“Development of bifunctional catalytic materials for the selective hydrotreating of dibenzothiophenes via the HYD route of hydrodesulfurization”

VÍCTOR GABRIEL BALDOVINO MEDRANO

UNIVERSIDAD INDUSTRIAL DE SANTANDER
FACULTAD DE INGENIERÍAS FISICO-QUÍMICAS
ESCUELA DE INGENIERÍA QUÍMICA
CENTRO DE INVESTIGACIONES EN CATÁLISIS (CICAT)
BUCARAMANGA
2009

"*Development of bifunctional catalytic materials for the selective hydrotreating of dibenzothiophenes via the HYD route of hydrodesulfurization*"

VÍCTOR GABRIEL BALDOVINO MEDRANO

Tesis presentada como requisito para acceder al Titulo de:
Doctor en Ingeniería Química

Director
Prof. Aristóbulo Centeno Hurtado

Co-directora
Prof. Sonia A. Giraldo

UNIVERSIDAD INDUSTRIAL DE SANTANDER
FACULTAD DE INGENIERÍAS FISICO-QUÍMICAS
ESCUELA DE INGENIERÍA QUÍMICA
CENTRO DE INVESTIGACIONES EN CATÁLISIS (CICAT)
BUCARAMANGA
2009

AGRADECIMIENTOS

A los profesores Aristóbulo Centeno y Sonia Azucena Giraldo cuyo apoyo permanente y oportunos consejos fueron un faro durante esta travesía.

A los miembros del Centro de Investigaciones en Catálisis con quienes además de las discusiones académicas sostenidas compartí momentos importantes en mi formación personal.

Al personal de la la *Unité de catalyse et chimie des matériaux divisés, Université catholique de Louvain*, bajo la dirección del Profesor E.M. Gaigneaux por su acogida y colaboración durante la realización de la pasantía doctoral.

Una larga lista de amigos muy significativos para mí podría ser inscrita en esta parte, pero todos ellos saben su contribución a la culminación de esta etapa y al comienzo de una nueva. Las palabras no serán suficientes y todas las memorias siguen vivas y latiendo en mi presente, tanto como lo harán en las gratas recordaciones del mañana.

El mundo está bien hecho. Todo tiene un origen y un final que da comienzo a un nuevo día. Si bien una Tesis Doctoral es un camino largo y solitario, se siente a la distancia el calor de aquellos cuyo amor incondicional no ha de abandonarme hasta que mis pasos se borren de este universo temporal. Gracias, Nurys, Víctor y mis hermanos.

Víctor Gabriel Baldovino Medrano

Contents

Chapter IV: What does chlorine have to do with the development of the HYD route of hydrodesulfurization?...147

Figures

Chapter III

 Part I

Part II

Tables

RESUMEN

TITULO: *Desarrollo de materiales catalíticos bifuncionales para la hidrodesulfuración de dibenzotiofenos por la ruta de hidrogenación*[*]

AUTOR: VÍCTOR GABRIEL BALDOVINO MEDRANO[**]

PALABRAS CLAVES: Hidrodesulfuración profunda de Diesel, dibenzotiofenos, ruta de hidrodesulfuración por hidrogenación, naftaleno, Pd-Pt, acidez "suave"

DESCRIPCIÓN

La hidrodesulfuración (HDS) de di-β-dibenzotiofenos es necesaria para obtener combustibles tipo Diesel que cumplan con las regulaciones ambientales presentes y por consiguiente su utilización tenga un menor impacto negativo tanto en el medioambiente como en la salud. Dichas moléculas presentan fuertes impedimentos estéricos que impiden su hidrodesulfuración directa (DDS) sobre los catalizadores empleados, su HDS procede casi exclusivamente por la ruta de hidrodesulfuración por hidrogenación (HID). En esta Tesis Doctoral se desarrollaron sistemas catalíticos bifuncionales Pd-Pt soportados para la HDS de dibenzotiofeno por la ruta HID.

Entre los aportes de la Tesis se encuentran: (i) El planteamiento de un mecanismo de reacción específico de la ruta HID. (ii) La preparación de catalizadores Pd-Pt soportados cuya selectividad HID/DDS puede controlarse a través de la relación atómica Pd/(Pd+Pt). (iii) El establecimiento de una correlación entre las sinergias en HID y en hidrogenación de aromáticos bajo atmósfera de H_2S. (iv) El planteamiento de un modelo de fase activa Pd-Pt en HDS. (v) Se mostró que la selectividad HID/DDS puede ser drásticamente modificada a partir de cambios "suaves" en la acidez del soporte catalítico de la fase activa Pd-Pt.

Toda la evidencia experimental obtenida indica que el éxito en la manipulación de la selectividad HID/DDS está ligada a una conveniente sintonización entre las características intrínsecas de la fase activa y el balance de sitios ácidos Lewis-Brønsted de naturaleza "suave" del soporte catalítico. Esta denominada acidez suave es muy relevante para la futura aplicación de dichos materiales en un proceso de HDS profunda de Diesel, porque reduce los riesgos de envenenamiento por moléculas nitrogenadas básicas y deposición de coque. En adición, los catalizadores Pd-Pt son estables y no son envenenados por el H_2S, y tienen simultáneamente alta actividad en HDS y en hidrogenación de aromáticos.

_____

ABSTRACT

TITLE: *Development of bifunctional catalytic materials for the selective hydrotreating of dibenzothiophenes via the HYD route of hydrodesulfurization*[*]

AUTHOR: VÍCTOR GABRIEL BALDOVINO MEDRANO[**]

KEYWORDS: Deep hydrodesulfurization of Diesel oils, dibenzothiophenes, HYD route of hydrodesulfurization, naphthalene, Pd-Pt, "soft" acidity.

DESCRIPTION

Deep hydrodesulfurization (HDS) of Diesel oils require the elimination of sulfur from sterically hindered di-β-dibenzothiophenes. Steric hindrance impedes the elimination of sulfur by a direct hydrodesulfurization (DDS) mechanism. Therefore, the HDS of di-β-dibenzothiophenes proceeds almost exclusively via the parallel and simultaneous hydrogenation route of hydrodesulfurization (HYD). For this reason, the development of HYD is crucial to deep HDS of Diesel fuels. In this Ph.D. Thesis a series of bifunctional Pd-Pt supported catalysts for the HDS of dibenzothiophene via HYD were prepared.

The main contributions of the work were: (i) The proposal of a specific mechanism for the HYD route. (ii) The preparation of a series of supported Pd-Pt catalysts over which the HYD/DDS selectivity can be controlled from the Pd/(Pd+Pt) molar ratio. (iii) The establishment of a correlation between the synergy in HYD and the synergy in the hydrogenation of aromatic molecules. (iv) The proposal of a model of Pd-Pt active phase in HDS reactions. (v) A demonstration that the HYD/DDS selectivity can be drastically modified by soft changes in the acidity of the support of the Pd-Pt active phase.

All of the collected evidence demonstrates that in order to exert an effective control on the HYD/DDS it is necessary to correctly tune out the intrinsic properties of the Pd-Pt active phase and the Lewis-Brønsted acid balance of the carrier. In this regard, soft acidity changes can be very relevant when considering a future utilization of the designed materials in a refinery unit for deep HDS to prevent poisoning by basic nitrogen molecules and coking. In addition, it was demonstrated that the Pd-Pt catalysts are stable in HDS not being poisoned by H_2S and that they keep their high activity and selectivity to HYD in the presence of an aromatic.

_____

Chapter I: General Introduction

1. The hydrotreating process and its relevance to human health and to the environment

The hydropurification or hydrotreatment (HDT) of oil fractions is at the heart of any oil refinery. After performing the primary separation of the crude oil in an atmospheric distillation unit, the separated oil fractions destined to be converted into fuels must be purified by removal of the different heteroatoms contained in the organic molecules which compose them. In agreement with the type of heteroatom to be removed HDT can be subdivided into reactions of hydrodesulfurization (HDS) as referred to sulfur removal, hydrodenitrogenation (HDN), i.e. nitrogen removal, hydrodeoxygenation (HDO), for oxygen removal, and finally hydrodemetallization (HDM), for heavy metals removal. In addition, those processes intended to transform the structure and molecular weight of certain molecules; such as catalytic hydrocracking, isomerization and hydrogenation of non saturated molecules (aromatics, olefins) make part of HDT. Consequently, the purpose of the HDT process is the production of fuels fulfilling the environmental standards established by governmental regulations regarding the maximum allowed contents of pollutants from the combustion of fossil fuels. Of particular concern are the emissions of SO_x, NO_x and soot from the exhaust gases from transportation vehicles, all of them being hazardous to human health and to the environment. SO_x (SO_2 + SO_3) is the cause of respiratory diseases in both human beings and animals, as well as it has a negative impact in vegetation. Furthermore, such gases are known precursors of sulfates and acid rain which besides damaging the aquatic and terrestrial ecosystems also deteriorate buildings such as historical monuments [1]. NO_x have similar adverse effects as SO_x. Gas-phase soot is constituted by polycyclic aromatic compounds which are known mutagens and probable carcinogens [2]. Soot, SO_x and NO_x simultaneously released in

exhaust gases constitute the so-called particulate matter (PM). PM levels in the air are strictly controlled by environmental authorities worldwide due to its high negative impact in human health. Therefore, giving that the effect of such emissions from thousands of millions of vehicles unchains a series of complex phenomena affecting us all, it can be properly said that part of the welfare of human society and of natural living beings relies to some extent in the design of very efficient HDT processes, because of the dependence of our society on fossil fuels.

2. Why is deep hydrodesulfurization of diesel oils in the spotlight of hydrotreating?

An analysis of the composition of any refinery oil fraction indicates that among the heteroatoms sulfur concentration is the highest [3]. In a conventional refinery scheme hydrodesulfurization of the oil cuts is necessary to reduce corrosion of the diverse units and pipelines, prevent poisoning of the noble metal catalysts used in reforming units, and meeting the particular specifications of the finished products [3]. There has been a growing demand for diesel-powered cars in the last few years [4, 5] and such demand will surely grow more in the upcoming years due to the boom of biodiesel and to the basic fact that diesel engines are more energetically efficient than Otto engines, i.e. those employing gasoline [5, 6]. For this reason, the production of diesel fuel in refineries is becoming more and more important every day. The refinery cut oil fraction in the range 473 – 723 K from the atmospheric distillation unit and lighter gas oil cut from vacuum distillation are raw materials to produce diesel fuels from petroleum [3]. Within these cuts the Light Cycle Oil (LCO) from the fluid catalytic cracking units (FCC) was the main component of diesel fuels for many years [7]. This was very advantageous for refiners from the economic and operative point of view, because LCO hydrotreatment is very complicated due to its extremely high sulfur, nitrogen and aromatics content [5, 7]. However, with the increasing tightening in environmental legislations concerning the sulfur contents of diesel fuels around the globe (current maximum sulfur

content of diesel fuel in the United States, Japan and the European Union is 10 wppm [8-10]), LCO utilization for diesel fuel production has steeply decreased being replaced by the lighter straight run gas oil (SRGO) in the last two decades [7]. Refiners have had to face a very challenging scenario from this situation; because year after year they are obliged to comply the tougher environmental regulations while hydrotreating sourer (i.e. crudes of higher sulfur contents) and heavier crude oils in their units. Furthermore, they face a very important LCO surplus which must be upgraded to balance the economics of the refinery [5]. A recent analysis of this situation made by R.G. Leliveld, and S.E. Eijsbouts [5] concluded that the most convenient economic option for refiners is the search for new more active and selective catalytic systems for the hydrotreatment of LCO and related oil cuts to avoid significant capital investments in new additional upgrading units. On the other hand, new applications of diesel fuels have been envisaged in the emerging field of fuel cells for generating electricity in power plants, automobiles and residential houses which will require a very extreme reduction in sulfur content (below 0.1 wppm) of this liquid hydrocarbon [11]. Therefore, the need of more environmentally friendly fuels puts hydrodesulfurization in the spotlight of HDT, because this type of reaction continues to be a driving force in the development of new technologies in refining industry.

3. Need for new more active and selective catalytic systems for deep hydrodesulfurization of diesel oils.

A typical refinery cut contains a large amount of sulfur-containing organic molecules. Such molecules are normally classified into two main families: aliphatic type sulfur containing molecules; which comprise mercaptanes, sulfides and disulfides, mostly present in light refinery cuts, and thiophenic type molecules, i.e. thiophenes, benzothiophenes and dibenzothiophenes (DBTs) [3, 12]. The relative concentration of each type of organosulfur compounds in the corresponding oil cuts from the atmospheric distillation unit is, of course, given by their boiling points. Therefore, lighter oil cuts are very rich in thiophenes and

benzothiophenes, whereas alkyl-benzothiophenes and dibenzothiophenes are major constituents of heavier fractions used to produce diesel fuels [3, 12, 13]. The deeper the level of hydrodesulfurization of the heavy oil fractions, the higher the concentration of more refractory dibenzothiophenes [12, 13]. At the conditions of a classical industrial HDT unit (T = 573 − 693 K and H_2 partial pressures between 3 and 10 MPa) refractory dibenzothiophenes are un-efficiently converted over conventional γ-Al_2O_3 supported MoS_2 based catalytic systems [5, 12, 13]. Consequently, when producing cleaner diesel fuels the HDT reactor must be operated at extreme reaction conditions which besides reducing the lifespan of the catalysts deteriorate some properties of the finished product [3, 5, 12, 13]. Moreover, the concentration of nitrogen containing organic compounds and aromatics of the heavier oil cuts is quite high; for example, the average total aromatics content of LCO is between 60-90% [5]. Intense competition between parallel hydrodesulfurization, hydrodenitrogenation and hydrodearomatization (HDA) reactions thus takes place during the catalytic HDT of cuts destined to produce diesel fuel oils [3, 5, 12, 14-18]. Furthermore, as the regulations concerning the contents of aromatics and nitrogen in diesel fuels have also been strictly adjusted [8-10] these compounds must be simultaneously hydrotreated with high efficiency. The requirement of producing the so-called ultra-low sulfur diesel (ULSD) -i.e. maximum sulfur content ≤ 10 wppm- to comply the environmental legislation in the classical HDT units is thus impossible, because conventional Co(Ni)-Mo(W)S_2/γ-Al_2O_3 do not possess enough hydrogenating capacity required to perform simultaneous deep HDS, HDN and HDA at moderate reaction conditions [3, 12, 13]. Moreover, an increase in the reaction temperature of the catalytic units is not convenient due to the fact that HDA reactions are exothermic (ΔH_{rxn} = 63-71 kJ/mole H_2 [19]) and are in equilibrium with dehydrogenation reactions. Regardless the H_2 partial pressure of the catalytic reactors for temperatures beyond 623 K dehydrogenation reactions are thermodynamically favored [20]. Aiming to satisfy the needs

of the refining industry a plethora of new designs of HDT processes [3, 5, 7, 15-18, 21-23] and new catalytic formulations [5, 13, 19, 20, 22-26] has boomed both the academic community and the market in the last two decades. An analysis of the relevant literature in the field indicates that secondary HDS reactor units for the production of ULSD in which highly hydrogenating and selective catalysts are used at moderate reaction conditions and with acceptable H_2 consumption is mandatory in modern refineries [5].

4. Target molecules of ultra deep hydrodesulfurization: di-β-dibenzothiophenes.

In 1978, Houalla et al. [27] published a rigorous kinetics study on the hydrodesulfurization of dibenzothiophenes over sulfided CoMo/γ-Al_2O_3 catalysts establishing the basic reaction network of their catalytic transformation. Dibenzothiophenes were found to react by two parallel reaction pathways called the hydrogenation route of desulfurization (HYD[1]) and the direct desulfurization route (DDS), where DDS was found to be predominant. Aside from this result, the authors remarked that: "The effect of the methyl groups in the 4 and 6 positions -of the dibenzothiophene molecule- (considered in view of the lack of an effect of methyl groups in the positions farther removed from the sulfur atom) suggests that they sterically hinder the adsorption that leads to hydrodesulfurization-in which the sulfur atom evidently interacts with the surface-but that they do not hinder the adsorption that leads to hydrogenation, in which the benzenoid ring(s) evidently interact(s) with the surface" [27]. The advent of the tighter legislation regarding the sulfur content of diesel fuels during the 90's produced keen interest in the reactivity of this type of substituted dibenzothiophenes, named β-dibenzothiophenes (β-DBTs), because their relative concentration in heavy oil cuts steeply augments with the level of hydrodesulfurization [12, 13, 14, 22].

When reducing sulfur content of diesel fuels β-dibenzothiophenes are the bull's eye of hydrodesulfurization. Among the typical organ-sulfur containing type compounds of the cuts

---

[1]The reader should note that the abbreviation HYD is used here exclusively to designate the hydrogenation route of hydrodesulfurization and not hydrogenation reactions.

used to produce diesel oils (Fig. 1) the kinetic studies on the reactivity of such compounds over conventional CoMo y NiMo/γ-Al$_2$O$_3$ established that the reactivity of this type of molecules decreases in the order: alkyl-benzothiophenes > DBT and alkyl-substituted-DBTs > mono-substituted β- DBTs > di-alkyl-substituted β-DBTs (di-β-DBTs) [12, 28-33].

Alkyl-benzothiophenes

Dibenzothiophene (DBT)

Alkyl-substituted-DBTs

Mono-alkyl-substituted-β-DBTs

Di-alkyl-substituted-β-DBTs
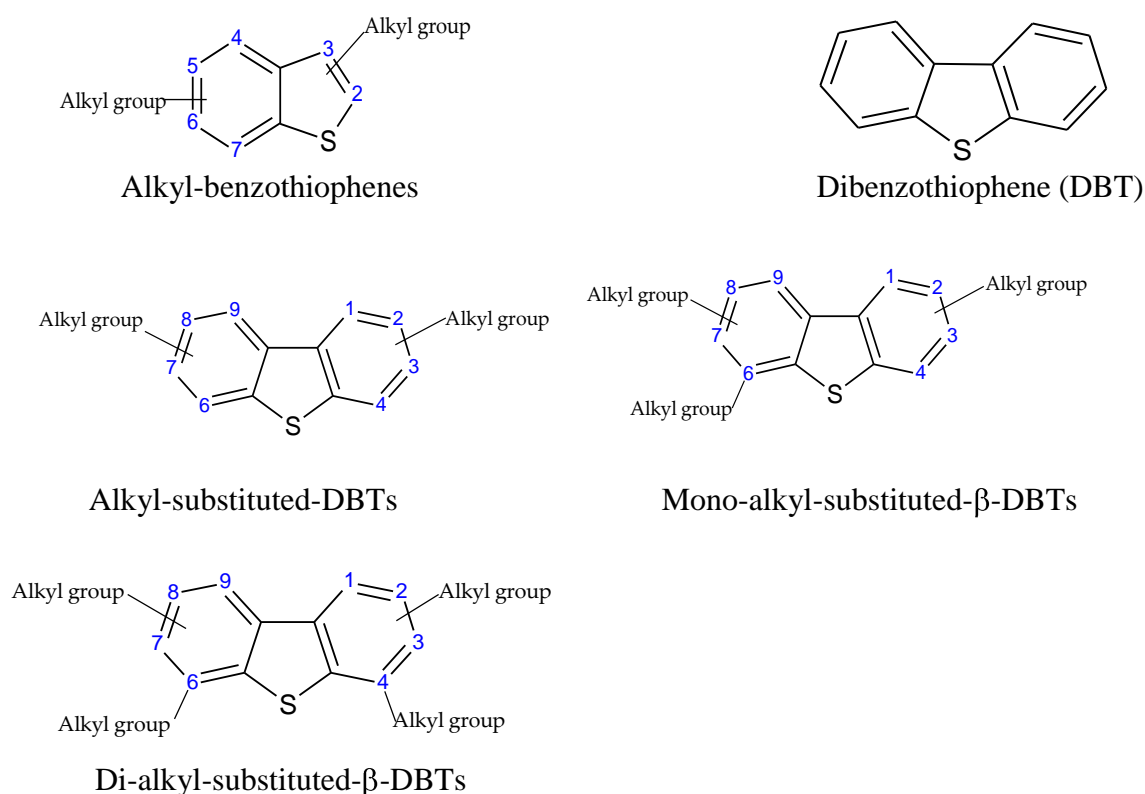
Fig. 1 Substituted benzothiophenes, dibenzothiophenes and alkyl-dibenzothiophenes usually contained in heavy refinery cuts.

Over conventional catalysts, the reaction rate differences in activity between dibenzothiophene and its alkyl derivatives, particularly, di-β-DBTs has been found to be around four to six times lower as compared to DBT [15, 23, 24, 26]. When aiming to reduce the sulfur content of diesel fuels below 10ppm, di-β-DBTs must be efficiently hydrodesulfurized [11-14, 22, 23, 28-34].

5. Mechanisms of reaction of dibenzothiophenes: the importance of the HYD route in the hydrodesulfurization of di-β-dibenzothiophenes.

Houalla et al. [27] established that dibenzothiophenes react by parallel HYD and DDS over conventional sulfided catalysts. DDS implies the direct scission of the C-S-C bond of the thiophene ring of DBT, whereas, HYD requires saturation of one benzenic ring of the DBT backbone before C-S-C bond scission [12, 14, 22, 23, 27-31, 34-36]. The precise mechanism of DDS and HYD has remained an object of controversy since long ago. After years of intense debate two different mechanisms stand as the most accepted ones. The first one is based on the ideas originally proposed by Lipsch and Schuit [37] in 1969; who considered the direct hydrogenolysis of the C-S-C bond of thiophenic rings over catalyst's active sites by the transfer of H to the aforementioned bond. This model has been further refined and supported by experiments of desulfurization of thiophene, benzothiophene and dibenzothiophene with transition metal complexes and theoretical calculations over MoS_2 clusters [38-43]. In this case it has been proposed that DDS and the final C-S-C bond scission in HYD occur by direct attachment by σ-adsorption or η^1 (S) adsorption, of the sulfur heteroatom on the sulfur edge [42]. Moreau et al. [41] concluded that hydrogenolysis of carbon sp^2-substituent bonds over various metallic complexes results from the attack on the carbon bearing the substituent by a soft nucleophilic species like a hydride ion. From density functional calculations, Prins et al. [43] determined that moderate activation energy is necessary to dissociate alkanethiol via direct adsorption of the S heteroatom to Mo atoms in MoS_2 clusters, and by further discussion on the mechanism of arylthiols, like thiophenol, they proposed that such molecules are also prone to direct hydrogenolysis. On the base of these arguments, they thus concluded that the hydrogen atoms on the catalyst surface react directly with the C-S-C bond of dibenzothiophenes. The second mechanism for the scission of the C-S-C bond in hydrodesulfurization reactions assumes the existence of partially hydrogenated di-hydrointermediates [44-47] (Fig. 2). In this model, both DDS and HYD share a common dihydroderivative of dibenzothiophene which is further either sequentially hydrogenated

(HYD) and finally desulfurized or directly desulfurized by cleavage of the C-S-C bonds. Regardless the reaction pathway, scission of the C-S-C bond occurs via an acid-base catalyzed elimination process leading to the re-aromatization of the partially hydrogenated cycle [44-47]. Actually, Mijoin et al. [47] proposed that there is not one but nine possible di-hydrointermediates, the selectivity HYD/DDS would depend on the distribution of these intermediates. Though chemically possible, a very strong argument against this mechanism is that none of these di-hydrointermediates has ever been detected in HDS reactions performed under standard conditions.
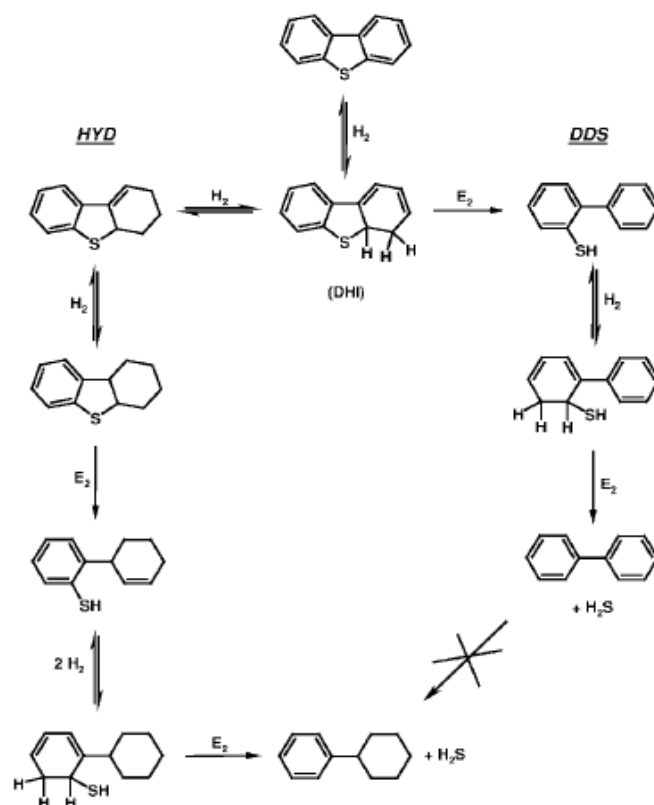
Fig. 2. Hydrodesulfurization reaction mechanism of dibenzothiophene involving the formation of a dihydro-dibenzothiophene intermediate proposed by Mijoin at al. [47].

Nevertheless, the very recent study of the group of Prins [48]; this group of research being by the way one of chief contradictors of the validity of the di-hydrointermediates mechanism, admits that it is possible that the C-S-C bond scission can simultaneously occur by direct hydrogenolysis or by the proposed elimination reaction [44-47].

Besides the dispute concerning the nature of the chemical reaction which leads to C-S-C scission, there is also certain debate around the way in which the dibenzothiophenes are adsorbed or coordinated to the catalytic active phase during desulfurization. While some authors present evidence supporting a preferential adsorption of the (di)-(benzo)-thiophene molecules by the vertical or perpendicular or "one-end" σ-adsorption mode of the S heteroatom [37, 49, 50], others have demonstrated that flat π-adsorption is energetically favored [51-54]. Cristol et al. [42] theoretically showed that for the hydrodesulfurization of dibenzothiophenes the HYD/DDS selectivity is the result of adsorption competition effects between the perpendicular $\eta^1(S)$ adsorption and the flat π-adsorption mode (comprising η^3, η^5, or η^6 coordination of the aromatic rings of dibenzothiophene with the catalytic active phase). Trying to explain the differences in reactivity between dibenzothiophene and 4,6-dimethyl-DBT, they concluded that as the $\eta^1(S)$ adsorption of the molecule on the vacancies of the MoS_2 phase is hindered by a conjunction of steric and aromaticity effects present in 4,6-dimethyl-DBT, this molecule can practically only react via the development of HYD. Regardless the prevalent adsorption mode of (di)-(benzo)-thiophene, it is totally agreed that HYD occurs by the formation of a π-complex of the aromatic structure of the molecule with the active sites [42, 43, 45-48, 51, 55]. A convenient model which reconciles the sometimes discordant points of view in this sense is the multipoint coordination model proposed by Kwart et al. [56] for the hydrodesulfurization of thiophene over MoS_2 catalysts. In this model the adsorbed thiophene molecule is in contact with to the active surface in more than one point, and not solely coordinated either by π or by σ adsorption of the S heteroatom. The study of Yang et al. [51] indicated that in fact flat adsorption (π-adsorption) was more energetically favorable over perpendicular adsorption (σ-adsorption), and that π-adsorption involves multipoint interactions of the sulfur atom, the thiophene, and aromatic rings of dibenzothiophenes with the catalytic surface. In conclusion, the analysis of the literature

indicates that there are adsorption-competition effects playing a role in the selectivity HYD/DDS and that the hydrodesulfurization reaction is taking place by competitive parallel reaction mechanisms.

The interplay between the phenomena mentioned above is crucial to understand the hydrodesulfurization of di-β-dibenzothiophenes, because, as discussed above, these molecules mostly react via HYD under standard reaction conditions and when using not highly acidic catalysts [29, 35, 57-62]. As appointed before, the reactivity of di-β-DBTs is driven by the steric hindrance imposed by the β substituents and it is also related to the electron density around the S atom (or aromaticity) [42, 57]. Even though early works attributed reaction rate differences between dibenzothiophene and di-β-DBTs to a difference in the adsorption energy [35, 58], such hypothesis was discarded because it was demonstrated that the adsorption constants of dibenzothiophene and 4,6-dimethyl-DBT are rather similar [59-61]. During the development of HYD hydrogenation of the benzenic structure of the dibenzothiophenes confers flexibility to the molecule which reduce the steric effects thus facilitating the removal of the S heteroatom; regardless the mechanism of C-S-C bond scission [57]. Fig. 3, adapted from [57], shows this:
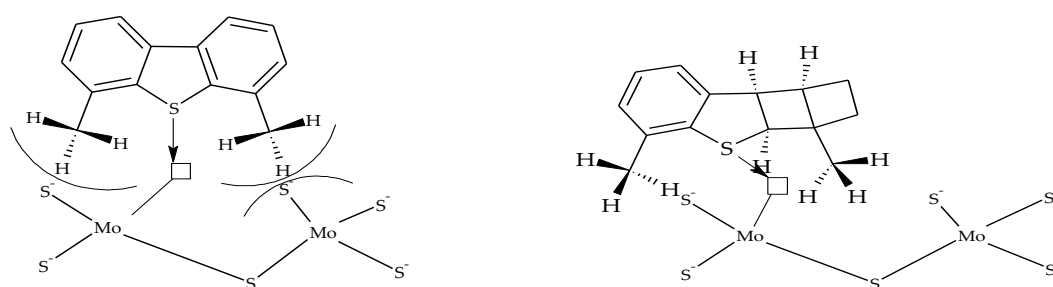
a) Effect of flexibility increase on a possible frontal approach of the sulfur heteroatom to the catalytic active sites.
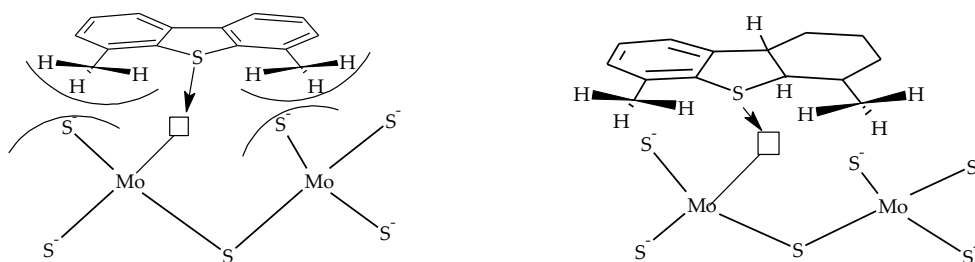
b) Effect of flexibility increase in a possible lateral approach to catalytic active sites.

Fig. 3. Increase in the flexibility of the DBT backbone of 4,6-dimethyl-DBT through a partial hydrogenation of the molecule [57].

Another way to diminish steric hindrance in di-β-DBTs is to perform the isomerization, de-alkylation or cracking of the dibenzothiophene structure previous to sulfur extraction. Fig. 4 summarizes these alternatives for 4,6-dimethyl-DBT [57]. Isomerization consists on shifting 4,6 alkyl-substituents to 3,7- or 2,8- positions then eliminating steric hindrance. De-alkylation is the breaking of the one of the alkyl-substituents. Cracking consists on breaking the C-C bond of the thiophenic ring.
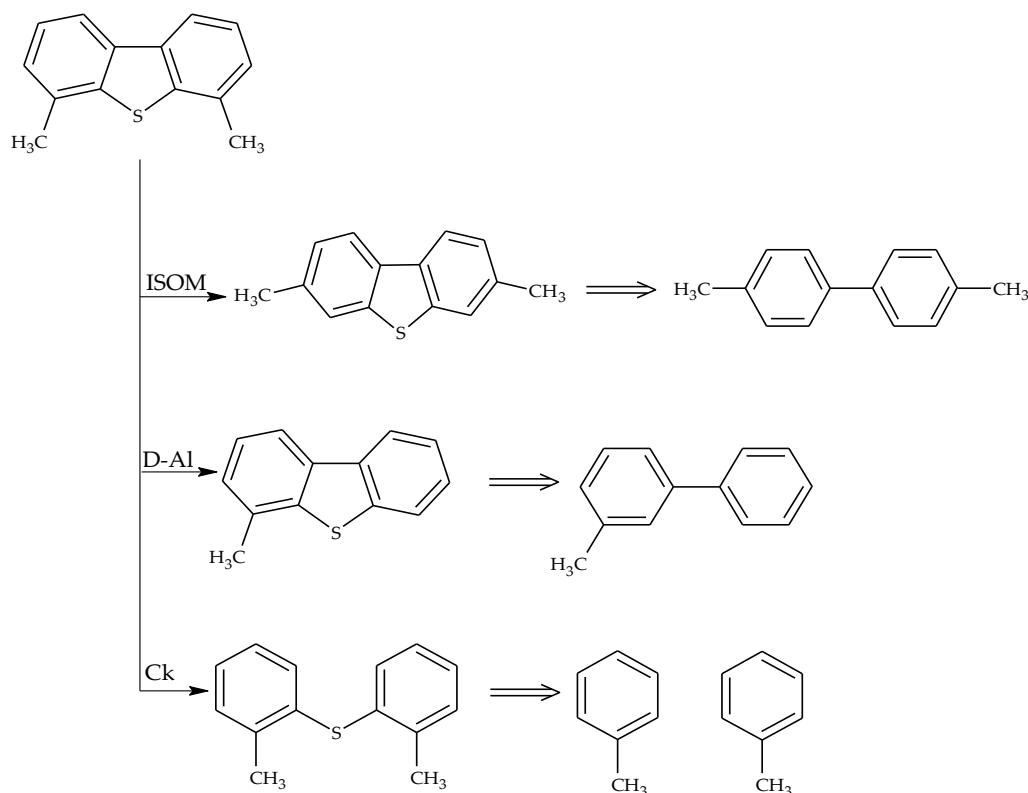
Fig. 4. General scheme of isomerization (ISOM), de-alkylation (De-Al) and cracking (Ck) pathways for the HDS of 4,6-dimethyl-DBT [57].

All of these reaction routes require the use of catalytic systems with medium or strong acidic properties [57, 63-69]. Considering the deep HDS of diesel fuels, in which parallel HDA and HDN reactions cannot be avoided, the use of catalytic materials with strong acidic properties

is not convenient, due to its tendency to be deactivated by coking and the HDN of basic nitrogen containing molecules [12, 14-18]. Conversely, the acidic properties of the materials can contribute to develop HYD [33, 69, 70]. As deep HDS necessarily entails HDA and HDN, the design of new catalytic systems with a proper balance of their functionalities and high hydrogenating capacity is desired. As it has been discussed in this section, a first crucial step in the pursuit of such goal is an in-depth comprehension of the mechanistic dynamics of the HYD route of hydrodesulfurization.

6. A brief literature review of the catalytic materials intended to be used for deep hydrodesulfurization and potentially able to develop the HYD route of hydrodesulfurization of dibenzothiophenes.

According to the discussion presented above, it is of prime interest to develop catalytic materials with the capacity to develop the HYD route of hydrodesulfurization of dibenzothiophenes. The properties which are necessary to direct the hydrodesulfurization of dibenzothiophenes whether by HYD or DDS can be classified as follows: i) physicochemical and structural properties of the active phase, and ii) acidic properties of the support. Naturally, the most important characteristic is the hydrogenating capacity of the catalytic active phase, which will be somehow reflected by the selectivity of the metals composing such active phase in hydrotreating reactions (i). For conventional HDS catalysts, some results indicate that the use of Co as a promoter of the MoS_2 phase favors DDS selectivity, whereas Ni promotion is thought to lead to higher HYD rates [12, 28-30, 32]. For that reason, it has been stated that Ni-MoS_2 based catalytic systems are more suitable for the production of ULSD, this fact being related to its higher hydrogenating capacity [12, 22, 71, 72]. Nevertheless, some authors attribute such difference to the effect of H_2S partial pressure on the nature of the catalytic active sites [63, 73], moreover, both metals have been proposed to basically promote DDS or the scission of the C-S-C bond in HYD [47, 73, 74]. Therefore, it seems clear, that even for

conventional HDS catalysts the role of the promoter (Co or Ni) on the desulfurization selectivity is not fully established.

On the other hand, noble metals, which are highly active hydrogenating catalysts, have been tested in HDT reactions, and among them, Pt and Pd, which are commonly used in reforming and hydrogenation reactions, have been the focus of attention. The results in literature show that either sulfided [75-77] or reduced [20, 24, 78, 79] Pt and Pd catalysts can be more active in HDS as compared to conventional HDS catalysts. Indeed, it has been found that Pt has an activity in the hydrodesulfurization of dibenzothiophenes as high as that of conventional Ni(Co)Mo catalysts [78, 79] and that Pd is more effective to develop the HYD route of hydrodesulfurization of 4,6-dimethyl-DBT than conventional MoS_2 based systems [20, 79]. Also the incorporation of Pt and Pd as promoters of MoS_2 based catalytic systems (Co(Ni)-Mo(W)S_2) has been studied [80-86]. For Pt-Mo, at a specific Pt/Mo ratio a high activity in the hydrodesulfurization of dibenzothiophene is obtained [84, 86]. The addition of low amounts of Pt to bimetallic sulfided Co(Ni)-MoS_2 catalysts has also been tested and slight improvements in HDS activity have been registered [87]. In the case of Pd-Mo catalysts poor activity in HDS has been reported [83, 85, 88]. The use of bimetallic Pt-Pd alloyed catalysts in hydrotreating has draw a lot of attention due to the capacity of these materials to overcome sulfur poisoning in HDA reactions under H_2S atmospheres [20, 89-92], hence, they have been recommended for second stage reactors performing deep HDA or deep HDS of heavy refinery streams [20, 79, 91, 93-101]. Consequently, the use of such alloys can result in HDS selective catalysts to HYD [79, 101].

Active phase-support interactions can be critical to both catalytic activity and selectivity [102]. For HDS catalysts, the active phase-support interactions play a role in controlling the catalytic functionalities [103-111]. As commented before, the use of acidic supports is advantageous in the hydrodesulfurization of di-β-DBTs, because additional Brønsted acidic

13

sites can perform the isomerization and/or cracking of the β-substituents of dibenzothiophene [57, 63-69] and favor the development of HYD [33, 69, 70]. Consequently, zeolites [12, 20, 23, 33, 63, 64, 66, 68, 94, 112-115], mixed oxides [12, 23, 109, 116], amorphous silica-alumina (ASA) [90, 95, 113, 117-119] and diverse mesoporous materials [109, 114, 117] have been tested as HDS catalyst's supports. Other authors have modified supports acidity by the addition of small amounts of phosphorus, fluorine and boron. By this method they have prepared more active HDS catalysts either by improving active phase dispersion (Mo, Co and Ni), and/or generating acidic sites on the support [34, 67]. However, the use of acidic supports requires a proper tuning of the acidic function of the catalyst and the functionalities of the active phase given that highly acidic supports can lead to extensive coke deposition on the catalyst surface, then deactivating the catalyst [63]. An interesting alternative is to prepare controlled acidic supports by means of changing the molar ratio of the elements constituting the oxide. This is the case of alumino-silicate type supports [95, 113, 117-122], for which the acid-base balance of the material can be directed from the Si/Al ratio used in their preparation process. Of special interest can be those alumino-silicates of low Si/Al ratios, for which "soft" acidity can be expected, because of their lower affinity to basic nitrogen molecules and less tendency to be deactivated by coke deposition.

7. The aims, methodology and scope of this study.

The conjunct analysis of the facts presented so far lead to conclude that in order to design a highly efficient material for the deep hydrodesulfurization of di-β-dibenzothiophenes it was necessary to prepare a series of catalysts possessing an appropriate balance in their catalytic functionalities, more precisely the hydrogenating capacity of the active phase and the acid properties of the carrier. To be able to correctly tune up both properties it was necessary to carry out a sequence of experiments conducting to a comprehension of the relationship between the physicochemical properties of the catalysts and the development of HYD. But,

before starting the search for an efficient catalytic system for deep hydrodesulfurization it was mandatory to choose the most convenient dibenzothiophene molecule from the family of dibenzothiophenes. Though, when aiming to study deep hydrodesulfurization, most authors opt for 4,6-dimethyl-DBT as model molecule, because this is the actual type of molecule from which sulfur must be eliminated in the industrial process, after considering that the hydrodesulfurization of 4,6-dimethyl-DBT will always be driven to HYD by steric effects, it was decided to select the non-sterically hindered dibenzothiophene molecule in this research because: (i) dibenzothiophene allows a real direct measurement of the intrinsic selectivity HYD/DDS of a given catalytic system because its hydrodesulfurization is not driven by any steric effect and thus is the result of the interactions established between the molecule and the catalytic active phase; (ii) the effect of the competition between the hydrogenation of an aromatic ring (HDA) -studied here- and the selectivity to HYD is more properly followed when using dibenzothiophene than with 4,6-dimethyl-DBT, because the former is more analog to aromatics; (iii) if a catalytic material is more selective to HYD than to DDS in the hydrodesulfurization of dibenzothiophene it will logically be quite active in the hydrodesulfurization of 4,6-dimethyl-DBT, as it has been demonstrated in literature [123]; and (iv) last, but not least, from the engineering and economical point of view dibenzothiophene is more versatile than 4,6-dimethyl-DBT, because the former is readily available in the market and cheaper, thus facilitating the reproduction of the catalytic results obtained by providing the possibility of making a larger number of replicas. Once this decision was taken a series of catalytic tests was planned comprising: (i) the hydrodesulfurization of dibenzothiophene as to measure the intrinsic HYD/DDS selectivity of the prepared catalysts; (ii) the simultaneous hydrodesulfurization of dibenzothiophene - hydrogenation of naphthalene as to determine the influence of adsorption competition effects between the hydrogenation reaction and HYD; (iii) hydrogenation of naphthalene in the

15

absence and presence of H_2S, to determine certain key properties of the active phase of the catalytic materials for the efficient development of HYD; and, (iv) stability tests of the catalytic materials.

The results of the study were then analyzed and organized sequentially to show stepwise how was designed the catalytic system over which dibenzothiophene is efficiently hydrodesulfurized via HYD and not via DDS. For a better comprehension of the process of tuning of the convenient properties of the active phase of the materials with the acid-base properties of the carrier, the present research was initially conducted over active phases supported on a commercial γ-Al_2O_3. Later on, the effect of the modification of the acid-base properties of the γ-Al_2O_3 support on the HYD selectivity was determined by means of certain selected changes in the nature and physicochemical properties of the support.

Before presenting the results of this research, the second part of this introductory section is devoted to an analysis of previous works performed at CICAT [124-126] in which the author discusses whether Ni- or Pt- promoted MoS_2 systems supported on γ-Al_2O_3 and boron modified γ-Al_2O_3 are suitable for the selective hydrodesulfurization of dibenzothiophene, at moderate reaction conditions, via HYD. The aim of this was twofold; to determine the viability of the use of this type of active phase for the designated purpose and to verify if acidity can promote HYD (boron modified γ-Al_2O_3 carriers). From the analysis presented in this section Ni- and Pt- promoted MoS_2 systems were discarded as potential materials to develop a selective HDS of dibenzothiophene via HYD. Concerning the acidity effect on HYD selectivity, it was detected that, indeed, the acidic balance of the carrier plays a role in the development of the HYD route of hydrodesulfurization.

In Chapter II the development of the HYD route over monometallic Pd/γ-Al_2O_3 catalysts was studied and complemented by an analysis of the behavior of Pt/γ-Al_2O_3 in this same type of reaction. For Pt/γ-Al_2O_3 the author selected some data from the work of Estupiñán [126] and

performed an analysis of the functionalities of this metal in hydrotreatment with particular emphasis on the selectivity to HYD. Therefore, the functionalities of both monometallic systems related to HYD selectivity were carefully analyzed, as to provide a solid base for the interpretation of the behavior of bimetallic Pd-Pt systems in the hydrodesulfurization of dibenzothiophene which is presented in Chapter III. This considering that both metals, Pt and Pd, are active in HDS and their selectivity to HYD can be different. On the other hand, the more appropriate method of activation of the noble metal catalysts was selected from the analysis of the influence of this variable on the catalytic performance. Finally, the analysis of the performed catalytic tests for Pd constituted a first step for the comprehension of the mechanism of the HYD route of hydrodesulfurization and its relationship with the basic properties which the active phase of the materials intended to be selective to HYD must possess, and with the mechanisms of hydrogenation of aromatics. This last relationship was very useful in the process, because it was determined that the mechanism of HYD share some key similarities with the mechanisms proposed to explain the stereoselectivity differences in the hydrogenation of naphthalene over supported metallic catalysts.

On the basis of the information obtained in Chapter II, the study was then directed to the selectivity to HYD over Pd-Pt/γ-Al$_2$O$_3$ alloyed systems as a function of the Pd/(Pd+Pt) atomic ratio of the alloy. As in the case of Chapter II, results in Chapter III are presented in two parts; the first thoroughly analyzing the hydrogenating function of Pd-Pt by the use of naphthalene hydrogenation as a very practical test molecule which can be employed to determine and verify some of the phenomena occurring in the active phase of the working catalyst. In part II, dibenzothiophene hydrodesulfurization under different reaction conditions and over the same group of materials was studied. The results were correlated with those obtained in Part I, pointing out to the common points of both reactions and to their relationship with the chemical properties of Pd-Pt which allow them to develop the HYD route of

hydrodesulfurization. Finally, the stability of the active phase of these materials in HDT was also studied. Therefore, in Chapter III the basic chemical properties of the Pd-Pt active phase relevant to HYD and the fundamentals of the dynamics of mechanism of the HYD route of hydrodesulfurization of dibenzothiophenes was established, thus providing rigorous engineering and physicochemical fundaments to the design of new catalytic materials for deep HDS.

Chapter IV is intended to establish a link between the properties of the active phase of Pt and Pd in hydrodesulfurization and the modification of the acidic balance of the carrier; thus, it constitutes the first step of the tuning process between these two variables. For this purpose, different modifications in the preparation method of the monometallic Pt and Pd catalysts were essayed. The return to the monometallic systems was based on the assumption that the functioning of the Pd-Pt active phase in the hydrodesulfurization reaction can be basically interpreted to correspond to a promotion of Pd by Pt (Chapter III). The results obtained led to conclude that significant enhancement of HYD over Pd is obtained only by a slight change in the acidic balance of the catalysts. This finding was clearly demonstrated experimentally in Chapter V for the bimetallic Pd-Pt system, for which "soft" modifications in the acid balance of the carrier were put into practice by supporting on different carriers of not very large differences in acidity. The scope of the Thesis is then completed as in Chapter V a totally new Pd-Pt supported material was prepared over which the HYD route of hydrodesulfurization of dibenzothiophene was fully developed, and the variables intervening in the appropriate tuning of the properties of the active phase and the acid properties of the material were established.

References

[1] http://www.ec.gc.ca/cleanair-airpur/SOx-WSBBB2123F-1_En.htm, consulted 29 April 2009.

[2] http://en.wikipedia.org/wiki/Soot, consulted 29 April 2009.

[3] J.G. Speigth, The Desulfurization of Heavy Oils and Residua, Marcel Dekker Inc. (2000) New York.

[4] http://www.greencarcongress.com/2008/02/european-automo.html, consulted 29 April 2009.

[5] R.G. Leliveld, S.E. Eijsbouts, Catal. Today 130 (2008) 183.

[6] http://en.wikipedia.org/wiki/Diesel_engine, consulted 29 April 2009.

[7] G.C. Laredo, R. Saint-Martin, M.C. Martínez, J. Castillo, J.L. Cano, Fuel 83 (2004) 1381.

[8] www.epa.gov/EPA-AIR/2001/January/Day-18/a01b.pdf, consulted 29 April 2009.

[9] http://www.env.go.jp/en/headline/headline.php?serial=226, consulted 29 April 2009.

[10] http://europa.eu/scadplus/leg/en/lvb/l28077.htm, consulted 29 April 2009.

[11] X. Ma, L. Sun, C. Song, Catal. Today 77 (2002) 107.

[12] D.D. Whitehurst, T. Isoda, I. Mochida, Adv. Catal. 42 (1998) 345.

[13] T.G. Kaufmann, A. Kaldor; G.F. Stuntz, M.C. Kerby, L.L. Ansell, Catal. Today 62 (2000) 77.

[14] T.C. Ho, Catal. Today 98 (2004) 3.

[15] J. Ancheyta, M.S. Rana, E. Furimsky, Catal. Today 109 (2005) 3.

[16] E. Furimsky, F.E. Massoth, Catal. Rev.-Sci. Eng. 47 (2005) 297.

[17] J. Ancheyta-Juárez, E. Aguilar-Rodríguez, D. Salazar-Sotelo, G. Betancourt-Rivera, M. Leiva-Nuncio, Appl. Catal. A: Gen. 180 (1999) 195.

[18] J.G. Speight, Catal. Today 98 (2004) 55.

[19] A. Stanislaus, B.H. Cooper, Catal. Rev.-Sci. Eng.36 (1994) 75.

[20] Y. Yoshimura, M. Toba, T. Matsui, M. Harada, Y. Ichihashi, K.K. Bando, H. Yasuda, H. Ishihara, Y. Morita, T. Kameoka, Appl. Catal. A: Gen. 322 (2007) 152.

[21] E. Ito, J.A. Rob van Veen, Catal. Today 116 (2006) 446.

[22] C. Song, Catal. Today 86 (2003) 211.

[23] I. Mochida, K. Sakanishi, X. Ma, S. Nagao, T. Isoda, Catal. Today 29 (1996) 185.

[24] Active Phases for Hydrotreating Catalysis, C. Geantet, M. Vrinat (Eds.), Special Issue Appl. Catal. A: Gen. 322 (2007).

[25] New developments in sulfide catalysis: Linking industrial needs to fundamental challenges - Proceedings of the 4th International Symposium on Molecular Aspects of Catalysis by Sulfides (MACS-IV), S. Eijsbouts, J.A.Rob van Veen, E.J.M. Hensen, G. Mul (Eds.), Catal. Today 130 (2008) 1-264.

[26] International Symposium on Advances in Hydroprocessing of Oils Fractions (ISAHOF 2007), J. Ancheyta, G.F. Froment (Eds.), Catal. Today 130 (2008) 265-536.

[27] M. Houalla. N.K. Nag, A.V. Sapre, D.H. Broderick, B.C. Gates, AlChE J. 24 (1978) 1015.

[28] M.J. Girgis, B.C. Gates, Ind. Eng. Chem. Res. 30 (1991) 2021.

[29] X. Ma, K. Sakanishi, I. Mochida, Ind. Eng. Chem. Res. 33 (1994) 218.

[30] B.C. Gates, H. Topsøe, Polyhedron 16 (1997) 3213.

[31] T. Kabe, A. Ishihara, H. Tajima, Ind. Eng. Chem. Res. 31 (1992) 1577.

[32] .S. Shih, S. Mizrahi, L.A. Green, M.S. Sarli, Ind. Eng. Chem. Res. 31 (1992) 1232.

[33] P. Michaud, J.L. Lemberton, G. Pérot, Appl. Catal. A 169 (1998) 343.

[34] S.K. Bej, S.K. Maity, U.T. Turaga, Energy & Fuels 18 (2004) 1227.

[35] M. Houalla, D.H. Broderick, A.V. Sapre, N.K. Nag, V.H. de Beer, B.C. Gates, H. Kwart, J. Catal. 61 (1980) 523.

[36] N. Hermann, M. Brorson, H. Topsøe, Catal. Lett. 65 (2000) 169.

[37] J.M.J.G. Lipsch, G.C.A. Schuit, J. Catal. 15 (1969) 179.

[38] R.A. Sanchez-Delgado, J. Mol. Catal. 86 (1994) 287.

[39] T.S. Smit, K.H. Johnson, Chem. Phys. Lett. 212 (1993) 525.

[40] A. Iretskii, J.J. García, G. Picazo, P.M. Maitlis, Catal. Lett. 51 (1998) 129.

[41] C. Moreau, J. Joffre, C. Saenz, J.C. Alfonso, J.-L. Portefaix, J. Mol. Catal. A: Chem. 161 (2000) 141.

[42] S. Cristol, J.-F. Paul, E. Payen, D. Bougeard, F. Hutschka, S. Clémendot, J. Catal. 224 (2004) 138.

[43] R. Prins, M. Egorova, A. Röthlisberger, Y. Zhao, N. Sivasankar, P. Kukula, Catal. Today 111 (2006) 84.

[44] O. Weisser, S. Landa, Sulphide Catalysts. Their Properties and Applications, Pergamon Press, Oxford, 1973.

[45] M. Zdražil, Appl. Catal. 4 (1982) 107.

[46] G.H. Singhal, R.L. Espino, J.E. Sobel, J. Catal. 67 (1981) 446.

[47] J. Mijoin, G. Pérot, F. Bataille, J.L. Lemberton, M. Breysse, S. Kasztelan, Catal. Lett. 71 (2001) 139.

[48] H. Wang, R. Prins, Appl. Catal. A: Gen. 350 (2008) 191.

[49] J. Joffre, P. Geneste, D.A. Lerner, J. Catal. 97 (1986) 543.

[50] A.J. Gellman, M.H. Farias, M. Salmeron, G.A. Somorjai, Surf. Sci. 136 (1984) 217.

[51] H. Yang, C. Fairbridge, Z. Ring, Energy Fuels 17 (2003) 387.

[52] M. Zdražil, J. Sedlaciek, Collect. Czech. Chem. Commun. 42 (1977) 3133.

[53] M. Neurock, R.A. van Santen, J. Am. Chem. Soc. 116 (1994) 4427.

[54] P. Raybaud, J. Hafner, S. Kresse, H. Toulhoat, Phys. Rev. Lett. 80 (1998) 1481.

[55] N.K. Nag, Appl. Catal. 10 (1984) 53.

[56] H. Kwart, G.C.A. Schuit, B.C. Gates, J. Catal. 61 (1980) 128.

[57] S.K. Bej, S.K. Maity, U.T. Turaga, Energy & Fuels 18 (2004) 1227.

[58] D.R. Kilanowski, H. Teeuwen, V.H.J. de Beer, B.C. Gates, G.C.A. Schuit, H. Kwart, J. Catal. 65 (1978) 129.

[59] V. Lamure-Meille, E. Schulz, M. Lemaire, M. Vrinat, Appl. Catal. A 131 (1995) 143.

[60] T. Kabe, A. Ishihara, Q. Zhang, Appl. Catal. A: Gen. 97 (1993) L1.

[61] V. Meille, E. Schulz, M. Lemaire, M. Vrinat, J. Catal. 170 (1997) 29.

[62] H. Kim, J.J. Lee, J.H. Koh, S.H. Moon. Appl. Catal. B: Env. 50 (2004) 17.

[63] G. Pérot, Catal. Today 86 (2003) 111.

[64] P. Michaud, J.L. Lemberton, G. Pérot, Appl. Catal. A: Gen. 169 (1998) 343.

[65] M. Breysse, G. Djega-Mariadassou, S. Pessayre, C. Geantet, M. Vrinat, G. Pérot, M. Lemaire, Catal. Today 84 (2003) 129.

[66] F. Richard, T. Boita, G. Pérot, Appl. Catal. A: Gen. 320 (2007) 69.

[67] P. Torres-Mancera, J. Ramírez, R. Cuevas, A. Gutiérrez-Alejandre, F. Murrieta, R. Luna, Catal. Today 107-108 (2005) 551.

[68] T. Klimova, J. Reyes, O. Gutiérrez, L. Lizama, Appl. Catal. A: Gen. 335 (2008) 159.

[69] C. Leyva, M.S. Rana, F. Trejo, J. Ancheyta, Catal. Today 141 (2009) 168.

[70] Y. Ogawa, M. Toba, Y. Yoshimura, Appl. Catal. A: Gen. 246 (2003) 213.

[71] W. Ripperger, W. Saum, J. Less-Common Met. 54 (1977) 353.

[72] M.V. Landau, D. Berger, M. Herskowitz, J. Catal. 159 (1996) 236.

[73] M. Egorova, R. Prins, J. Catal. 225 (2004) 417.

[74] F. Bataille, J.L. Lemberton, P. Michaud, G. Pérot, M. Vrinat, M. Lemaire, E. Schulz, M. Breysse, S. Kasztelan, J. Catal. 191 (2000) 409.

[75] T.A. Pecoraro, R.R. Chianelli, J. Catal. 67 (1981) 430.

[76] R.R. Chianelli, G. Berhault, P. Raybaud, S. Kasztelan, J. Hafner, H. Toulhoat, Appl. Catal. A: Gen. 227 (2002) 83.

[77] H. Toulhoat, P. Raybaud, S. Kasztelan, G. Kresse, J. Hafner, Catal. Today 50 (1999) 629.

[78] E. Dhainaut, H. Charcosset, C. Cachet, L. de Mourgues, Appl. Catal. 2 (1982) 75.

[79] A. Niquille-Röthlisberger, R. Prins, J. Catal. 242 (2006) 207.

[80] P. Grange, X. Vanhaeren, Catal. Today 36 (1997) 375.

[81] Z. Vít, J. Cinibulk, D. Gulková, Appl. Catal. A: Gen. 272 (2004) 99.

[82] Z. Vít, D. Gulková, L. Kaluža, M. Zdražil, J. Catal. 232 (2005) 447.

[83] M.H. Pinzón, L.I. Meriño, A. Centeno, S.A. Giraldo, en: B. Delmon, G.F. Froment, P. Grange (Eds), Stud. Surf. Sci. Catal. 127 (1999) 97.

[84] M. Vergara, S.A. Giraldo, A. Centeno, ION 16 (2000) 63.

[85] B. Pawelec, R. Navarro, J.L.G. Fierro, J.F. Cambra, F. Zugazaga, M.B. Güemez, P.L. Arias, Fuel 76 (1997) 61.

[86] M.H. Pinzón, A. Centeno, S.A. Giraldo, Appl. Catal. A: Gen. 302 (2006) 118.

[87] S. Pessayre, C. Geantet, R. Bacaud, M. Vrinat, T.S. N'Guyen, T. Soldo, J.L. Aceman, M. Breysse, Ind. Eng. Chem. Res. 46 (2007) 3877.

[88] D. Pérez-Martínez, S.A. Giraldo, A. Centeno, Appl. Catal. A: Gen. 315 (2006) 35.

[89] B. Pawelec, A.M. Venezia, V. La Parola, E. Cano-Serrano, J.M. Campos-Martin, J.L.G. Fierro, Appl. Surf. Sci. 242 (2005) 380.

[90] B. Pawelec, V. La Parola, S. Thomas, J.L.G. Fierro, J. Mol. Catal. A: Chem. 253 (2006) 30.

[91] H. Du, C. Fairbridge, H. Yang, Z. Ring, Appl. Catal. A: Gen. 294 (2005) 1.

[92] T.-B. Lin, C.-A. Jan, J.-R. Chan, Ind. Eng. Chem. Res. 34 (1995) 4284.

[93] H.R. Reinhoudt, R. Troost, A.D. van Langeveld, S.T. Sie, J.A.R. van Veen, J.A Moulijn, Fuel Proc. Tech. 61 (1999) 133.

[94] L. Le Bihan, Y. Yoshimura, Fuel 81 (2002) 491.

[95] V.L. Barrio, P.L. Arias, J.F. Cambra, M.B. Güemez, B. Pawelec, J.L.G. Fierro, Fuel 82 (2003) 501.

[96] E.W. Qian, K. Otani, L. Li, A. Ishihara, T. Kabe, J. Catal. 221 (2004) 294.

[97] A. Ishihara, F. Dumeignil, J. Lee, K. Mitsuhashi, E.W. Qian, T. Kabe, Appl. Catal. A: Gen. 289 (2005) 163.

[98] K.K. Bando, T. Kawai, K. Asakura, T. Matsui, L. Le Bihan, H. Yasuda, Y. Yoshimura, S.T. Oyama, Catal. Today 111 (2006) 199.

[99] W. Qian, Y. Yoda, Y. Hirai, A. Ishihara, T. Kabe, Appl. Catal. A: Gen. 184 (1999) 81.

[100] S. Albertazzi, G. Busca, E. Finocchio, R. Glöckler, A. Vaccari, J. Catal. 223 (2004) 372.

[101] A. Röthlisberger, R. Prins, J. Catal. 235 (2005) 229.

[102] Y. Okamoto, M. Breysse, G.M. Dhar, C. Song, Catal Today 86 (2003) 1.

[103] I. Babich, J. Moulijn, Fuel 82 (2003) 607.

[104] P. Baeza, M. Ureta-Zañartu, N. Escalona, J. Ojeda, F. Gil-Llambías, B. Delmon, Appl. Catal. A: Gen. 274 (2004) 303.

[105] J. Choi, F. Maugé, C. Pichon, J. Olivier-Fourcade, J.C. Jumas, C. Petit-Clair, D. Uzio, Appl. Catal. A: Gen. 267 (2004) 203.

[106] A. Venecia, F. Raimondi, V. La Parola, G. Deganello, J. Catal. 194 (2000) 393.

[107] V. La Parola, G. Deganello, A. Venecia, Appl. Catal. A: Gen. 260 (2004) 237.

[108] D. Mey, S. Brunet, C. Canaff, F. Maugé, C. Bouchy, F. Diehl, J. Catal. 227 (2004) 436.

[109] M. Breysse, P. Afanasiev, C. Geantet, M. Vrinat, Catal. Today 86 (2003) 5.

[110] C.-E. Hédoire, C. Louis, A. Davidson, M. Breysse, F. Maugé, M. Vrinat, J. Catal. 220 (2003) 433.

[111] H. Topsøe, B. Hinnemann, J.K. Nørskov, J.V. Lauritsen, F. Besenbacher, P.L. Hansen, G. Hytoft, R.G. Egeberg, K.G. Knudsen, Catal. Today 107-108 (2005) 12.

[112] H. Guo, Y. Sun, R. Prins, Catal. Today 130 (2008) 249.

[113] T. Isoda, Y. Takase, K. Kusakabe, S. Morooka, Energy & Fuels 14 (2000) 585.

[114] C. Song, K.M. Reddy, Appl. Catal. A: Gen. 176 (1999) 1.

[115] T. Klimova, M. Calderon, J. Ramirez, Appl. Catal. A: Gen. 240 (2003) 29.

[116] E. Lecrenay, K. Sakanishi, I. Mochida, T. Suzuka, Appl. Catal. A: Gen. 175 (1998) 237.

[117] X. Li, A. Wang, Z. Sun, C. Li, J. Ren, B. Zhao, Y. Wang, Y. Chen, Y. Hu, Appl. Catal. A: Gen. 254 (2003) 319.

[118] M.A. Ali, T. Tatsumi, T. Masuda, Appl. Catal. A: Gen. 233 (2002) 77.

[119] W. Robinson, J. van Veen, V. de Beer, R. van Santen, Fuel. Process. Technol. 61 (1999)103.

[120] D. Eliche-Quesada, E. Rodríguez-Castellón, A. Jiménez-López, Micropor. Mesopor. Mater. 99 (2007) 268.

[121] A. Corma, A. Martínez, V. Martínez-Soria, J. Catal. 169 (1997) 487.

[122] A. Wang, Y. Wang, T. Kabe, Y. Chen, A. Ishihara, W. Qian, J. Catal. 199 (2001) 19.

[123] C.-M. Wang, T.-C. Tsai, I. Wanga, J. Catal. 262 (2009) 206.

[124] L.E. González, K. Rojas, Undergraduate work, Escuela de Ingeniería Química, Centro de Investigaciones en Catálisis, Universidad Industrial de Santander, Bucaramanga (2008).

[125] M.A. Beltrán, W.R. Sarmiento, Undergraduate work, Escuela de Ingeniería Química, Centro de Investigaciones en Catálisis, Universidad Industrial de Santander, Bucaramanga (2008).

[126] A. Estupiñán, Master Thesis, Escuela de Ingeniería Química, Centro de Investigaciones en Catálisis, Universidad Industrial de Santander, Bucaramanga (2008).

An analysis of the selectivity of MoS$_2$ based catalytic systems to the hydrogenation route of hydrodesulfurization

1. Introduction

Classical MoS$_2$ based catalytic systems for hydrotreatment (HDT) reactions are among the most intensively studied materials in catalysis science. There are plenty of reviews dedicated to analyze the nature and functioning of their active phase [1-15]. Nowadays, some studies have indicated that Ni-MoS$_2$/γ-Al$_2$O$_3$ catalysts, which have a higher hydrogenating capacity as compared to Co-MoS$_2$/γ-Al$_2$O$_3$ [16-20], are more selective to the HYD route of di-β-DBTs. Nevertheless, other authors [21-23] present evidence that the addition of Ni and in particular of Co as promoters of monometallic MoS$_2$/γ-Al$_2$O$_3$ mostly enhances the conversion of DBTs via the direct route of hydrodesulfurization (DDS). Alternatively, the promotion of HDT catalysts with low amounts of Pt results in a strong synergy effect [24-30], but the selectivity of the Pt-Mo catalytic system to the hydrogenation route of hydrodesulfurization (HYD) in the HDS of dibenzothiophenes has only been started to be analyzed very recently [24, 31, 32]. In this regard, it could be preliminary expected that the addition of the highly hydrogenating Pt to Mo based systems would enhance HYD selectivity.

On the other hand, it has been recognized that the acidic characteristics of the carrier play a key role in the hydrodesulfurization of di-β-DBTs [16-18, 33-39] and can improve selectivity to HYD [33, 39, 40]. However, the relationship between acidity and the selectivity HYD to DDS is not fully understood yet. A simple and economic way to increase the acidity of the alumina support of conventional HDT catalysts consists in the preparation mixed γ-Al$_2$O$_3$-B$_2$O$_3$ type oxides by boron impregnation [37, 41-51]. But, some contradiction in regard to the effect of boron in HDS can be noticed in literature, which is most likely due to differences in the reaction conditions used in each one of these studies [43-51].

26

As a first approach to the design of a catalytic material able to develop the HYD route of desulfurization of the non-sterically hindered DBT molecule, in this section, an analysis of the potentiality of promoted MoS_2 based catalytic systems for this task is presented along with an analysis of their hydrogenation function. For this purpose, Mo/γ-Al_2O_3 catalysts were promoted with Co, Ni and Pt and tested in the hydrogenation of NP and the hydrodesulfurization of DBT at different reaction conditions. Afterwards, the effect of boron as a modifier of the acid properties of the γ-Al_2O_3 carrier in the hydrogenating function of Ni and Pt promoted Mo/γ-Al_2O_3 was analyzed.

2. Experimental

2.1. Preparation of catalysts

The supported Co-Mo, Ni-Mo and Pt-Mo catalysts were prepared by sequential wetness impregnation. Mo, from an aqueous solution of the ammonium heptamolybdate tetrahydrated $((NH_4)_6Mo_7O_{24}.4H_2O$, Merck) precursor, was impregnated first for bimetallic Co-Mo and Ni-Mo, whereas for Pt-Mo it was impregnated after Pt. More details on the preparation of these materials can be found in previous works [25, 26, 52, 53]. The metallic contents of the conventional Co-Mo and Ni-Mo catalysts were: 2wt.% CoO - 10wt.% MoO_3, and 4.5wt.% NiO - 9wt.%MoO_3, respectively. These two catalysts were simply designated as CoMo and NiMo. In the case of the Pt promoted Mo/γ-Al_2O_3 catalysts the nominal contents of Pt and MoO_3 were: 0.5, 1 and 2 wt.% Pt and 2, 8 and 15 wt.% MoO_3, These bimetallic catalysts were labeled according to their nominal Pt and MoO_3 contents as follows: Pt(0.5)Mo(2), Pt(1)Mo(2), Pt(0.5)Mo(8), Pt(0.5)Mo(15), and Pt(2)Mo(15); the nominal metallic contents are indicated in parentheses. On the other hand, the modification of the alumina support by boron addition was performed by impregnation of an aqueous solution of H_3BO_3 (Merck), with the required concentration as to obtain the corresponding nominal contents of B_2O_3 in the support, followed by the sequential impregnation of the metallic precursors. The effect of

boron was studied for the Ni-Mo and Pt-Mo catalysts. For the Ni-Mo/γ-Al$_2$O$_3$-B$_2$O$_3$ catalysts, B$_2$O$_3$ contents were: 0, 2, 3, 6 and 8 wt.%. In the case of the Pt-Mo catalysts, B$_2$O$_3$ contents were: 2, 4 and 6 t.%. The index -B(x) was added to catalysts labels to indicate their B$_2$O$_3$ nominal content.

2.2. Catalysts activation

A standard activation procedure was carried out *in situ* before the catalytic tests. First, drying of the calcined catalysts (0.5 g) at 393 K under N$_2$ (Oxígenos de Colombia, 99.995%) flow (100 mL/min) for 1 h was done, followed by sulfidation with a H$_2$S (15 vol. %) – (Aga-fano, 99.5%) in H$_2$ (Oxígenos de Colombia, 99.995%) gaseous mixture, at 673 K and atmospheric pressure, during 3 h. The activation mixture flow (100 mL/min) was kept until reaching reaction temperature and beginning the pressurization of the reaction system with H$_2$. Further details of the experimental set-up have been reported before [54, 55].

2.3. Characterization of the catalysts

2.3.1. Textural properties

BET surface area (S$_{BET}$), pore volume (V$_P$) and average pore diameter (D$_P$), as determined by the BJH method, were measured by the conventional nitrogen (Aga-fano, 99.999%) adsorption-desorption technique in a NOVA 1200 (Quantachrome) apparatus. Before the analysis, the samples of the catalysts (c.a. 0.2 g) were outgassed in vacuum (1x10^{-3} mmHg, T = 363 K) overnight.

2.3.2. Total acidity

NH$_3$ TPD analysis was used to determine total acidity of the catalysts. A Chembet 3000 (Quantachrome) apparatus was used. Previous to each test, catalyst activation was performed at the same conditions as mentioned in section 2.2. Sulfidation of the samples, at the conditions mentioned in Section 2.2. was followed by N$_2$ evacuation (15 min) at 373 K. NH$_3$ was adsorbed at this temperature by flowing it during 15 min. Once the adsorption step was

completed He evacuation of the system was carried out for 2 h. NH_3 TPD was performed by heating the sample (at 10 K/min) until 773 K under N_2 flow and then collecting desorbed ammonia in a 0.4 vol.% H_3BO_3 solution. The amount of desorbed NH_3 (μeq NH_3/g cat.) was calculated by titration of the NH_3-H_3BO_3 solution with a 0.01N standard aqueous solution of H_2SO_4. Specific acidity (μeq NH_3/m^2) was calculated from the ratio: total acidity to BET surface area.

2.4. Catalytic tests

Catalytic tests were performed in a continuous high-pressure fixed-flow reactor system comprehensively described in previous works [52-54, 56-58]. The volume of the catalytic bed was c.a. 2 mL and it was composed of 0.5 g of catalyst diluted in borosilicate glass-beads. Three types of catalytic tests were performed: (i) NP hydrogenation under an H_2S atmosphere, (ii) dibenzothiophene HDS, and (iii) simultaneous DBT hydrodesulfurization and NP hydrogenation. The composition of the liquid feed was 3 wt.% of naphthalene and/or 2 wt.% dibenzothiophene, as model molecules representing typical components of a standard diesel oil, 2 wt.% of hexadecane, as GC internal standard, all of them diluted in cyclohexane. To generate the H_2S atmosphere during the hydrogenation of NP, dimethyldisulfide was added to the liquid feed in such a concentration as to obtain 4074 wppm of H_2S (which corresponds to the H_2S concentration obtained at a molar conversion of c.a. 60% of dibenzothiophene). Standard reaction conditions were P = 5 MPa, hydrogen flow = 15 LN/h, liquid feed flow = 30 mL/h and a H_2/(liquid feed) ratio = 500 NL/L. At these conditions, the absence of any diffusion limitations had been verified [52, 53, 57]. Temperature for the catalytic test (i) was 563 K. For test (ii), temperature was varied between 563 - 603 K, whereas test (iii) was performed at 583 K. For the sake of clarity, Table 1 provides a summary of the catalysts' codes used along with the reaction temperature used in the different catalytic tests.

Table 1. Summary of the prepared catalysts and temperature of the different reaction tests carried out.

Catalyst code†	x = B_2O_3 wt.%	Temperature (K)	Reaction
NiMo	----		
NiMo-B(x)	2		
	3		
	6	563	(i) Naphthalene hydrogenation under an H_2S environment
	8		
Pt(0.5)Mo(2)	----		
Pt(0.5)Mo(2)-B(x)	2		
	4		
	6		
CoMo	----	573	
NiMo	----	563	
NiMo-B(x)	2	583	
	3		
	6	543, 563 and 583	(ii) Dibenzothiophene hydrodesulfurization
	8	583	
Pt(0.5)Mo(2)	----	563, 583 and 603	
Pt(0.5)Mo(15)	----		
Pt(2)Mo(15)			
Pt(0.5)Mo(2)-B(x)		583	
Pt(1)Mo(2)-B(x)	4		
Pt(0.5)Mo(15)-B(x)			
NiMo-B(x)	8		(iii) Simultaneous dibenzothiophene hydrodesulfurization - naphthalene hydrogenation
Pt(0.5)Mo(2)		583	
Pt(0.5)Mo(8)	----		
Pt(0.5)Mo(15)			

†Nominal metallic contents are indicated in parentheses.

Reaction products were identified using an HP 6890 GC, provided with an FID detector and a HP-1 (100 m x 0.25 mm x 0.5 μm) column. All catalytic tests were conducted until steady state (aprox. 5 h). The catalytic activity was expressed as the total reactant conversion (%C):

$$\%C_i = 100 \times \frac{(n_0^i - n_f^i)}{n_0^i} \qquad \text{(Eq. 1)}$$

Where: i = naphthalene or dibenzothiophene; n_0 = initial moles of reactant; and, n_f = final moles of reactant.

The yield (*%y*) of the different reaction products was defined according to IUPAC recommendations [59]:

$$\% y_j = 100 \times \frac{n_j}{n_0^i} \qquad \text{(Eq. 2)}$$

Where: j = reaction product.

The selectivity to the HYD route of hydrodesulfurization (S_{HYD}) was calculated from the ratio:

$$S_{HYD} = \frac{(\%C_{DBT} - \% y_{BP})}{\% y_{BP}} \qquad \text{(Eq. 3)}$$

BP = biphenyl, the product from the direct route of desulfurization.

In the simultaneous reaction, the selectivity to convert dibenzothiophene was defined as:

$$S_{DBT} = \frac{\%C_{DBT}}{\%C_{NP}} \qquad \text{(Eq. 4)}$$

The experimental error in the mass balance of the reaction system, as from the chromatography analysis, and the reproducibility of the catalytic tests was found to be between 10-15 %.

3. Results and discussion

3.1. Preliminary experiments: influence of the reaction temperature on the HYD selectivity over NiMo and PtMo catalysts

The influence of the reaction temperature in the activity and particularly in the selectivity to HYD of these two selected catalysts: NiMo-B(6) and Pt(0.5)Mo(2) was studied. Table 2 shows the obtained results.

Table 2. Effect of temperature on the activity (%C_{DBT}) and HYD selectivity (S_{HYD}) in the hydrodesulfurization of dibenzothiophene over NiMo-B(6) and Pt(0.5)Mo(2) catalysts. N.D. = not determinated.

Catalyst	Temperature (K)							
	543		563		583		603	
	%C_{DBT}	S_{HYD}	%C_{DBT}	S_{HYD}	%C_{DBT}	S_{HYD}	%C_{DBT}	S_{HYD}
NiMo-B(6)[a]	27.4	0.28	54.4	0.34	84.7	0.40	N.D.	N.D.
Pt(0.5)Mo(2)[b]	N.D.	N.D.	35.4	0.01	49.2	0.01	70.8	0.02

Other reaction conditions are: P = 5 MPa; Liquid feed flow = 30 mL/h; (H_2/liquid feed) ratio = 500 LN/L.
[a]Data taken from L.E. González and K. Rojas [60].
[b]Data taken from M.A. Beltrán and W.R. Sarmiento [61].

The conversion of dibenzothiophene increases with reaction temperature as it has been determined in previous literature works [4, 17, 20]. The selectivity to HYD of both catalysts increases very slightly with reaction temperature, indicating that, at the conditions of the present study, the development of the HYD route of hydrodesulfurization over the promoted alumina supported MoS_2 catalysts is inherently linked to the intrinsic functionalities of these materials; which agrees with the absence of thermodynamic limitations in hydrogenation (T > 623 K) [20].

3.2. Evaluation of the development of the HYD route of hydrodesulfurization of dibenzothiophene over MoS_2/γ-Al_2O_3 based catalytic systems.

This section is divided into two main parts which discuss the role of the precursor, Co, Ni and Pt, of the MoS_2/γ-Al_2O_3 catalysts in the development of the HYD route of hydrodesulfurization of dibenzothiophene, and the influence of the modification of the acid properties of the bimetallic catalysts in HYD.

The reaction products detected in the HDS of dibenzothiophene were BP and cyclohexylbenzene (CHB) and non quantitative traces of the partially hydrogenated tetrahydro(TH)-dibenzothiophene intermediate. Tetralin and traces of decalins were detected in the hydrogenation of NP.

3.2.1. Influence of the promoter on the selectivity to HYD of MoS$_2$/γ-Al$_2$O$_3$ based catalysts.

Table 3 shows the steady state results obtained in the HDS of dibenzothiophene for CoMo, NiMo and Pt-Mo catalysts. The reaction temperature for conventional CoMo and NiMo was adjusted as to compare their selectivity to HYD at dibenzothiophene iso-conversion. Reaction temperature for Pt-Mo catalysts was kept constant at 583 K. It can be seen in Table 3 that though NiMo is more active that CoMo in the HDS reaction, both catalysts do not display a significant difference in the HYD selectivity. This result is in agreement with reports ascribing the difference in HYD selectivity of Ni(Co)-MoS$_2$ to an effect of the H$_2$S partial pressure on the nature of the active sites of these catalytic systems [7, 23, 34, 62-66]. Wang and Prins [66] studied the HDS of dibenzothiophene over Mo/γ-Al$_2$O$_3$ and found that an increase in the H$_2$S partial pressure inhibits the conversion of the molecule to both desulfurized reaction products: biphenyl, from DDS, and cyclohexylbenzene, from HYD, respectively, but the conversion to partially hydrogenated intermediates of HYD only changed slightly. Farag [65] observed that the H$_2$S partial pressure can significantly modify the selectivity in the HDS of dibenzothiophene over nanosize MoS$_2$ catalysts, but did not have a strong effect on the selectivity over Co-Mo/γ-Al$_2$O$_3$. Therefore, within the scope of the presented results, both conventional γ-Al$_2$O$_3$ supported Ni- and Co-MoS$_2$ catalysts poorly develop HYD when working under a similar H$_2$S partial pressure. On the other hand, the role of Pt in bimetallic Pt-Mo/γ-Al$_2$O$_3$ catalysts for HDT reactions has been studied in literature [24-32]. Some studies have experimentally showed the simultaneous presence of metallic Pt, PtS$_x$ and MoS$_2$ species on the surface of sulfided Pt-Mo/γ-Al$_2$O$_3$ [67, 68]. Results from CICAT-UIS [29, 32, 58, 69, 70] have provided evidence of a double role of Pt in Pt-Mo catalysts in HDT reactions; Pt is a promoter of the sulfided Mo active phase and also possesses its own active sites for hydrotreatment. Therefore, such a mixture of metallic Pt particles-sulfided PtS$_x$ species and sulfided Mo can completely work either independently or

simultaneously independently and "cooperatively". However, as the present results indicate, though Pt can be performing such double role, and is a very active catalyst in aromatics hydrogenation, its presence in the bimetallic system does not particularly promote selectivity to HYD.

In conclusion, the analysis of the results presented here show that neither Co, Ni nor Pt promoted $MoS_2/\gamma-Al_2O_3$ catalysts are able to efficiently develop the HYD route of hydrodesulfurization of dibenzothiophene.

Table 3. Average steady state conversion (%C_{DBT}), products distribution (%y) and selectivity to HYD (S_{HYD}) in the hydrodesulfurization of dibenzothiophene CoMo, NiMo and PtMo catalysts.

Catalyst	%C_{DBT}	%y_{BP}	%y_{CHB}	S_{HYD}
CoMo[a]	75.4	69.4	6.0	0.09
NiMo[b]	78.0	70.9	7.1	0.10
Pt(0.5)Mo(2)[c,†]	49.2	48.4	0.8	0.02
Pt(0.5)Mo(15)[c,†]	41.0	36.0	5.0	0.14
Pt(2)Mo(15)[c,†]	49.5	42.3	7.2	0.17

[a]Reaction temperature = 573 K; [b]T = 563 K and [c]T = 583 K.
[†]Data taken from M.A. Beltrán and W.R. Sarmiento [61].

3.2.2. Influence of the boron modification of the acid properties of the $\gamma-Al_2O_3$ support on the hydrogenation function of Ni and Pt promoted Mo catalysts.

To investigate the effect of the acid properties of the support on the hydrogenation function of the boron modified Ni-Mo and Pt-Mo catalysts, the results from naphthalene hydrogenation reactions (test (i)) and dibenzothiophene hydrodesulfurization (test (ii)) were correlated with the total acidity of the materials as measured in the NH_3 TPD experiments. In first place, Table 4 presents the textural properties and the acidity of NiMo-B(x) and the textural properties of some selected PtMo-B(x) catalysts. Concerning the textural properties of the catalysts, the results of the textural characterization show that the effect of boron on the catalysts' surface area (S_{BET}) depends on the boron concentration, without causing significant changes in the porous structure (V_p and D_p). For the group of Ni-Mo catalysts, it is observed that for those catalysts containing a B_2O_3 wt.% up to 3 there is an increase in S_{BET}, while for

those with higher B_2O_3 wt.% contents S_{BET} decreases, as compared to NiMo. The S_{BET} of the PtMo-B(x) catalysts confirm that for a B_2O_3 wt.% higher than 3, S_{BET} decreases. Usman et al. [42] showed that at low boron concentration, B_2O_3 is well dispersed on the alumina support without significantly changing its textural properties. Torres-Mancera et al. [37] ascribed the effect of boron on the support's textural properties to a partial dissolution of alumina during H_3BO_3 impregnation. On the other hand, the acidity measurement performed for the group of NiMo-B(x) catalysts, shows that both total and specific acidity monotonously increase with the B_2O_3 wt.%. This behavior agrees with previous literature reports [37, 41-51] that show that such acidity increase is due to a change in the balance of Lewis and Brønsted acidic sites of the γ-Al_2O_3 carrier which is a function of boron concentration. It has been observed that the amount of Lewis acidic sites slightly increase at B_2O_3 concentrations up to 3 wt.%, but such Lewis sites tend to decrease and disappear at B_2O_3 concentrations higher than 5 wt.% [41, 43]. Sibeijn et al. [41] examined the changes in the distribution of the basic, neutral and acidic Al-OH hydroxyl groups of γ-Al_2O_3 due to the incorporation of rhenium and boron by infrared analysis of pyridine adsorption. They determined that whereas the noble metal is essentially deposited onto the Lewis (Al^{3+}) sites of γ-Al_2O_3, new B-OH groups are formed on the surface of the boron modified support. As the number of these B-OH groups increases with boron concentration at the expense of a consumption of Al-OH hydroxyls, they concluded that boron is deposited to Al-OH hydroxyls and not to Lewis Al^{3+} sites. The authors also proposed that boron species thus deposited onto γ-Al_2O_3 tend to polymerize once they saturate the Al-OH groups. This tendency causes lessening of the textural properties of the materials at high boron concentrations. The relationship between the chemical nature of the boron species present on the surface of γ-Al_2O_3-B_2O_3 mixed oxides and the modification of the acid balance of these materials was established by a combination of ^{11}B magic angle spinning (MAS) Nuclear Magnetic Resonance (NMR) and TPD of adsorbed pyridines characterization

performed by Sato et al. [52]. Their results indicate that the amount and strength of Brønsted acidic sites of such materials is related to the presence of BO_4 species; which increase with the load of boron. The NH_3 TPD results presented in Table 4 for NiMo-B(x) concord with the acidity increase of the γ-Al_2O_3-B_2O_3 carriers with boron load, and they also reproduce the results reported by other authors for the acidity of Co(Ni)-MoS_2/γ-Al_2O_3-B_2O_3 catalysts [43, 47, 51].

Table 4. Textural properties and acidity of NiMo-B(x) and some selected PtMo-B(x) catalysts.

Catalyst	S_{BET} (m^2/g)	V_p (cm^3/g)	D_p (nm)	Total acidity $(\mu eqNH_3/g\ cat.)$	Specific acidity $(\mu eqNH_3/m^2)$
γ-Al_2O_3	220	0.62	11.6	N.D.	N.D.
NiMo[a]	185	0.50	10.8	329	1.78
NiMo-B(2)[a]	205	0.51	11.2	389	1.90
NiMo-B(3)[a]	191	0.46	10.9	397	2.08
NiMo-B(6)[a]	166	0.43	11.1	465	2.80
NiMo-B(8)[a]	126	0.37	11.3	576	4.57
Pt(0.5)Mo(2)[b]	212	0.55	11.3	N.D.	N.D.
Pt(0.5)Mo(2)-B(4)[b]	209	0.55	10.6	N.D.	N.D.
Pt(0.5)Mo(2)-B(6)[b]	196	0.53	10.9	N.D.	N.D.

[a]Data taken from L.E. González and K. Rojas [60].
[b]Data taken from M.A. Beltrán and W.R. Sarmiento [61].

Considering the aspects discussed above and on the grounds of the literature [41, 43-45] a qualitative description of the changes in the acid balance of NiMo-B(x) as a function of the boron concentration can be hypothesized: two main zones of distribution of acidic sites can be present on the catalysts: at low B_2O_3 concentrations there is an equilibrium between the number of Brønsted and Lewis acidic sites, and at higher boron concentrations, Lewis acidic sites tend to disappear and then mostly Brønsted sites are present on the catalyst's surface. Such Brønsted sites would possess an intermediate acidic strength which is increased with the amount of BO_4 species.

We will now proceed to correlate the results obtained in the catalytic tests (i) and (ii) with the acidity for NiMo-B(x) as a function of the B_2O_3 content. Fig. 5 shows the steady state %C_{DBT},

products distribution ($\%y_{BP}$ and $\%y_{CHB}$) and specific acidity of NiMo-B(x) as a function of the B_2O_3 wt.%. As observed, boron addition at low concentrations does not significantly impact DBT conversion, but, at higher boron concentration HDS activity decreases. Other authors have reported similar trends [45, 49]. It is interesting to analyze the changes in reaction products distribution during DBT hydrodesulfurization as presented in Fig. 5. Biphenyl and cyclohexylbenzene were almost the only detected products. Partially hydrogenated TH-dibenzothiophene and hexahydro(HH)-dibenzothiophene intermediates were detected only as traces. The fact that at practically total conversion of DBT the $\%y_{CHB}$ is lower than that obtained at lower $\%C_{DBT}$ shows that biphenyl is not being further hydrogenated to cyclohexylbenzene. This is in agreement with the results presented by Orozco et al. [71]. Moreover, as previously discussed, but now considering that there are certain differences on the conversion of DBT, possible H_2S partial pressure effect in products distribution can also in this case ruled out because: first, at the range of $\%C_{DBT}$ observed, the change in the H_2S partial pressure is not as high as to induce such effects; and second, the registered trend in the $\%y_{BP}$ and $\%y_{CHB}$ with the increase in $\%C_{DBT}$ is opposite to the experimental results reported in literature, where, it would be expected that the higher the H_2S partial pressure the lower the $\%y_{BP}$ and the higher the $\%y_{CHB}$ or of TH-dibenzothiophene. Therefore, it can be assumed that the present catalytic trends are mainly due to the modification of the chemical properties of NiMo provoked by boron. It is observed that boron incorporation has a remarkably negative effect in the development of DDS. Conversely, the $\%y_{CHB}$, thus HYD selectivity, increases to some extent. This behavior has been reported for boron modified Co-Mo/Al_2O_3 catalysts [45, 49].
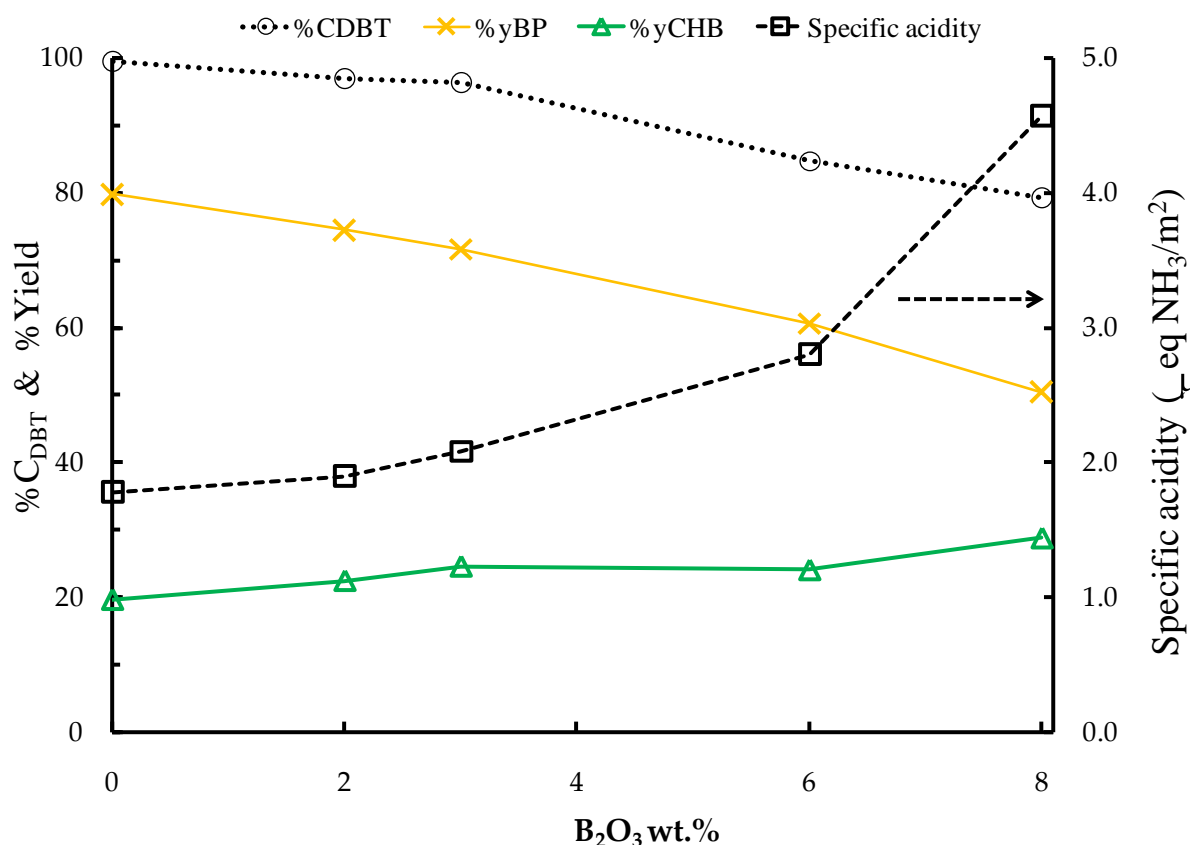
Fig. 5. Steady state performance and specific acidity of NiMo-B(x) catalysts during dibenzothiophene HDS as a function of the B_2O_3 wt.%.
Reaction conditions: T = 583 K, P = 5 MPa, liquid feed flow 30 mL/h, H_2/liquid feed ratio = 500 NL/L.
*Data taken from L.E. González and K. Rojas [60].

Dumeignil et al. [45] observed that the increase in the B/Al of sol-gel prepared Co-Mo/Al_2O_3-Al_2O_3 catalysts lowered the conversion of dibenzothiophene via DDS and slightly favored the yields to HYD reaction products; CHB and TH-dibenzothiophene. From the correlation between the catalytic behavior in dibenzothiophene hydrodesulfurization and specific acidity presented in Fig. 5, for the NiMo-B(x) series, it is not possible to reach a clear conclusion regarding the specific influence of acidity on the development of HYD. The change in the DDS/HYD selectivity can be also due to the changes in the structure of the active phase of the NiMo catalysts. Other authors have established that the dispersion and the structure of the active phase of Al_2O_3-B_2O_3 supported HDT catalysts is affected by the B_2O_3 concentration due to changes induced by the conformation of the BO_4 in the alumina surface [42, 45, 47-49]. The presence of these BO_4 polymeric species reduces the interaction between Mo and the

alumina support, then increasing the size of the Mo oxide clusters [42], as a result, a less dispersed MoS_2 active phase and changes in the location of the promoter in the sulfided active phase occur [45, 47-49].

To try to gain better insight in the changes on the hydrogenation function of the catalysts induced by boron, it was decided to correlate the results obtained in the hydrogenation of naphthalene (test (i)) with the acidity, assuming that there is an evolution in the nature and distribution of the acid sites with the increase in the B_2O_3 according to the hypothesis previously announced, and summarized next to facilitate the comprehension of the present discussion: at boron concentrations up to 3 wt.% B_2O_3 there is a simultaneous increase in the amount of both Lewis and Brønsted sites of the catalyst, whereas for B_2O_3 wt.% higher than 3%, there is a further increase in the amount of Brønsted sites along with a decrease in the amount of Lewis sites. Fig. 6 shows the effect of boron concentration on the catalytic performance in the hydrogenation of naphthalene and the specific acidity of NiMo-B(x). In general, Fig. 6 shows a volcano curve for $\%C_{NP}$ as a function of the boron content. For B_2O_3 contents up to 6 wt.% there is an activity increase as compared to the NiMo catalyst, whereas for the content of 8 wt.% no significant change is registered. Li et al. [47] ascribed this trend to a better dispersion of the oxidic NiO and MoO_3 precursors at low boron concentration. Though it can be considered that the trend registered in the hydrogenation of naphthalene can be also a consequence of a combination of the changes in the dispersion of the MoS_2 active phase and Ni and the acidity increase of the catalysts, it can be assumed that the latter is playing the central role in this case due to fact that hydrogenation reactions are often considered as structure insensitive, i.e. not taking place at an specific site of the catalytic surface, and because, and more evidently, up to 6 wt.% B_2O_3 the activity of the NiMo-B(x) catalysts is c.a. 20% higher than the one of NiMo. In this last regard, it seems that not only acidity increase is important but also the distribution and strength of Brønsted and Lewis

acidic sites (Fig. 6). It can be speculated that the best catalytic performance of NiMo-B(x) in the hydrogenation reaction is related to an appropriated balance between the relative concentration of Brønsted and Lewis acid sites of intermediate acidic strength. Comparatively, the increase in HYD selectivity, as a function of acidity and B_2O_3 content, is not as high as the activity increase in naphthalene hydrogenation. This can be partly ascribed to the lower aromaticity of naphthalene as compared with dibenzothiophene, which makes the latter more refractory to be hydrogenated.

The trend for HYD and acidity observed in Fig. 5 agrees well with the hypothesis that an increase in Brønsted acidic sites of the support of MoS_2 based catalysts favors the HYD route of desulfurization [33, 39, 40]. Therefore, it also likely that the development of HYD over conventional MoS_2 based catalysts is more related to the presence of Brønsted sites of higher acidic strength as compared to those required for naphthalene hydrogenation.
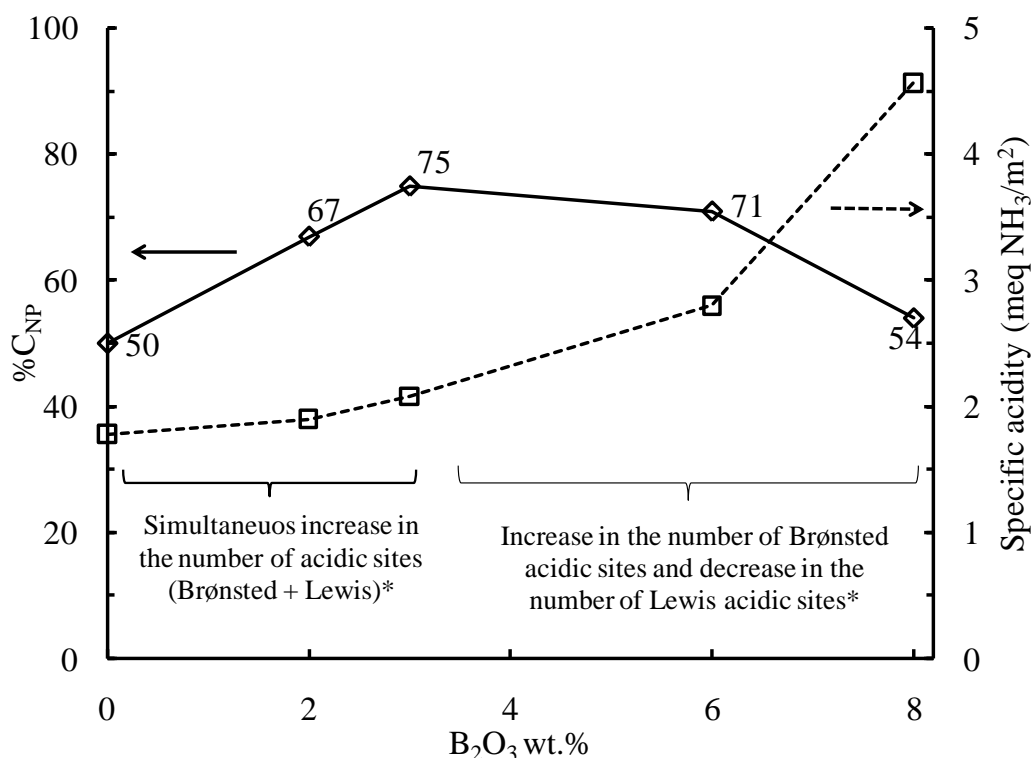
Fig. 6. Steady state performance of NiMo-B(x) catalysts during the hydrogenation of naphthalene, under an H_2S atmosphere, as a function of the B_2O_3 wt.%.
Reaction conditions: T = 563 K, P = 5 MPa, liquid feed flow 30 mL/h, H_2/liquid feed ratio = 500 NL/L, additional H_2S concentration in the reaction atmosphere c.a. 4074 wppm.
*Data taken from L.E. González and K. Rojas [60].

The behavior of the PtMo-B(x) catalysts in tests (i) and (ii) is presented in Figs. 7 and 8. Fig. 7 shows the steady state activity of Pt(0.5)Mo(2)-B(x) in the hydrogenation of NP as a function of the B_2O_3 content. A very poor performance of the catalysts in the hydrogenation reaction is evidenced. Moreover, the addition of boron causes a slight decrease in the catalytic activity, which is not directly related to boron concentration. Given the results obtained for the NiMo-B(x) catalysts, it was decided to modify the Pt(0.5)Mo(2) and Pt(0.5)Mo(15) catalysts by addition of 4 wt.% B_2O_3. The best catalytic performance for NiMo-B(x) was obtained around this boron load. In Fig. 8 a comparison of the steady state activity and selectivity of this group of catalysts is presented. The incorporation of boron has a negative effect on the HDS activity which is stronger than that determined for NiMo-B(x), and the effect in HYD selectivity is weak.
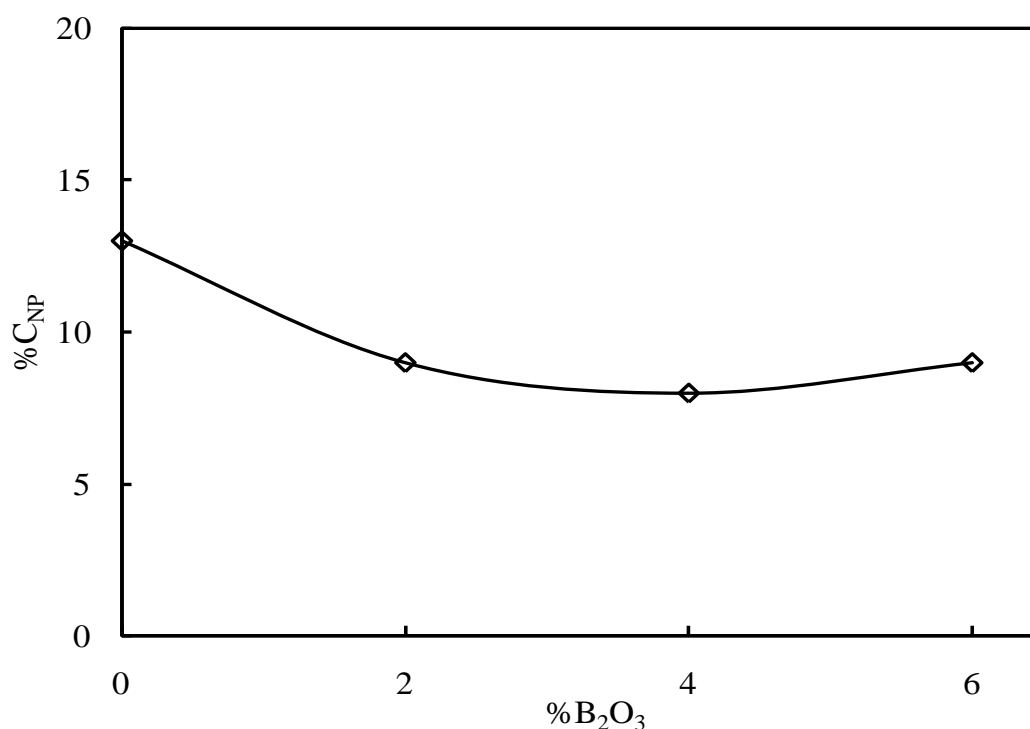
Fig. 7. Steady state performance of Pt(0.5)Mo(2)-B(x) catalysts during the hydrogenation of naphthalene, under an H_2S atmosphere, as a function of the B_2O_3 wt.%.
[*]Data taken from M.A. Beltrán and W.R. Sarmiento [61].

Therefore, taking into account the evidence presented so far, the effect of the acidity increase, due to boron incorporation, in the hydrogenation function of the Pt promoted MoS_2 catalysts

is weak, and neither leads to a development of the HYD route of hydrodesulfurization of DBT nor to strengthen the hydrogenating function of these materials.
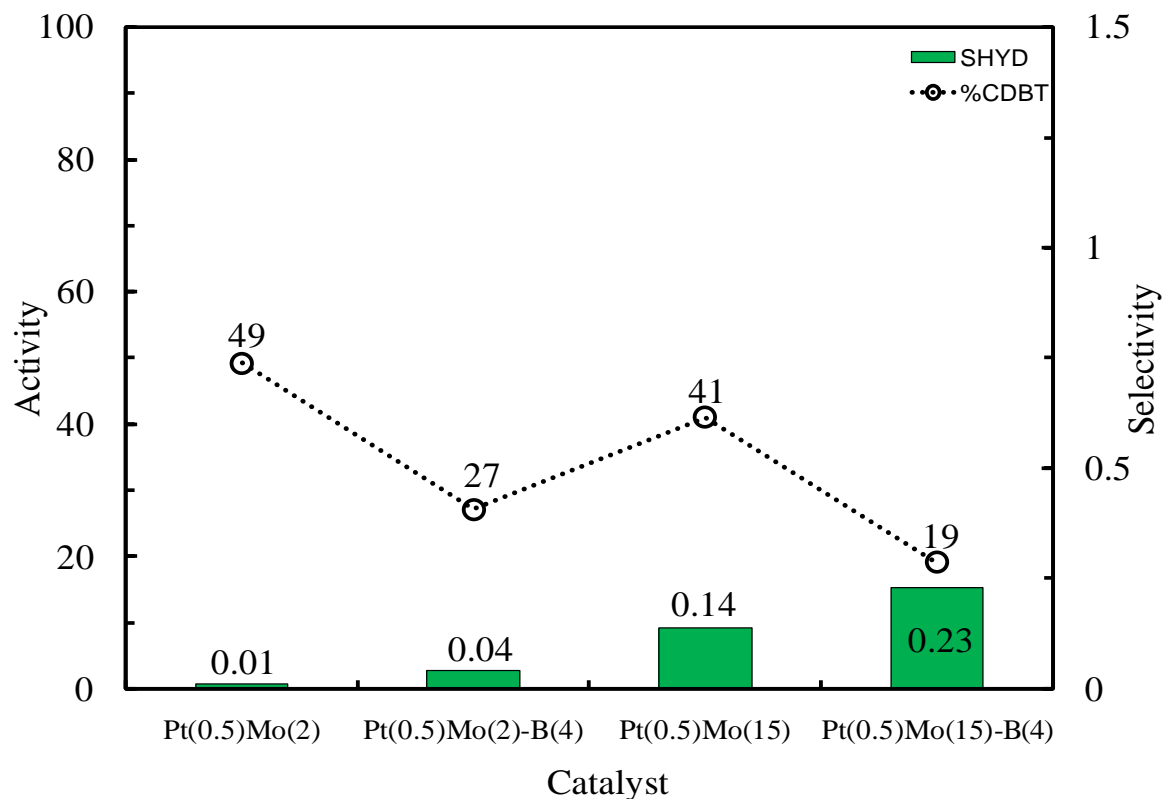
Fig. 8. Effect of boron on the activity and HYD selectivity of Pt(0.5)Mo(2) and Pt(0.5)Mo(15).
[*]Data taken from M.A. Beltrán and W.R. Sarmiento [61].

Finally, the main conclusion obtained from the experiments presented in this section is that a controlled increase in the acidity of the MoS_2 based promoted catalysts can be of benefit to its hydrogenating function, depending on the type of promoter. Nevertheless, the effect of acidity in the development of the HYD route of hydrodesulfurization of dibenzothiophene over γ-Al_2O_3 supported Ni-Mo and Pt-Mo systems is rather weak; these catalysts always performing the hydrodesulfurization reaction via DDS.

3.3. Influence of the presence of naphthalene on the reactivity of dibenzothiophene over Ni-Mo and Pt-Mo catalysts

The simultaneous hydrodesulfurization of dibenzothiophene – hydrogenation of naphthalene reaction was performed over NiMo-B(8) and three of the prepared Pt(0.5)Mo(2, 8 and 15) catalysts. Results are presented in Table 5.

Table 5. Steady state performance of NiMo-B(8) and Pt(0.5)Mo catalysts in simultaneous dibenzothiophene hydrodesulfurization – naphthalene hydrogenation reaction at T = 583 K.

Catalyst	%C_{DBT}	%C_{NP}	S_{HYD}	S_{DBT}
NiMo-B(8)[a]	68.1	62.1	0.4	1.1
Pt(0.5)Mo(2)[b]	53.0	10.0	N.D.	5.3
Pt(0.5)Mo(8)[b]	43.0	11.0	N.D.	3.9
Pt(0.5)Mo(15)[b]	39.0	8.0	N.D.	4.9

[a]Data taken from L.E. González and K. Rojas [60].
[b]Data taken from A. Estupiñán [69].

In regard to the reactivity of dibenzothiophene, the results show only slight differences with those registered for the independent tests. This behavior is in agreement with the generally accepted idea of the existence of different active sites for desulfurization and hydrogenation reactions in MoS_2 based catalytic systems [2, 3, 6, 7, 8-10, 12-14, 64]. The presence of naphthalene does not drastically change the selectivity to HYD of Ni-Mo. In the case of the Pt(0.5)Mo(2, 8 and 15) catalysts, the selectivity to HYD was not determined, because of the extremely low yield of cyclohexylbenzene observed during the reactions, making its chromatography quantification unfeasible. The results confirm that the Pt-Mo system is intrinsically more selective to DDS than conventional Co-Mo and Ni-Mo. With regard to the selectivity to the hydrodesulfurization reaction, it can be seen that the hydrogenation of naphthalene is qualitatively more competitive to HDS on the NiMo-B(x) catalyst, as compared to Pt-Mo. Indeed, in a parallel way to the HYD/DDS selectivity in the independent reaction tests, Pt-Mo is extremely selective to HDS. In a very recent work [32], performed within the frame of this Thesis, it is actually demonstrated that for the Pt-Mo catalytic system, the selectivity HYD/DDS in the hydrodesulfurization of DBT can be indirectly described by

the selectivity HDS to naphthalene hydrogenation. Considering adsorption competitions effects between the flat π–mode of adsorption of both the aromatic rings of naphthalene and dibenzothiophene, it is possible to explain the slight decrease in HYD selectivity of the Ni-Mo and Pt-Mo catalysts. But at this point, a definitive conclusion on this subject cannot be attained.

4. Conclusions

The results presented allow concluding that the HYD route of hydrodesulfurization of dibenzothiophene is not efficiently developed by promoted MoS_2/γ-Al_2O_3 based catalysts, regardless of the nature of promoter: Co, Ni or Pt. This is an intrinsic property of these systems, even when possessing a very good capacity to perform the hydrogenation of aromatics, as it is the case of NiMo. Conversely, it was demonstrated that a proper modification of the acid properties of the alumina support can contribute to the development of HYD. Finally, adsorption competition effects between the HYD route of hydrodesulfurization of dibenzothiophene and the hydrogenation of naphthalene can take place, but such effects did not significantly modify the reactivity of dibenzothiophene over the studied promoted MoS_2/γ-Al_2O_3 systems.

References

[1] O. Weisser, S. Landa, Sulfide Catalysts, Their Properties and Applications, Pergamon Press (1973) New York.

[2] P. Grange, Catal. Rev. -Sci. Eng. 21 (1980) 135.

[3] E. Furimsky, Catal. Rev. -Sci. Eng. 22 (1980) 371.

[4] M.L. Vrinat, Appl. Catal. 6 (1983) 137.

[5] M. Zdražil, Catal. Today 3 (1988) 269.

[6] R. Prins, V.H.J. De Beer, G.A. Somorjai, Catal. Rev. -Sci. Eng. 31 (1989) 1.

[7] B. Delmon, G.F. Froment, Catal. Rev. -Sci. Eng. 38 (1996) 69.

[8] H. Topsøe, B.S. Clausen, F.E. Massoth, Hydrotreating Catalysis, Springer-Verlag (1996) Berlin.

[9] S. Eijsbouts, Appl. Catal. A: Gen. 158 (1997) 53.

[10] J. Grimblot, Catal. Today 41 (1998) 111.

[11] A.N. Startsev, J. Mol. Catal. A: Chem. 152 (2000) 1.

[12] M. Breysse, E. Furimsky, S. Kasztelan, M. Lacroix, G. Pérot, Catal. Rev. -Sci. Eng. 44 (2002) 651.

[13] R.R. Chianelli, M.H. Siadati, M. Pérez De la Rosa, Catal. Rev. -Sci. Eng. 48 (2006) 1.

[14] M. Sun, J. Adjaye, A.E. Nelson, Appl. Catal. A: Gen. 263 (2004) 131.

[15] International symposium on advances in hydroprocessing of oils fractions (ISAHOF 2007), J. Ancheyta J, G.F. Froment (Eds), Catal. Today 130 (2008) 265 - 536.

[16] M.V. Landau, D. Berger, M. Herskowitz, J. Catal. 159 (1996) 236.

[17] D.D. Whitehurst, T. Isoda, I. Mochida, Adv. Catal. 42 (1998) 345.

[18] C. Song, Catal. Today 86 (2003) 211.

[19] W. Ripperger, W. Saum, J. Less-Common Met. 54 (1977) 353.

[20] M.J. Girgis, B.C. Gates, Ind. Eng. Chem. Res. 30 (1991) 2021.

[21] F. Bataille, J.-L. Lemberton, P. Michaud, G. Pérot, M. Vrinat, M. Lemaire, E. Schulz,

[22] J. Mijoin, G. Pérot, F. Bataille, J.L. Lemberton, M. Breysse, S. Kasztelan, Catal. Lett. 71 (2001) 139.

[23] M. Egorova, R. Prins, J. Catal. 225 (2004) 417.

[24] R. Navarro, B. Pawelec, J.L.G. Fierro, P.T. Vasudevan, Appl. Catal. A: Gen. 148 (1996) 23.

[25] M.H. Pinzón, L.I. Meriño, A. Centeno, S.A. Giraldo, Stud. Surf. Sci. Catal. 127 (1999) 97.

[26] M. Vergara, S.A. Giraldo, A. Centeno, ION 16 (2000) 63.

[27] Z. Vít, J. Cinibulk, D. Gulková, Appl. Catal. A: Gen. 272 (2004) 99.

[28] Z. Vít, D. Gulková, L. Kaluža, M. Zdražil, J. Catal. 232 (2005) 447.

[29] M.H. Pinzón, A. Centeno, S.A. Giraldo, Appl. Catal. A 302 (2006) 118.

[30] S. Pessayre, C. Geantet, R. Bacaud, M. Vrinat, T.S. N'Guyen, Y. Soldo, J.L. Hazemann, M. Breysse, Ind. Eng. Chem. Res. 46 (2007) 3877.

[31] V.G. Baldovino-Medrano, S.A. Giraldo, A. Centeno, Información Tecnológica 20:6 (2009) In press.

[32] V.G. Baldovino-Medrano, S.A. Giraldo, A. Centeno, Fuel (2009), Under review.

[33] P. Michaud, J.L. Lemberton, G. Pérot, Appl. Catal. A: Gen. 169 (1998) 343.

[34] G. Pérot, Catal. Today 86 (2003) 111.

[35] M. Breysse, G. Djega-Mariadassou, S. Pessayre, C. Geantet, M. Vrinat, G. Pérot, M. Lemaire, Catal. Today 84 (2003) 129.

[36] F. Richard, T. Boita, G. Pérot, Appl. Catal. A: Gen. 320 (2007) 69.

[37] P. Torres-Mancera, J. Ramírez, R. Cuevas, A. Gutiérrez-Alejandre, F. Murrieta, R. Luna, Catal. Today 107-108 (2005) 551.

[38] T. Klimova, J. Reyes, O. Gutiérrez, L. Lizama, Appl. Catal. A: Gen. 335 (2008) 159.

[39] C. Leyva, M.S. Rana, F. Trejo, J. Ancheyta, Catal. Today 141 (2009) 168.

[40] Y. Ogawa, M. Toba, Y. Yoshimura, Appl. Catal. A: Gen. 246 (2003) 213.

[41] M. Sibeijn, J.A.R. Vanveen, A. Bliek, J.A. Moulijn, J. Catal. 145 (1994) 416.

[42] U. Usman, M. Takaki, T. Kubota, Y. Okamoto, Appl. Catal. A: Gen. 286 (2005) 148.

[43] M. Lewandowski, Z. Sarbak, Fuel 79 (2000) 487.

[44] S. Sato, M. Kuroki, T. Sodesawa, F. Nozaki, G.E. Maciel, J. Mol. Catal. A: Chem. 104 (1995) 171.

[45] F. Dumeignil, K. Sato, M. Imamura, N. Matsubayashi, E. Payen, H. Shimada, Appl. Catal. A: Gen. 287 (2005) 135.

[46] T.-C. Huang, B.-C. Kang, J. Mol. Catal. A: Chem. 103 (1995) 163.

[47] D. Li, T. Sato, M. Imamura, H. Shimada, A. Nishijima, Appl. Catal. B: Env. 16 (1998) 255.

[48] D. Li, T. Sato, M. Imamura, H. Shimada, A. Nishijima, J. Catal. 170 (1997) 357.

[49] Usman, T. Kubota, I. Hiromitsu, Y. Okamoto, J. Catal. 247 (2007) 78–85.

[50] D. Ferdous, A. K. Dalai, J. Adjaye, Ind. Eng. Chem. Res. 45 (2006) 544.

[51] L. Ding, Z. Zhang, Y. Zheng, Z. Ring, J. Chen, Appl. Catal. A: Gen. 301 (2006) 241.

[52] J. Vargas, Master Thesis, Centro de Investigaciones en Catálisis, Escuela de Ingeniería Química, Universidad Industrial de Santander, Bucaramanga (2000).

[53] M. Vergara, Master Thesis, Centro de Investigaciones en Catálisis, Escuela de Ingeniería Química, Universidad Industrial de Santander, Bucaramanga (2001).

[54] L.I. Meriño, Master Thesis, Centro de Investigaciones en Catálisis, Escuela de Ingeniería Química, Universidad Industrial de Santander, Bucaramanga (1999).

[55] L.I. Meriño, A. Centeno, S.A. Giraldo, Appl. Catal. A: Gen. 197 (2000) 61.

[56] P. Amorocho, R.A. Lucero, Undergraduate work, Centro de Investigaciones en Catálisis, Escuela de Ingeniería Química, Universidad Industrial de Santander, Bucaramanga (2002).

[57] M.H. Pinzón, Master Thesis, Escuela de Ingeniería Química, Centro de Investigaciones en Catálisis, Universidad Industrial de Santander, Bucaramanga (2000).

[58] M.H. Pinzón, Ph.D. Thesis, Escuela de Ingeniería Química, Centro de Investigaciones en Catálisis, Universidad Industrial de Santander, Bucaramanga (2006).

[59] J. Haber, Pure Appl. Chem. 63 (1991) 1227.

[60] L.E. González, K. Rojas, Undergraduate work, Escuela de Ingeniería Química, Centro de Investigaciones en Catálisis, Universidad Industrial de Santander, Bucaramanga (2008).

[61] M.A. Beltrán, W.R. Sarmiento, Undergraduate work, Escuela de Ingeniería Química, Centro de Investigaciones en Catálisis, Universidad Industrial de Santander, Bucaramanga (2008).

[62] P. Grange, X. Vanhaeren, Catal. Today 36 (1997) 375.

[63] Y.W. Li, B. Delmon, J. Mol. Catal. A: Chem. 127 (1997) 163.

[64] V. Rabarihoela-Rakotovao, S. Brunet, G. Pérot, F. Diehl, Appl. Catal. A: Gen. 306 (2006) 34.

[65] H. Farag, Appl. Catal. A: Gen. 331 (2007) 51.

[66] H. Wang, R. Prins, J. Catal. 258 (2008) 153.

[67] Z. Paál, T. Koltai, K. Matusek, J.-M. Manoli, C. Potvin, M. Muhler, U. Wild and P. Tétényi, Phys. Chem. Chem. Phys. 3 (2001) 1535.

[68] Z. Paál, P. Tétényi, M. Muhler, U. Wild, J-M. Manoli and C. Potvin, J. Chem. Soc., Faraday Trans. 94 (1998) 459.

[69] A. Estupiñán, Master Thesis, Escuela de Ingeniería Química, Centro de Investigaciones en Catálisis, Universidad Industrial de Santander, Bucaramanga (2008).

[70] D. Pérez-Martínez, S.A. Giraldo, A. Centeno, Appl. Catal. A: Gen. 315 (2006) 35.

[71] E.O. Orozco, M. Vrinat, Appl. Catal. A: Gen. 170 (1998) 195.

Chapter II: The hydrogenation route of hydrodesulfurization over γ-Al₂O₃ supported monometallic Pd and Pt catalysts

Abstract

In this Chapter the functionalities of monometallic Pd and Pt/γ-Al₂O₃ catalysts in reactions of hydrodesulfurization of dibenzothiophene under several reaction conditions is presented. The study is focused in understanding those functionalities that control the selectivity of both monometallic noble metals to HYD. The experimental evidence presented for Pd is compared with an analysis of the functionalities of monometallic Pt/γ-Al₂O₃ in simultaneous HDS of dibenzothiophene and hydrogenation of naphthalene reactions. In this case, the author allowed himself to revisit some of the results presented by Estupiñán[‡] in his Master Thesis developed at CICAT-UIS for Pt/γ-Al₂O₃, and propose new interpretations concerning the subject of the present Ph.D. Thesis: the selective HDS of dibenzothiophene via HYD. Further in Chapter IV, new experiments performed by the author are presented which confirmed the propositions presented here. The results evidenced that the active phase of the noble metals possesses a metallic character, but the reactivity of dibenzothiophene over Pt and Pd is different. On the other hand, adsorption competition effects between hydrogenation and hydrodesulfurization reactions were evidenced. The similarities observed between the mechanistic dynamics of HYD and the hydrogenation of aromatics led to propose an alternative reaction mechanism for HYD over Pd/γ-Al₂O₃.

Keywords: Pd and Pt/γ-Al₂O₃, dibenzothiophene HDS, naphthalene hydrogenation, HYD route of hydrodesulfurization, direct route of hydrodesulfurization.

[‡] A. Estupiñán, Master Thesis, Escuela de Ingeniería Química, Centro de Investigaciones en Catálisis, Universidad Industrial de Santander, Bucaramanga (2008))

1. Introduction

The new generation of hydrotreating catalysts must have the capacity to desulfurize highly refractory di-β-dibenzothiophenes while performing the deep hydrogenation of aromatic molecules [1]. Dibenzothiophenes are desulfurized via the parallel DDS and HYD reaction routes [2, 3]. As previously discussed in the Introductory Chapter, developing highly-hydrogenating selective catalysts is desirable for deep hydrodesulfurization. Chianelli and co-workers [4, 5] found that unsupported *platinum metals sulfides* (PtS, PdS, RuS_2) are more active than MoS_2 in the HDS of dibenzothiophene (DBT). So far, noble metal based catalysts have been tested in deep hydrodesulfurization and aromatics hydrogenation [6-9]. On one hand, Pd is able to selectively hydrogenate sulfur containing molecules. Mashkina and co-workers [10, 11] hydrogenated thiophene and benzothiophene on Pd. Röthlisberger and Prins [7, 12] tested Pd in the hydrodesulfurization of dibenzothiophene and 4,6-dimethyl-DBT. Their results show that Pd has a higher selectivity to HYD in the hydrodesulfurization of dibenzothiophene as compared to Ni-MoS_2 and Pt catalysts [7]. Significant amounts of partially hydrogenated products were found during the hydrodesulfurization of 4,6-dimethyl-DBT [12]. On the other hand, Pt/γ−Al_2O_3 is a known reforming catalyst and much of its interaction with sulfur is understood up to date due to such studies [13-19]. Besides their wide use in naphtha reforming, Pt catalysts were recognized a long time ago as effective catalysts for hydrodesulfurization [4, 5, 20]. In particular, the outstanding hydrogenating capacity of platinum makes it a potential catalyst for deep HDS and deep aromatics hydrogenation (HDA). Nevertheless it is known that the main disadvantage of noble metal catalysts is their low tolerance to H_2S. An increase in the

support acidity and/or the combination of Pt with other transition metals has been proposed to overcome this problem [8, 21-28].

The combination Pt-Pd supported on acidic materials has been found to be very effective for HDA in the presence of sulfur [8, 23-28]. Nevertheless, the higher thiotolerance exhibited by Pt-Pd catalysts is not only restricted to the use of acidic supports [29]. The catalytic properties of Pt-Pd based systems have also started to attract interest for deep HDS [7-9, 30, 31]. Though some aspects related to the interactions between Pt and Pd have begun to be understood [26], few reports are devoted to the study of the catalytic functionalities of each metal within the bimetallic system [7, 12]. One of the significant findings of these studies is that Pd can provide hydrogenation sites in HDS [12], whereas Pt supplies hydrogenolysis sites [7].

Within this context, in this Chapter, the functionalities of monometallic Pd and Pt in reactions of hydrodesulfurization of DBT and/or hydrogenation of naphthalene (NP) were analyzed. To gain insight into the nature of the active phase of both noble metals under a hydrotreating reaction environment the hydrogenation function of both metals is analyzed as a function of different activation procedures; reduction, reduction-sulfidation, sulfidation with pure H_2S, and non-activation.

2. Experimental

2.1. Catalyst preparation

One Pd/γ-Al$_2$O$_3$ catalyst prepared from a PdCl$_2$ precursor (Aldrich 99.0%) was chosen to study the HDS of dibenzothiophene. The wet impregnation technique was used. The same γ-Al$_2$O$_3$ support employed in Chapter I (See section 2.1., Page 27) was used. The nominal content of Pd was adjusted to 2 wt.% and verified by atomic absorption. To obtain sulfided

Pd catalysts with different chemical states of Pd and analyze their thiotolerance, two additional catalysts were prepared using Li_2PdCl_4 and palladium acetate $(Pd(C_2H_3O_2)_2)$ (Aldrich 98.0%) as precursors. Impregnating solutions were obtained as follows: $PdCl_2$ was diluted in an aqueous solution of HCl to obtain $PdCl_4^{-2}$ species [33]. Li_2PdCl_4 was diluted in water (deionized and distilled), and $Pd(C_2H_3O_2)_2$ was diluted in acetone. These solutions were kept in contact with the carrier until impregnation process completeness. Then, the exceeding solvent was vacuum evaporated. Drying (12 h) and calcination (4 h at 773 K) of these solids were performed under air flow. Catalyst labels were assigned according to the Pd precursor: Pd_{Cl} ($PdCl_2$), Pd_{Li} (Li_2PdCl_4), and Pd_{Ac} ($Pd(C_2H_3O_2)_2$).

The preparation of the 2 wt% Pt/γ-Al_2O_3 catalyst is reported in the work of Estupiñán [34]. Conventional CoMo (15 wt% MoO_3, 3 wt% CoO) and NiMo (9 wt% MoO_3, 4.5 wt% NiO) catalysts were prepared using the procedure described by Portela et al. [32].

2.2. Catalyst activation

Catalysts were activated according to the procedures described in Chapter I (Section 2.2., Page 28). All Pd catalysts were activated with a H_2S (15 vol.%)/H_2 mixture. Pd_{Cl} was also activated with pure H_2 or pure H_2S. According to the activating agent, the indexes: S15 = mixture H_2S (15 vol.%)/H_2, H = pure H_2, and S = pure H_2S were added to catalyst labels. The Pt catalysts were activated at similar conditions [34]. Thorough cleaning of the catatest was performed to guaranty the absence of H_2S in the system when activation was performed with pure H_2. The conventional CoMo and NiMo catalysts; the latter ones were only activated with the S15 mixture. Finally, a sample of Pt/γ-Al_2O_3 was tested without

activation, being labeled with the letter N. This experiment was performed to qualitative evaluate the evolution of the active phase of the catalyst under the reaction atmosphere.

2.3. Catalysts characterization

2.3.1. XPS analysis of sulfided Pd catalysts.

The Pd sulfided catalysts were analyzed by XPS. They were maintained in iso-octane before the XPS analysis to avoid air exposure. The XPS apparatus was an Axis Ultra spectrometer from Kratos working with non-monochromatic Mg radiation (10 mA, 15 kV) and a charge compensation device (charge balance fixed at -2.3 V). The pressure in the analysis chamber was around 10^{-6}Pa. The angle between the normal of the sample surface and the lens axis was 0°. The hybrid lens magnification mode was used with the slot aperture resulting in an analyzed area of 700 μm x 300 μm. The pass energy for the analyzer was 40 eV. In these conditions, the energy resolution gives a full width at half maximum (FWHM) of the $Ag_{3d5/2}$ peak of about 1 eV. The following sequence of spectra was recorded: C_{1s}, O_{1s}, Al_{2p}, Pd_{3d}, S_{2p}. The binding energies (BE) were calibrated by fixing the C–(C, H) contribution of the C_{1s} adventitious carbon at 284.8 eV. Peaks were considered to be combinations of Gaussian and Lorentzian functions in a 70:30 ratio working with a linear baseline. Data treatment was performed with the CasaXPS program (Casa Software Ltd., UK) [36].

2.3.2. TPR analysis of Pt/γ-Al₂O₃ catalysts

TPR experiments were carried out in a ChemBET3000 TPR/TPD apparatus (Quantachrome) provided with a TCD. Samples of 0.1 g of the calcined catalyst were placed into a U-shaped quartz reactor and dried in N_2 flow at 393 K for 2 h. Then, they

were activated under the same conditions as described in Section 2.2. The complete procedure for this analysis was described by Estupiñán [34]. An additional set of experiments was performed as follows: the *in situ* activated samples were cooled down to the temperature used in the catalytic tests (583 K) and, then, maintained under an H_2S-H_2 atmosphere with the same composition as the one observed in the catalytic tests under steady state conditions, during a time period equal to the time on stream of the catalytic test. This procedure was marked as TPR-SRE (SRE = simulated reaction environment). For these samples, the brand -SRE was added. All TPR patterns were registered during heating of the samples from 298 K to 1123 K (heating rate 10 K/min) in a flow (30 mL/min) of highly pure H_2.

2.4. Catalytic tests

Four types of tests were performed: (i) naphthalene or tetralin (TTL) hydrogenation without the presence of H_2S, (ii) naphthalene hydrogenation under an H_2S environment, (iii) dibenzothiophene hydrodesulfurization, and, (iv) simultaneous hydrodesulfurization of dibenzothiophene - naphthalene hydrogenation. The composition of the liquid charge was systematically changed according to the reaction test performed. The liquid feed charge was prepared according to the standard procedure. Temperature was varied between T = 543 - 603 K depending on the type of catalytic test, while keeping the usual reaction conditions. Liquid products were analyzed using a HP 6890 GC equipped with an FID, an HP-1 capillary column (100 m x 0,25 mm x 0,5 μm), and a split injector. Catalytic tests were conducted until reaching steady state.

2.4.1. Hydrogenation of aromatic rings (naphthalene and tetralin)

Test (i) was performed on reduced samples of Pd_{Cl} (Pd_{Cl}^H), in order to characterize the interaction of metallic Pd with aromatic rings. A concentration of 3 wt.% NP (commercial grade) or 2 wt.% TTL (Aldrich 98%) was used for these tests. Test (ii) was carried out on reduced Pd_{Cl}^H and reduced-sulfided Pd_{Cl}^{S15}, Pd_{Li}^{S15}, and Pd_{Ac}^{S15} catalysts, to analyze the effect of the chemical state of Pd in its thiotolerance in aromatics hydrogenation. Naphthalene content was the same as mentioned above, and H_2S (concentration c.a. 4074 ppm) was generated from decomposition of dimethyldisulfide (DMDS) added to the reactor liquid feed. At the present conditions, all DMDS is transformed to H_2S [37].

2.4.2. Independent dibenzothiophene hydrodesulfurization and simultaneous hydrodesulfurization of dibenzothiophene and naphthalene hydrogenation.

In the case of Pd/γ-Al_2O_3, these reactions were carried out only on samples of Pd_{Cl} activated with different agents (Pd_{Cl}^H, Pd_{Cl}^{S15} or Pd_{Cl}^S). Also, the effect of temperature on the hydrodesulfurization of dibenzothiophene over Pd_{Cl}^H was studied. These tests were performed at the following reaction conditions: T = 583 K; P = 5 MPa; Liquid feed flow = 30 mL/h; (H_2/liquid feed) ratio = 500 LN/L. For the samples of Pt/γ-Al_2O_3 only the simultaneous dibenzothiophene hydrodesulfurization - naphthalene hydrogenation reaction was carried out. An additional catalytic test was carried out for the reduced catalyst (Pt^H), in order to establish its sulfur tolerance and changes in its selectivity due to an increase in the H_2S partial pressure. The general procedure used on the test was as follows: initially, the catalyst was evaluated at the usual conditions, allowing it to reach steady state. Once this condition was achieved, DMDS was added to the liquid charge in such an amount as to obtain a concentration of 50% excess of H_2S in the reaction environment, as compared with

the initial H$_2$S concentration in steady state. Afterward, the catalyst was allowed to attain a new steady state. When the latter condition was met, DMDS was withdrawn from the liquid charge and the catalyst was permitted to reach a steady state condition again. Further details on the procedure can be found in [34].

2.4.3. Expression of the results

The activity was determined from Eq. 1 (Chapter I) and products distribution as *%y$_j$* (Eq. 2, Chapter I), For naphthalene and tetralin tests without H$_2$S presence, the selectivity to *trans*-decalin over the *cis*-decalin isomer (*S$_{trans-}$*) was defined as the ratio:

$$S_{trans-} = \frac{\% y_{trans-}}{\% y_{cis-}}$$ (Eq. 5)

For naphthalene hydrogenation under an H$_2$S environment, turnover numbers (*TON^{XPS}*) were defined as the ratio k$_{NP}$, as obtained from an average of three samples at steady state conditions to Pd/Al atomic relation determined by XPS as expressed by:

TON^{XPS} = k$_{NP}$/(Pd/Al atomic ratio)^{XPS} (Eq. 6)

Where, k_{NP} is the specific rate constant (k_{NP} [=] L.s^{-1}g^{-1}) calculated considering a pseudo-first order kinetics [38] from the expression:

$$k_{NP} = \frac{F_0}{wC_0} \ln\left(-\chi\right)$$ (Eq. 7)

Where, F_0 corresponds to the molar feed rate of the reactant (naphthalene) in mol/s; w to the catalyst weight in g; C_0 to the initial concentration of reactant, and χ to the conversion after reaching the steady state.

This calculation of TON^{XPS} provides a qualitative idea of the intrinsic activity of surface Pd atoms in steady state conditions. Considering that the alumina support can be taken as a

common and valid reference to determine the relative distribution of Pd among these catalysts, the surface Pd/Al atomic ratio is a good qualitative descriptor of the surface atomic dispersion. Even though this method is not fully accurate, the use of conventional methods to measure dispersion is not especially recommended in this case, given that sulfided phases are being examined [39].

To compare the thiotolerance of the reduced-sulfided (Pd_{Cl}^{S15}, Pd_{Li}^{S15}, and Pd_{Ac}^{S15}) catalysts to the one of reduced Pd_{Cl}^{H} during naphthalene hydrogenation at steady state conditions, a % of the relative activity (*%RA*) was defined as k_{NP} for Pd_{Cl}^{H} minus k_{NP} for the corresponding reduced sulfided catalyst divided by k_{NP} for Pd_{Cl}^{H}:

$$\%RA = 100 \times \frac{k_{NP}\left(Pd_{Cl}^{H}\right) - k_{NP}\left(Pd_{Cl,Li,Ac}^{S15}\right)}{k_{NP}\left(Pd_{Cl}^{H}\right)} \qquad \text{(Eq. 8)}$$

Where, the corresponding catalyst has been indicated after k_{NP}.

The catalytic selectivity was expressed in two different ways, the first, was the total selectivity to HYD (S_{HYD}) as determined from Eq. 3 (Chapter I), and, second as the ratio:

$$S_{HYD}^{DS} = \frac{\% y_{CHB}}{\% y_{BP}} \qquad \text{(Eq. 9)}$$

i.e. between completely desulfurized products (*CHB* = cyclohexylbenzene, and *BP* = biphenyl).

For the simultaneous reactions, S_{DBT} was calculated according to Eq. 4 (Chapter I). It must be noticed that this selectivity is indicating the capacity of the catalyst to hydrogenate naphthalene over converting dibenzothiophene. In addition, a selectivity (S_{HDS}) representing the capacity of the catalyst to desulfurize dibenzothiophene compared to the activity in naphthalene hydrogenation was defined as:

$$S_{HDS} = \frac{\left(\% \, y_{CHB} + \% \, y_{BP} \right)}{\% \, C_{NP}}$$ (Eq. 10)

3. Results

3.1. XPS analysis of the catalysts sulfided during activation

Table 1 shows the XPS results of the Pd catalysts sulfided during activation. As observed, the Pd/Al atomic ratio for the catalysts activated with the H_2S/H_2 mixture follows the order $Pd_{Ac}^{S15} > Pd_{Li}^{S15} > Pd_{Cl}^{S15}$. The S/Pd atomic ratio was found to remain almost constant for these catalysts. The BE of the $Pd_{3d5/2}$ peak decreases in the order $Pd_{Cl}^{S15} > Pd_{Li}^{S15} > Pd_{Ac}^{S15}$. All BE values are higher than the one of metallic Pd (335.0 ± 0.1 eV) [40]; hence, the oxidation state of Pd is between +2 and +4 [41]. Given BE values for $Pd_{3d5/2}$ and S_{2p} and the S/Pd ratio, it is concluded that at similar activation conditions, this group of catalysts has similar sulfur saturation degrees but displays different electronic states of Pd. On the other hand, the S/Pd atomic ratio reported for Pd_{Cl}^{S} in Table 1 shows that activation with pure H_2S leads to an extensive sulfur saturation of the catalyst. Indeed, the S/Pd atomic ratio for Pd_{Cl}^{S} is almost twice of the Pd_{Cl}^{S15}. Additionally, activation with pure H_2S causes a larger positive BE shift of the $Pd_{3d5/2}$ peak.

3.2. TPR characterization of Pt/γ-Al₂O₃

From the data presented by Estupiñán [34] the author selected those presented in Fig. 1 which shows the TPR pattern of the sample sulfided with pure H_2S (Pt^S), the activated γ-Al_2O_3 support (γ-$Al_2O_3^{S15}$), and the patterns of the different samples after the SRE treatment (Pt^H-SRE; Pt^N-SRE; Pt^{S15}-SRE; Pt^S-SRE; and γ−$Al_2O_3^{S15}$-SRE). The γ-$Al_2O_3^{S15}$ shows a wide peak around 500 K, which can be ascribed to the chemical adsorption of H_2S

[43, 44]. The size of this peak decreases after the SRE treatment. Therefore, most part of the chemisorbed H_2S is desorbed under the atmosphere of the reaction environment. It is known that after treating alumina under H_2 atmospheres sulfur can be removed from its surface [13-17]. The profile of Pt^S shows a very wide peak in the region 500 - 750 K. This peak is attributed to a combination of the H_2S chemically adsorbed on the support and PtS [45-47]. The profile of Pt^S-SRE indicates that under the atmosphere of the reactor most of the H_2S chemisorbed on the support is desorbed, as well as some part of the PtS has been reduced. This is also the case of the Pt^{S15}-SRE sample. The samples Pt^H-SRE, and Pt^N-SRE show no peaks.
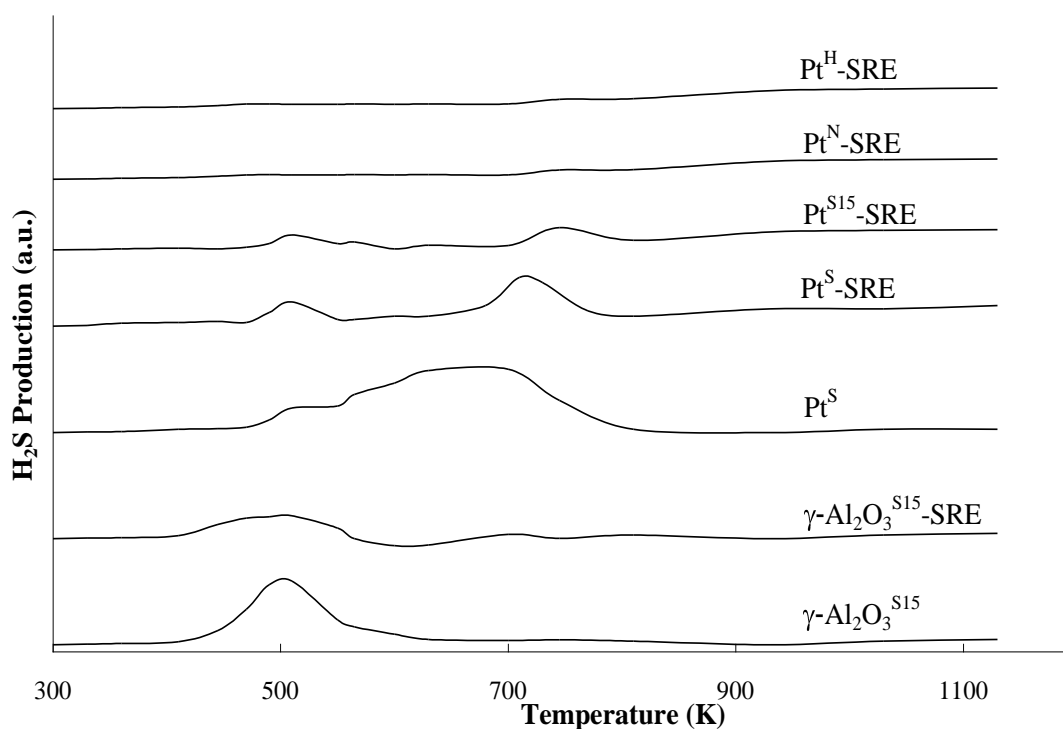
Fig. 1. TPR patterns of the Pt catalyst samples and γ-Al_2O_3 support after activation with different agents (H = reduction with pure H_2; S15 = reduction-sulfidation with 15 vol. % H_2S in H_2; S = sulfidation with pure H_2S; and N = no activation), after activated and after activated and maintained under a simulated reaction environment during 6 h.
*Data taken from A. Estupiñán [34].

Table 1. XPS analysis of Pd/γ-Al$_2$O$_3$ catalysts after activation by sulfidation either with a H$_2$S (15 vol.%)-H$_2$ mixture or H$_2$S.

Catalyst	% Atomic			Binding Energy (BE) (eV)		FWHM		Atomic Ratio	
	Pd 3d$_{5/2}$	S 2p	Al 2p	Pd 3d$_{5/2}$	S 2p	Pd 3d$_{5/2}$	S 2p	S/Pd	Pd/Al
Pd$_{Cl}^{S15}$	0.27	0.39	30.98	336.43	162.01	2.2	2.7	1.4	0.009
Pd$_{Li}^{S15}$	0.50	0.62	29.91	336.00	161.73	2.3	2.3	1.2	0.017
Pd$_{Ac}^{S15}$	0.64	0.84	30.65	335.65	161.99	2.0	2.3	1.3	0.021
Pd$_{Cl}^{S}$	0.18	0.48	31.09	336.55	162.34	1.7	2.7	2.7	0.006

3.3. Catalytic tests

The results for the independent naphthalene hydrogenation and dibenzothiophene hydrodesulfurization reactions for Pd/γ-Al$_2$O$_3$ are described first, and, afterwards, those corresponding to the simultaneous reactions.

3.3.1. Naphthalene or tetralin hydrogenation without the presence of H$_2$S

Reaction products detected were tetralin, *cis*-decalin, and *trans*-decalin. Table 2 presents the activity and the selectivity *trans*- to *cis*-decalin (S$_{trans-}$) at steady state for Pd$_{Cl}^{H}$. It is observed that Pd is highly selective to tetralin. Moreover, the activity in tetralin hydrogenation to decalins is low. Concerning S$_{trans-}$, *trans*-decalin is always favored over *cis*-decalin. This trend is similar either for naphthalene or tetralin, as in both cases S$_{trans-}$ remains constant. Similar results have been reported in literature [48, 49].

Table 2. Steady state catalytic performance of Pd$_{Cl}^{H}$ in naphthalene and tetralin hydrogenation without the presence of H$_2$S. T = 543 K.

Reaction	Activity				Selectivity
	%C$_{NP}$	%y$_{TTL,}$ %C$_{TTL}$	%y$_{trans-}$	%y$_{cis-}$	S$_{trans-}$
Naphthalene hydrogenation	85.0	84.1	0.7	0.2	3.5
Tetralin hydrogenation	0	3.4	2.6	0.8	3.3

3.3.2. Naphthalene hydrogenation under an H_2S environment

Table 3 presents the steady state results for this reaction on Pd_{Cl}^H, Pd_{Cl}^{S15}, Pd_{Li}^{S15}, and Pd_{Ac}^{S15}. All catalysts displayed very low activity and only yielded tetralin. This is in agreement with the low thiotolerance of monometallic noble metal based catalysts [21]. On the other hand, TON^{XPS} decreased in the order $Pd_{Cl}^{S15} > Pd_{Li}^{S15} > Pd_{Ac}^{S15}$. Thus, it can be said that, in general, Pd atoms on the surface of Pd_{Cl}^{S15} possess a relatively higher intrinsic activity than those of the other two catalysts.

Table 3. Steady state performance of Pd/γ-Al$_2$O$_3$ catalysts in naphthalene hydrogenation under a H$_2$S atmosphere. T = 563 K.

Catalyst	$\%C_{NP}$	%RA	TON^{XPS}
Pd_{Cl}^H	15.3	N.D.	N.D.
Pd_{Cl}^{S15}	7.2	49	1.6
Pd_{Li}^{S15}	11.6	21	1.3
Pd_{Ac}^{S15}	7.6	49	0.7

3.3.3. Dibenzothiophene hydrodesulfurization

Fig. 2 (a, b and c) shows the evolution of the catalytic performance with time on stream for Pd_{Cl} activated with different agents. In this figure, selectivity evolution is obtained from the dynamic change in products yields. Table 4 displays the steady-state catalytic behavior as a function of the activating agent and temperature. Detected reaction products were biphenyl, cyclohexylbenzene, TH-dibenzothiophene and HH-dibenzothiophene.
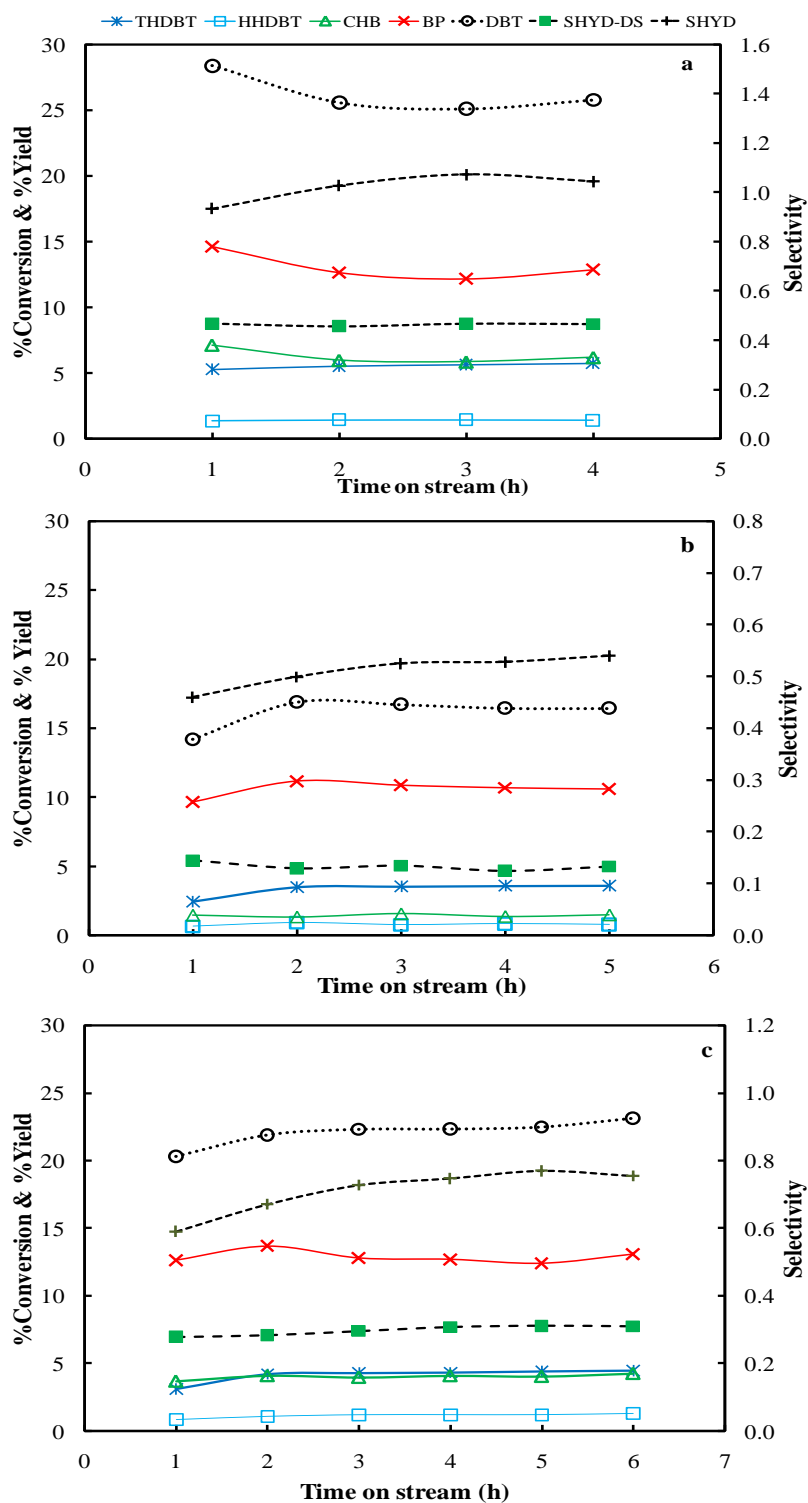
Fig. 2. Activity and selectivity versus time on stream for a Pd_{Cl}, in independent DBT hydrodesulfurization, as a function of the activating agent: a) Reduced in H_2 (Pd_{Cl}^H); b) reduced-sulfided in H_2S(15 vol.%)/H_2 (Pd_{Cl}^{S15}); c) sulfided with pure H_2S (Pd_{Cl}^S).

3.3.3.1. Effect of the activating agent

For Pd_{Cl}^{S15}, an initial raise in dibenzothiophene conversion was observed (Fig. 2b). Changes in yields of products for Pd_{Cl}^{S15} were also observed as compared to Pd_{Cl}^{H}. Thus, a comparison between the yields of the different HYD products of Pd_{Cl}^{H} and Pd_{Cl}^{S15} shows that the order of the former corresponded to $\%y_{CHB} \sim \%y_{THDBT} > \%y_{HHDBT}$, whereas the order of the latter corresponded to $\%y_{THDBT} > \%y_{CHB} \sim \%y_{HHDBT}$. On the other hand, the decrease in the yields of HYD products registered for Pd_{Cl}^{S15} demonstrate that inhibition of HYD can occur due to sulfidation of the catalyst. Notwithstanding, once steady state is reached, it can be seen that DDS was not deeply affected (see $\%y_{BP}$ in Table 4). Finally, the trends for Pd_{Cl}^{S} (Figure 2c) are similar to those for Pd_{Cl}^{S15}. In general, comparing $\%y_{BP}$ for the three samples of the Pd_{Cl} catalyst in these experiments as a function of the activating agent (Table 4), only small changes are observed. Therefore, the activation procedure does not markedly impact DDS on Pd (see $\%y_{BP}$, Table 4). Conversely, as appointed before, HYD is negatively affected when activation by sulfidation is carried out. Thus, $\%y_{THDBT}$ and S_{HYD} decreased in the order $Pd_{Cl}^{H} > Pd_{Cl}^{S} > Pd_{Cl}^{S15}$. Where, S_{HYD} for Pd_{Cl}^{S15} is half the one of Pd_{Cl}^{H}. Finally, S_{HYD}^{DS} for Pd_{Cl}^{H} is approximately thrice the one of Pd_{Cl}^{S15}.

3.3.3.2. Effect of reaction temperature on the selectivity for dibenzothiophene conversion over Pd

The steady state catalytic performance of Pd_{Cl}^{H} in the hydrodesulfurization of dibenzothiophene as a function of reaction temperature is presented in Table 4. Dibenzothiophene conversion increases with temperature, but its values are far below the predicted thermodynamic equilibrium [50]. In general, S_{HYD} decreased and S_{HYD}^{DS} showed a small increase with temperature increase. Thus, higher temperatures enhanced the rate of

hydrogenolysis of the C-S-C bond. The results obtained evidence that the hydrodesulfurization of dibenzothiophene over Pd is highly controlled by kinetics.

Table 4. Steady state catalytic performance of Pd_{Cl} and temperature effect over Pd_{Cl}^H in independent DBT hydrodesulfurization.

Catalyst	T (K)	Activity					Selectivity	
		%y_{THDBT}	%y_{HHDBT}	%y_{CHB}	%y_{BP}	%C_{DBT}	S_{HYD}^{DS}	S_{HYD}
	563	4.8	1.5	3.7	7.8	17.9	0.47	1.31
Pd_{Cl}^H	583	5.7	1.4	6.2	12.5	25.9	0.48	1.08
	603	6.6	1.2	10.2	18.3	36.4	0.53	0.98
Pd_{Cl}^{S15}	583	3.6	0.8	1.4	10.8	16.7	0.1	0.5
Pd_{Cl}^S	583	4.4	1.3	4.1	12.7	22.7	0.3	0.8

3.3.4. Reactivity of dibenzothiophene over Pd and Pt/γ-Al₂O₃ in the presence of naphthalene

Table 5 presents the steady state catalytic behavior of Pd_{Cl} as a function of the activating agent, and Fig. 3 features the catalytic conversion and the reaction products distribution as a function of time on stream.

Table 5. Steady state catalytic performance of Pd_{Cl} in the simultaneous reactions of dibenzothiophene hydrodesulfurization and naphthalene hydrogenation.

Catalyst	Activity						Selectivity			
	%C_{NP}	%y_{THDBT}	%y_{HHDBT}	%y_{CHB}	%y_{BP}	%C_{DBT}	S_{HYD}^{DS}	S_{HYD}	S_{HDS}	S_{DBT}
Pd_{Cl}^H	26.3	4.3	1.2	3.4	15.1	24.0	0.23	0.59	0.70	0.91
Pd_{Cl}^{S15}	15.7	3.5	1.0	2.0	12.5	19.0	0.16	0.52	0.92	1.21
Pd_{Cl}^S	17.0	5.1	1.5	4.2	11.1	21.8	0.38	0.96	0.90	1.28

Reaction conditions: T = 583 K, P = 5 MPa; Liquid feed flow=30 mL/h; (H₂/liquid feed) ratio = 500 LN/L.
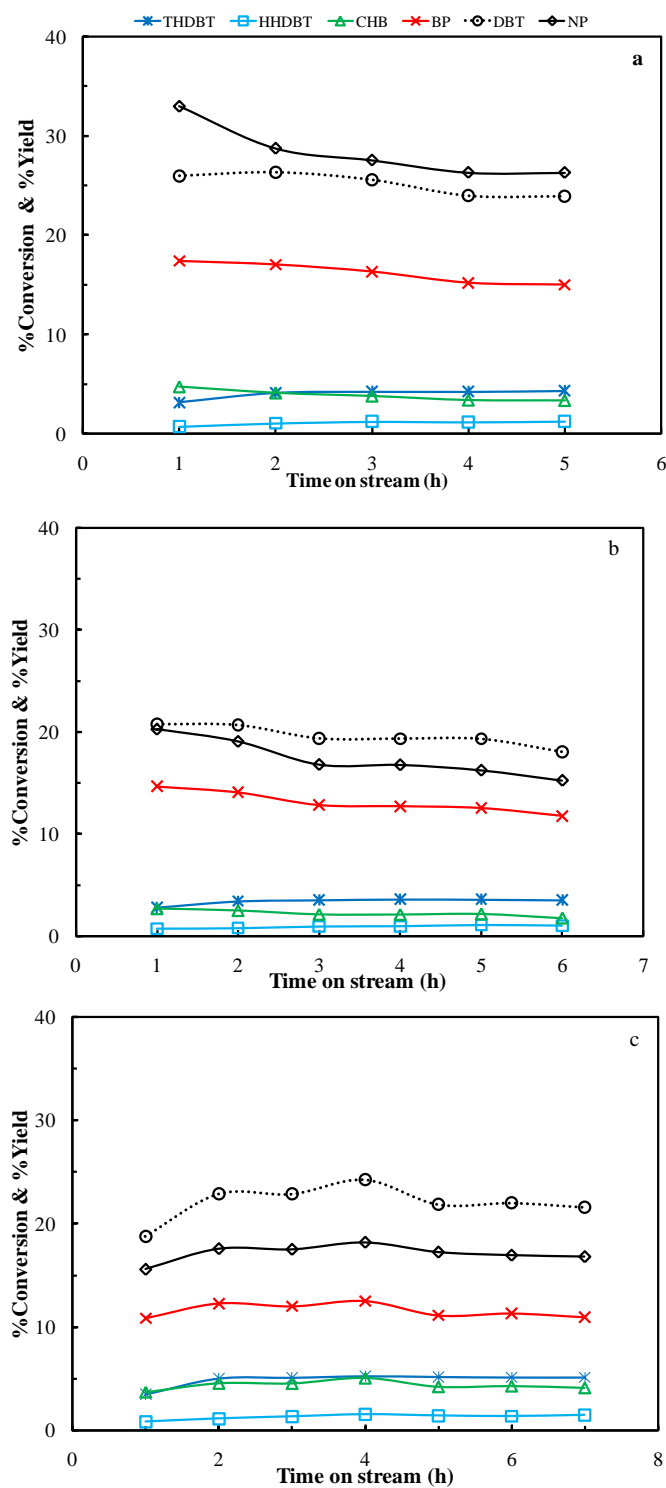
Fig. 3. Activity versus time on stream for Pd_{Cl} in the simultaneous reaction of dibenzothiophene hydrodesulfurization and naphthalene hydrogenation, as a function of the activation agent: a) Reduced in H_2 (Pd_{Cl}^H); b) reduced-sulfided in H_2S(15 vol.%)/H_2 (Pd_{Cl}^{S15}); c) sulfided with pure H_2S (Pd_{Cl}^S).

As reported in Table 5 for $Pd_{Cl}{}^{H}$, a comparison of the results in dibenzothiophene hydrodesulfurization and those obtained in the simultaneous reactions demonstrates that the presence of naphthalene inhibits HYD. Comparing Tables 4 and 5, the yields of the products from HYD (Tables 4 and 5) on the reduced sample decrease for the simultaneous reaction. Consequently, HYD selectivities, S_{HYD}^{DS} and S_{HYD}, are approximately half of those registered for the independent test. An increase in DDS can be observed comparing the $\%y_{BP}$ in Tables 4 and 5. Conversely, in this particular case, the evolution of dibenzothiophene conversion with time on stream shows a similar pattern to the one observed in the independent reaction (Figures 2a and 3a respectively). Additionally, it is remarkable that reduced Pd was more selective to naphthalene hydrogenation than to the conversion of dibenzothiophene, whether to desulfurized products ($1/S_{HDS} = 1.42$) or to all dibenzothiophene reaction products ($1/S_{DBT} = 1.1$). Nevertheless, as observed in Figure 3a, the initial conversion of naphthalene diminishes to a higher extent than the decrease in dibenzothiophene conversion.

For $Pd_{Cl}{}^{S15}$, the presence of naphthalene does not cause large changes on the performance in the hydrodesulfurization of dibenzothiophene (Figure 3b). Therefore, steady state HYD selectivities remained rather unchanged in the simultaneous reaction. Comparing the selectivity observed for $Pd_{Cl}{}^{S15}$ to the one for $Pd_{Cl}{}^{H}$ at steady state conditions (Table 5), a decrease in S_{DBT} and S_{HDS} was obtained. However, selectivity results still denote a higher favorability to the conversion of naphthalene than to the hydrodesulfurization of dibenzothiophene, i.e. conversion to desulfurized products. Similar trends in this reaction were observed for $Pd_{Cl}{}^{S}$.

Finally, comparing the selectivity trends of the sulfided samples of Pd_{Cl} (Pd_{Cl}^S and Pd_{Cl}^{S15}) to those of the reduced sample (Pd_{Cl}^H), it is observed in Table 5 that selectivity to naphthalene hydrogenation (i.e. $1/S_{HDS}$ and $1/S_{DBT}$) decreases when sulfidation was performed in the activation stage. This latter trend is similar to the one registered for HYD in the hydrodesulfurization of dibenzothiophene.

On the other hand, the average steady state activity and selectivity of the different samples of the Pt/γ-Al_2O_3 catalyst and that of the conventional $Co(Ni)$-Mo^{S15} catalysts, on both reactions, are reported in Table 6.

Table 6. Activity and selectivity of Pt/γ-Al_2O_3 (activated with different agents), CoMo, and NiMo catalysts in simultaneous HDS of dibenzothiophene and hydrogenation of naphthalene.

Catalyst code[a]	Activity				Selectivity		H_2/H_2S ratio[b]
	$\%C_{DBT}$	$\%C_{NP}$	$\%y_{BP}$	$\%y_{CHB}$	S_{DBT}	S_{HYD}	
Pt^{N*}	76	31	67	9	2.45	0.13	297
Pt^{H*}	80	41	70	10	1.95	0.14	279
Pt^{S15*}	61	25	55	6	2.44	0.11	366
Pt^{S*}	50	18	45	5	2.78	0.11	354
$NiMo^{S15}$	87	55	68	19	1.58	0.28	----
$CoMo^{S15}$	78	40	59	19	1.95	0.32	----

[a]Indexes are referred to the type of activating mixture: H = pure H_2; S15 = 15 vol% H_2S in H_2; S = pure H_2S; and N = non-activated.
[b]Used for the TPR-SRE experiments
Reaction conditions: T = 583 K; P = 5 MPa; liquid flow rate = 30 mL/h; H_2/liquid charge volume ratio = 500 NL/L.
*Data taken from A. Estupiñán [34].

In this case, the activity trend in HDS followed the order: $NiMo^{S15} > CoMo^{S15} \approx Pt^H \approx Pt^N > Pt^{S15} > Pt^S$, while in the hydrogenation of naphthalene followed the order: $NiMo^{S15} > CoMo^{S15} \approx Pt^H > Pt^N > Pt^{S15} \approx Pt^S$. It can be observed in Table 6 that the activity of the reduced and non-activated samples is similar to that of the $Co(Ni)$-Mo^{S15} catalysts for dibenzothiophene HDS. It can be seen that the use of H_2S in the activation step decreased

the activity of Pt/γ−Al$_2$O$_3$ as in the case of Pd/γ-Al$_2$O$_3$. Regarding the selectivity to HYD or to hydrodesulfurization, small differences were found among the catalysts samples. Moreover, the HYD selectivity of all of the Pt/γ-Al$_2$O$_3$ samples was lower than the conventional sulfided catalysts.

Concerning the evolution with time on stream of the performance of the samples of Pt/γ-Al$_2$O$_3$ in this catalytic test, Fig. 4 shows it. It can be observed that the activity of Pt^H (trace a) remains steady in both reactions. Pt^{S15} (trace c) shows a steady behavior in HDS and an initial increase in HDA. Pt^S (trace d) displays an initial increase in both HDS and HDA activity. The activity of the Pt^N sample (trace b) shows a similar trend to that of Pt^S.
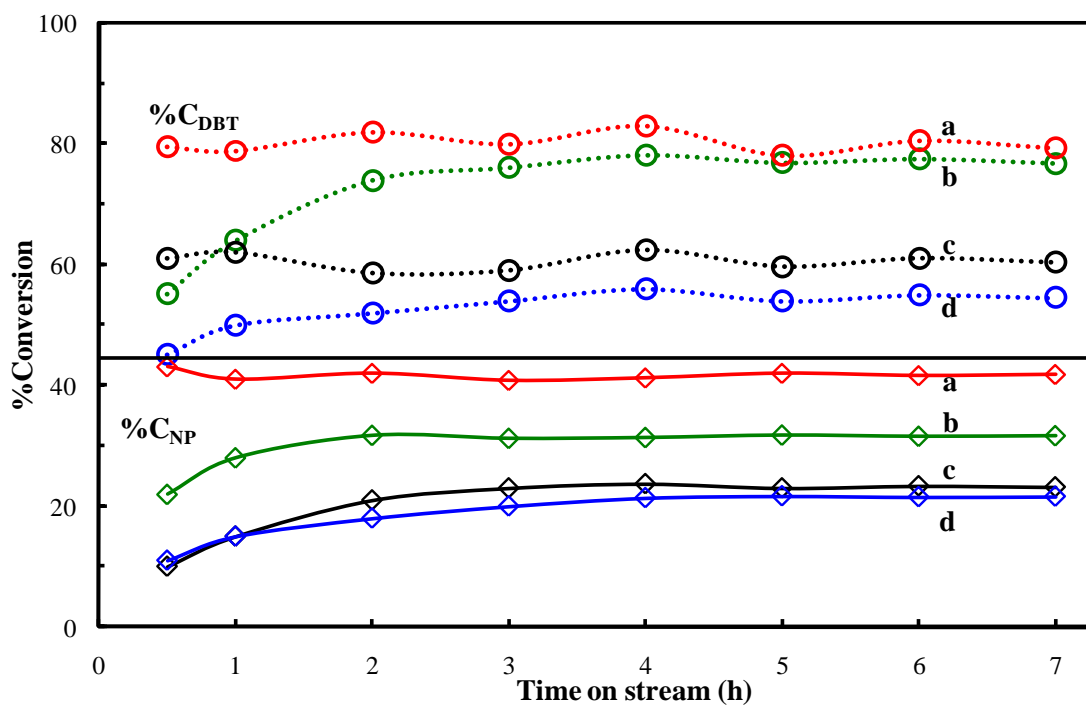
Fig. 4. Activity versus time on stream for Pt/γ-Al$_2$O$_3$: a) reduced (Pt^H); b) non-activated (Pt^N); c) reduced-sulfided (Pt^{S15}); d) sulfided with pure H$_2$S sample (Pt^S).
[*]Data taken from A. Estupiñán [34].

3.3.5. Catalytic activity and selectivity in the stability test for Pt^H.

Fig. 5 shows the catalytic performance of Pt^H in the sulfur tolerance test. Both the $\%C_{DBT}$ and the $\%C_{NP}$ decrease with increasing the H_2S concentration in the reaction environment. Nonetheless, after withdrawing the excess H_2S the catalytic activity in both reactions is reestablished to its initial extent. This behavior evidences that no poisoning of the catalyst occurs with increasing the H_2S concentration of the reaction atmosphere. On the other hand, it can be seen that the selectivity, whether HDS to naphthalene hydrogenation or DDS to HYD, of Pt^H catalyst does not experience any change during this test.
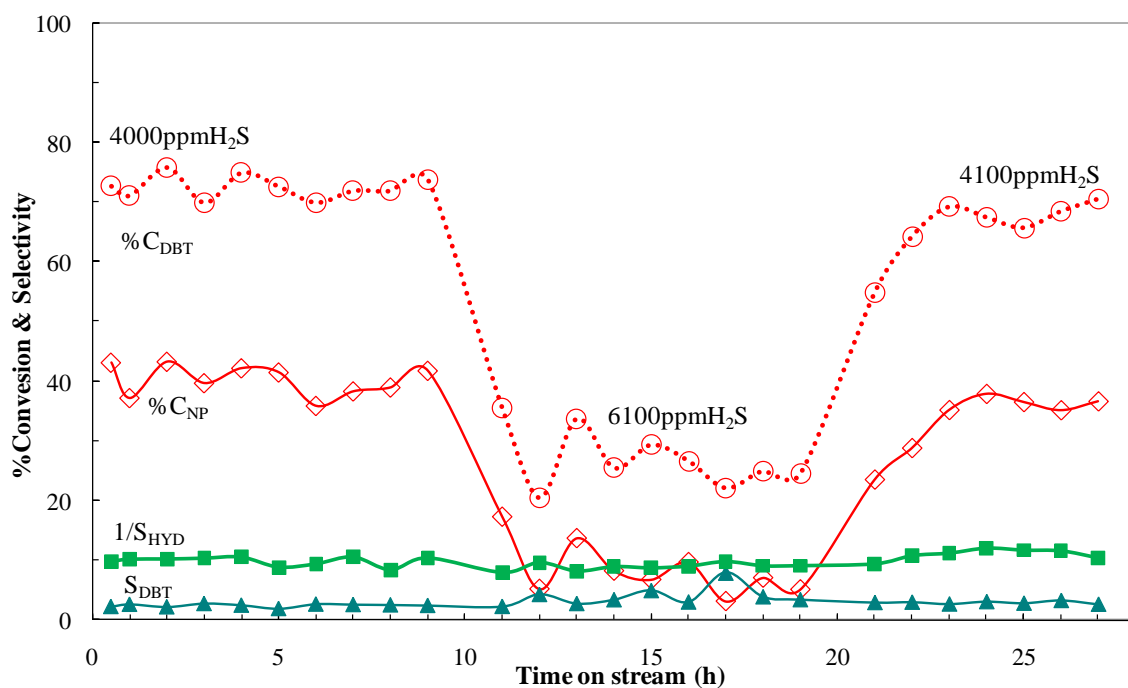
Fig. 5. Activity and selectivity as a function of time on stream for the reduced $Pt/\gamma-Al_2O_3$ catalyst (Pt^H) in the sulfur tolerance test.
[*]Data taken from A. Estupiñán [34].

4. Discussion

The discussion is focused on the reactivity of dibenzothiophene over Pd and Pt/γ-Al$_2$O$_3$ and the nature of the active phase of these two noble metals under hydrotreating reaction conditions.

4.1. Reactivity of dibenzothiophene over Pd/γ-Al$_2$O$_3$

Pd showed a high selectivity to the kinetically controlled HYD route, being highest than the one reported for MoS$_2$-based catalysts [51-54]. Selectivity trends can be explained in terms of an adsorption competition of DBT over catalyst active sites. It has been proposed that HYD comprises the formation of a π-complex between the DBT aromatic backbone and the catalyst active phase [55, 56], whereas the hydrogenolysis of the S heteroatom over MoS$_2$ is considered to proceed via perpendicular σ–adsorption. Studies on DBT desulfurization over organometallic Pt complexes have shown certain similarities to this mechanism [57]. Thus, whereas DDS can be considered to occur on a "single step", HYD comprises a series of sequential hydrogenation steps and a final hydrogenolysis of the C-S-C bond [51-53]; such mechanism is supposed to be similar as the one in DDS [52, 55]. Egorova and Prins suggested that this is only possible after desorption and re-adsorption of the HH-dibenzothiophene intermediate [52]. Considering the above discussion and the results presented so far, in this Thesis it is suggested that HYD over Pd takes place by the mechanism depicted in Scheme 1:
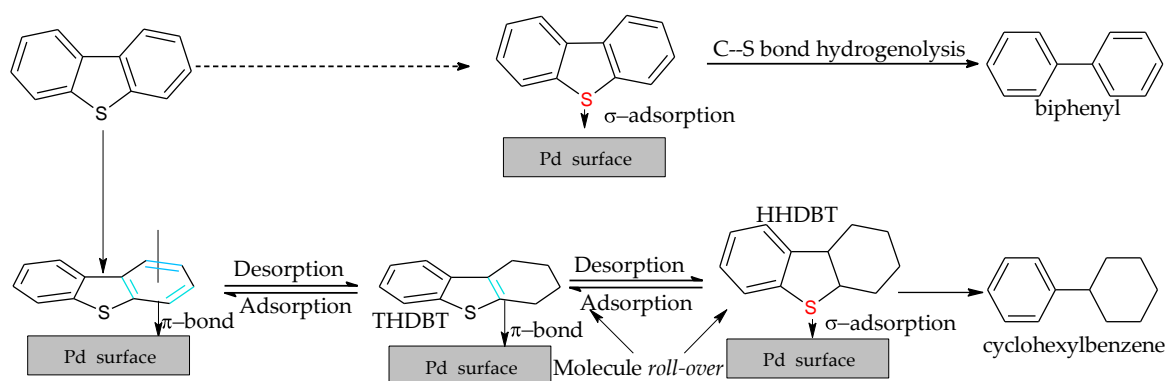
Scheme 1. Proposed reaction scheme for the conversion of dibenzothiophene over Pd.

This mechanism consists on a sequential series of adsorption-desorption steps, leading to the sequential saturation of one of the aromatic rings of DBT from TH-dibenzothiophene to HH-dibenzothiophene. Then, the HH-dibenzothiophene intermediate *rolls over* the Pd surface to make possible the C-S-C bond hydrogenolysis as in DDS. *Roll over* mechanisms have been suggested to explain aromatics hydrogenation on Pd [48, 49, 58], due to the marked stereoselectivity of this metal to *trans*-isomers. In the case of naphthalene hydrogenation, the reaction and characteristics of the active phase of this metal were analyzed long ago by Weitkamp [48]. This author demonstrated that the conversion of TTL to *trans*-decalin implies an adsorption-desorption equilibrium between the $\Delta^{9,10}$-octalin and the $\Delta^{1,9}$-octalin intermediates on the Pd surface, whereas conversion to *cis*-decalin proceeds directly from the saturation of the olefin-type bond of $\Delta^{9,10}$-octalin; the production of the *trans*-decalin isomer requires turning over of the octalin intermediate on the catalyst. The theoretical reason for this argument is that the addition of atomic H to an unsaturated bond must always occur by the same side of the molecule. Therefore, from the theoretical point of view, when *trans*-isomers are produced during a reaction, the adsorbed intermediates necessarily change their mode of coordination to the catalytic surface [48].

Inoue et al. [59] provided experimental evidence of this mechanism using the isotopic exchange of cyclopentane and deuterium over Pt/SiO_2 catalysts as a model reaction. Considering this theory, other authors have also suggested a similar reaction mechanism for aromatics hydrogenation on Pd [49, 58]. The results presented here suggest that the dibenzothiophene aromatic backbone also interacts strongly with the Pd active phase given the high yield of HYD products observed. Therefore, it is possible that both hydrogenation reactions, namely, naphthalene hydrogenation and the HYD route of hydrodesulfurization, on Pd comprise a *roll over* type mechanism.

4.2. Reactivity of dibenzothiophene over Pd and Pt/γ-Al$_2$O$_3$ in the presence of naphthalene

Selectivity changes observed in the simultaneous dibenzothiophene hydrodesulfurization and naphthalene hydrogenation reactions indicate active site competition between these two molecules. In particular, for Pd, the presence of naphthalene caused inhibition of the HYD route. Additionally, naphthalene showed a higher conversion compared to dibenzothiophene. These findings are in agreement with the mechanism proposed for the HYD route on Pd, given the assumption that the naphthalene hydrogenation mechanism shares a similar dynamics than that of HYD. Conversely, selectivity results point out the preferential hydrogenation of the olefin-type bond of naphthalene in the presence of dibenzothiophene. In naphthalene hydrogenation, the obtained results confirm that Pd is highly selective to tetralin. Weikamp ascribed this behavior to a preferential adsorption of naphthalene through the olefin-type bonds of the molecule [48]. Indeed, Pd is known to be the most selective catalyst to saturate olefin bonds attached to aromatic rings [48, 60]. This trend has also been reported in the selective hydrogenation of the olefin-type bonds of

thiophene and benzothiophene. Mashkina and Sakhaltueva [10] studied the selective hydrogenation of thiophene to TH-thiophene over a series of transition metal sulfides and found that Pd was the most active in this reaction. Zirka et al. [11] hydrogenated benzothiophene to 2,3-dihydro-benzothiophene on Pd. Therefore, as in the case of naphthalene hydrogenation to tetralin, Pd has the capacity of selectively hydrogenate the olefin bond of these S-containing molecules. Such behavior matches the selectivity shift in the hydrodesulfurization of dibenzothiophene in the presence of naphthalene. Given that it appears that DDS is favored by HYD inhibition, it seems that naphthalene presence changes the mode of adsorption of the dibenzothiophene molecule over the Pd active phase. On the other hand, for $Pt/\gamma-Al_2O_3$ the same competitive effects can be present, but in this case it is the HDS reaction which is most favored, as in an analog way as DDS is prevalent over HYD. The studies carried out in reforming catalysts point out to the fact that the sulfur heteroatom is readily hydrogenolyzed over metallic Pt catalysts [13-16, 19], therefore dibenzothiophene would be directly adsorbed through the sulfur atom on the active phase of Pt. It must be remarked that the selectivity of $Pt/\gamma-Al_2O_3$ towards DDS reaction pathway is at the same level than that of conventional Ni(Co)-Mo[S15] catalysts. This behavior has been previously documented in literature [7, 9, 31, 61]. Niquille-Röthlisberger et al. [7] found that alumina supported Pt is selective to DDS. Also. Fujikawa et al. [25] that the hydrogenation activity of Pd-Pt catalysts increased with Pd content, and concluded that the main hydrogenation active site for aromatics hydrogenation is surface Pd and not Pt.

4.3. Pd and Pt active phase under a hydrotreating environment

The behavior of Pd under hydrotreating reaction conditions strongly suggests that its active phase is possibly not constituted by sulfur vacancies, having rather a metallic nature.

The XPS results of the catalysts activated with the H_2S/H_2 mixture (Pd_{Cl}^{S15}, Pd_{Li}^{S15} and Pd_{Ac}^{S15}) show that their sulfur coverage is comparable. According to the determined S/Pd ratio and the BE of the $Pd_{3d5/2}$ peaks, their stoichiometry corresponds to PdS_x, with x < 1.5. However, Pd sulfides stoichiometry cannot be accurately determined at the present conditions because sulfur can also be retained over the γ-Al_2O_3 support [42]. Therefore, a mixture of different Pd sulfided species can be present as determined in previous studies [62-65]. According to Hensen et al. [62], activation with H_2S/H_2 can result in a mixture of metallic Pd, Pd_4S and PdS species, where, PdS is the most thermodynamically stable phase [62, 64]. On the other hand, XPS analysis of Pd_{Cl}^S, i.e. activation with pure H_2S, leads to the formation of PdS_2 [62-65] along with H_2S adsorbed on the alumina support [42]. The different Pd species obtained during the activation step can be readily transformed under the HDT reaction environment [9, 26, 62, 64-66]. This is evidenced in the evolution of the catalytic performance in the tests performed for the reduced and sulfided samples of Pd_{Cl} (Figs. 2 and 3). In such case, a dynamic equilibrium between the different Pd sulfided species, metallic Pd and the H_2S-H_2 atmosphere should be established. Considering the thermodynamic stability of Pd sulfides under H_2 atmospheres, it can be said that under the conditions used here, the equilibrium PdS_n $_{(n=1,\ 2)(s)}$ + $H_{2(g)}$ $\leftrightarrow$ $Pd_{(s)}$ + $H_2S_{(g)}$ is shifted to metallic Pd, i.e. the existence of thermodynamically stable Pd sulfide phases is not favored [62]. The same analysis can be performed for Pt/γ-Al_2O_3. Starting from the equilibrium,

$PtS_{(s)} + H_{2(g)} \leftrightarrow Pt^0_{(s)} + H_2S_{(g)}$ and using the values of standard molar enthalpy of formation and standard molar Gibbs energy of formation at 298 K [67], both, $\Delta H^0_{rxn} = 61$ kJ/mol and $\Delta G^0_{rxn} = 42.7$ kJ/mol at 298 K, can be estimated. The value of ΔH^0_{rxn} indicates that the reaction is endothermic and thus favored by increasing temperature. At T = 583 K it was calculated a $\Delta G^0_{rxn} = -25.21$ kJ/mol which shows that PtS can be readily decomposed under the conditions used here. This, of course, does not completely rules out the formation of metastable Pd and Pt sulfided phases. Such phases can be formed, especially, from irreversible adsorbed sulfur species [16], as in reforming catalysts [16, 66] or due to metal-support interactions [4, 13-15, 44]. The fact that the evolution of the activity of $Pd_{Cl}{}^H$ during the desulfurization experiments is contrary to the one of the sulfided samples ($Pd_{Cl}{}^{S15}$ and $Pd_{Cl}{}^S$) indicates reduction-sulfidation dynamics of the Pd phases occurring under the reaction atmosphere. Indeed, Kabe et al. [32] proved that regardless the noble metal, Pt or Pd, the sulfided catalysts lost most of the sulfur present on their surface during the HDS of dibenzothiophene. Conversely, the initial decrease observed in the activity of the reduced Pd_{Cl} sample, during the HDS tests, indicates that sulfidation under such conditions has a negative effect in both hydrodesulfurization and hydrogenation. Furthermore, as discussed above, it is actually the HYD route of hydrodesulfurization of DBT which is mostly affected because DDS suffers rather small changes as a function of the activating agent. These trends are in good agreement with the fact that the reduced sample of Pd_{Cl} is more thiotolerant than the sulfided catalysts ($Pd_{Cl}{}^{S15}$, $Pd_{Li}{}^{S15}$ and $Pd_{Ac}{}^{S15}$) in the hydrogenation of naphthalene. In addition, when correlating TON^{XPS} obtained for the reduced-sulfided catalysts with the BE of the $Pd_{3d5/2}$ peak, it can be said that those Pd atoms

with a higher positive shifting of BE display a better activity in hydrogenation under and H_2S atmosphere. Such behavior is similar to that reported in thiotolerance tests of reduced noble metal catalysts [16, 21, 26]. Arcoya et al. [68] found that lower electron donating $Pd^{\delta+}$ species possess a higher thiotolerance in aromatics hydrogenation compared to completely reduced metallic Pd^0 species. On the other hand, the results obtained for Pt/γ-Al_2O_3 can be interpreted in the following terms which are in accord with the remarks done above for Pd. The results of the thiotolerance test (Fig. 5) point out to the fact that H_2S, dibenzothiophene and naphthalene compete to adsorb on the same catalytic active site, where H_2S would be preferentially adsorbed over the catalyst surface, but its dissociative adsorption, to produce H^+ and SH^- species, does not lead in this case to a change of selectivity, neither to the HDS reaction compared to naphthalene hydrogenation, nor to the reaction route of dibenzothiophene. This result evidences that also over Pt, HYD is not promoted by the generation of sulfided species. When activation of Pt/γ-Al_2O_3 by sulfidation takes place the evolution of the catalytic activity (Fig. 4) follows a trend which is alike to that of Pd. Therefore, basically, also in this case a dynamic equilibrium between (metallic Pt particles) and (sulfided Pt particles) is occurring. When the catalyst is non activated such equilibrium is reached under the reaction environment. The TPR patterns of Pt^{S15}-SRE and Pt^S-SRE evidences that such mixture of metallic and sulfided Pt particles exists. This finding is in agreement with the results presented by other authors. Paál et al. [44] have presented evidence on the coexistence of metallic Pt particles and PtS in PtMo/γ-Al_2O_3 catalysts using TEM microscopy, XRD and ISS. Matsubayashi et al. [24] found using EXAFS that after sulfidation of a Pt/USY-zeolite catalyst a part of the platinum

remained as metallic Pt. Bando et al. [32] prepared Pt-Pd/Al$_2$O$_3$ and Pt-Pd/SiO$_2$ catalysts, and performed *in situ* EXAFS characterization during the simultaneous HDS of dibenzothiophene and HDA of tetralin; they detected the concurrence of sulfided and metallic Pt particles during the essays.

In conclusion, it seems that the active sites of Pd and Pt/γ-Al$_2$O$_3$ in hydrodesulfurization reactions should possess a more metallic character than expected, without discarding the existence of sulfided phases, which, from the presented evidence, have a detrimental effect in the development of HYD, as well as in naphthalene hydrogenation.

5. Conclusions

In this Chapter the development of the HYD route of hydrodesulfurization over monometallic Pd and Pt/γ-Al$_2$O$_3$ catalysts and the functionalities of these catalytic materials in hydrodesulfurization and aromatics hydrogenation were analyzed. The selected approach consisted on performing a thorough analysis of the catalytic tendencies and dynamics of a series of reaction tests with naphthalene, tetralin, and dibenzothiophene, at conditions typical of the HDT process over Pd and in analyzing some results for Pt/γ-Al$_2$O$_3$ using the thermodynamics of the sulfidation reactions of noble metals and a comparison between the mechanisms of the HYD route of hydrodesulfurization of dibenzothiophene and naphthalene hydrogenation as a basis of the aforementioned analysis. Results indicated that the development of HYD depends on the specific interactions of the dibenzothiophene molecule with the noble metals. Thus, Pt/γ-Al$_2$O$_3$ is as active as conventional Co(Ni)-Mo sulfides and even more selective to DDS than the latter, whereas Pd/γ-Al$_2$O$_3$ is moderately active but the conversion of dibenzothiophene takes place by a competition between both

DDS and HYD reaction routes. Analogously, Pt is very selective to HDS in simultaneous tests of dibenzothiophene hydrodesulfurization - naphthalene hydrogenation, while the reactivity of both dibenzothiophene and naphthalene over Pd is more competitive. Furthermore, the results of the simultaneous catalytic tests evidenced the existence of adsorption competition effects between naphthalene and dibenzothiophene. The trends registered for Pd showed a specific competition between the hydrogenation of the aromatic and the HYD route of hydrodesulfurization. On the basis of a comparison between the mechanism of naphthalene hydrogenation over Pd and the mechanistic dynamics of HYD, it was suggested that HYD takes place by a sequential adsorption – desorption equilibrium followed by *roll over* of the partially hydrogenated intermediates of dibenzothiophene over the catalytic surface.

On the other hand, both Pd and Pt exhibited the best catalytic performance when activated by hydrogen reduction. The sulfidation of the catalysts in the activation stage negatively impacted the catalytic performance of both noble metals. The concomitant analysis of the evolution of the catalytic performance the thermodynamics of the sulfidation - reduction reactions of Pd and Pt, and some results of characterization evidenced that under the HDT reaction environment a change in the relative distribution of noble metal sulfided particles and metallic ones occurs. The results of such analysis indicated that the active phase of Pd and Pt has the character of a metallic active phase. Finally, it must be pointed out that sulfidation deters the development of HYD.

References

[1] R.G. Leliveld, S.E. Eijsbouts, Catal. Today 130 (2008) 183.

[2] R. Shafi, G.J. Hutchings, Catal. Today 59 (2000) 423.

[3] F. Bataille, J.-L. Lemberton, P. Michaud, G. Pérot, M. Vrinat, M. Lemaire, E. Schulz, M. Breysse, S. Kasztelan, J. Catal. 191 (2000) 409.

[4] T.A. Pecoraro, R.R. Chianelli, J. Catal. 67 (1981) 430.

[5] R.R. Chianelli, T.A. Pecoraro, T.R. Halbert, W.-H. Pan, E.I. Stiefel, J. Catal. 86 (1984) 226.

[6] H.R. Reinhoudt, R. Troost, A.D. van Langeveld, S.T. Sie, J.A.R. van Veen, J.A. Moulijn, Fuel Proc. Tech. 61 (1999) 133.

[7] A. Niquille-Röthlisberger, R. Prins, J. Catal. 242 (2006) 207.

[8] V.L. Barrio, P.L. Arias, J.F. Cambra, M.B. Güemez, B. Pawelec, J.L.G. Fierro, Fuel 82 (2003) 501.

[9] T. Kabe, W. Qian, Y. Hirai, L. Li, A. Ishihara, J. Catal. 190 (2000) 191.

[10] A.V. Mashkina, L.G. Sakhaltueva, Kin. Catal. 43 (2002) 107.

[11] A.A. Zirka, G.L. Ryzhova, Yu.G. Slizhov, A.V. Mashkina, React. Kinet. Catal. Lett. 23 (1983) 7.

[12] A. Röthlisberger, R. Prins, J. Catal. 235 (2005) 229.

[13] C.R. Apesteguía, J. Barbier, J.F. Plaza De Los Reyes, T.F. Garetto, J.M. Parera, Appl. Catal. 1 (1981) 159.

[14] C.R. Apesteguía, J. Barbier, J. Catal. 78 (1982) 352.

[15] C.R. Apesteguía, T.F. Garetto, C.E. Brema, J.M. Parera, Appl. Catal. 10 (1984) 291.

[16] C.R. Apesteguía, J.F. Plaza De Los Reyes, T.F. Garetto, J.M. Parera, Appl. Catal. 4 (1982) 5.

[17] J. Barbier, P. Marecot, L. Tifouti, M. Guenin, R. Frety, Appl. Catal. 19 (1985) 375.

[18] L. Pönitzsch, M. Wilde, P. Tétényi, M. Dobrovolszky, Z. Paál, Appl. Catal. A: Gen. 86 (1992) 115.

[19] P.G. Menon, G.B. Marin, G.F. Froment, Ind. Eng. Chem. Prod. Res. Dev. 21 (1982) 52.

[20] J.B. McKinley, Catalysis, In: P.H. Emmett (Ed), Vol. 5, Reinhold (1957) New York.

[21] A. Stanislaus, B.H. Cooper, Catal. Rev.-Sci. Eng. 36 (1994) 75.

[22] H. Du, C. Fairbridge, H. Yang, Z. Ring, Appl. Catal. A: Gen. 294 (2005) 1.

[23] H.Yasuda, Y. Yoshimura, Catal. Lett. 46 (1997) 43.

[24] N. Matsubayashi, H. Yasuda, M. Imamura, Y. Yoshimura, Catal. Today 45 (1998) 375.

[25] T. Fujikawa, K. Tsuji K, H. Mizuguchi, H. Godo, K. Idei, K. Usui, Catal. Lett. 63 (1999) 27.

[26] Y. Yoshimura, M. Toba, T. Matsui, M. Harada, Y. Ichihashi, K.K. Bando, H. Yasuda, H. Ishihara, Y. Morita, T. Kameoka, Appl. Catal. A: Gen. 322 (2007) 152.

[27] R.M. Navarro, B. Pawelec, J.M. Trejo, R. Mariscal, J.L.G. Fierro, J. Catal. 189 (2000) 184.

[28] V.L. Barrio, P.L. Arias, J.F. Cambra, M.B. Güemez, B. Pawelec, J.L.G. Fierro, Catal. Commun. 5 (2004) 173.

[29] S. Albertazzi, G. Busca, E. Finocchio, R. Glöckler, A. Vaccari, J. Catal. 223 (2004) 372.

[30] H.R. Reinhoudt, R. Troost, A.D. van Langeveld, S.T. Sie, J.A.R. van Veen, J.A. Moulijn, H.R. Reinhoudt, R. Troost, A.D. van Langeveld, S.T. Sie, J.A.R. van Veen, J.A. Moulijn, Fuel. Proc. Techn. 61 (1999) 133.

[31] R. Navarro, B. Pawelec, J.L.G. Fierro, P.T. Vasudevan, J.F. Cambra, M.B. Guemez, P.L. Arias, Fuel. Proc. Techn. 61 (1999) 73.

[32] K.K. Bando, T. Kawai, K. Asakura, T. Matsui, L. Le Bihan, H. Yasuda, Y. Yoshimura, S.T. Oyama, Catal. Today 111 (2006) 199.

[33] Cr. Conţescu, M.I. Vass, Appl. Catal. 33 (1987) 259.

[34] A. Estupiñán, Master Thesis, Escuela de Ingeniería Química, Centro de Investigaciones en Catálisis, Universidad Industrial de Santander, Bucaramanga (2008).

[35] L. Portela, P. Grange, B. Delmon, J. Catal. 156 (1995) 243.

[36] M.A. Soria, P. Ruiz, E.M. Gaigneaux, Catal. Today 128 (2007) 168.

[37] S. Texier, G. Berhault, G. Pérot, F. Diehl, Appl. Catal. A: Gen. 293 (2005) 105.

[38] M. Vrinat, D. Letourneur, R. Bacaud, V. Harlé, B. Jouguet, C. Leclercq, Stud. Surf. Sci. Catal. 127 (1999) 153.

[39] P. Grange, Catal. Rev. -Sci. Eng. 21 (1980)135.

[40] Y. Matsumoto, M. Soma, T. Onishi, K. Tamaru, J. Chem. Soc., Faraday Trans. I 76 (1980) 1122.

[41] J.A. Rodriguez, S. Chaturvedi, T. Jirsak, Chem. Phys. Lett. 296 (1998) 421.

[42] O. Saur, T. Chevreau, J. Lamotte, J. Travert, J.-C. Lavalley, J. Chem. Soc., Faraday Trans. I 77 (1981) 427.

[43] J. Oudar, Catal. Rev.-Sci. Eng. 22 (1980) 171.

[44] Z. Paál, P. Tétényi, M. Muhler, U. Wild, J.-M. Manoli, C. Potvin, J. Chem. Soc., Faraday Trans. 94 (1998) 459.

[45] S.A. Giraldo de León, P. Grange, B. Delmon, Catal. Lett. 47 (1997) 51.

[46] P.J. Mangnus, A. Riezebos, A.D. Vanlangeveld, J.A. Moulijn, J. Catal. 151 (1995) 178.

[47] D. Pérez-Martínez, S.A. Giraldo, A. Centeno, Appl. Catal. A: Gen. 315 (2006) 35.

[48] A.W. Weitkamp, Adv. Catal. 18 (1968) 1.

[49] S. Dokjampa, T. Rirksomboon, S. Osuwan, S. Jongpatiwut, D.E. Resasco, Catal. Today 123 (2007) 218.

[50] M.L. Vrinat, Appl. Catal. 6 (1983) 137.

[51] V. Vanrysselberghe, G.F. Froment, Ind. Eng. Chem. Res. 35 (1996) 3311.

[52] M. Egorova, R. Prins, J. Catal. 225 (2004) 417.

[53] M. Houalla, N.K. Nag, A.V. Sapre, D.H. Broderick, B.C. Gates, AlChE J. 24 (1978) 1015.

[54] T.A. Zepeda, B. Pawelec, J.L.G. Fierro, A. Olivas, S. Fuentes, T. Halachev, Micropor. Mesopor. Mater. 111 (2008) 157.

[55] N.K. Nag, Appl. Catal. 10 (1984) 53.

[56] S. Cristol, J.-F. Paul, E. Payen, D. Bougeard, F. Hutschka, S. Clémendot, J. Catal. 224 (2004) 138.

[57] A. Iretskii, J.J. García, G. Picazo, P.M. Maitlis, Catal. Lett. 51 (1998) 129.

[58] A.K. Neyestanaki, P. Mäki-Arvela, H. Backman, H. Karhu, T. Salmi, J. Väyrynen, D. Yu. Murzin, J. Mol. Catal. A: Chem. 193 (2003) 237.

[59] Y. Inuoe, J.M. Herrmann, H. Schmidt, R.L. Burwell, J.B. Butt, J.B. Cohen, J. Catal. 53 (1978) 401.

[60] H.-U. Blaser, A. Indolese, A. Schnyder, H. Steiner, M. Studer, J. Mol. Catal. A: Chem. 173 (2001) 3.

[61] E. Dhainaut, H. Charcosset, C. Cachet, L. de Mourgues, Appl. Catal. 2 (1982) 75.

[62] E.J.M. Hensen, H.J.A. Brans, G.M.H.J. Lardinois, V.H.J. de Beer, J.A.R. van Veen, R.A. van Santen, J. Catal. 192 (2000) 98.

[63] M. Zdražil, Catal. Today 3 (1988) 269.

[64] A. Vázquez, M.J. Yañez, S. Fuentes, M. Avalos-Borja, Catal. Lett. 28 (1994) 351.

[65] Z. Paál, T. Koltai, K. Matusek, J.-M. Manoli, C. Potvin, M. Muhler, U. Wild, P. Tétényi, Phys. Chem. Chem. Phys. 3 (2001) 1535.

[66] J.M. Parera, C.R. Aspesteguia, J.F. Plaza de los Reyes, T.F. Garetto, React. Kinet. Catal. Lett. 15 (1980) 167.

[67] D.R. Lide (ed), CRC Handbook of Chemistry & Physics 5 (2006-2007).

[68] A. Arcoya, X.L. Seoane, N.S. Figoli, P.C. L'Argentiere, Appl. Catal. 62 (1990) 35.

[69] Z. Paál, P. Tétényi, M. Muhler, U. Wild, J.-M. Manoli, C. Potvin, J. Chem. Soc., Faraday Trans. 94 (1998) 459.

Chapter III: Designing an efficient catalytic system for the selective hydrodesulfurization of dibenzothiophenes

Abstract

In this Chapter it is proven that the selectivity HYD/DDS during the hydrodesulfurization of dibenzothiophene over bimetallic Pd-Pt/γ-Al$_2$O$_3$ catalysts can be controlled with the Pd/(Pd+Pt) atomic ratio of this type of alloy. Moreover, a synergetic effect exists in the development of HYD over Pd-Pt/γ-Al$_2$O$_3$ which is in correspondence with the one observed in the hydrogenation of aromatic molecules under H$_2$S and with the stereoselectivity *trans*-decalin/*cis*-decalin trend during the hydrogenation of naphthalene. In order to establish the nature of this synergetic effect, naphthalene hydrogenation was used as an alternative *in situ* characterization method (Part I) later on complemented with other techniques (Part II). The analysis of these results indicated that the presence of Pd$^{\delta+}$ surface particles in the Pd-Pt alloyed particles and the H$_2$ uptake capacity of Pd-Pt are crucial factors for the development of HYD.

The stability of these catalytic materials under different reaction conditions was analyzed. It was found that: (i) naphthalene does not significantly inhibit the HYD route; (ii) H$_2$S can specifically inhibit the C-S-C bond scission step of both hydrodesulfurization reaction pathways; (iii) coke deposition has a poisoning effect on those functionalities of Pd-Pt related to HYD.

Part I: Hydrogenation of aromatic rings over Pd-Pt catalysts.

Abstract

The hydrogenation of naphthalene, at usual hydrotreatment reaction conditions, was used as a model reaction to determine the properties of the hydrogenation function and the characteristics of Pd-Pt/γ-Al$_2$O$_3$ catalysts in HDT as a function of the Pd/(Pd+Pt) molar ratio. Naphthalene hydrogenation was performed in the absence and in the presence of H$_2$S. The selectivity trends reflected changes in the interaction between the aromatic molecule and the catalytic active phase as a function of the Pd/(Pd+Pt) molar ratio which were correlated with the naphthalene reaction mechanism. Therefore, the model reaction served as a qualitative descriptor of phenomena such as Pd surface enrichment of the alloyed Pd-Pt clusters and Pd like catalytic behavior of the Pd-Pt active phase in hydrotreatment reactions, often reported in literature. The effects of coke deposition during naphthalene hydrogenation and the presence of H$_2$S were also interpreted in terms of changes in the dynamics of the mechanism of naphthalene hydrogenation.

Keywords: Pd-Pt catalysts; molar ratio influence; Naphthalene hydrogenation; selectivity; stereoselectivity.

1. Introduction

Deep hydrodesulfurization requires the development of alternative routes of desulfurization to withdraw the sulfur heteroatom from sterically hindered di-β-dibenzothiophenes [1-3]. The HDS of these molecules proceeds mostly via the HYD route of hydrodesulfurization [3, 4]. HYD implies flat π-bonding of one of the benzene rings of DBT to catalyst's active sites [5-7]; such as those formed during aromatics hydrogenation [8]. Therefore, studying the hydrogenation of aromatic rings can provide valuable information for understanding the HYD route of hydrodesulfurization of dibenzothiophenes. Moreover, parallel hydrodearomatization (HDA) reactions take place during deep HDS [1].

In order to use classical Co-(Ni)-Mo(W)S$_2$ formulations in deep HDS it is necessary to design and build new units operating at very low space velocities and being provided with secondary reactors [9]. Noble metal based catalysts possess superior hydrogenating capacity and their alloys can overcome H$_2$S poisoning [10, 11]. Pd-Pt catalysts are highly thiotolerant [11] and more active in the hydrodesulfurization of 4,6-dimethyl-DBT than conventional Co-(Ni)-Mo(W)S$_2$ catalysts [12], because they can hydrodesulfurize this molecule via HYD [13]. During the late 70's the formation of an alloy between Pd and Pt in the surface of supported Pd-Pt catalysts was proved [14, 15]. Pd surface enrichment of the alloyed Pd-Pt clusters under HDT environments has been observed [16]. In addition, there is a relationship between the composition, the geometrical arrangement of the Pd-Pt surface and the adsorption competition between H$_2$ and H$_2$S [17]. To investigate the properties of Pd, Pt and Pd-Pt catalysts under real HDT conditions the use of naphthalene hydrogenation as a model reaction has been proposed [16, 18]. The advantage of this method is that the mechanism of naphthalene hydrogenation is well known, and the registered selectivity

trends have been associated to changes in the strength of the interaction between the aromatic nucleus and the catalytic active phase [19-21]. Weitkamp [19] proposed that a high selectivity to tetralin (TTL) or to *trans*-decalin (*trans*-DCL) implies strong interactions between the catalytic surface and the aromatic backbone of naphthalene. Highly active hydrogenating catalysts, such as Pt, are always more selective to *cis*-decalin and yield low amounts of tetralin [19, 20]. As demonstrated in Chapter II, Pd, which has a lower hydrogenation activity, is particularly selective to both tetralin and *trans*-decalin [19-21]. Furthermore, based on such stereoselectivity difference, Yoshimura et al. [16] showed that the active phase of Pd-Pt displayed a Pd-like behavior when the Pd/(Pd+Pt) molar ratio of the catalyst is fixed at 0.8. Therefore, naphthalene hydrogenation constitutes a powerful tool to investigate the hydrogenation function of Pd-Pt systems under HDT environments as well as it can provide a useful qualitative description of the interaction between the Pd-Pt active phase and aromatic backbones. This information also serves as a fundamental basis to comprehend some of the factors which play a significant role in the development of HYD. Consequently, it was decided to analyze the performance of Pd-Pt/γ-Al$_2$O$_3$ in naphthalene hydrogenation as a function of the Pd/(Pd+Pt) molar ratio under different reaction conditions to establish which functionalities of these catalytic systems allow them to develop HYD [12, 13, 22].

2. Experimental

2.1. Catalyst preparation

A series of bimetallic Pd-Pt/γ-Al$_2$O$_3$ catalysts of different Pd/(Pd+Pt) molar ratios were prepared by incipient wetness co-impregnation. An aqueous solution of PdCl$_2$ and H$_2$PtCl$_6$.4H$_2$O (both provided by Sigma-Aldrich), containing the desired amounts of Pt and

Pd, was prepared and impregnated onto the *Procatalyse* γ-Al$_2$O$_3$ support using a 20% excess of the impregnating solution as referred to the support's pore volume. The wetted solid was dried at ambient conditions for one day. Then, it was dried at 393 K for 12 h and calcined at 773 K for 4 h in air flow. The Pd/(Pd+Pt) molar ratio was varied from 0 (pure Pt) to 1 (pure Pd). Catalysts were labeled according to their real metallic contents as shown in parenthesis after the corresponding metal.

2.2. Catalysts activation

Catalysts were in situ activated before catalytic tests. Samples of 0.5 g of the calcined catalysts were dried at 393 K under N$_2$ flow for 1 h, and subsequently, they were reduced in hydrogen flow (100 mL/min) at 673 K for 3h.

2.3. Catalysts characterization

2.3.1. Metallic contents and textural properties

The metallic contents of the catalysts were established by atomic absorption technique in a 2380 Perking Elmer spectrometer following the ASTM 1977-91 standard. BET surface area, pore volume, distribution and pore size; using the BJH method, were determined by nitrogen adsorption-desorption isotherms in a Nova 1300 (Quantachrome) apparatus.

2.3.2. TGA profiles of spent catalysts

TGA profiles of the catalysts spent on the hydrogenation of NP, without the presence of H$_2$S, were obtained in a 2050 TGA apparatus from TA Instrument, to determine the presence of carbonaceous residua from the reactions. Previous to TGA analysis, spent catalysts were subjected to Soxhlet extraction during 24 h, using cyclohexane as solvent, as to remove different residua from reaction tests. TGA analysis consisted on heating the samples from room temperature until 473 K under N$_2$ and held for 30 min at such

conditions. Then N_2 was switch-off allowing O_2 flow and heating until 873 K at a rate of 10 K/min. This temperature was kept until constant sample weight.

2.4. Catalytic tests

The hydrogenation of naphthalene (commercial grade) was studied without and in the presence of H_2S. Reaction conditions were chosen according to the following criteria: to recreate the conditions of temperature and pressure of a typical hydrotreatment reactor, to avoid thermodynamic limitations in hydrogenation [10] and to obtain a constant *trans*-decalin to *cis*-decalin ratio far from the conditions at which *cis*-decalin can isomerize to *trans*-decalin [20, 23]. In addition, to permit a proper analysis of the *trans*-decalin to *cis*-decalin stereoselectivity (S_{trans-}) naphthalene conversion was kept close or at 100% in the absence of H_2S, to discard the possible self-inhibitory effect of naphthalene in the complete saturation of the tetralin intermediate to decalins [10, 23].

The composition of the liquid charge was 3 wt.% naphthalene and 2 wt.% hexadecane, as chromatography internal standard, dissolved in cyclohexane. Reaction conditions and the quantitative analysis of the products of reaction were described in Chapter II. Temperature was varied in the range 503 - 583K.

An additional test was performed by adding dibenzothiophene to the liquid feed (2 wt.%) during a typical hydrogenation test performed at 583 K on a selected Pd-Pt/γ-Al_2O_3 catalyst (Pd/(Pd+Pt) molar ratio = 0.8) working under steady state conditions. The catalytic results were expressed as presented in Chapter II, Section 2.4.3.

3. Results and discussion

3.1. Metallic contents and textural properties of the catalysts

Table 1 shows the metallic contents, Pd/(Pd+Pt) molar ratios, and textural properties of the prepared Pd-Pt catalysts. It can be seen that the textural properties of the catalysts are not very different from those of the bare γ-Al$_2$O$_3$ support. These results show that the incorporation of Pd and Pt to the support does not negatively influences the final textural properties of the catalysts, in spite of the strong pH (pH = 0 - 1) of the impregnating solutions prepared from chlorides which can cause alumina dissolution during the impregnation process [24].

Table 1. Metallic contents and textural properties of the prepared Pd-Pt/γ-Al$_2$O$_3$ catalysts as measured by atomic absorption and nitrogen adsorption isotherms, respectively.

Catalyst[†]	Pd/(Pd+Pt) molar ratio	BET surface area (m^2/g)	Average pore diameter (Å)	Pore volume (cm^3/g)
γ-Al$_2$O$_3$	---	211.4	111.9	0.6
Pt(1.3)	0.0	196.9	111.1	0.6
Pd(0.2)-Pt(1.5)	0.2	196.4	112.0	0.5
Pd(0.7)-Pt(0.9)	0.6	199.9	111.0	0.6
Pd(1.0)-Pt(0.5)	0.8	199.2	112.0	0.6
Pd(1.4)-Pt(0.3)	0.9	205.6	111.1	0.6
Pd(1.9)	1.0	200.6	109.8	0.6

[†]Metallic contents (wt.%), as determined from atomic absorption, are indicated in parentheses.

3.2. Catalytic tests

The results obtained in the hydrogenation of naphthalene without the presence of H$_2$S as a function of the Pd/(Pd+Pt) molar ratio will be discussed first analyzing the selectivity trends registered from the standpoint of the functionalities of the Pd-Pt catalysts as

interpreted from mechanistic considerations for the hydrogenation reaction. Then the effect of H_2S will be analyzed.

3.2.1. *Naphthalene hydrogenation without the presence of H_2S*

Reaction products detected in these tests were tetralin, *cis*-decalin and *trans*-decalin. Table 2 shows the steady state catalytic and selectivity of the monometallic Pt(1.3) and Pd(1.9) catalysts as a function of reaction temperature.

Table 2. Steady state catalytic activity and selectivity of monometallic γ-Al_2O_3 supported Pt and Pd catalysts as a function of reaction temperature.

Catalyst	Temperature (K)	$\%C_{NP}$	$\%y_{TTL}$	$\%y_{cis\text{-}DCL}$	$\%y_{trans\text{-}DCL}$	$S_{trans\text{-}}$
	583	100.0	1.3	21.1	77.6	3.7
Pt(1.3)	563	100.0	4.2	33.1	62.7	1.9
	503	93.1	77.5	8.0	7.5	0.9
Pd(1.9)	583	97.9	94.6	0.7	2.6	3.7
	543	88.7	87.7	0.2	0.8	3.5

At 583 and 563 K, Pt(1.3) is highly active and selective to decalins. The fact that at these temperatures the $S_{trans\text{-}}$ is higher than 1 for Pt indicates that, in this case, isomerization of *cis*-decalin to *trans*-decalin is occurring [20, 23]. Calculations presented in literature indicate that *trans*-decalin is the thermodynamically favored isomer [19], and when the conversion of tetralin is high (as it is indicated by the low $\%y_{TTL}$ at 583 and 563 K) *cis*-decalin is converted to *trans*-decalin. Only at 503 K, in which the yield to decalins is lower than 20%, the $S_{trans\text{-}}$ ratio was found to be close to 1 which is the value usually reported in literature [19, 20, 23]. Therefore, at this temperature it can be assumed that no further isomerization of *cis*-decalin to *trans*-decalin for Pt is taking place, and thus the stereoselectivity registered corresponds to that intrinsically related to the properties of the

active phase and not to isomerization due to mere thermal effects. On the other hand, the

results for Pd indicated a low conversion of tetralin to decalins. This guaranties the absence

of further thermal isomerization of *cis*-decalin to *trans*-decalin. Pd is always selective to

trans-decalin; with S_{trans-} values of 3.7 at 583 K and 3.5 at 543 K. Therefore, for Pd

reaction temperature does not to significantly modify S_{trans-} stereoselectivity because of the

low conversion of tetralin to decalins. Other authors have reported similar values of

stereoselectivity [19]. As previously appointed, the selectivity in the hydrogenation of

naphthalene provides qualitative information on the interaction between an aromatic

nucleus and a catalytic surface [16, 18, 19, 21]. naphthalene hydrogenation consists of a

series of dehydrogenation-hydrogenation adsorption-desorption equilibrium steps leading

to stepwise saturation from naphthalene to tetralin then to decalins, passing through

intermediates such as $\Delta^{9,10}$-octalin and $\Delta^{1,9}$-octalin [19] (Scheme 1).
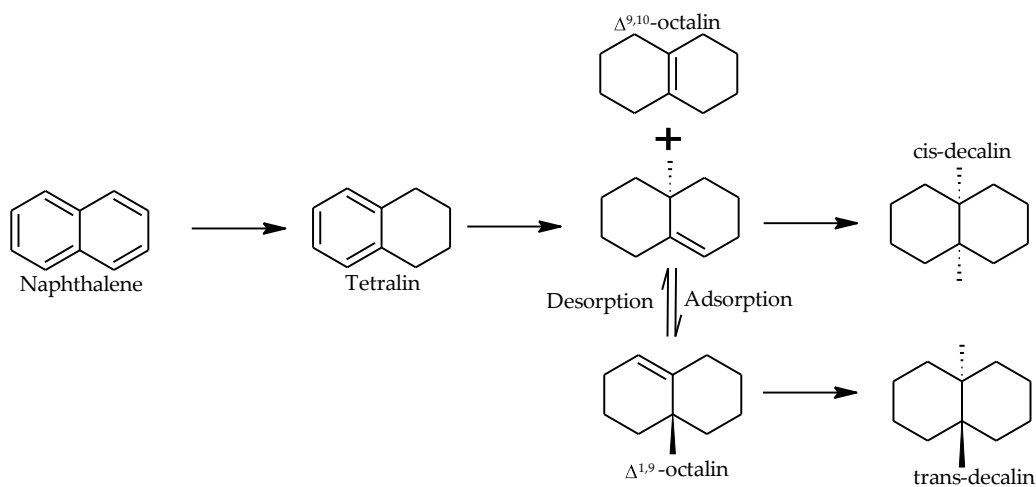
Scheme 1. Reaction mechanism of naphthalene hydrogenation [19].

Decalins stereoselectivity is determined by the strength of the interaction of the octalin

intermediates with the catalytic surface. A theoretical reason for this assumption is that the

92

addition of atomic H can only occur by the same side of the molecule (i.e. *syn* mode). Thus, the production of *trans*-decalin implies desorption and re-adsorption of the intermediate by its opposite side [19]. This has been associated to the *roll over* phenomenon and mechanism [25]. Moreover, the same mechanism has been found to operate for the hydrogenation of other aromatic molecules over Pd [26]. In addition, the high selectivity of Pd to tetralin is ascribed to an adsorption of naphthalene by their olefin type bonds [18]. This assumption is very well founded on the fact that this is the only metal able to selectively hydrogenate olefins in the presence of aromatics [18, 27]. As Pd is always more selective to tetralin and to *trans*-decalin compared to Pt (Table 2) it can be inferred that this metal has a stronger interaction with the aromatic nucleus than the latter [18, 20, 23].

The effect of the Pd/(Pd+Pt) molar ratio in the S_{trans-} stereoselectivity was studied under those conditions which guaranty no further isomerization of *cis*-decalin to *trans*-decalin. The results are presented in Fig. 1. Accordingly, the S_{trans-} values for the monometallic Pt and Pd catalysts reported in Fig. 1 correspond to those measured at 503 K for Pt and 543 K for Pd, respectively. Taking advantage of the initial deactivation of the bimetallic Pd-Pt catalysts (as it will be discuss later), which led to decalins yields lower than 20%, the S_{trans-} ratios, in this case, were determined at 543 K after reaching steady state conversions.
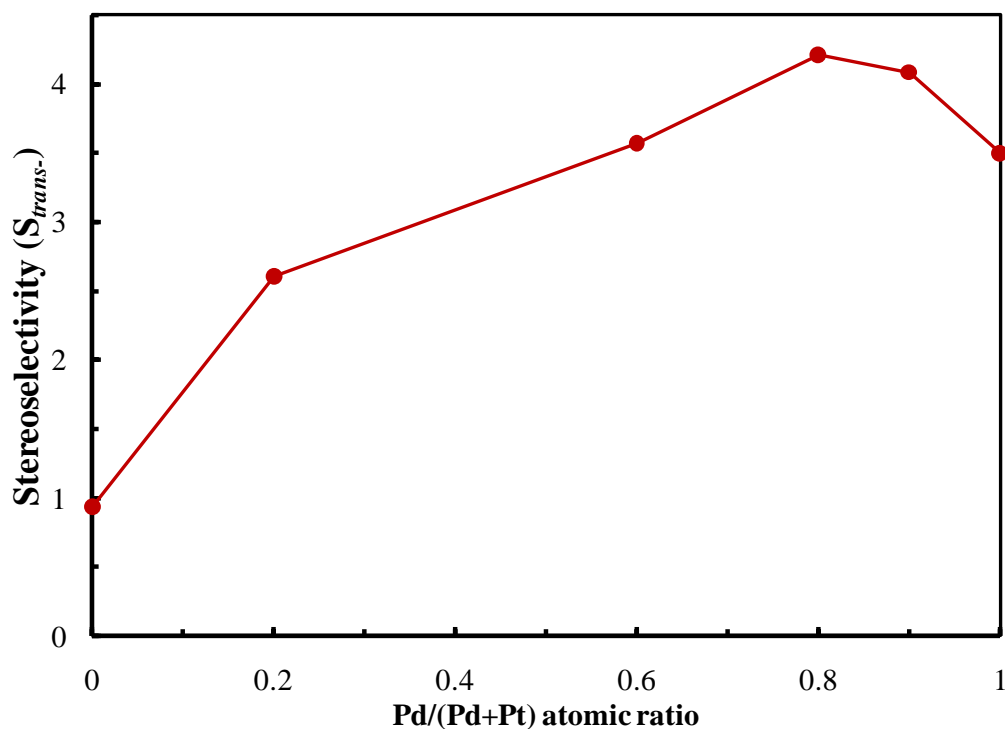
Fig. 1. Steroselectivity *trans*-decalin to *cis*-decalin (S_{trans-}) as a function of the Pd/(Pd+Pt) molar ratio for Pd-Pt/γ-Al$_2$O$_3$ catalysts during the hydrogenation of naphthalene. Reaction conditions: T = 503 K for Pt(1.3); T = 543 K for monometallic Pd(1.9) and bimetallic Pd-Pt catalysts, P = 5 MPa, liquid feed flow 30 mL/h, H$_2$/liquid feed ratio = 500 NL/L.

It is observed that S_{trans-} increases according to the higher concentration of Pd in the bimetallic catalysts. Even at a very low Pd concentration, i.e. Pd/(Pd+Pt) molar ratio of 0.2, the system displays a higher selectivity to the *trans*-decalin isomer. For the catalysts with higher Pd contents S_{trans-} is between 3.5 and 4.0, with a slightly higher S_{trans-} value for the catalyst with a Pd/(Pd+Pt) atomic ratio of 0.8. S_{trans-} ratios for the bimetallic Pd-Pt catalysts tend to approach that of monometallic Pd as the Pd concentration increases. This trend is similar to that reported by Guillon et al. [28] for the stereoselectivity in *o*-xylene hydrogenation. From the point of view of the interaction between the naphthalene molecule and the Pd-Pt active phase, the behavior presented in Fig. 1 is directly related to changes in the dynamics of the mechanism of hydrogenation. Such changes can be correlated to earlier

catalytic results concerning dehydrogenation reactions over Pd-Pt catalysts [14, 15, 29]. The works of Gomez and co-workers [14, 15, 29] led to the conclusion that the use of supported Pd-Pt alloys decrease the activity in catalytic dehydrogenation to a high extent as compared to pure Pt depending on the Pd/(Pd+Pt) molar ratio [15]. This catalytic property of the Pd-Pt system is well reflected by the changes in decalins stereoselectivity registered here. Indeed, as mentioned before, the stereoselectivity in the hydrogenation of naphthalene is directly controlled by an adsorption-desorption equilibrium comprising a series of hydrogenation-dehydrogenation steps between the different partially hydrogenated intermediates [19]. Therefore, the changes in stereoselectivity observed in Fig. 1 can be directly related to changes in the strength of the interaction between the aromatic structures and the Pd-Pt surface and to a modification in the dynamics of the above mentioned equilibrium occurring during naphthalene hydrogenation. Such changes can thus be controlled only by a modification of the Pd/(Pd+Pt) molar ratio. Dokjampa et al. [20] proposed that the differences in *trans-* to *cis-* stereoselectivity are intrinsically associated to the rate of hydrogenation of the octalin intermediates over the catalytic surface, i.e. the rate of hydrogen activation and transfer from the metal to the aromatic backbone. Indeed, the results of H_2 uptake for the bimetallic Pd-Pt alloys [22] displayed a volcano type plot as a function of the Pd/(Pd+Pt) molar ratio comparable to the trend in *trans-* to *cis-* stereoselectivity (Fig. 1).

Hydrogenation-dehydrogenation equilibrium in aromatics hydrogenation reactions have been demonstrated to conduct to coke deposition over alumina supported noble metal catalysts prepared from chlorided precursors [30, 31]. In general, all of the prepared Pd-Pt catalysts were found to retain surface chlorine after activation (See Part II: Section 3.2.).

Fig. 2 presenting the TGA profile of the selected Pd(1.0)-Pt(0.5) catalyst, Pd/(Pd+Pt) molar ratio = 0.8, illustrates this behavior. Coke deposition is evidenced by weight loss of the spent catalysts after 673 K, as in agreement with Barman et al. [32]. Similar trends were registered for the other catalysts, where no significant quantitative differences in the amount of deposited coke over the catalysts were determined. The changes in the catalytic Pd-Pt system induced by coke deposition can be followed from the behavior of both selected catalysts as a function of time on stream as presented in Fig. 3. In both cases though naphthalene conversion remains constant at 100% important selectivity shifts are observed. During the first four hours of reaction both catalysts yield mainly *trans*-decalin and lower amounts of tetralin and *cis*-decalin. During the subsequent hours of reaction tetralin yield sharply increases, then becoming the main reaction product, *trans*-decalin yield markedly decreases and *cis*-decalin only exhibit a slight decrease until reaching the final steady state. The TGA results and the above described trend evidence the important role of coke in the dynamics of the behavior of the Pd-Pt active phase in hydrogenation reactions. Jongpatiwut et al. [23] reported deactivation of Pd-Pt catalysts during the hydrogenation of phenanthrene and naphthalene as a consequence of coke deposition. Karpiński and Kocieślski [33] determined that the surface of Pd-Pt alloyed films as well as that of Pd films experiences deep carbonization and poisoning during the isomerization of C_5 and C_6 alkanes. In alkyne hydrogenation over Pd catalysts significant amounts of subsurface carbon and Pd-C species are claimed to be responsible for the high selectivity of this metal to partially saturate the alkyne molecules to alkenes by altering the process of hydrogen transfer from Pd to the unsaturated molecule [34].
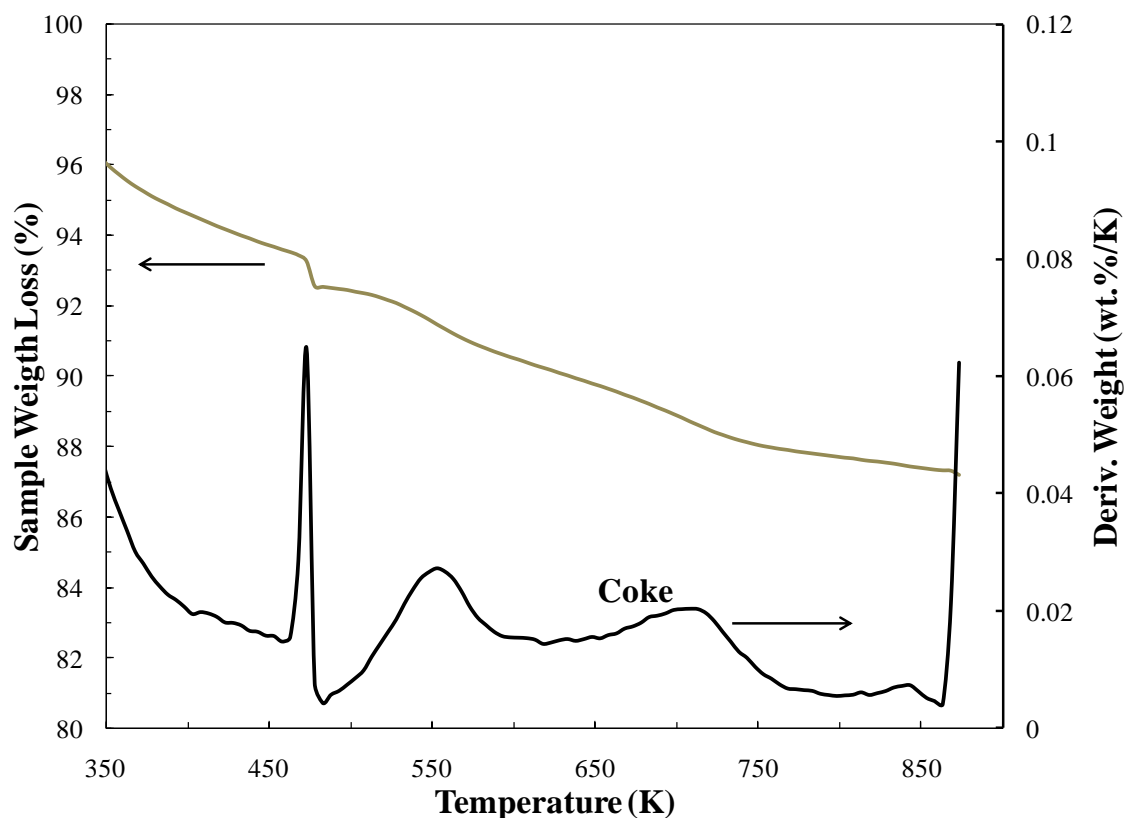
Fig. 2. TGA profile of a selected spent Pd-Pt/γ-Al$_2$O$_3$ catalyst (Pd/(Pd+Pt) molar ratio = 0.8) after the hydrogenation of naphthalene in the absence of H$_2$S.

One may assume that a similar transformation of the Pd-Pt active phase can occur during the hydrogenation of naphthalene, shifting the selectivity from decalins to tetralin. Such behavior can be related to a modification in the rate of hydrogen transfer from the Pd-Pt surface to the adsorbed π-complexes of naphthalene and those of the partially hydrogenated intermediates as early discussed. The effect of coke deposition on the selectivity in the hydrogenation of naphthalene keeps a certain resemblance with the behavior of sulfided Co-(Ni)-MoS$_2$ catalysts in this reaction [35, 36]. Redey and Hall proposed that this was due to the heterolytic chemisorption of hydrogen on the sulfided active phase which allows a stronger interaction of the aromatic backbone of naphthalene by the slower addition of H

by opposite sides of the molecule [36]. On the other hand, it is also possible that the electronic state of the metals can be related to stereoselectivity [16, 28]. A correlation between the increase in Pd electronic density, stereoselectivity and the Pd/(Pd+Pt) molar ratio has been observed [28]. In addition, from decalins stereoselectivity it has been suggested that the electronic properties of the metallic sites of the alloyed Pd-Pt clusters were closer to those of Pd [16]. XPS analysis of the prepared Pd-Pt/γ-Al$_2$O$_3$ catalysts showed that after reduction the surface of the Pd-Pt alloys becomes enriched by electron deficient Pd$^{\delta+}$ species [22, Part II: Section 3.2.] probably resulting from a combination of the ionic interaction between Pd and Pt in the alloyed clusters [37] and to the formation of stronger noble metal-O-Al bridges promoted by chlorine [38]. Finally, as demonstrated by Stakheev et al. [39], the presence of such electron deficient Pd$^{\delta+}$ species is definitively playing a role in the coke deposition over the Pd-Pt/γ-Al$_2$O$_3$ catalysts, thus reflected in the complex dynamics of the hydrogenation mechanism.

3.2.2. *Naphthalene hydrogenation under an H$_2$S environment*

Fig. 4 presents the %C$_{NP}$, under an H$_2$S atmosphere, as a function of the Pd/(Pd+Pt) molar ratio as measured at 563 K. It is important to recall that the results correspond to the simultaneous hydrogenation of naphthalene and decomposition of DMDS; the latter generating the H$_2$S atmosphere. The only product detected was tetralin. The monometallic Pd and Pt catalysts displayed a very low activity; with Pd being a slightly more active. It must be noticed that the Pd(0.2)-Pt(1.5) catalyst, Pd/(Pd+Pt) molar ratio = 0.2, presents a very low activity; almost as low as that of Pt(1.3), and a little lower than that of Pd(1.9). The increase in the Pd concentration of the catalysts augments their hydrogenating activity

under an H_2S atmosphere. The maximum at the Pd/(Pd+Pt) molar ratio = 0.8 corresponds to the metallic composition reported to possess the best catalytic behavior in HDA [11, 16, 28, 40].
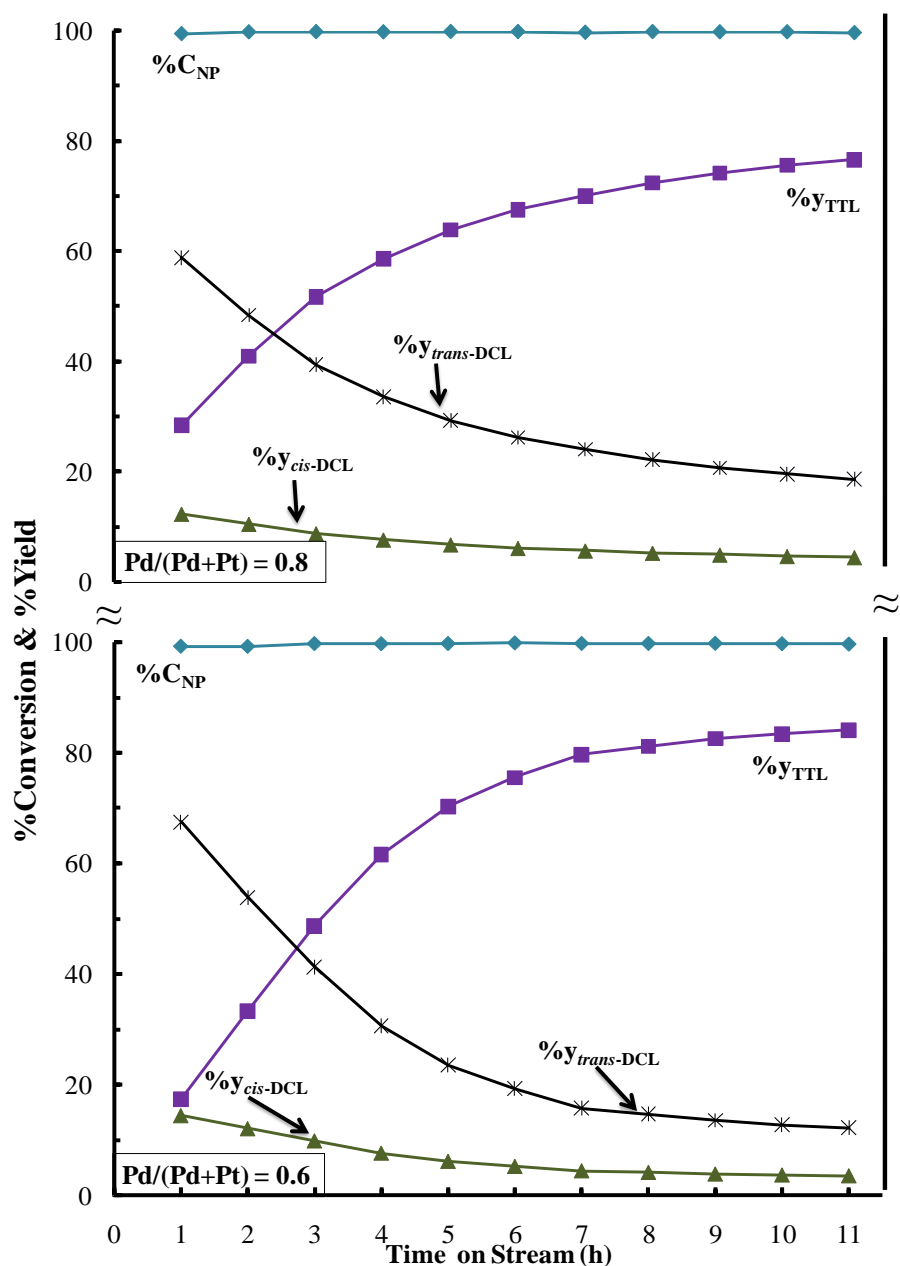
Fig. 3. Evolution of the activity of selected bimetallic Pd-Pt/γ-Al$_2$O$_3$ catalysts of different Pd/(Pd+Pt) molar ratios (0.6 and 0.8) during the hydrogenation of naphthalene in the absence of H_2S.
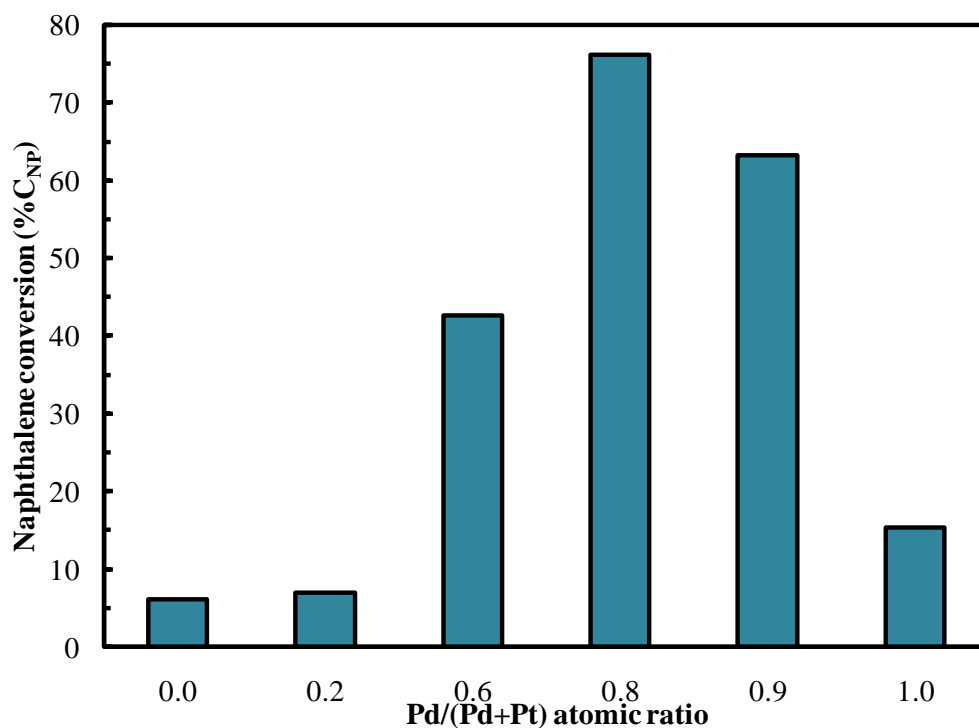
Fig. 4. Naphthalene conversion (%C_{NP}) under an H$_2$S environment for Pd-Pt/γ-Al$_2$O$_3$ catalysts of different Pd/(Pd+Pt) molar ratios. Reaction conditions: T = 563 K, P = 5MPa, liquid feed flow 30 mL/h, H$_2$/liquid feed ratio = 500 NL/L, H$_2$S concentration in the reaction atmosphere c.a. 4074 wppm.

From a comparison of the catalytic performance of monometallic Pt and Pd with that of bimetallic Pd-Pt, a synergetic effect in hydrogenation under an H$_2$S atmosphere is evident. Such synergetic effect is a function of the Pd/(Pd+Pt) molar ratio. Recalling the behavior presented in Fig. 1 which evidenced that the increase in Pd concentration in the Pd-Pt system results in S$_{trans-}$ ratios similar to that of Pd, it can be assessed that Pt promotes the functionalities of the electron deficient Pd$^{δ+}$ particles existing at the surface of the Pd-Pt clusters [22, Part II: Section 3.2.], which are less sensitive to the H$_2$S environment. XPS characterization of the calcined and reduced catalysts showed Pd surface enrichment of the Pd-Pt alloys [22, Part II: Section 3.2.]. Matsubayashi et al. [41] using EXAFS reported that

the formation of the Pd-Pt alloy after reduction allowed the survival of Pd metallic particles after sulfidation with an H_2S-H_2 mixture. Fujikawa et al. [42] have suggested that "the active phase of Pd-Pt in aromatics hydrogenation is composed of the Pd dispersed on Pt particle structure". Bando et al. [43] have shown, using in situ XAFS measurements, that after reduction of a Pd-Pt/Al_2O_3 catalyst dissolution of Pt atoms into Pd metal particles takes place. Afterward, during the HDT model reaction the formation of sulfided phases co-existing with metallic sites was observed. They suggested that segregated Pt atoms were more accessible to sulfur. Jacquin et al. [44] concluded that Pd was preferentially located at the surface of Pd-Pt alloyed clusters. Recently, theoretical DFT calculations performed by Jiang et al. [17] demonstrated that the sulfur tolerance of bimetallic Pd-Pt clusters is related to the atomic distribution of Pd and Pt on bimetallic Pt(1 1 1)-nPd surfaces. Their results show that H_2S adsorption over Pt is preferential than on Pd and also that H_2 adsorption on the bimetallic clusters is much more competitive to both H_2S and S atom adsorption. As it is known, the strong adsorption of H_2S on metallic surfaces reduces drastically their capacity to activate and transfer atomic hydrogen [10, 45]. From the above discussion and the results observed in Fig. 4 it can be concluded that a modification of the surface structure of the Pd-Pt alloyed clusters by the presence of H_2S and the subsequent change in the dynamics of H transfer from the catalytic surface to the aromatic structure of naphthalene deeply influences the catalytic selectivity in the hydrogenation of naphthalene. Thus no decalins are detected and only tetralin is produced. Guczi et al. [15] pointed out that the structure of the surfaces intermediates of a reaction are a function of the rate of H transfer from the catalytic active phase. The results of Karpiński and Kocieślski [33] regarding the effect of the Pd(Pd+Pt) molar ratio on the conversion of n-hexane over alloyed Pd-Pt films

indicated a synergetic effect for the aromatization of this molecule to benzene which is similar to the synergy in naphthalene hydrogenation observed in Fig. 4. Therefore, as discussed in a precedent section, the composition of the Pd-Pt alloy is clearly modulating the strength of the interaction between naphthalene and their partially hydrogenated intermediates and the catalyst active phase by a modification of the hydrogenation-dehydrogenation equilibrium during the reaction as a result of changes in the rate of H transfer. This is also in agreement with several reports studying the thermodynamics of the Pd-Pt-H system [46, and references therein]. Of course, as appointed before, the presence of H_2S has also a deep impact in the dynamics of H transfer from the Pd-Pt bimetallic clusters and then displaces the equilibrium during naphthalene hydrogenation as reflected by the registered selectivity shift. On the other hand, it must be noticed that the activity and selectivity of the bimetallic Pd-Pt system in the hydrogenation of naphthalene under an H_2S atmosphere is similar to that of conventional MoS_2 based catalysts, which also present very low or no yield to decalins [35]. This means, according to Weitkamp's postulates, that both catalytic systems are only able to saturate the olefin adsorbed type bonds of the molecule then producing tetralin [19]. Besides, it is important to recall that tetralin is the main reaction product detected in the hydrogenation of naphthalene over monometallic Pd without the presence of H_2S (Table 2) [19-21]. Consequently, the presence of H_2S inhibits to some extent the hydrogenating capacity of the Pd-Pt catalysts but does not change its "Pd-like" [16] behavior.

3.2.3. *Effect of the addition of dibenzothiophene on the steady state hydrogenation of naphthalene*

Fig. 5 shows the effect of adding dibenzothiophene to the liquid feed during the hydrogenation of naphthalene over the Pd(1.0)-Pt(0.5) catalyst at 583 K, once steady state

conversion and selectivity have been reached. The catalytic behavior without the presence of dibenzothiophene is similar to that observed in Fig. 3; i.e. though conversion of naphthalene remains at 100% there is an important shift in the catalytic selectivity due to coke deposition during this stage of the reaction. After dibenzothiophene addition a strong decrease in the conversion of naphthalene was registered, with a sharp change in the catalytic selectivity. Henceforth, partially saturated tetralin intermediate constituted the only reaction product, and then the production of decalins was completely stopped. As it is shown in Part II of this Chapter, the severe negative effect of dibenzothiophene on the catalytic performance can be mainly ascribed to the production of H_2S from its hydrodesulfurization. Adsorption-competition effects between both molecules have been demonstrated not to cause such a strong effect on the hydrogenation of naphthalene over Pd-Pt [21, 22].

Comparing the behavior of this catalyst as from Figs. 4 and 5, it must be remarked that though a lower temperature was used in the simultaneous hydrogenation of naphthalene and decomposition of DMDS (Fig. 4) to H_2S, the negative effect of H_2S from dibenzothiophene hydrodesulfurization is much stronger. The experimental evidence presented for the tests of naphthalene hydrogenation in the absence of H_2S lead to conclude that the coked catalytic surface of Pd-Pt/γ-Al$_2$O$_3$ is more susceptible to H_2S and thus its hydrogenating capacity is drastically reduced. In this sense, Miller and Koningsberger [47] established that coke deposits on Pt based catalysts can decrease metallic active sites availability, then enhancing sulfur poisoning. Finally, Jongpatiwut et al. [23] demonstrated that when performing this type of model reaction, i.e. addition of dibenzothiophene to a "stabilized" Pd-Pt catalyst

during aromatics hydrogenation, coke formation is accelerated due to the presence of H_2S, thus its negative effect on the catalytic performance is even more severe.
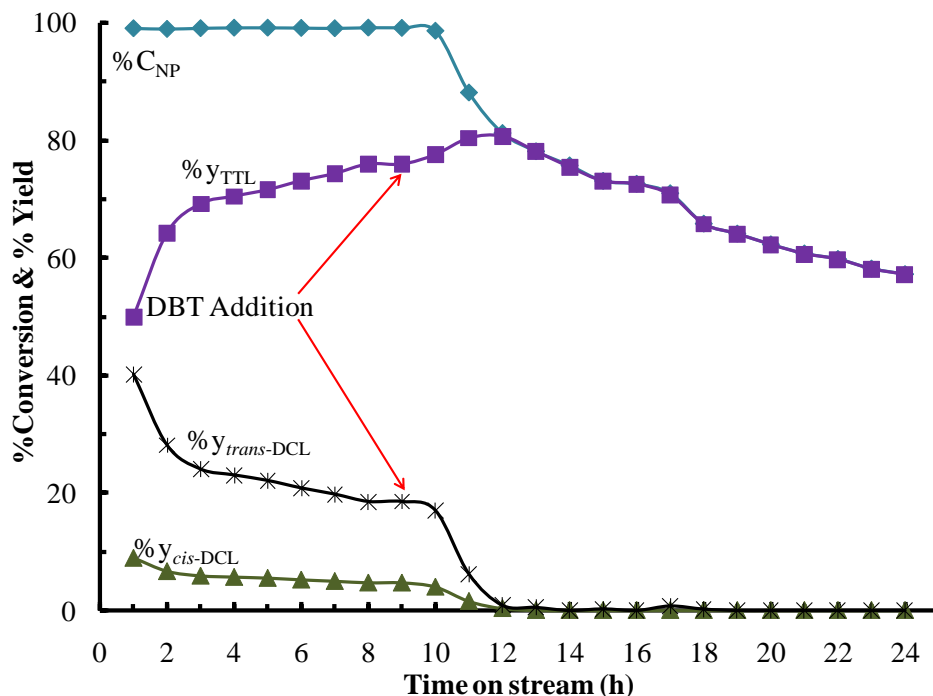
Fig. 5. Effect of the addition of DBT, once steady state has been reached, on the catalytic performance of a Pd-Pt/γ-Al$_2$O$_3$ catalyst with Pd/(Pd+Pt) molar ratio of 0.8 with time on stream. Reaction conditions: T = 583 K, P = 5 MPa, liquid feed flow = 30 mL/h, H_2/liquid feed ratio = 500 NL/L; 2 wt.% of dibenzothiophene.

4. Conclusions

The hydrogenation of naphthalene was used as a model reaction to evaluate the catalytic properties of the hydrogenating function of Pd-Pt/γ-Al$_2$O$_3$ catalysts. The analysis of the catalytic behavior of the Pd-Pt system in this model reaction was correlated with the accepted mechanism of naphthalene hydrogenation. Hence, it was established that the interaction between the naphthalene aromatic backbone and the active phase of the Pd-Pt/γ-Al$_2$O$_3$ catalysts is controlled by the Pd/(Pd+Pt) molar ratio. Moreover, from such analysis it was confirmed that the supported bimetallic surface is enriched by metallic Pd particles and

that the hydrogenation function of the Pd-Pt active phase has a "Pd-like" behavior. It was found that though H_2S decreases the hydrogenation activity of the Pd-Pt/γ-Al$_2$O$_3$ catalysts, the active phase of the system retains its main hydrogenation functionalities.

Coking of the catalysts during naphthalene hydrogenation shifted the catalytic selectivity favoring the production of the partially hydrogenated tetralin intermediate thus changing the strength of the interaction between the aromatic molecule and the catalyst's active phase. Furthermore, it was determined that coke deposition over Pd-Pt/γ-Al$_2$O$_3$ makes the catalyst more susceptible to H_2S deactivation during aromatics hydrogenation.

References

[1] C. Song, Catal. Today 86 (2003) 211.

[2] T. Kabe, A. Ishihara, Q. Zhang, Appl. Catal. A: Gen. 97 (1993) Ll.

[3] M.V. Landau, D. Berger, M. Herskowitz, J. Catal. 159 (1996) 236.

[4] M. Houalla, N.K. Nag, A.V. Sapre, D.H. Broderick, B.C. Gates, AlChE J. 24 (1978) 1015.

[5] K. Teraishi, J. Mol. Catal. A: Chem. 126 (1997) 73.

[6] H. Yang, C. Fairbridge, Z. Ring, Energy Fuels 17 (2003) 387.

[7] N.K. Nag, Appl. Catal. 10 (1984) 53.

[8] J.J. Rooney, G. Webb, J. Catal. 3 (1964) 488.

[9] B.H. Cooper, K.G Knudsen, World Refining 10 (2000) 14.

[10] Stanislaus, B.H. Cooper, Catal. Rev.-Sci. Eng. 36 (1994) 75.

[11] T.-B. Lin, C.-A. Jan, J.-R. Chan, Ind. Eng. Chem. Res. 34 (1995) 4284.

[12] H.R. Reinhoudt, R. Troost, A.D. van Langeveld, S.T. Sie, J.A.R. van Veen, J. A. Moulijn, Fuel Proc. Tech. 61 (1999) 133.

[13] A. Niquille-Röthlisberger, R. Prins, J. Catal. 242 (2006) 207.

[14] R. Gómez, S. Fuentes, F.J. Fernández del Valle, A. Campero, J.M. Ferreira, J. Catal. 38 (1975) 47.

[15] L. Guczi, Z. Schay, Stud. Surf. Sci. Catal. 27 (1986) 313.

[16] Y. Yoshimura, M. Toba, T. Matsui, M. Harada, Y. Ichihashi, K.K. Bando, H. Yasuda, H. Ishihara, Y. Morita, T. Kameoka, Appl. Catal. A: Gen. 322 (2007) 152.

[17] H. Jiang, H. Yang, R. Hawkins, Z. Ring, Catal. Today 125 (2007) 282.

[18] A.D. Schmitz, G. Bowers, C. Song, Catal. Today 31 (1996) 45.

[19] A.W. Weitkamp, Adv. Catal. 18 (1968) 1.

[20] S. Dokjampa, T. Rirksomboon, S. Osuwan, S. Jongpatiwut, D.E. Resasco, Catal. Today 123 (2007) 218.

[21] V.G. Baldovino-Medrano, S.A. Giraldo, A. Centeno, J. Mol. Cat. A: Chem. 301 (2009) 127.

[22] V.G. Baldovino-Medrano, S.A. Giraldo, A. Centeno, J. Catal. (2009) DOI: 10.1016/j.jcat.2009.08.004.

[23] S. Jongpatiwut, Z. Li, D.E. Resasco, W.E. Alvarez, E.L. Sughrue, G.W. Dodwell, Appl. Catal. A: Gen. 262 (2004) 241.

[24] Balint, A. Miyazaki, K.-i. Aika, Chem. Mater. 13 (2001) 932.

[25] Y. Inuoe, J.M. Herrmann, H. Schmidt, R.L. Burwell, J.B. Butt, J.B. Cohen, J. Catal. 53 (1978) 401.

[26] A.K. Neyestanaki, P. Mäki-Arvela, H. Backman, H. Karhu, T. Salmi, J. Väyrynen, D.Yu. Murzin, J. Mol. Catal. A: Chem. 193 (2003) 237.

[27] H.-U. Blaser, A. Indolese, A. Schnyder, H. Steiner, M. Studer, J. Mol. Catal. A 173 (2001) 3.

[28] E. Guillon, J. Lynch, D. Uzio, B. Didillon, Catal. Today 65 (2001) 201.

[29] J. Haro, R. Gómez, J.M. Ferreira, J. Catal. 45 (1976) 326.

[30] J. Barbier, Appl. Catal. 23 (1986) 225.

[31] M. Guisnet, P. Magnoux, Appl. Catal. A: Gen. 212 (2001) 83.

[32] B.N. Barman, L. Skarlos, D.J. Kushner, Energy Fuels 11 (1997) 593.

[33] Z. Karpiński, T. Kocieślski, J. Catal. 56 (1980) 430.

[34] D. Teschner, E. Vass, M. Hävecker, S. Zafeiratos, P. Schnörch, H. Sauer, A. Knop-Gericke, R. Schlögl, M. Chamam, A. Wootsch, A.S. Canning, J.J. Gamman, S.D. Jackson, J. McGregor, L.F. Gladden, J. Catal. 242 (2006) 26.

[35] J. Shatbai, N.K. Nag, F.E. Massoth, in M.J. Phillips, M. Ternan (Eds.) "Proceedings, 9th International Congress on Catalysis, Calgary, 1988", Vol. 1, Chemical Institute of Canada, Ottawa, 1988, p. 1.

[36] A. Redey, W.K. Hall, J. Catal. 119 (1989) 534.

[37] N. Matsubayashi, H. Yasuda, M. Imamura, Y. Yoshimura, Catal. Today 45 (1998) 375.

[38] A. Sarkany, G. Stefler, J.W. Hightower, Appl. Catal. A: Gen. 127 (1995) 77.

[39] A.Yu. Stakheev, L. M. Kustov, Appl. Catal. A: Gen. 188 (1999) 3.

[40] T. Fujikawa, K. Idei, T. Ebihara, H. Mizuguchi, K. Usui, Appl. Catal. A: Gen. 192 (2000) 253.

[41] N. Matsubayashi, H. Yasuda, M. Imamura, Y. Yoshimura, Catal. Today 45 (1998) 375.

[42] T. Fujikawa, K. Tsuji, H. Mizuguchi, H. Godo, K. Idei, K. Usui, Catal. Lett. 63 (1999) 27.

[43] K.K. Bando, T. Kawai, K. Asakura, T. Matsui, L. Le Bihan, H. Yasuda, Y. Yoshimura, S.T. Oyama, Catal. Today 111 (2006) 199.

[44] M. Jacquin, D.J. Jones, J. Rozière, A.J. López, E. Rodríguez-Castellón, J.M.T. Menayo, M. Lenarda, L. Storaro, A. Vaccari, S. Albertazzi, J. Catal. 228 (2004) 447.

[45] F.J. Castro, G. Meyer, G. Zampieri, J. Alloys Comp. 330-332 (2002) 612.

[46] H. Noh, Ted B. Flanagan, T. Sonoda, Y. Sakamoto, J. Alloys Comp. 228 (1995) 164.

[47] J.T. Miller, D.C. Koningsberger, J. Catal. 162 (1996) 209.

Part II: Development of the HYD route of hydrodesulfurization over Pd-Pt catalysts.

Abstract

The hydrodesulfurization of dibenzothiophene on a series of Pd-Pt/γ-Al$_2$O$_3$ catalysts was studied as a function of the Pd/(Pd+Pt) molar ratio at different reaction conditions. Catalytic tests comprised: (i) influence of reaction temperature on HDS over monometallic Pd and Pt, (ii) effect of the presence of naphthalene and H$_2$S over the Pd-Pt performance in hydrodesulfurization, and (iii) effect of performing naphthalene hydrogenation before hydrodesulfurization. It was determined that a synergetic effect exists in the development of the HYD route of dibenzothiophene HDS over Pd-Pt/γ-Al$_2$O$_3$ being in correspondence with the hydrogenation of aromatic molecules under H$_2$S atmospheres. From the results of tests (ii) and (iii) it was concluded that naphthalene does not significantly inhibit HYD over Pd-Pt. H$_2$S was encountered mainly to inhibit C-S-C bond scission step of both hydrodesulfurization reaction pathways. Finally, coke deposition from naphthalene hydrogenation (test iii) was found to have a poisoning effect on the functionalities of Pd-Pt. Results of characterization; H$_2$ and CO chemisorption, TPR and XPS, showed that the presence of Pd$^{\delta+}$ surface particles in the Pd-Pt alloyed clusters and the H$_2$ uptake capacity of Pd-Pt are crucial factors for the development of HYD.

Keywords: Pd-Pt catalysts; molar ratio influence; dibenzothiophene hydrodesulfurization; HYD pathway; H$_2$S and coke effect.

1. Introduction

The hydrodesulfurization of sterically hindered di-β-dibenzothiophenes proceeds almost exclusively by HYD [1-3]. Flat π adsorption of a dibenzothiophene type structure on a catalytic surface involves multipoint interactions with the sulfur atom, the thiophenic and aromatic rings [4-8]. Theoretical calculations on MoS_2 clusters have shown that cleavage of the C-S-C bond of di-β-dibenzothiophenes via direct sulfur $\eta^1 S$ adsorption (DDS) is not an energetically favored process [4, 9]. It is generally agreed that both DDS and HYD are parallel reaction routes for the hydrodesulfurization of dibenzothiophenes. The C-S-C bond scission step in both routes has the same nature either in DDS or in HYD [5, 6, 10, 11]. It can be said that contrary to di-β-dibenzothiophenes, the hydrodesulfurization of dibenzothiophene measures the intrinsic catalytic selectivity either to HYD or DDS of a given catalytic system, because during the reaction no steric effects drive selectivity [4, 9]. On the other hand, HYD involves a simultaneous hydrogenation-dehydrogenation-C-S-C bond scission equilibrium between the benzenic rings of dibenzothiophene, the thiophenic system and the partially hydrogenated tetrahydro-(TH) and hexahydro-(HH) intermediates [11-13]; for such intermediates, the decrease in the resonance energy of the DBT backbone facilitates the rupture of the C-S-C bond [6]. Though over monometallic MoS_2 catalysts HYD and DDS are very competitive [10, 12-14], the addition of promoters enhances the HDS activity mostly by favoring DDS [14, 15, see also Chapter I]. Even highly hydrogenating metals such as Pt present such promoting effect on MoS_2 [15]. Reinhoudt et al. [16] compared the activity of γ-Al_2O_3 and ASA supported promoted MoS_2 and Pd-Pt catalysts in the hydrodesulfurization of β-dibenzothiophenes. The rate of HDS of such

molecules over Pd-Pt/ASA catalysts was as higher as 5 fold than that of MoS_2 based systems [16]. The alloyed Pd-Pt bimetallic system is able to develop the HYD route of hydrodesulfurization of 4,6-dimethyl-DBT [11, 17]. The reasons for such capacity are not fully established yet. The author has successfully used selectivity and stereoselectivity trends in naphthalene hydrogenation to study the properties of the hydrogenation function of Pd-Pt alloyed catalysts as a function of the Pd/(Pd+Pt) molar ratio at the usual reaction conditions of hydrotreatment (Chapter III, Part I). This allowed confirming that Pd surface enrichment of the alloyed Pd-Pt particles occur under an HDS environment [17] and that Pt acts as a promoter of certain functionalities of Pd [18]. Moreover, the catalytic trends registered demonstrated that the hydrogenating active sites under an H_2S atmosphere possess the character of metallic Pd [17, 18].

In this part of the study, it was decided to study the development of the HYD route of hydrodesulfurization of dibenzothiophene as a function of the Pd/(Pd+Pt) molar ratio and under different reaction conditions for the same group of Pd-Pt/γ-Al_2O_3 catalysts as presented in Part I of the present Chapter. This permits to improve the present state of knowledge on the capacity of Pd-Pt to hydrodesulfurize di-β-dibenzothiophenes via HYD, thus envisaging the critical variable in the design of an effective material for the selective hydrodesulfurization of diesel oil.

2. Experimental

2.1. Catalysts preparation

A series of bimetallic Pd-Pt/γ-Al_2O_3 catalysts of total (Pd+Pt) metallic contents below 2 wt.% and different Pd/(Pd+Pt) molar ratios were prepared as reported in Part I, Section 2.1. The Pd/(Pd+Pt) molar ratio was varied from 0 to 1, i.e. from monometallic Pt to

monometallic Pd. Metallic contents were verified by atomic absorption analysis and are indicated within parentheses in the catalyst's labels after the corresponding metal.

2.2. Catalysts characterization

2.2.1. Hydrogen chemisorption

Hydrogen chemisorption measurements were performed in a Micromeritics ASAP 2010C instrument. All catalysts were in situ reduced in hydrogen at 673 K before the measurements. After this step, evacuation was performed by flowing He for 2 h at 673 K, under vacuum at 673 K for 30 min, and finally under vacuum at the temperature selected for the measurement for another 30 min. Hydrogen chemisorption isotherms were determined at 343 K to avoid the formation of the β-Pd-H hydride phase [19], this was also verified by TPR measurements. The reported hydrogen uptake values were taken from the volume difference between two hydrogen adsorption isotherms; the second one measured after an evacuation time of 45 min, extrapolated to zero pressure (strongly adsorbed hydrogen). For the calculation of dispersion from these measurements the ratio $H/M = 1$ was assumed between the metallic phases (Pd, Pt and Pd-Pt) and hydrogen.

2.2.2. CO chemisorption

CO chemisorption measurements were conducted on a Micromeritics Pulse Chemisorb 2700 apparatus. Samples of the calcined catalysts, c.a. 0.15 g, were dried using hydrogen (30 mL/min) at 393 K and subsequently at 493 K during 30 min at each temperature before performing its final reduction under the same hydrogen flow at 673 K for 2 h. At this same temperature, helium (30 mL/min) was flowed into the system during 90 min. The system was then cooled down to 318 K at which CO pulses were repeatedly injected until saturation of the sample. Dispersion was determined according to the procedure presented

by Hermans et al. [20]. For the monometallic catalysts the ratios CO/Pt = 1 and CO/Pd = 0.68 were assigned as recommended by Navarro et al. [21]. For the bimetallic Pd-Pt catalysts the stoichiometric factor was calculated according to the formula: $X_{Pt}*1+X_{Pd}*0.68$, where X is the molar fraction of the metal in the alloy.

2.2.3. *Temperature programmed reduction* (TPR)

Temperature programmed reduction (TPR) experiments were performed in a u-shaped fixed-bed quartz micro-reactor containing samples of c.a. 100 mg of the calcined catalysts to which a layer of approximately 1 cm of glass beads was added to guaranty plug-flow. Before the analysis, drying of the samples under He flow (50 mL/min) was performed at 413 K until stabilization of the H_2O signal as registered with a QMC 311 Balzers quadrupole mass spectrometer coupled to the reactor. After cooling the reactor, TPR patterns were then registered by increasing temperature from 308 K to 1073 K at a temperature rate of 10 K/min. TPR analysis was performed by flowing a 5 vol.% H_2 in He (flow rate = 50 mL/min) gas mixture. The MS signals corresponding to H_2 (m/z = 2), H_2O (m/z = 18), HCl (m/z = 36) and Cl^+ (m/z = 37); corresponding to diverse chlorine containing compounds, were monitored. Recorded signals were treated by using a Gaussian mathematical function.

2.2.4. *X-Ray photoelectron spectroscopy (XPS)*

XPS analyses were performed in the same instrument and at the same conditions described in Chapter II, Section 2.3.1. The following sequence of spectra was recorded: survey spectrum, C 1s, O 1s, Al 2p, Al 2s, Pd 3d, Pt 4d, Cl 2p, and C 1s again to check the stability of charge compensation in function of time and the absence of degradation of the sample during the analyses. This time the Pd 3d doublet was decomposed in three components with

Pd $3d_{5/2}$ binding energies fixed at 335 (Pd^0), 336 (Pd^{2+}) and 338 eV (Pd^{4+}) [22]. The algebraic sum of the surface atomic concentration of ($Pd^{2+}+Pd^{4+}$) species was defined as the total concentration of surface electron deficient $Pd^{\delta+}$ species. For the Pt 4d peak the energy separation for the doublet was fixed at 16.8 eV [22].

2.3. Catalytic tests

Catalysts were reduced in H_2 at 673 K before reaction tests according to the procedures previously described in Part I of this Chapter. Further details on the experimental set up have already been presented (Chapter I, Section 2.4.). For a better understanding of the functionalities of Pd-Pt in hydrodesulfurization a comparison between monometallic Pt and Pd is introduced, recalling part of the results of the experiments presented in Chapter II; in particular the effect of reaction temperature on Pd (See Chapter II, Section 3.3.3.2.)

The catalyst with a Pd/(Pd+Pt) molar ratio of 0.8, Pd(1.0)-Pt(0.5), was selected for two long run tests. The first consisted on performing the hydrodesulfurization of dibenzothiophene until reaching steady state and then adding naphthalene to the liquid feed. Once a new steady state was reached, dimethyldisulfide (DMDS) was incorporated to the feed as to generate an additional H_2S concentration of c.a. 4074 wppm. When stable conversions were achieved, DMDS was withdrawn from the system, closing the cycle which began with naphthalene addition. As described, this experiment allows studying the influence of the incorporation of naphthalene to a stabilized Pd-Pt catalyst on the performance in hydrodesulfurization, as well as the influence of an increase in the H_2S concentration on the simultaneous HDS - naphthalene hydrogenation reaction thus performed. For the second experiment, the hydrogenation of naphthalene was performed first. At steady state

conditions dibenzothiophene was then introduced to the liquid feed, and once a new steady state was attained, naphthalene was taken out of the feed. Specific details on this experiment as well as some of its results were included in Part I of the present Chapter. This second experiment allowed establishing the role of coke deposition due to naphthalene hydrogenation in the development of HYD.

The catalytic results are expressed in the usual terms currently employed along this Thesis.

3. Results and discussion

The catalytic trends and the characteristics of the Pd-Pt active phase in the hydrodesulfurization of dibenzothiophene as a function of the Pd/(Pd+Pt) molar ratio are analyzed first. Afterwards, the analysis is focused on the trends observed during the long run tests.

3.1. Hydrodesulfurization of dibenzothiophene

Reaction products detected in these tests were: cyclohexylbenzene (CHB), biphenyl (BP), and partially hydrogenated TH-dibenzothiophene (THDBT) and HH-dibenzothiophene (HHDBT).

Table 1 shows the effect of reaction temperature on the activity ($\%C_{DBT}$) and reaction products distribution for monometallic Pd(1.9) and Pt(1.3), respectively. For both catalysts $\%C_{DBT}$ increases with temperature. As reported [16, 17, 24], Pt is much more active than Pd, therefore, the competition between HYD and DDS depends on the nature of the noble metal [11, 24]. In general, the yields of both desulfurized products, i.e. cyclohexylbenzene and biphenyl, increased with temperature over both catalysts, with biphenyl as the main reaction product. For Pt the yield of biphenyl was an order of magnitude higher than that of cyclohexylbenzene indicating a very high selectivity to DDS [24-26]. Over Pd, the yield to

cyclohexylbenzene is c.a. half the one corresponding to biphenyl. Both partially

hydrogenated intermediates, TH-dibenzothiophene and HH-dibenzothiophene, were

observed for Pd, and instead, over Pt only a very low amount of TH-dibenzothiophene was

detected. A noticeable difference between Pt and Pd is that over the former the yield of TH-

dibenzothiophene decreases with raising temperature, while over Pd it increases with

temperature. The trend observed for TH-dibenzothiophene over Pt is similar to that

registered for HH-dibenzothiophene over Pd; though in this case such decrease is very

slight. The behavior of Pd shows that HYD is kinetically controlled and becomes more

competitive to DDS on those catalysts displaying lower HDS rates; as for un-promoted

MoS_2 [12-14, 24].

Table 1. Effect of reaction temperature on the hydrodesulfurization of dibenzothiophene over monometallic γ-Al_2O_3 supported Pd and Pt catalysts.

Catalyst[†]	Temperature (K)	%C_{DBT}	%y_{THDBT}	%y_{HHDBT}	%y_{CHB}	%y_{BP}
	563	50.4	1.9	0	3.6	45.9
Pt(1.3)	583	69.2	1.0	0	5.3	63.2
	603	87.7	0.5	0	7.1	80.0
	563	17.9	4.8	1.5	3.7	7.8
Pd(1.9)	583	25.9	5.7	1.4	6.2	12.5
	603	36.4	6.6	1.2	10.2	18.3

[†]Numbers in parentheses indicate metallic contents.

Up to date, the mechanism of DDS remains an object of controversy, because evidence

supporting an elimination type mechanism and/or direct C-S-C bond hydrogenolysis has

been extensively documented [5, 6, 10-14]. However, there is a good agreement in the fact

that the same mechanism can operate either in DDS or in the final C-S-C bond scission step

of HYD [6, 7, 9-11, 14]. In HYD, the formation of a π-complex between the catalyst active

phase and the dibenzothiophene benzenic backbone is formed leading to its sequential saturation [4-8]. Thus, the literature [11, 24, 27] indicates that during HYD a dynamic competition between hydrogenation-dehydrogenation reactions and the scission of the C-S-C bond of dibenzothiophene occurs. As the resonance energy of the aromatic rings decreases from dibenzothiophene to TH-dibenzothiophene and then to HH-dibenzothiophene C-S-C bond scission is favored [6]. It has been proved that the rate of interconversion between TH-dibenzothiophene and HH-dibenzothiophene can be significant for Pd [13]. Given that the hydrogenation of HH-dibenzothiophene to HH-dibenzothiophene can lead either to *trans*-HHDBT or *cis*-HHDBT [13], it is possible that the *cis*- to *trans*- stereoselectivity could be playing a role in such step when considering a C-S-C bond scission step proceeding via elimination [11]. It must be recalled that metallic Pd catalysts are highly selective to *trans*-isomers in aromatics hydrogenation [Part I: Section 3.2.1., 28-31]. This implies both a strong interaction between its hydrogenation active sites and the aromatic rings, and a slower rate of hydrogen transfer from the Pd active phase to the π-unsaturated double bonds of the aromatic backbone [28]. Indeed, Table 2 displaying the results of H_2 chemisorption for the prepared Pd-Pt catalysts, shows that at the same temperature (343 K) the Pd(1.9) catalyst has a lower capacity to chemisorb H_2 than Pt(1.3). Only for a temperature of 308 K the results of H_2 chemisorption display a similar value for both monometallic catalysts, but it must be considered that the metallic content of Pt(1.3) is lower than that of Pd(1.9).

Table 2. H_2 and CO chemisorption results for the prepared Pd-Pt/γ-Al$_2$O$_3$ catalysts.

| Catalyst[a] | Chemisorption | | | |
| | n_{ads}^{STP} (µmol/µmol metal) | | %Dispersion | |
	H$_2$ (343 K)	CO (308 K)	H$_2$	CO
Pt(1.3)	0.19[b]	0.37	37.9[b]	36.9
	0.57		114.0	
Pd(0.2)-Pt(1.5)	0.22	0.45	43.8	36.8
Pd(0.9)-Pt(0.7)	0.26	0.37	51.4	30.4
Pd(1.0)-Pt(0.5)	0.29	0.37	57.1	30.4
Pd(1.4)-Pt(0.3)	0.17	0.25	33.0	20.8
Pd(1.9)	0.10	0.20	20.6	13.5

[a]Numbers in parentheses indicate metallic contents.
[b]Measured at 308 K

These differences in the H$_2$ chemisorption capacity of both supported catalysts can be directly related to the development of the HYD route of hydrodesulfurization of dibenzothiophene as in parallel with the hydrogenation of non-sulfur containing aromatic molecules [28-31]. Pt is highly active in both the hydrodesulfurization reactions via DDS [24-26] and aromatics hydrogenation without the presence of H$_2$S [28, 29]. By possessing a higher H$_2$ chemisorption capacity, Pt catalysts are able to rapidly transfer hydrogen to the unsaturated bonds of aromatic molecules thus being more selective to *cis*-isomers [28, 29, 32]. Moreover, as evidenced by the value of Pt dispersion as calculated from H$_2$ uptake at 343 K, which is higher than 100% (Table 2), it can be said that hydrogen spillover effects [33, 34] are playing a significant role on the catalytic performance of Pt/γ-Al$_2$O$_3$ in hydrodesulfurization.

For the bimetallic Pd-Pt catalysts the dynamics in the hydrodesulfurization of dibenzothiophene is controlled by the Pd/(Pd+Pt) molar ratio. Fig. 1 displays both %C$_{DBT}$ and S_{HYD}^{DS} as a function of the Pd/(Pd+Pt) molar ratio at 583 K along with the H$_2$ uptake of

the Pd-Pt catalysts (as reported in Table 2). Concerning the catalytic activity, the trend registered in Fig. 1 leads to conclude that the Pd-Pt alloys have low or no synergy effects regarding the hydrodesulfurization activity. In fact, it can be observed that those catalysts with higher Pt contents, Pd/(Pd+Pt) molar ratio = 0.2 and 0.6, respectively, are more active than the one containing the highest Pd load, Pd/(Pd+Pt) = 0.9. At a Pd/(Pd+Pt) molar ratio of 0.8 the highest activity among the bimetallic catalysts is registered, but without surpassing that of monometallic Pt. On the other hand, the development of the HYD route of hydrodesulfurization also changes as a function of this variable. Selectivity to HYD, S_{HYD}^{DS}, increases with the Pd content (Fig. 1) until a maximum, $S_{HYD}^{DS} \approx 1$, located at the same Pd/(Pd+Pt) molar ratio as the maximum in activity, Pd/(Pd+Pt) molar ratio = 0.8; thus, a strong synergetic effect in HYD is found. In this sense, the catalytic behavior of Pd-Pt in the development of the HYD route of reaction resembles that in aromatics hydrogenation under H_2S atmospheres [17, 35, 36].

Comparing the hydrogen uptake of the Pd-Pt alloys with that corresponding to the monometallic Pt and Pd catalysts (Table 2), at the same temperature (343 K), it is observed that the alloyed catalysts have a higher H_2 chemisorption capacity than monometallic Pd, with a maximum located at Pd/(Pd+Pt) molar ratio = 0.8, but compared to Pt all of the alloys chemisorb lower amounts of hydrogen.
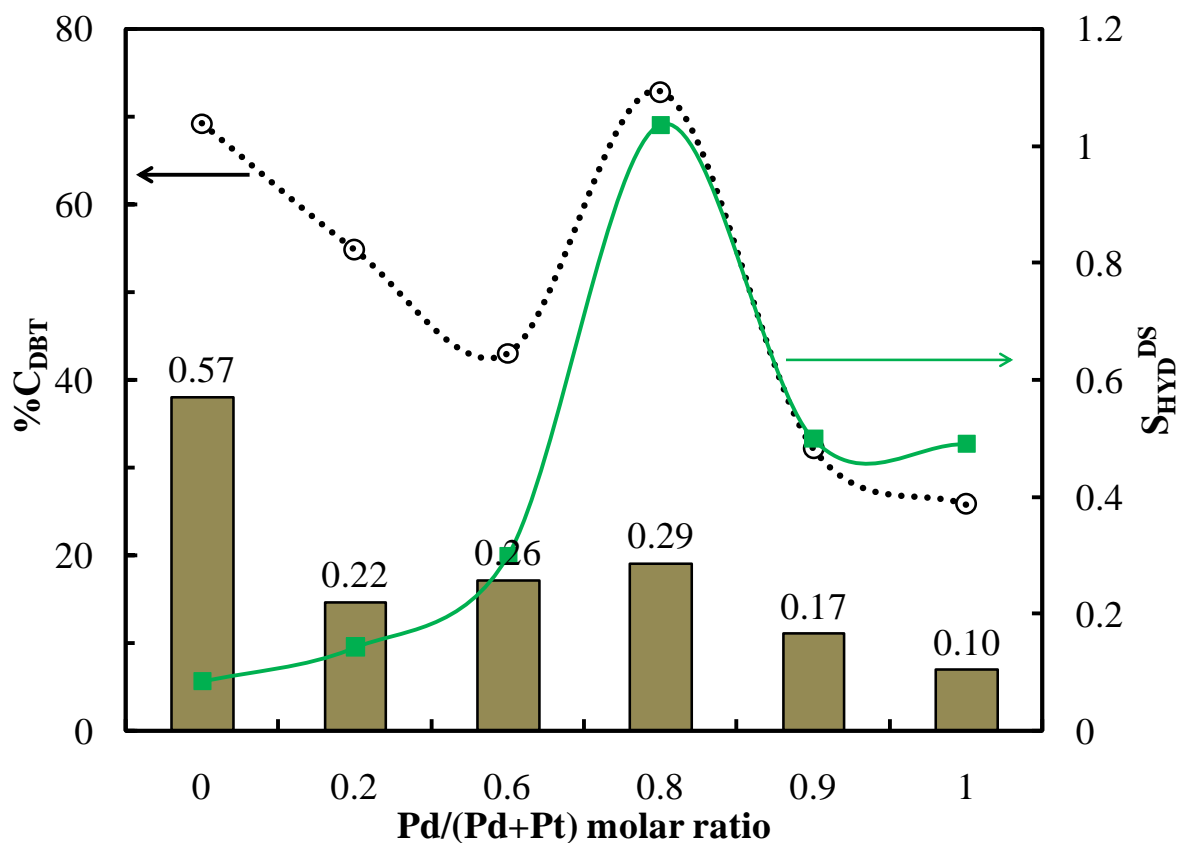
Fig. 1. Steady state activity (%C_{DBT}) and selectivity cyclohexylbenzene to biphenyl (S_{HYD}^{DS}) for Pd-Pt/γ-Al$_2$O$_3$ catalysts in the hydrodesulfurization of dibenzothiophene as a function of the Pd/(Pd+Pt) molar ratio. (▢) μmol H$_2$ chemisorbed/μmol metal; (⊙) %C_{DBT}; (-■-) S_{HYD}^{DS}. Reaction conditions: T = 583 K, P = 5 MPa, liquid feed flow 30 mL/h, H$_2$/liquid feed ratio=500 NL/L.

From Fig. 1, a direct relationship between H$_2$ uptake and S_{HYD}^{DS} selectivity for the Pd-Pt alloys is evidenced. Both variables describe a volcano curve as a function of the composition of the alloy. Fig. 2 shows the reaction products distribution (at 583 K) as a function of the Pd/(Pd+Pt) molar ratio.
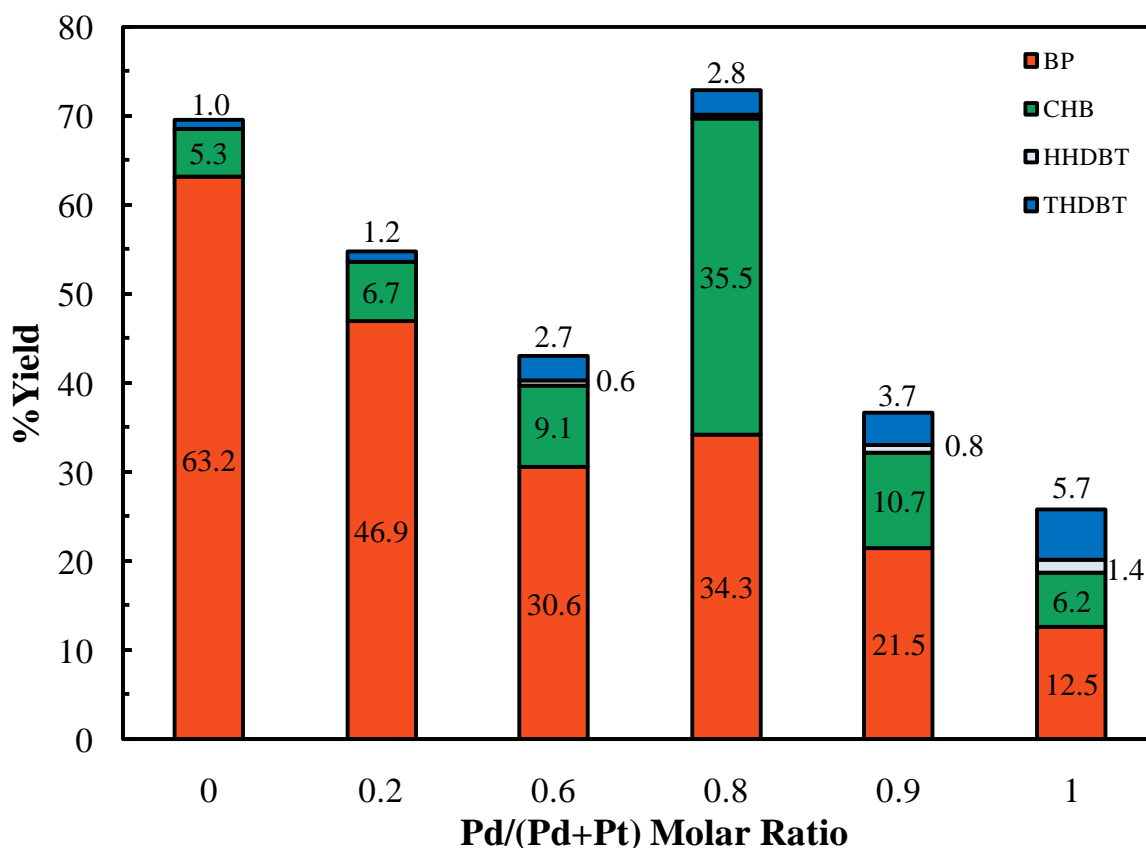
Fig. 2. Steady state products distribution for Pd-Pt/γ-Al$_2$O$_3$ catalysts in the hydrodesulfurization of DBT as a function of Pd/(Pd+Pt) molar ratio.

Special attention must be paid to the fact that for monometallic Pd the algebraic sum of the yields of cyclohexylbenzene, TH-dibenzothiophene and HH-dibenzothiophene is slightly higher than that one corresponding to biphenyl. Moreover, Pd yielded similar amounts of partially hydrogenated products and cyclohexylbenzene (Fig. 2 and Table 1). From the standpoint of the addition of Pt to the system, this effect can be regarded as if the presence of a small amount of this metal on the Pd-rich alloyed particles simultaneously accelerates both the hydrogenation of the dibenzothiophene benzenic backbone and the extraction of the S heteroatom from the dibenzothiophene, TH-dibenzothiophene and/or the HH-dibenzothiophene intermediates as to produce cyclohexylbenzene [11-13]. Further

hydrogenation of biphenyl to cyclohexylbenzene can be neglected [37, Chapter I, Section 3.2.]. The registered trend demonstrates that this variable modifies the competitive hydrogenation-dehydrogenation-C-S-C bond scission equilibrium by a fine tuning of the rate of hydrogen transfer from the catalytic surface to the dibenzothiophene molecule. Considering the promoting effect in the hydrogenation of aromatics of Pt on Pd in the bimetallic Pd-Pt alloys [Chapter III, Part I] and in the hydrodesulfurization of dibenzothiophene, additional remarks on the HYD mechanism of dibenzothiophene hydrodesulfurization over this system should be pointed. A common feature in both cases is that during the adsorption-desorption steps implicated in both reactions, the reactive molecules must change its mode of adsorption or coordination to the Pd-Pt active phase. To allow C-S-C bond scission, regardless the considered mechanism, dibenzothiophene and/or its partially hydrogenated intermediates must adsorb in π-mode, desorb and re-adsorb in σ-mode before the extraction of the S heteroatom [9-13]. Therefore, in Chapter II, it has been proposed that the HYD route of hydrodesulfurization of dibenzothiophene over Pd proceeds via a *roll-over* mechanism [31] similar to that proposed for the hydrogenation of aromatic molecules [29, 30, 32]. The dynamics of *roll-over* is related to the rates of H_2 activation and addition to the aromatic rings [29]. A lower rate of H addition to the benzenic backbone of dibenzothiophene promotes a stronger interaction between the molecule and the catalytic active phase thus favoring HYD.

3.2. *Characteristics of the Pd-Pt active phase in dibenzothiophene HDS*

Given the results obtained for the dispersion of the Pd-Pt catalysts from H_2 chemisorption it was decided to corroborate these values by CO chemisorption (Table 2) as presented in section 2.2.2. The adopted stoichiometry for Pd [21] and the Pd-Pt alloys is in agreement

with the fact that CO can be adsorbed in both linear and bridge mode over this Pd [38] and considering the composition of the alloys. According to the results in Table 2, overestimation of the dispersion of the metallic phase of the Pd-Pt/γ-Al$_2$O$_3$ catalysts is inevitable when using H$_2$ chemisorption at the present conditions. From CO chemisorption, with the exception of the Pd(1.0)-Pt(0.5) catalyst, the increase in the concentration of Pd in the alloy leads to a decrease in the dispersion of the Pd-Pt active phase over the γ-Al$_2$O$_3$ support. Therefore, no direct correlation between dispersion and the development of HYD can be established. Apart from dispersion, literature [40-42] reports that other geometrical effects thus play a central role in controlling the catalytic properties of the Pd-Pt system. It has been theoretically determined that the structural composition of the Pd-Pt alloy controls the dynamics in the adsorption, dissociation and migration of hydrogen species, H$_2$S and the S atom [42]. This effect seems to be very important to the capacity of the active phase of these catalysts of keeping the character of a supported monometallic Pd catalyst under the H$_2$S atmosphere of the hydrotreatment reaction environment [17, 42]. It is well accepted that the alloyed Pd-Pt particles consist in a Pt-rich core surrounded by a Pd-rich shell [43]. The results of the XPS characterization presented in Table 3 for the calcined and reduced catalysts show a decrease in the surface Pd/(Pd+Pt) atomic ratio of the bimetallic catalysts: precisely from 0.17, calcined, to 0.08, reduced, for Pd(0.2)-Pt(1.5), 0.55 to 0.31 for Pd(0.9)-Pt(0.7), 0.86 to 0.62 for Pd(1.0)-Pt(0.5) and 1.06 to 0.61 for Pd(1.4)-Pt(0.3), respectively. This behavior is indicative of Pd surface segregation after reduction [44]. XPS analysis also demonstrates that during reduction there is a change in the proportions of metallic Pd^0 and electron deficient Pd^{4+} and Pd^{2+} surface species present at the surface of the catalysts. It can

be seen that the $Pd^{\delta+}/Pd^0$ surface atomic ratio increases after reduction. The value of $Pd^{\delta+}/Pd^0$ atomic ratio decreased in the order: $Pd(1.0)-Pt(0.5) > Pd(1.4)-Pt(0.3) \approx Pd(0.9)-Pt(0.7)$. Thus, the bimetallic catalyst displaying the best performance both in HDS and naphthalene hydrogenation (Part I of the present Chapter) shows the highest increase in the amount of electron deficient $Pd^{\delta+}$ species as compared to metallic Pd^0 ones.

Fig. 3 shows the XPS spectra of monometallic Pt(1.3) -a- and bimetallic Pt(1.5)-Pd(0.2) -b- both calcined and after reduction.
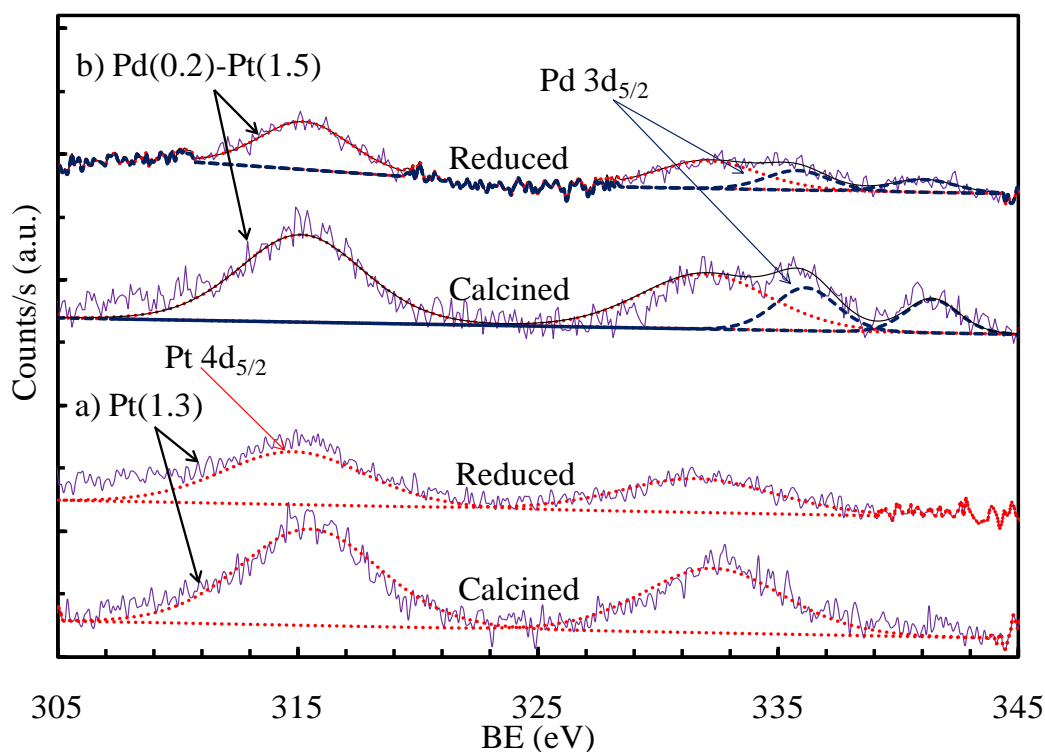
Fig. 3. XPS spectra of a) Pt(1.3) and b) Pd(0.2)-Pt(1.5); calcined and reduced samples. (•••) Pt 4d; (- - -) Pd 3d.

Table 3. XPS analysis of the Pd $3d_{5/2}$ peak of prepared Pd-Pt/γ-Al$_2$O$_3$ alloyed catalysts after calcination and reduction.

Catalyst	%At.						Surface atomic ratios				
Pd(1.9)	Pd 3d (Pd^0)	Pd 3d (Pd^{2+})	Pd 3d (Pd^{4+})	Pt 4d	Cl 2p	Al 2p - 2s†	Pd/(Pd+Pt)	Pd/Al	Pt/Al	Pd$^{\delta+}$/Pd^0	Cl/Al
Calcined	0.04	0.13	0.05	----	0.59	36.25	1.00	0.006	----	4.02	0.016
Reduced	0.08	0.09	0.06	----	0.57	28.49	1.00	0.008	----	1.92	0.020
Pt(1.3)											
Calcined	----	----	----	0.29	0.62	24.76	0.00	----	0.012	----	0.025
Reduced	----	----	----	0.25	0.61	21.00	0.00	----	0.012	----	0.029
Pd(0.2)-Pt(1.5)											
Calcined	N.D.	0.04	N.D.	0.19	0.56	23.93	0.17	0.002	0.008	N.D.	0.023
Reduced	0.02	0.01	0.02	0.15	0.63	21.79	0.08	0.001	0.007	N.D.	0.029
Pd(0.9)-Pt(0.7)											
Calcined	0.03	0.07	0.02	0.11	0.51	24.77	0.55	0.005	0.004	2.83	0.021
Reduced	0.01	0.05	0.04	0.18	0.60	19.70	0.31	0.005	0.009	11.00	0.030
Pd(1.0)-Pt(0.5)											
Calcined	0.06	0.11	0.03	0.08	0.51	24.47	0.86	0.008	0.003	2.24	0.020
Reduced	0.01	0.15	0.07	0.05	0.70	20.74	0.62	0.011	0.002	17.80	0.034
Pd(1.4)-Pt(0.3)											
Calcined	0.08	0.13	0.04	0.03	0.60	24.60	0.88	0.010	0.001	1.96	0.024
Reduced	0.01	0.11	0.04	0.08	0.61	21.09	0.61	0.008	0.004	11.21	0.029

†For the Pt containing catalysts the Al 2s line was selected

Regarding the positions of the Pt 4d and Pd 3d doublets it is observed that no large shift in the BE of both metal occurs neither by the formation of the alloy between both metals nor after reducing the catalysts. As observed in Fig. 3, the Pt 4d line in Pt(1.3) and Pd(0.2)-Pt(1.5) remains around 315 - 315.5 eV in all cases; monometallic and bimetallic catalysts whether calcined or reduced. The same trend was found for the other Pd-Pt/γ-Al$_2$O$_3$ catalysts. The Pt 4f line is found to be completely overlapped with the Al 2p line in all catalysts, as it has been determined for Pt/γ-Al$_2$O$_3$ of low metallic contents prepared from chlorided precursors [23].

XPS results presented in Table 3 show that residual chlorine is present on the surface of the series of prepared Pd-Pt/γ-Al$_2$O$_3$ catalysts, where the Cl/Al atomic ratio does not significantly change even after reduction. The same trend has been found by Karhu et al. [23] for monometallic chlorided Pt and Pd/γ-Al$_2$O$_3$. It has been possible to separate the Pt 4f line from the Al 2p line in Pt/γ-Al$_2$O$_3$ catalysts when a significant amount of Pt particles are in the metallic Pt^0 oxidation state [45, 46]. This is not feasible when the Pt metallic content is below 2 wt.% and chlorided precursors are employed [45]. The reason is the high resistance to reduction of the oxo-chlorided-platinum complexes formed during calcination [47]. Though after reduction the residual chlorine is not directly attached to Pt [48] its presence facilitates the formation of stronger Pt-O-Al bridges between the metal and the support [49]. This phenomenon is common to both chlorided Pt and Pd/γ-Al$_2$O$_3$ [23, 50]. The study conducted by Persson et al. [51] showed that the surface of oxidized Pd-Pt is composed by a mixture of Pd^{2+} and Pd^{4+} species in the shell of the Pd-Pt particles. In fact, Hilaire et al. [52] determined that the surface of oxidized Pd-Pt alloys is completely

covered by a layer of Pd oxide. EXAFS measurements [53] provided evidence that the active phase of Pd-Pt in aromatics hydrogenation under H_2S atmospheres consists on "Pd dispersed on Pt particles". This is consistent with the results in dibenzothiophene hydrodesulfurization and naphthalene hydrogenation obtained in Part I of the present Chapter as well as with the actual XPS analysis. Within this context, the increase in the amount of $Pd^{\delta+}$ species compared to Pd^0 after reduction, as determined from XPS, would be partly explained by considering that during the process of surface enrichment of the Pd-Pt particles the dispersion of the Pd^0 species decreases whereas the dispersion of $Pd^{\delta+}$ increases (see Table 3), therefore if after reduction the total amount of Pd^0 species increases, these particles are less exposed during XPS because of the decrease of dispersion. On the other hand, the formation of an ionic bond between Pt and Pd upon alloying would be expected. However, such electronic effects are not easily identifiable by most characterization techniques because of its very low intensity [54]. The formation of a Pd-Pt alloy is confirmed by TPR results as showed in Fig. 4. It is observed that the TPR profile of the bimetallic samples, i.e. Pd(0.2)-Pt(1.5) -Fig. 4c-, Pd(0.9)-Pt(0.7) -Fig. 4d-, Pd(1.0)-Pt(0.5) -Fig. 4e- and Pd(1.4)-Pt(0.3) -Fig. 4f-, respectively, is not the simple superposition of those corresponding to monometallic Pt(1.3) -Fig. 4a- and Pd(1.9) -Fig. 4b-. Pt displays a wide reduction peak with a maximum located around 490 K and a small shoulder at 640 K as in agreement with other studies [47]. The signals corresponding to chlorine species (HCl and Cl^+, respectively) confirm the presence of oxo-chlorided-Pt and -Pd complexes. On the other hand, Pd exhibits a peak of hydrogen production around 336 K due to the decomposition of the β-Pd-H hydride phase [55]. The same peak was only

detected again for the Pd(1.5)-Pt(0.2) bimetallic catalyst, but it was shifted to a lower temperature (320 K) -Fig. 4f-. This can be attributed to an inhibition of the formation of the β-Pd-H hydride phase due to Pt addition [56]. Comparing Pt and Pd it can be observed that the latter is more easily reduced than the former. The evolvement profile of chlorine species from Pd(1.9) is even less complex than the one registered for Pt(1.3). The intense MS Cl^+ peak of Pd is located at the same position (467 K) of the H_2 reduction curve which is at a lower temperature than the peak for Pt. As observed in Fig. 4 (c, d, e and f) the production of chlorine species and H_2 consumption is lower for the bimetallic Pd-Pt/γ-Al_2O_3 catalysts than for Pt and Pd. With the exception of Pd(0.9)-Pt(0.7), the alloys exhibited a reduction maximum at the same temperature as monometallic Pd, i.e. around 467 K. It is not clear why the maximum in the H_2 signal of the Pd(0.9)-Pt(0.7) catalyst is located at a higher temperature but it evidences the complex nature of the interactions between both metals in the alloy. Nevertheless, it must be noticed that the signals of chlorine species have their maxima around 500 - 505 K for all of the alloys excepting Pd(1.0)-Pt(0.5) for which such maximum is at a lower temperature (442 K). Moreover, compared to the other alloys this catalyst exhibited the highest Cl^+ and HCl signals and H_2 consumption. In conclusion, the reducibility of the Pd-Pt/γ-Al_2O_3 catalysts is also a function of the Pd/(Pd+Pt) molar ratio. Furthermore, the profile of decomposition of surface oxo-chloride Pd and Pt complexes agrees with XPS results showing that after the activation step only a fraction of Pt and Pd has been reduced to its zero valent metallic state.
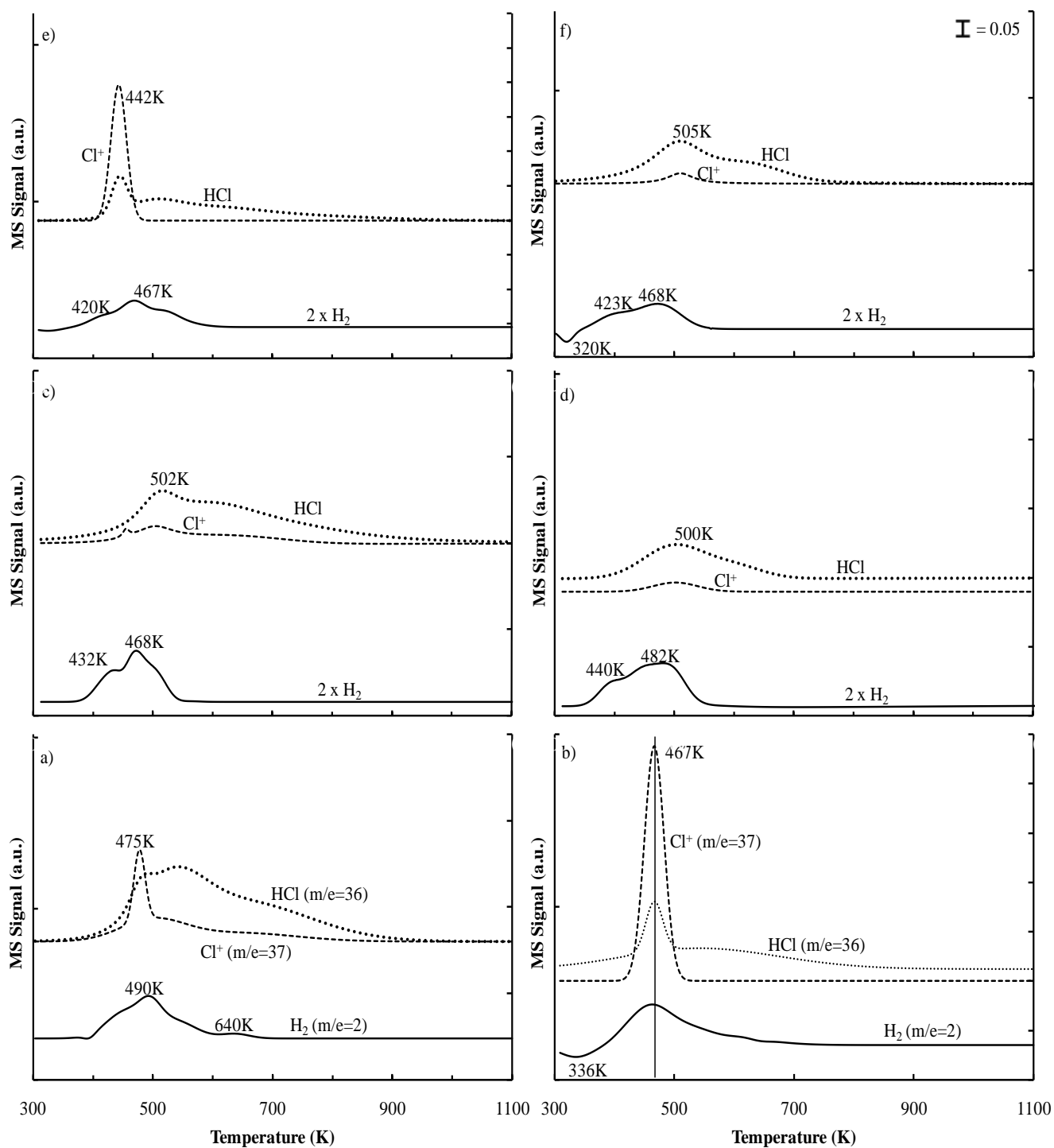
Fig. 4. Temperature programmed reduction profiles for calcined monometallic catalysts: a) Pt(1.3), b) Pd(1.9), c) Pd(0.2)-Pt(1.5), d) Pd(0.7)-Pt(0.9), e) Pd(1.0)-Pt(0.5), f) Pd(1.4)-Pt(0.3) (catalysts' codes as presented in Table 1). H_2 consumption, HCl and Cl^+ production Mass Spectrometer Signals vs Temperature.

Finally, considering the chemical changes of the Pd-Pt alloy after reduction, another simultaneous phenomenon contributing to the increase in the amount of $Pd^{\delta+}$ species after reduction can be a strengthen in the Pd-Pt ionic bond of the alloy leading to partial electronic transfer from Pd to Pt. Bando et al. [58] studied the chemical state of Pd-Pt/γ-Al_2O_3 after calcination and after reduction by EXAFS, and found that the bands assigned to Pd-(O, Cl) and Pt-(O, Cl) tend to disappear after reduction and new bands assigned to metal-metal bonds: Pd-Pd, Pt-Pt and Pd-Pt appear. Moreover, they suggested that the mixing of the Pd and Pt atoms increases with reduction temperature [57].

The above evidence contributes to improve the understanding on the way in which the active phase of Pd-Pt catalysts develops the HYD route of hydrodesulfurization of dibenzothiophene and its relationship with aromatics hydrogenation. Several authors have proposed that the main hydrogenation active sites of the bimetallic Pd-Pt alloys are Pd atoms keeping their metallic character under HDT reaction conditions [17, 24, 54]. Under sulfidation conditions it has been found that a mixture of metallic, Pt, Pd and Pd-Pt particles, and sulfided PtS_x and PdS_x species exists [17, 57-61]. According to the results of Qian et al. [59] the sulfur accommodated on the noble metals is highly labile and participates in the hydrodesulfurization reaction. As previously discussed, the structure of the Pd-Pt alloyed particles consists on a Pt-core surrounded by a Pd-shell. Bando et al. [58] demonstrated that sulfidation of the Pd-Pt particles proceeds from the core of the alloy and that Pt atoms are more accessible to sulfur. Niquille-Röthlisberger and Prins [24] suggested that the highly active hydrogenating active sites responsible for the development of the HYD route of hydrodesulfurization were Pd atoms keeping their metallic character. This is

in agreement with the model proposed by Fujikawa et al. [54]. From the results obtained here and the above discussion, in this Thesis it is proposed that for the prepared Pd-Pt/γ-Al$_2$O$_3$ catalysts the dynamic behavior of the Pd-Pt active phase during the hydrodesulfurization of dibenzothiophene consists on the sequential hydrogenation of the aromatic backbone of dibenzothiophene mainly over the electron deficient Pd$^{\delta+}$ containing Pd-Pt particle shell and further withdrawal of the S heteroatom mainly on core Pt atoms. This does not rule out neither the existence of intermetallic Pd-Pt active sites acting as HYD and S withdrawal active sites nor the existence of Pd particles performing S withdrawal from dibenzothiophene and its partially hydrogenated intermediates. Adsorption of H$_2$S and sulfur over such Pd$^{\delta+}$ containing Pd-Pt particle shell does not occur due to their high electron deficiency which significantly reduces noble metal affinity with the electron acceptor S heteroatom of dibenzothiophene. In an analogous way, some recent studies [8, 60] indicate that the active site for HYD on MoS$_2$ based catalysts possesses a metallic character (so-called "Brim-sites") [8] and do not adsorb H$_2$S [8, 60]. It must be remarked that the sulfided Pd and Pt species are neither thermodynamically stable [17, 26] nor the strength of the Pt-S, Pd-S bonds is high enough to form an active phase consisting on sulfur uncoordinated vacancies as that corresponding to MoS$_2$ based systems [59]. Finally, the contribution of additional metal-support interface sites for the adsorption of the dibenzothiophene aromatic backbone to the development of HYD over the chlorided Pd-Pt/γ-Al$_2$O$_3$ catalysts should not be completely neglected [61, 62].

3.3. Influence of naphthalene and H₂S on the hydrodesulfurization of dibenzothiophene over Pd-Pt/γ-Al₂O₃.

Fig. 5 shows the results of the first long-run test performed over a selected Pd-Pt/γ-Al₂O₃

catalyst (Pd(1.0)-Pt(0.5)) as a function of time on stream.
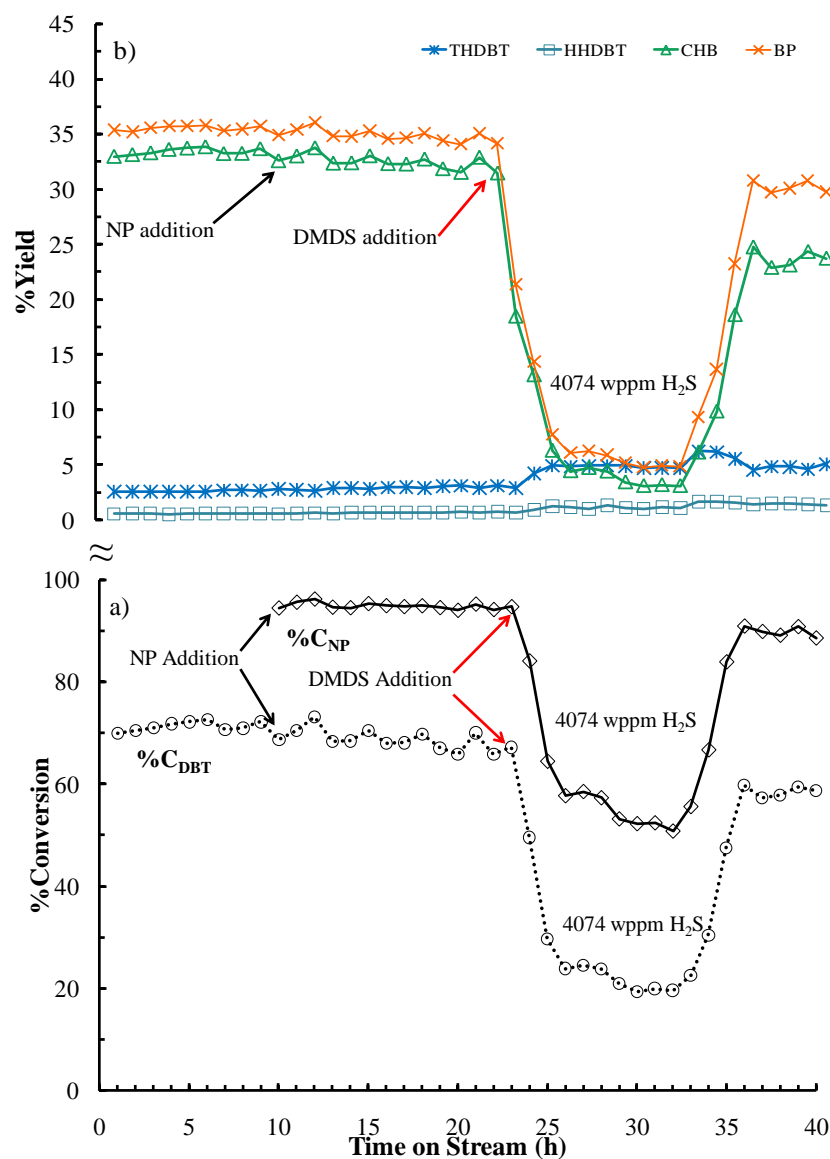
Fig. 5. Effect of the addition of naphthalene and subsequent increase of H₂S concentration in the evolution of the performance of Pd(1.0)-Pt(0.5) catalyst (Pd/(Pd+Pt) molar ratio=0.8) with time on stream during a hydrodesulfurization long-run test: a) Conversion of dibenzothiophene and naphthalene, b) products distribution.

The addition of naphthalene to the liquid feed during the hydrodesulfurization test neither significantly changes the activity (Fig. 5a) nor the selectivity in the hydrodesulfurization reaction (Fig. 5b). The catalyst displays a very high activity in the hydrogenation of naphthalene, $\%C_{NP}$ c.a. 100%, and simultaneously keeps its good selectivity to HYD. Naphthalene was converted mostly into tetralin with low amounts of *cis*-decalin and *trans*-decalin (not shown). The *trans*- to *cis*-decalin ratio was about 4 which is similar to that registered in the absence of H_2S in the reaction atmosphere (Part I: Section 3.2.1.). Such trend confirms that during hydrodesulfurization the catalyst's active phase keeps the functionalities exhibited in aromatics hydrogenation. It must be noticed that the conversion of naphthalene is always higher than that of dibenzothiophene. Such differences have been ascribed to differences in resonance energies [63, 64]. Comparing the present results with those previously reported [26, 31, Chapter II], it is particularly remarked that $Pt/\gamma-Al_2O_3$ [26, Chapter II, Section 3.2.4.] is more selective to the hydrodesulfurization reaction than to naphthalene hydrogenation, while an inverse trend is observed for $Pd/\gamma-Al_2O_3$ [31, Chapter II, Section 3.2.4.]. Further increase in the H_2S concentration caused an inhibition effect on both reactions, but did not change the Pd-Pt catalytic functionalities (Fig. 5). Accordingly, the selectivity remained invariable regarding either naphthalene hydrogenation to dibenzothiophene hydrodesulfurization or HYD to DDS, as in the case of monometallic $Pt/\gamma-Al_2O_3$. A slight increase in the production of both dibenzothiophene partially hydrogenated intermediates is observed, in particular of the TH-dibenzothiophene intermediate. This points out the fact that at very high H_2S concentrations the dynamics of the mechanism of dibenzothiophene hydrodesulfurization over Pd-Pt can be modified. A

similar behavior has been recently reported for un-promoted MoS_2 [13]. It is often considered that H_2S partial pressure has a more negative effect on DDS than in HYD [2, 3, 10, 14, 65, 66]. The trend observed in Fig. 5b shows that over Pd-Pt alloyed catalysts, both reaction pathways are negatively affected by H_2S to a similar extent, and that increasing H_2S partial pressure only partial hydrogenation of dibenzothiophene to TH-dibenzothiophene is favored. Thus, it can be considered that HYD is stopped at this step. The shift in the dynamics of the simultaneous hydrogenation and hydrodesulfurization reactions caused by H_2S can be related to a modification in the rate of atomic hydrogen transfer from the catalytic surface to the reacting molecules [26, 65, 66]. Finally, after withdrawing the excess H_2S concentration from the reaction environment it is observed that the Pd-Pt catalyst recovers almost all of its initial activity only merely changing its selectivity. It is interesting to observe in Fig. 5b that while the yield of HH-dibenzothiophene and TH-dibenzothiophene remained at the same level than in the stage under high H_2S concentration, the gap between the yields of cyclohexylbenzene and biphenyl widens, as compared to the initial stages of the reaction test, in favor of the latter. This indicates that a small but irreversible change in the dynamics of the HYD pathway has been caused by the presence of a very high concentration of H_2S. The above described effects can be ascribed to the adsorption of irreversible sulfur species [59]. From the present results, H_2S mostly has a strong inhibitory effect and a slight poisoning effect on the catalytic performance of the Pd-Pt alloyed particles [17, 59].

3.4. Effect of performing hydrogenation of naphthalene previous to the hydrodesulfurization of dibenzothiophene

Fig. 6a presents the catalytic performance (activity and S_{HYD}^{DS}) as a function of time on stream in the second long-run test; which consisted on performing naphthalene hydrogenation previous to dibenzothiophene hydrodesulfurization. The results of this test are quite different from the one described in the previous section. In this case, a significant deactivation of the catalyst is observed when adding dibenzothiophene. Such negative effect concerns deactivation in naphthalene hydrogenation, a poor activity in the hydrodesulfurization of dibenzothiophene, and a strong decrease in the selectivity to the HYD route. While on the first long-run test, i.e. addition of naphthalene during the hydrodesulfurization of dibenzothiophene S_{HYD}^{DS} remained as in the independent hydrodesulfurization of dibenzothiophene, in this case, S_{HYD}^{DS} is around half that value. The catalytic trends in hydrodesulfurization do not change after withdrawing naphthalene from the feed. In Part I of this Chapter, it has been determined that coke deposition decreases the hydrogenating capacity of the bimetallic Pd-Pt alloyed catalysts. When the surface of noble metal catalysts is "coked" they become more sensitive to H_2S presence in the reaction environment, because of an increase in the amount of irreversible adsorbed sulfur species [67]. This phenomenon has been ascribed to a diminution in the amount of available metallic active sites which in turn reduces the capacity of the catalyst to activate and transfer atomic hydrogen [67]. Jongpatiwut et al. [64] demonstrated that when performing this type of model reaction, aromatics hydrogenation followed by addition of dibenzothiophene, coke formation is accelerated due to the presence of H_2S, thus its negative effect on the catalytic performance is even more severe. Fig. 6b displays products

distribution from the hydrodesulfurization of dibenzothiophene (%yield) as a function of time on stream in this catalytic test. It is observed that during the subsequent hours of dibenzothiophene addition biphenyl yield decreases until reaching a stationary state. Conversely, the yield of cyclohexylbenzene in the presence of naphthalene, though slightly, constantly decreases. Additionally, TH-dibenzothiophene and HH-dibenzothiophene production was found to be almost the double of that registered in the test in which naphthalene was added to the feed of the already stabilized Pd-Pt catalyst in the hydrodesulfurization of dibenzothiophene (Fig. 5b). After withdrawing naphthalene from the liquid feed, a slight increase in the yields of both desulfurized products is observed, particularly for biphenyl. The above described behavior evidences that adsorption competition effects are present during simultaneous aromatics hydrogenation and hydrodesulfurization of dibenzothiophenes [31, 64]. On the other hand, it is shown that coke formation during aromatics hydrogenation can severely change the functionalities of the active phase of the Pd-Pt alloyed particles. In this regard, coke deposition on the catalytic surface of Pd-Pt was found to deeply affect the hydrogenation-dehydrogenation dynamics in the hydrogenation of naphthalene.

Finally, correlating the results obtained in both long-run catalytic tests it can be concluded that when the Pd-Pt surface has not been previously "coked", the presence of H_2S in the reaction environment has a less negative effect in the hydrogenating function of the Pd-Pt alloy. This phenomenon has been well described for noble metal based reforming catalysts [68]. In those studies, reversible sulfur adsorbed species increase the selectivity to hydrogenation-dehydrogenation reactions over parallel C-C hydrogenolysis then avoiding coke poisoning of the metallic surface [68].
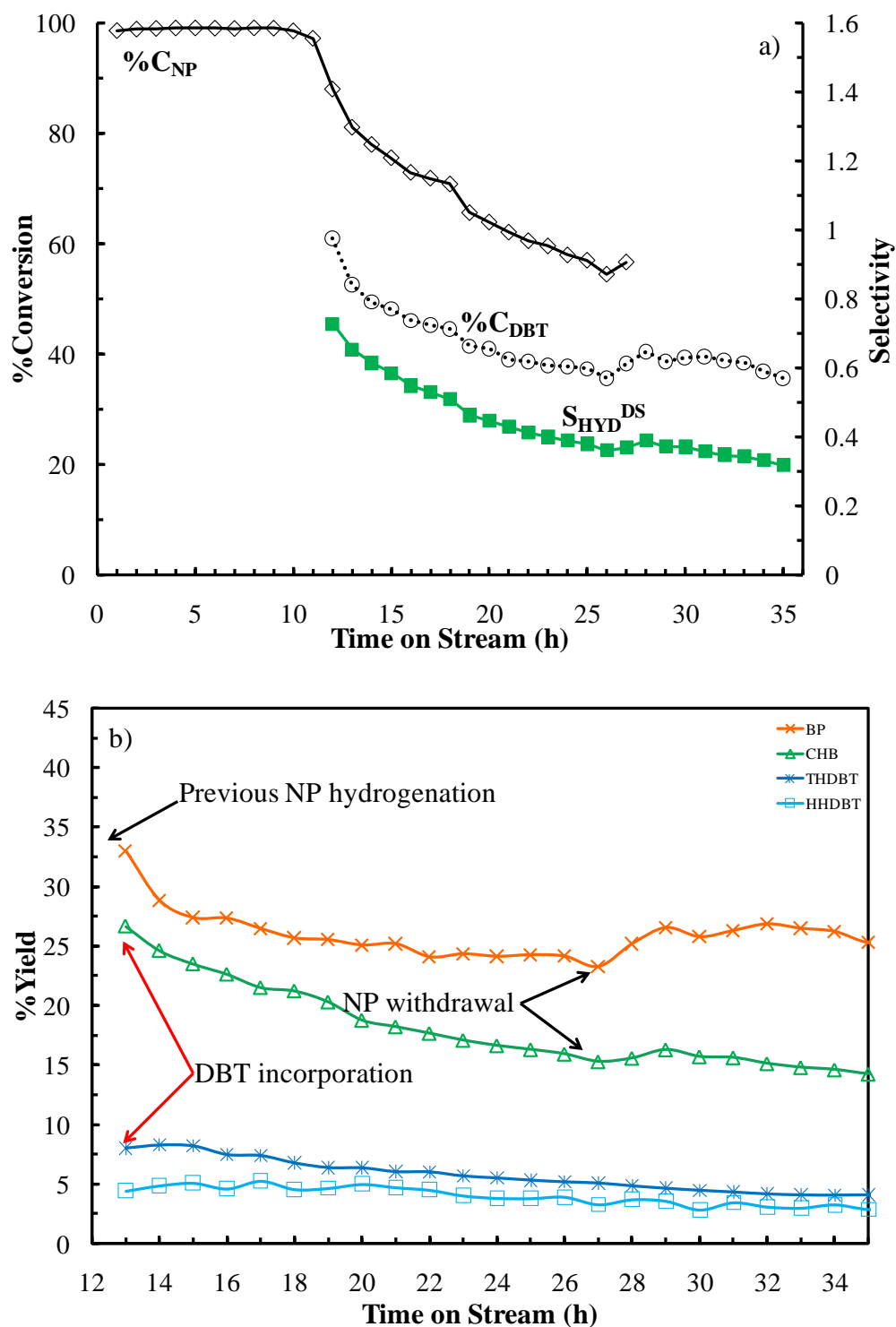
Fig. 6. Effect of performing naphthalene hydrogenation first and its subsequent withdraw from liquid feed on the catalytic performance of Pd(1.0)-Pt(0.5) with time on stream during a long-run test: a) Activity and Selectivity S_{HYD}^{DS}, b) products distribution.

4. Conclusions

The hydrodesulfurization of dibenzothiophene over Pd-Pt/γ-Al$_2$O$_3$ catalysts as a function of the Pd/(Pd+Pt) molar ratio was studied at different reaction conditions. It was determined that no synergy effects on the HDS activity over the Pd-Pt alloyed system exists. Instead, a synergetic effect for the development of the HYD route of hydrodesulfurization was observed in agreement with the synergy of Pd-Pt in aromatics hydrogenation under an H$_2$S atmosphere. Consequently, the dynamics of hydrogenation-dehydrogenation-C-S-C bond breaking during the hydrodesulfurization of dibenzothiophene can be controlled from the Pd/(Pd+Pt) molar ratio of the alloy. Characterization results showed that the development of HYD is related to the existence of a Pd-Pt active phase possessing some of the functionalities of monometallic Pd and comprising the interaction between electron deficient Pd$^{\delta+}$ particles and platinum, the formers enriching the surface of the Pd-Pt alloy.

On the other hand, concerning the stability of the catalysts, the addition of naphthalene during a dibenzothiophene hydrodesulfurization reaction over a Pd-Pt catalyst of Pd/(Pd+Pt) molar ratio = 0.8, working at steady state conditions, was found to change neither the HDS activity nor the HYD selectivity. At high H$_2$S excess concentration an inhibition of all catalytic functionalities of Pd-Pt was observed rather than poisoning. This inhibition effect hinders the C-S-C bond scission step of both the HYD and DDS reaction. Finally, coke deposition due to naphthalene hydrogenation was encountered to have a more severe and irreversible deactivating effect over the functionalities of Pd-Pt than H$_2$S.

References

[1] C. Song, Catal. Today 86 (2003) 211.

[2] D.D. Whitehurst, T. Isoda, I. Mochida, Adv. Catal. 42 (1998) 345.

[3] M.V. Landau, D. Berger, M. Herskowitz, J. Catal. 159 (1996) 236.

[4] H. Yang, C. Fairbridge, Z. Ring, Energy Fuels 17 (2003) 387.

[5] H. Kwart, G.C.A. Schuit, B.C. Gates, J. Catal. 61 (1980) 128.

[6] M. Zdražil, Appl. Catal. 4 (1982) 107.

[7] P. Raybaud, J. Hafner, G. Kresse, H. Toulhoat, Phys. Rev. Lett. 80 (1998) 1481.

[8] F. Besenbacher, M. Brorson, B.S. Clausen, S. Helveg, B. Hinnemann, J. Kibsgaard, J.V. Lauritsen, P.G. Moses, J.K. Nørskov, H. Topsøe Catal. Today 130 (2008) 86.

[9] S. Cristol, J.-F. Paul, E. Payen, D. Bougeard, F. Hutschka, S. Clémendot, J. Catal. 224 (2004) 138.

[10] J. Mijoin, G. Pérot, F. Bataille, J.L. Lemberton, M. Breysse, S. Kasztelan, Catal. Lett. 71 (2001) 139.

[11] R. Prins, M. Egorova, A. Röthlisberger, Y. Zhao, N. Sivasankar, P. Kukula, Catal. Today 111 (2006) 84.

[12] H. Wang, R. Prins, Appl. Catal. A: Gen. 350 (2008) 191.

[13] H. Wang, R. Prins, J. Catal. 258 (2008) 153.

[14] F. Bataille, J.-L. Lemberton, P. Michaud, G. Pérot, M. Vrinat, M. Lemaire, E. Schulz, M. Breysse, S. Kasztelan, J. Catal. 191 (2000) 409.

[15] V.G. Baldovino-Medrano, S.A. Giraldo, A. Centeno. Información Tecnológica 20:6 (2009), In press.

[16] H.R. Reinhoudt, R. Troost, A.D. van Langeveld, S.T. Sie, J.A.R. van Veen, J.A. Moulijn, Fuel Proc. Tech. 61 (1999) 133.

[17] Y. Yoshimura, M. Toba, T. Matsui, M. Harada, Y. Ichihashi, K.K. Bando, H. Yasuda, H. Ishihara, Y. Morita, T. Kameoka, Appl. Catal. A: Gen. 322 (2007) 152.

[18] N. Matsubayashi, H. Yasuda, M. Imamura, Y. Yoshimura, Catal. Today 45 (1998) 375.

[19] W. Palczewska, Adv. Catal. 24 (1975) 245.

[20] S. Hermans, C. Diverchy, O. Demoulin, V. Dubois, E.M. Gaigneaux, M. Devillers. J. Catal. 243 (2006) 239.

[21] R.M. Navarro, B. Pawelec, J.M. Trejo, R. Mariscal, J.L.G. Fierro, J. Catal. 189 (2000) 184.

[22] L.M. Tosta Simplício, S. Teixeira Brandão, E. Andrade Sales, L. Lietti, F. Bozon-Verduraz, Appl. Catal. B: Environ. 63 (2006) 9.

[23] H. Karhu, A. Kalantar, I.J. Väyrynen, T. Salmi, D.Yu. Murzin, Appl. Catal. A: Gen. 247 (2003) 283.

[24] A. Niquille-Röthlisberger, R. Prins, J. Catal. 242 (2006) 207.

[25] E. Dhainaut, H. Charcosset, C. Cachet, L. de Mourgues, Appl. Catal. 2 (1982) 75.

[26] V.G. Baldovino-Medrano, S.A. Giraldo, A. Centeno, Fuel 87 (2008) 1917.

[27] M. Houalla, N. K. Nag, A.V. Sapre, D.H. Broderick, B.C. Gates, AlChE J. 24 (1978) 1015.

[28] A.W. Weitkamp, Adv. Catal. 18 (1968) 1.

[29] S. Dokjampa, T. Rirksomboon, S. Osuwan, S. Jongpatiwut, D.E. Resasco, Catal. Today 123 (2007) 218.

[30] A.K. Neyestanaki, P. Mäki-Arvela, H. Backman, H. Karhu, T. Salmi, J. Väyrynen, D.Yu. Murzin, J. Mol. Catal. A: Chem. 193 (2003) 237.

[31] V.G. Baldovino-Medrano, S.A. Giraldo, A. Centeno, J. Mol. Catal. A: Chem. 301 (2009) 127.

[32] A.K. Neyestanaki, P. Mäki-Arvela, H. Backman, H. Karhu, T. Salmi, J. Väyrynen, D.Yu. Murzin, J. Catal 218 (2003) 267.

[33] S. Khoobiar, J. Phys. Chem. 68 (1964) 411.

[34] Y. Wang, R.T. Yang, J. Catal. 260 (2008) 198.

[35] T.-B. Lin, C.-A. Jan, J.-R. Chang, Ind. Eng. Chem. Res. 34 (1995) 4284.

[36] E. Guillon, J. Lynch, D. Uzio, B. Didillon, Catal. Today 65 (2001) 201.

[37] E.O. Orozco, M. Vrinat, Appl. Catal. A: Gen. 170 (1998) 195.

[38] H. Conrad, G. Ertl, J. Koch, E.E. Latta, Surf. Sci. 43 (1974) 462.

[39] M. Boudart, Adv. Catal., 20 (1969) 153.

[40] L. Guczi, Z. Schay, Stud. Surf. Sci. Catal. 27 (1986) 313.

[41] M. Jacquin, D.J. Jones, J. Rozière, A.J. López, E. Rodríguez-Castellón, J.M.T. Menayo, M. Lenarda, L. Storaro, A. Vaccari, S. Albertazzi, J. Catal. 228 (2004) 447.

[42] H. Jiang, H. Yang, R. Hawkins, Z. Ring, Catal. Today 125 (2007) 282.

[43] R. Ferrando, J. Jellinek, R.L. Johnston, Chem. Rev. 108 (2008) 845.

[44] L. Fiermans, R. De Gryse, G. De Doncker, P.A. Jacobs, J.A. Martens, J. Catal. 193 (2000) 108.

[45] J.Z. Shyu, K. Otto, Appl. Surf. Sci. 32 (1988) 246.

[46] Z. Paál, P. Tétényi, M. Muhler, U. Wild, J-M. Manoli, C. Potvin, J. Chem. Soc., Faraday Trans. 94 (1998) 459.

[47] H. Lieske, G. Lietz, H. Spindler, J. Völter, J. Catal. 81 (1983) 8.

[48] S.D. Jackson, J. Willis, G.D. Mclellan, G. Webb, M.B.T. Keegan, R.B. Moyes, S. Simpson, P.B. Wells, R. Whyman, J. Catal. 139 (1993) 191.

[49] A. Sarkany, G. Stefler, J.W. Hightower, Appl. Catal. A: Gen. 127 (1995) 77.

[50] A. Stanislaus, B.H. Cooper, Catal. Rev.-Sci. Eng. 36 (1994) 75.

[51] K. Persson, A. Ersson, K. Jansson, J.L.G. Fierro, S.G. Järås, J. Catal. 243 (2006) 14.

[52] L. Hilaire, G.Diaz Guerrero, P. Légaré, G. Maire, G. Krill, Surf. Sci. 146 (1984) 569.

[53] T. Fujikawa, K. Tsuji, H. Mizuguchi, H. Godo, K. Idei, K. Usui, Catal. Lett. 63 (1999) 27.

[54] B. Coq, F. Figueras, J. Mol. Catal. A: Chem. 173 (2001) 117.

[55] N.K. Nag, J. Phys. Chem. B 105 (2001) 5945.

[56] I.T. Caga, J.M. Winterbottom, J. Catal. 57 (1979) 494.

[57] K.K. Bando, T. Matsui, Y. Ichihashi, K. Sato, T. Tanaka, M. Imamura, N. Matsubayashi, Y. Yoshimura, Phys. Scr. T115 (2005) 828.

[58] K.K. Bando, T. Kawai, K. Asakura, T. Matsui, L. Le Bihan, H. Yasuda, Y. Yoshimura, S.T. Oyama, Catal. Today 111 (2006) 199.

[59] E.W. Qian, K. Otani, L. Li, A. Ishihara, T. Kabe, J. Catal. 221 (2004) 294.

[60] V. Vanrysselberghe, G.F. Froment, Ind. Eng. Chem. Res. 35 (1996) 3311.

[61] P. Chou, M.A. Vannice, J. Catal. 107 (1987) 129.

[62] A.Yu. Stakheev, L.M. Kustov, Appl. Catal. A: Gen. 188 (1999) 3.

[63] B. Pawelec, R. Mariscal, R. M. Navarro, S. van Bokhorst, S. Rojas, J. L. G. Fierro, Appl. Catal. A: Gen. 225 (2002) 223.

[64] S. Jongpatiwut, Z. Li, D.E. Resasco, W.E. Alvarez, E.L. Sughrue, G.W. Dodwell, Appl. Catal. A: Gen. 262 (2004) 241

[65] H. Farag, Appl. Catal. A: Gen. 331 (2007) 51.

[66] V. Rabarihoela-Rakotovao, S. Brunet, G. Perot and F. Diehl, Appl. Catal. A: Gen. 306 (2006) 34.

[67] J.T. Miller, D.C. Koningsberger, J. Catal. 162 (1996) 209.

[68] C.R. Apesteguía, J. Barbier, J. Catal. 78 (1982) 352.

General Conclusions of Chapter III

The selective hydrodesulfurization of dibenzothiophene was performed over Pd-Pt/γ-Al$_2$O$_3$ catalysts. These catalytic materials exhibited a synergetic effect in the development of the HYD route of hydrodesulfurization of dibenzothiophene. Synergy is controlled by the Pd/(Pd+Pt) atomic ratio of the system, and was found to be in correspondence with the synergy of Pd-Pt in the hydrogenation of aromatics under H$_2$S atmospheres. Such correlation has not been reported yet in literature, thus constituting one of the contributions of this Ph.D. Thesis.

Naphthalene hydrogenation model reaction was demonstrated to be a very useful alternative *in situ* characterization method providing relevant information on the nature of the active phase of Pd-Pt. The trends in the selectivity to the different reaction products of this reaction can be interpreted from the dynamics of the mechanism of hydrogenation of the molecule and correlated to changes in the interaction of the molecule with the catalyst's active phase. The production of tetralin and *trans*-decalin was associated to a strong interaction dynamic between the adsorbed intermediates and the active phase, whereas *cis*-decalin production was assumed to imply a very fast saturation of the model molecule, thus it was considered to correspond to a weaker dynamic interaction. The results obtained by this method were further verified and complemented by other characterization techniques. The information gathered this way allowed verifying some studies in literature and, the most important; it provided new insights into the nature and functioning of the Pd-Pt active phase in hydrotreatment. In this sense, the development of HYD is related to the existence of a Pd-Pt active phase possessing some of the functionalities of monometallic Pd and

comprising the interaction between electron deficient $Pd^{\delta+}$ particles and Pt, the formers enriching the surface of the Pd-Pt alloy. The dynamics of the HYD route of hydrodesulfurization comprises a series of hydrogenation-dehydrogenation-C-S-C bond breaking which can be controlled from the Pd/(Pd+Pt) molar ratio of the Pd-Pt alloy. In such dynamics the hydrogen uptake capacity of the catalytic material; hence, the rate of hydrogen transfer from the catalytic surface to the molecule, rather than the dispersion of the active phase, is playing a key role.

The dynamics of HYD can be modified by a sharp increase in the H_2S partial pressure and coke deposition over the catalytic active surface. In this regard, the negative effect of H_2S in the activity and selectivity of the catalysts is above all inhibitory not poisonous. In a parallel way, as H_2S completely shifts the selectivity in naphthalene hydrogenation to the partially hydrogenated tetralin intermediate, in the hydrodesulfurization of dibenzothiophene the production of partially hydrogenated dibenzothiophene intermediates increases while the production of desulfurized cyclohexylbenzene and biphenyl is lowered. Consequently, the increase in H_2S partial pressure hinders the C-S-C bond scission step of both the HYD and DDS reaction pathways. On the other hand, coking of the catalyst, during aromatics hydrogenation, profoundly modifies the functioning of the catalytic active phase of Pd-Pt rendering it to a less active and poorly HYD selective state under an H_2S atmosphere. This effect was clearly evidenced when comparing the results of the reaction tests in which the order of naphthalene hydrogenation and dibenzothiophene hydrodesulfurization was switched. The severe negative effect of coke on the functionalities of Pd-Pt is practically irreversible, but is not present when performing

simultaneous aromatics hydrogenation and dibenzothiophene hydrodesulfurization reactions. In such case, Pd-Pt/γ-Al$_2$O$_3$ is very active, and more selective to naphthalene hydrogenation than to dibenzothiophene hydrodesulfurization keeping a very good selectivity to the HYD route of hydrodesulfurization.

The findings presented in this Chapter are very important in HDT because they provide new insights into the nature of the active sites necessary to prepare highly HYD selective catalytic systems. The author thus considers that from this point of view one of the principal objectives of the present Thesis has been achieved; which is to rationally and sequentially determine the main properties that the active phase of Pd-Pt catalysts possesses and its correlation with the development of the HYD route of hydrodesulfurization. Finally, it must be remarked that the correlations obtained here have not been previously reported in open scientific literature.

Chapter IV: What does chlorine have to do with the development of the HYD route of hydrodesulfurization?

Abstract

The influence of the metallic precursor and the pretreatment of γ-alumina supported Pt and Pd catalysts on the reactivity of dibenzothiophene over these catalysts was studied. It was found that the use of chlorided precursors induces changes in the chemical state of the metals and in the acid properties of the support which are partly a function of the type of noble metal. Such changes were found to positively affect the conversion of dibenzothiophene over both monometallic systems. Regardless of the preparation conditions, Pt keeps its high selectivity to the direct route of hydrodesulfurization of dibenzothiophene, whereas over Pd, the selectivity to the hydrogenation route of hydrodesulfurization (HYD) is greatly enhanced when employing a chlorided precursor. The use of a low temperature pretreatment of the chlorided catalysts enhanced dibenzothiophene conversion, and for Pd/γ-Al$_2$O$_3$ it doubled the selectivity to HYD. The registered trends were rather related to a change in the distribution of acid sites of the catalysts than to the effect of dispersion.

Keywords: Pt/γ-Al$_2$O$_3$; Pd/γ-Al$_2$O$_3$; chlorine; pretreatment conditions; dibenzothiophene; HYD pathway; acidity.

1. **Introduction**

Either alloyed or as monometallic catalysts Pt and Pd have shown very good catalytic performance in the hydrodesulfurization (HDS) of dibenzothiophene (DBT) type molecules [1-6, Chapters II and III]. 4,6-dimethyl-DBT is the most representative member of the family of highly refractory di-β-dibenzothiophenes, and is usually regarded as the target molecule to be hydropurified in heavy cut oils [7, 8]. Though the HDS of this molecule can proceed by the hydrogenation (HYD) or direct (DDS) routes of hydrodesulfurization, it has been both experimentally and theoretically demonstrated that the steric hindrance imposed by the alkyl-substituents of 4,6-dimethyl-DBT practically leaves no room for the scission of the sulfur heteroatom via DDS [7-9]; thus making conversion via HYD essential to achieve the required rate of HDS [7, 8]. Within this frame, it is very desirable to develop catalytic systems able to perform the HDS of dibenzothiophene via HYD. A material highly selective to HYD during the hydrodesulfurization of dibenzothiophene will clearly present a higher rate of reaction when tested with 4,6-dimethyl-DBT [10]. To accomplish this goal, it is quite important to understand those factors which control the development of HYD. In the precedent chapters, it has been shown that the particular nature of the noble metals; Pd or Pt is very important for this purpose. In addition, several studies have pointed out the role played by the chemical properties of the support in HYD [1-6, 10]. An increase in the acidity of the support can enhance HYD reaction rates [10-13]. Moreover, acidic supports can improve the resistance of the noble metals to sulfidation increasing their activity in aromatics hydrogenation under HDS environments [14-28]. In fact, γ-Al$_2$O$_3$ supported Pt and Pd catalysts are known as bifunctional catalysts [19, 20, 27]. Their chemical

characteristics can be modified in many possible ways, ranging from the selection of the metallic precursor [1, 21-31] to the conditions used in the activation stage [1, 5, 6, 32-35]. In this Chapter, it was decided to study the specific influence of the use of two different metallic precursors, organometallic and chlorided Pt and Pd precursors, and the conditions used during the pretreatment of the catalysts before performing the hydrodesulfurization of dibenzothiophene in the selectivity to HYD. Catalysts were characterized by hydrogen and ammonia chemisorption, temperature programmed reduction (TPR) and X-ray photoelectron spectroscopy.

2. **Experimental**

2.1. *Catalysts preparation*

A series of γ-alumina (Procatalyse, S_{BET} = 220 m^2/g, Vp = 0.62 cm^3/g, Dp = 11.6 nm) supported Pt and Pd catalysts were prepared by three different methods. The first method consisted in the impregnation of the support with Pd(II) acetylacetonate (Pd(acac)$_2$) and Pt(II) acetylacetonate (Pt(acac)$_2$) (Sigma-Aldrich) precursors, respectively, diluted in toluene, followed by drying (12 h, T = 393 K) and calcination in air flow (4 h, T = 773 K). The second one consisted in the impregnation of the support with chloride precursors: aqueous solutions of PdCl$_2$ and H$_2$PtCl$_6$ (Sigma-Aldrich), respectively, followed by drying and calcination under the same conditions of the first method. Those catalysts prepared with these two methods were in situ reduced before the catalytic tests at 673 K, for 3 h. And finally, the third method consisted in treating the same catalysts prepared by method 2 by drying at 363 K for 6 h and reduction at 473 K, for 4 h. Catalysts were labeled according to each preparation method as follows: Pt(MC),Pd(MC)-Org for the first method; Pt(MC),Pd(MC)-Cl-HT for the second one (HT = high temperature), and Pt(MC),Pd(MC)-

Cl-LT for the third one (LT = low temperature). MC stands for the metallic content of the catalysts as obtained from atomic absorption.

2.2. Catalyst characterization

2.2.1. Hydrogen chemisorption

Hydrogen chemisorption measurements were performed in the same apparatus mentioned in Chapter III, Part II: Section 2.2.1. The pretreatment of the samples (c.a. 0.15 g) comprised an initial evacuation stage under He flow for 30min at the temperature selected for the measurement, followed by oxidation under O_2 flow; reproducing the conditions of catalyst's calcination described in section 2.1. Subsequent evacuations under He flow were carried out, each one for 30 min, at the employed oxidation temperature and at the temperature selected for the measurements. Afterward, in situ reduction in hydrogen at the corresponding conditions of the catalytic test was performed. i.e. samples of Pt(MC),Pd(MC)-Org and Pt(MC),Pd(MC)-Cl-HT catalysts were reduced at 673 K, and the samples of Pt(MC),Pd(MC)-Cl-LT were reduced at 473 K. After this step, evacuation was performed by flowing He for 2 h at the employed reduction temperature, under vacuum for 30min, and finally under vacuum at the temperature selected for the measurement for another 30 min. Hydrogen chemisorption isotherms were determined at 308 K for Pt catalysts and at 343 K for Pd ones to avoid the formation of the β-Pd-H hydride phase [36], this was also verified by TPR measurements. The reported hydrogen uptake values are taken from the volume difference between two hydrogen adsorption isotherms; the second one measured after an evacuation time of 45 min, extrapolated to zero pressure (strongly adsorbed hydrogen).

2.2.2. *Ammonia chemisorption*

Ammonia chemisorption measurements were carried out at 318, 423 and 623 K in a Micromeritics ASAP 2010C apparatus. Samples of the catalysts were pretreated following the same protocol employed during H_2 chemisorption measurements (Section 2.2.1). By using this protocol, the obtained results describe the acidity of the catalysts at the beginning of the catalytic tests. Acidic sites' strength is classified as: weak (measured at 318 K), medium (measured at 423 K) and strong (measured at 623 K), as in agreement with a previous literature report [37]. The total number of acidic sites is defined as the algebraic sum (weak+medium+strong) acidic sites. The relative number of acidic sites, according to its strength, is the ratio: (number of corresponding acidic site)/(total number of acidic sites.). The method for the evaluation of the amount of ammonia chemisorbed is similar to that used in hydrogen chemisorption.

2.2.3. *Temperature programmed reduction* (TPR)

Temperature programmed reduction (TPR) experiments were performed in the same instrument and conditions presented in Chapter III, Part II: Section 2.2.3. The MS signals corresponding to H_2 (m/z = 2), H_2O (m/z = 18), HCl (m/z = 36) and Cl^+ (m/z = 37); corresponding to diverse chlorine containing compounds, were monitored. Recorded signals were treated by using a Gaussian mathematical function.

2.2.4. *X-Ray photoelectron spectroscopy (XPS)*

XPS analyses were performed in the same apparatus and using the same protocol presented in Chapter III, Part II: Section 2.2.4. The following sequence of spectra was recorded: survey spectrum, C 1s, O 1s, Al 2p, Al 2s, Pd 3d, Pt 4d, Cl 2p, and C 1s again to check the stability of charge compensation in function of time and the absence of degradation of the

sample during the analyses. The Pd 3d doublet was deconvoluted in three components with Pd $3d_{5/2}$ binding energies fixed at 335 (Pd^0), 336 (Pd^{2+}) and 338eV (Pd^{4+}) [23]. The algebraic sum of the surface atomic concentration of ($Pd^{2+}+Pd^{4+}$) species was defined as the total concentration of surface electron deficient $Pd^{\delta+}$ species. For the Pt 4d peak the energy separation for the doublet was fixed at 16.8 eV [22].

2.3. Catalytic tests

Catalysts were tested in the hydrodesulfurization of dibenzothiophene as it was described in precedent Chapters. Catalytic tests were conducted until reaching the steady state. Reaction products detected were: biphenyl (BP), cyclohexylbenzene (CHB) and hydrogenated intermediates: TH-dibenzothiophene (THDBT) and HH-dibenzothiophene (HHDBT).

Activity ($\%C_{DBT}$), products distribution ($\%y_i$) and selectivity (S_{HYD}) were expressed as in precedent Chapters.

3. Results and discussion

3.1. Chemical properties of the prepared catalysts

The results of H_2 and NH_3 chemisorption are displayed in Table 1. H_2 uptake, expressed as μmol H_2/μmol metal, followed the order: Pt(1.1)-Cl-HT > Pt(1.1)-Cl-LT > Pt(1.4)-Org, for Pt, and Pd(1.4)-Cl-HT > Pd(1.8)-Org > Pd(1.4)-Cl-LT, for Pd. For the chlorided Pt and Pd catalysts, the high temperature treatment increases H_2 uptake capacity compared to the low temperature treatment.

Table 1. H_2 and NH_3 chemisorption results for the prepared γ-Al_2O_3 supported Pd and Pt catalysts.

Catalyst[†]	n_{ads}^{STP} (μmol H_2/μmol metal)	n_{ads}^{STP} (μmol NH_3/g cat.)			Total Number of sites
		T (K)			
		308.15	423.15	623.15	
γ-Al_2O_3	----	376.0	236.5	65.7	678.1
Pt(1.4)-Org	0.29	361.4	218.2	69.6	649.3
Pt(1.1)-Cl-LT	0.38	443.0	190.9	105.8	739.7
Pt(1.1)-Cl-HT	0.56	527.1	289.9	178.0	995.0
Pd(1.8)-Org	0.13	390.4	197.1	88.6	676.1
Pd(1.4)-Cl-LT	0.10	481.9	168.4	135.1	785.4
Pd(1.4)-Cl-HT	0.21	601.1	393.9	105.0	1101.0

[†]Pt(MC),Pd(MC)-Org = catalysts prepared from acetylacetonate precursors, calcined at 773K and activated by H_2 reduction at 673 K; Pt,Pd-Cl-LT = catalysts prepared from chloride precursors, dried at 363 K and activated by H_2 reduction at 473 K; Pt,Pd-Cl-HT = catalysts prepared from chloride precursors and treated as those prepared with organometallic precursors. MC = metallic content as determined by atomic absorption.

Dispersion values of the noble metals as obtained from these measurements are not presented here due to fact that overestimation resulting from the hydrogen spillover phenomena for γ-Al_2O_3 supported Pt and Pd cannot be completely ruled out [16, 17, 38]. On the other hand, Pd catalysts are found to possess a lower H_2 uptake capacity than Pt ones. This fact cannot be attributed to the formation of β-Pd-H hydrides. Fig. 1 shows the TPR patterns of the γ-Al_2O_3 supported Pt and Pd catalysts. It can be seen in Fig. 1b that the peak corresponding to β-Pd-H appears below 343 K [36]; which is the temperature selected for the H_2 chemisorption experiments for Pd. Therefore, it can be assumed that, in general, regardless of the preparation method, the Pd catalysts have an intrinsically lower capacity to chemisorb hydrogen than Pt ones. Finally, as observed in Table 1, calcination at 773 K significantly enhances the H_2 uptake capacity of the catalysts.
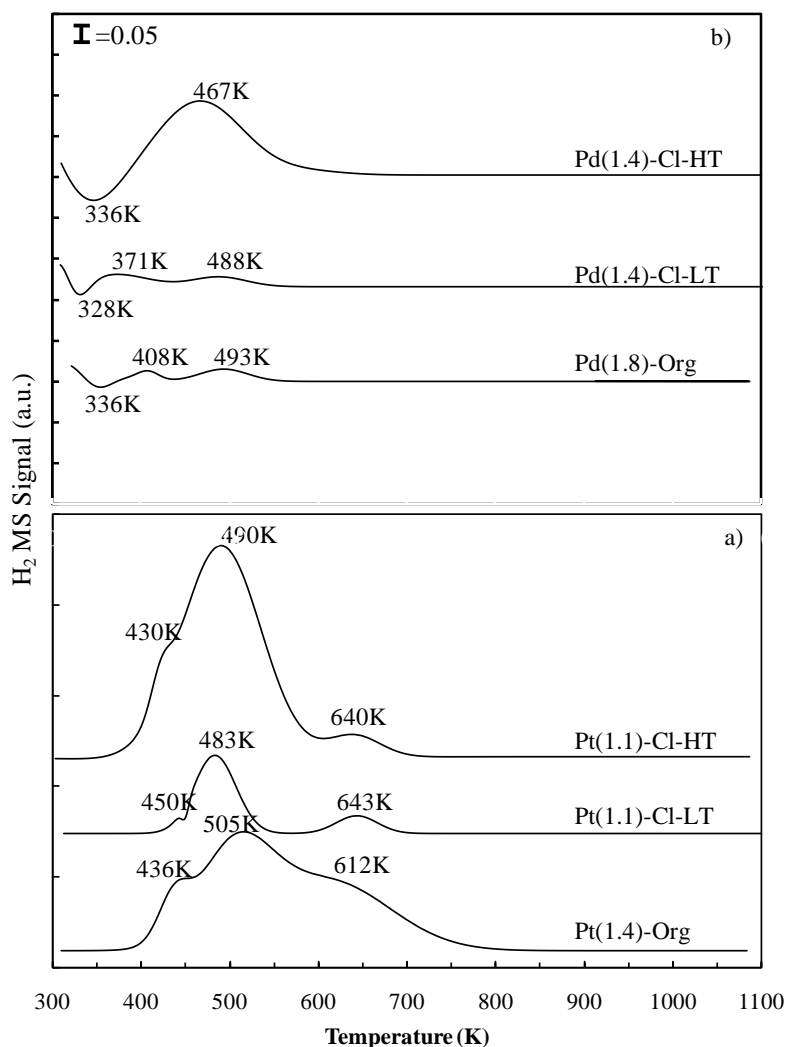
Fig. 1. TPR patterns for the prepared Pd and Pt catalysts: a) Pt catalysts: Pt(1.4)-Org., Pt(1.1)-Cl-LT, and Pt(1.1)-Cl-HT; b) Pd catalysts: Pd(1.8)-Org., Pd(1.4)-Cl-LT, and Pd(1.4)-Cl-HT. The H_2 Mass Spectrometer Signals are inverted.

The oxidation state of the calcined catalysts was studied by XPS and the results are presented in Table 2 and Fig. 2 for Pd, and in Table 3 and Fig. 3 for Pt. As described in the experimental section (2.2.4.), the Pd 3d doublet was decomposed into three components; Pd^0, Pd^{2+} and Pd^{4+}, the ratio $Pd^{\delta+}/Pd^0$ being estimated. The presence of zero valent metallic particles can be partly attributed to reduction of the noble metal in the analysis chamber of

154

the instrument [22]. It can be observed in Table 2 that the ratio $Pd^{\delta+}/Pd^0$ is highest for Pd(1.4)-Cl-HT, whereas Pd(1.8)-Org and Pd(1.4)-Cl-LT display closer values, with the latter exhibiting a slightly higher ratio. Surface chlorine after calcination is detected for the samples of Pd/γ-Al_2O_3 prepared from $PdCl_2$, as in agreement with many literature reports [22-27, 30]. This was also evidenced by the detection of MS peaks attributed to chlorine containing species (m/z = 35 and m/z = 37) during the TPR analysis (not shown). The Cl/Al ratio decreases after the HT treatment. In the precedent Chapter (Part II: Section 3.2.) it was demonstrated that chlorine remains on the surface of Al_2O_3 supported noble metal catalysts even after reduction. This was found to agree with previous literature reports it has been demonstrated [22, 24, 26, 27, 32, 39, 40]. The above results picture a catalytic surface for Pd/γ-Al_2O_3 composed of a mixture of metallic Pd^0, PdO, PdO_2 and/or $PdCl_xO_y$ species; the latter in the case of the use of the chloride precursor, before reduction. As observed in Chapter III a change in the relative distribution of these different species can occur after reduction. It has been postulated that the presence of Pd^{4+} species and $PdCl_xO_y$ imply a stronger metal-support interaction [15, 18, 22, 40, 41]. The process of adsorption of Pd and Pt acetylacetonate and chloride precursors on γ-Al_2O_3 has been studied [28, 42]. The extensive study conducted by Rob van Veen et al. [28] concluded that the acetylacetonate complexes of Pd and Pt chemisorb on the Al^{3+} CUS sites of γ-Al_2O_3 and physisorbed on the γ-Al_2O_3 surface. These authors also established that the extent of $Pt(acac)_2$ adsorption on γ-Al_2O_3 is lower than that of $Pd(acac)_2$. In the case of the chlorided Pd and Pt precursors, the formation of chloro- and chloro(aquo)-palladate and platinate complexes in the presence of H^+ leads to surface charging of the –OH groups of alumina and further attachment of these

complexes on the positively charged $-AlOH_2^+$ surface groups [29, 43]. After pretreatment of the catalysts, either calcination or reduction, chlorine atoms are no longer attached to the metals, but remain in the vicinity of the Pt and Pd particles [40, 44]. The TPR patterns displayed in Fig. 1a show a wide peak of reduction for Pt(1.4)-Org with shoulders located at 436 and 612 K, respectively, and a maximum at 505 K. For the Pt(1.1)-Cl-HT, which has been prepared at the same calcination temperature, this peak is sharper and stronger with the maximum shifted to 490 K and the shoulders to 430 K and 640 K, respectively. The Pt(1.1)-Cl-LT sample of the chlorided catalyst exhibits a very small shoulder at 450 K followed by the most intense peak at 483 K and a separated peak at 643 K. These peaks are attributed a mixture of Pt species; PtO, PtO_2 and/or $PtCl_xO_y$ [24, 27], which are analogous to those determined for Pd in XPS. The XPS results for Pt (Table 3) show that the oxidation state of Pt in the chlorided catalysts, Pt(1.1)-Cl-HT and Pt(1.1)-Cl-LT, is alike, whereas the Pt 4d doublet for Pt(1.4)-Org is shifted to a lower BE, $\Delta BE \approx 1$ eV. This is indicative of the presence of Pt particles in an oxidation state closer to metallic Pt^0. The Pt 4d doublet presented in Fig.3a illustrates the BE shift. Furthermore, a survey of the Pt 4f peak of these catalysts (Fig. 3b) shows that contrary to the chlorided catalysts; for which the Pt 4f doublet is fully overlapped with the Al 2p line, the Pt 4f doublet of Pt(1.4)-Org is partially separated from Al 2p, at a BE of 71.0 eV. This is actually the position of metallic Pt^0. At this point it seems that this behavior does not match with the registered TPR pattern of this catalyst, because compared to the chlorided Pt samples it is observed that Pt(1.4)-Org is reduced at a higher temperature (Fig. 1a).

Table 2. XPS analysis of the prepared Pd/γ-Al_2O_3 catalysts before activation.

Catalyst	$335eV$ (Pd^0) %At.	$336eV$ (Pd^{2+}) %At.	$338eV$ (Pd^{4+}) %At.	Cl $2p_{3/2}$ BE	Cl $2p_{3/2}$ %At.	Al 2p BE	Al 2p %At.	Pd/Al	$Pd^{\delta+}/Pd^0$	Cl/Al
Pd(1.8)-Org	0.092	0.125	0.031	----	----	74.3	35.661	0.007	1.696	----
Pd(1.4)-Cl-LT	0.098	0.138	0.050	198.3	0.993	74.3	35.553	0.008	1.918	0.028
Pd(1.4)-Cl-HT	0.044	0.130	0.047	198.3	0.562	74.3	36.245	0.006	4.023	0.016

Table 3. XPS analysis of the prepared Pt/γ-Al_2O_3 catalysts before activation.

Catalyst	Pt $4d_{5/2}$ BE	Pt $4d_{5/2}$ %At.	Cl $2p_{3/2}$ BE	Cl $2p_{3/2}$ %At.	Al 2s BE	Al 2s %At.	Pt/Al	Cl/Al
Pt(1.4)-Org	314.6	1.162	----	----	119.19	26.539	0.044	----
Pt(1.1)-Cl-LT	315.9	0.381	199.98	0.829	119.21	24.963	0.015	0.033
Pt(1.1)-Cl-HT	315.5	0.288	199.95	0.591	119.15	24.764	0.012	0.024

However, various studies [26, 31] have demonstrated that the Pt 4f doublet can be separated from Al 2p in those chlorided Pt/γ-Al$_2$O$_3$ catalysts containing high metallic contents in which sintered Pt particles are present. Another factor that could be playing a role in such trend is the possible formation of a spinel PtAl$_2$O$_4$ phase after calcination, which has a higher reduction temperature [24]. This is more plausible when using the Pt(acac)$_2$ precursor due to attachment of the to the Al^{3+} CUS sites of γ-Al$_2$O$_3$ [28] and not to –OH surface groups as in the case of the chloride precursor [29, 43]. Fig. 1b displays TPR patterns of the Pd catalysts. A peak corresponding to the decomposition of β-Pd-H hydride phase [36] was detected in all of the catalysts. Such peak is located at 336 K for both, Pd(1.8)-Org and Pd(1.4)-Cl-HT, catalysts which are calcined at the same temperature, and at 328 K for the Pd(1.4)-Cl-LT catalyst, which was only dried at 363 K. Both Pd(1.8)-Org and Pd(1.4)-Cl-LT exhibit two small reduction peaks instead of the wide reduction peak centered around 467 K displayed by Pd(1.4)-Cl-HT. These two peaks are found to be located at 408 and 493 K for Pd(1.8)-Org, and at 371 and 488 K for Pd(1.4)-Cl-LT, respectively. The registered trend indicates that, as in the case of Pt, the Pd species present on those catalysts prepared from chlorides are more reducible than those obtained after preparation with the Pd(acac)$_2$ precursor. As in the case of Pt, the attachment of the Pd(acac)$_2$ complex to the Al^{3+} CUS sites of γ-Al$_2$O$_3$ instead to the –OH surface groups of the carrier could lead to the formation of Pd-Al species, such as PdAl$_2$O$_4$ which are reduced at higher temperatures [24]. For the samples of the catalyst prepared from the chloride precursor, the wide peak centered at 467 K for the Pd(1.4)-Cl-HT sample reflects a complex pattern of reduction of the diverse Pd species of the catalyst. The TPR pattern of

the dried sample (Pd(1.4)-Cl-LT) can be interpreted as the separation of two contributions of the wide peak of Pd(1.4)-Cl-HT. The existence of different Pd-Cl-alumina complexes after impregnation of aqueous $PdCl_2^{4-}$ in which Pd is surrounded and in direct contact with chlorine has been determined [43]. After calcination at 773 K, several studies demonstrate that these species are converted mostly to PdO, and partly to Pd^{4+}, with chlorine still attached to the Al_2O_3 support, but no longer directly linked to Pd [45, 46]. The maximum located around 467 K in the TPR analysis of chlorided Pd/γ-Al_2O_3 catalysts is attributed to the reduction of the $PdCl_xO_y$ complex [46]. After calcination at 773 K there is a significant increase in the amount of $Pd^{δ+}$ as compared to the concentration of Pd^0 rather due to a decrease in the surface concentration of Pd^0 than to a drastic change in the distribution of $(Pd^{4+}+Pd^{2+})$.
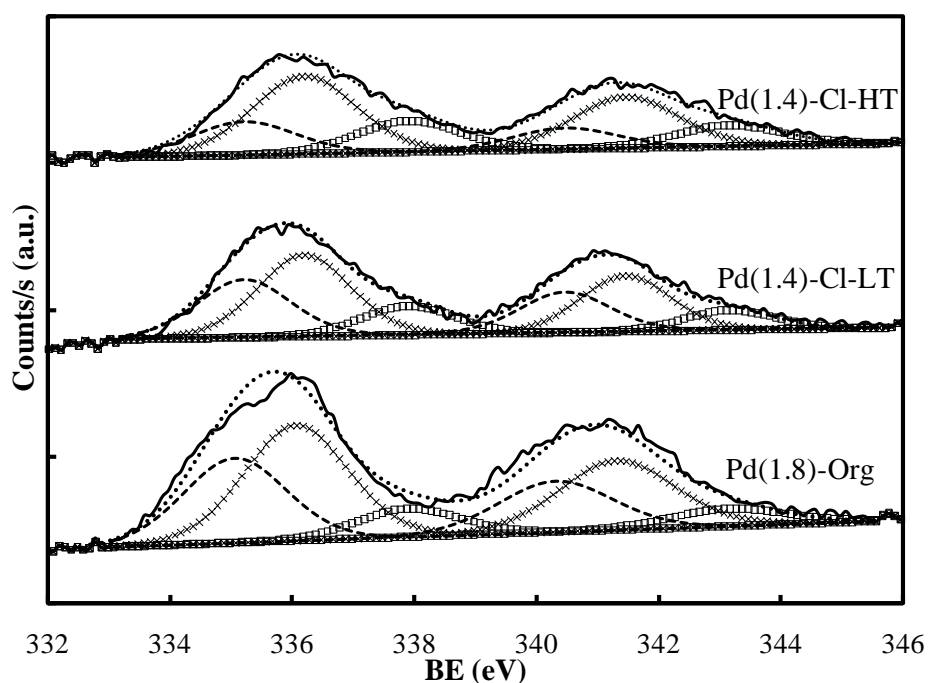
Fig. 2. XPS spectra decomposition of the Pd 3d doublet of Pd/γ-Al_2O_3 catalysts before activation. (- - -) Pd $3d_{5/2}$ at 335 eV (Pd^0); (xxx); Pd $3d_{5/2}$ at 336 eV (Pd^{2+}) and (□□□); Pd $3d_{5/2}$ at 338 eV (Pd^{4+}).
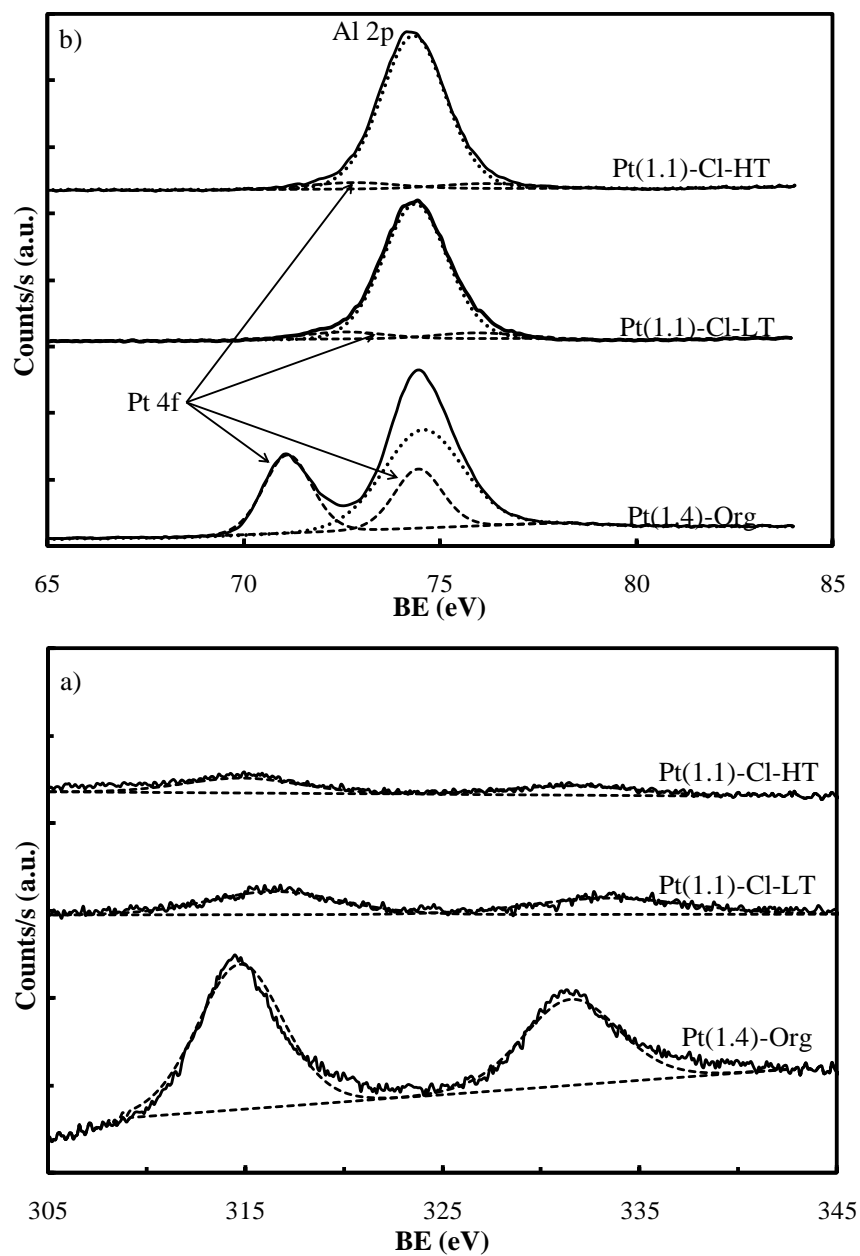
Fig. 3. XPS spectra of the Pt 4d doublet -Fig. 3a- and Al 2p line -Fig. 3b- of the Pt/γ-Al$_2$O$_3$ catalysts before activation.

Concerning the acidic properties of the materials, before the catalytic tests, the results of ammonia chemisorption are displayed in Table 1, and the relative density of acidic sites, as classified by its strength (see section 2.2.2. for details), is presented in Fig. 4.
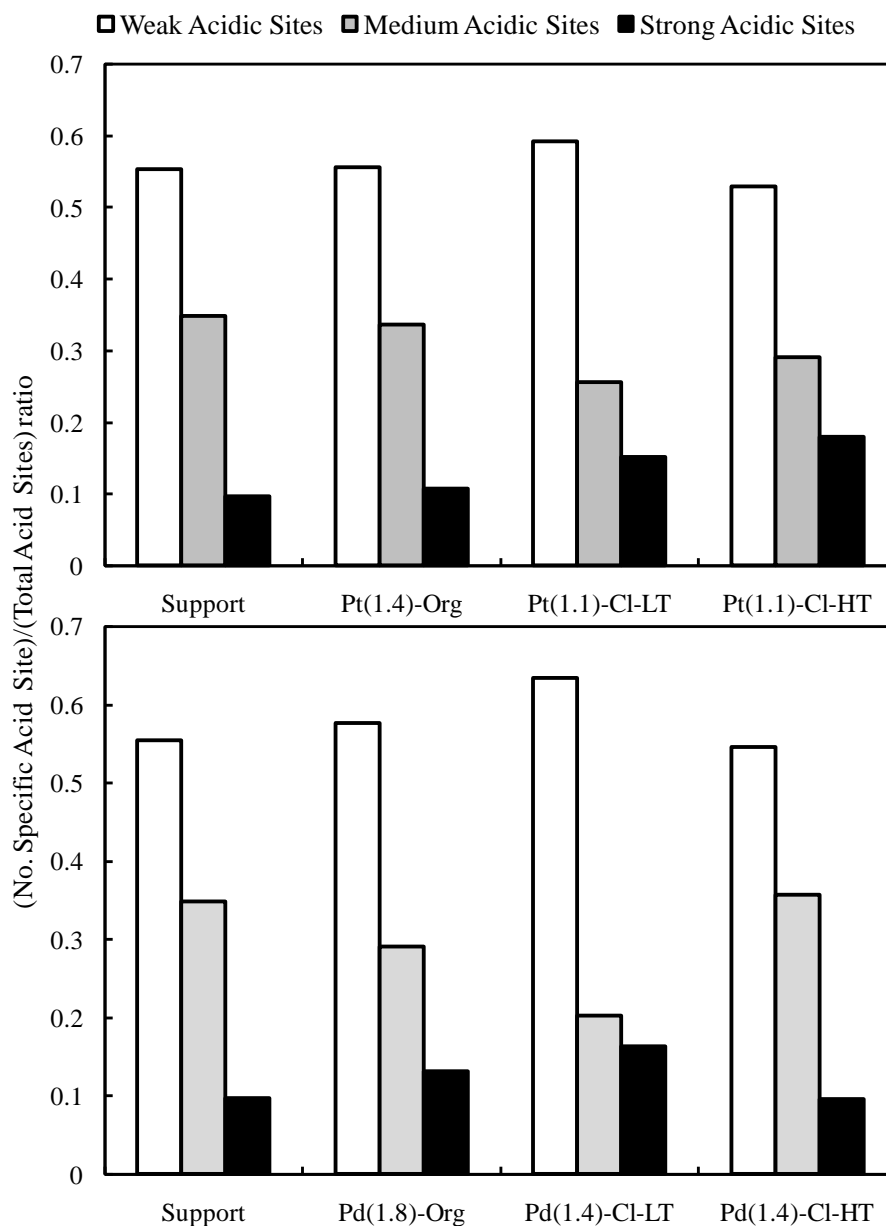
Fig. 4. Acidic sites distribution (relative number of acidic sites) for the prepared Pt and Pd/γ-Al$_2$O$_3$ catalysts according to their strength. Weak acidic sites from NH$_3$ chemisorption at T = 308 K; medium acidic sites from NH$_3$ chemisorption at T = 423 K, and strong acidic sites from NH$_3$ chemisorption at T = 623 K.

It can be seen in Table 1 that compared to the bare γ-Al$_2$O$_3$ support, which was reduced at the same condition of the HT catalysts, the Pt and Pd catalysts prepared from

acetylacetonates have a lower amount of total acidic sites. The Pd and Pt catalysts prepared from chlorides show a higher amount of total acidic sites, regardless of the pretreatment used. Pd catalysts have in all cases a higher concentration of acidic sites as compared to Pt ones, regardless the preparation conditions. It is interesting to follow the distribution of acidic sites according to their strength (Fig. 4). The distribution of weak, medium and strong acidic sites of those catalysts prepared from acetylacetonates is rather similar to that of the γ-Al_2O_3 support, indicating that the acidic properties of both materials are almost the same. Making a comparison of the density of acidic sites of the Pd and Pt catalysts as a function of the preparation method the following behavior is registered: (i) those catalysts prepared with chlorides and by the LT treatment showed the highest density of weak acidic sites, both for Pt and Pd, whereas those prepared with chlorides by the HT treatment exhibited the lowest density of them. (ii) In the case of the Pd catalysts, the highest density of medium acidic sites is registered for the Pd(1.4)-Cl-HT catalyst followed by Pd(1.8)-Org > Pd(1.4)-Cl-LT. This trend is not the same found for Pt, in this case: Pt(1.4)-Org > Pt(1.1)-Cl-HT > Pt(1.1)-Cl-LT. Finally, regarding the density of strong acidic sites (iii), for Pd, it followed the order: Pd(1.4)-Cl-LT > Pd(1.8)-Org > Pd(1.4)-Cl-HT, and for Pt: Pt(1.1)-Cl-HT > Pt(1.1)-Cl-LT> Pt(1.4)-Org. The results described above evidence small differences in the acidic balance of the catalysts as a function of the noble metal. Furthermore, from the results for the chlorided catalysts and those of the ones prepared from acetylacetonates, it is clear that the presence of residual chlorine influences such acidic balance. It is well known that chlorine significantly modifies the acidic properties of γ-Al_2O_3 due to a polarization of its surface –OH groups [47, 48]. During the decomposition of the metallic precursors, either

in the calcination or reduction stage, the interaction of the gaseous HCl produced has been found to induce the formation of new acidic sites on the alumina surface [47-49]. In particular, it seems that, regardless of the calcination temperature of the catalyst, the formation of Brønsted acidic sites occurs when reduction at low temperatures takes place, whereas at higher temperatures the apparition of strong Lewis acidic sites takes place [47-49]. The results of NH_3 chemisorption presented here are not useful to distinguish the precise nature of the acidic sites induced by chlorine, but reflect that, indeed, changes in the distribution of the strength of the acidic sites of the catalysts are happening during the pretreatment stage. The importance of such changes in the HYD selectivity will be further discussed in this document.

3.2. Catalytic performance in the hydrodesulfurization of dibenzothiophene

The conversion of dibenzothiophene and the yield to the different reaction products; biphenyl, cyclohexylbenzene, TH-dibenzothiophene and HH-dibenzothiophene, as a function of the preparation method are presented in Fig. 5 for Pt and in Fig. 6 for Pd. A decrease in dibenzothiophene conversion is observed for both Pt and Pd/γ-Al$_2$O$_3$ during the first two hours of reaction, after which the steady state is attained. This can be attributed to the irreversible adsorption of sulfur on the noble metal particles [1, 50]. The Pt catalysts are more active than the Pd ones, as in agreement with the results presented in Chapters II and III, as well as with other literature reports [3-5, 32, 50, 51]. The conversion of dibenzothiophene over the noble metals is a function of the nature of the metal and the preparation method.
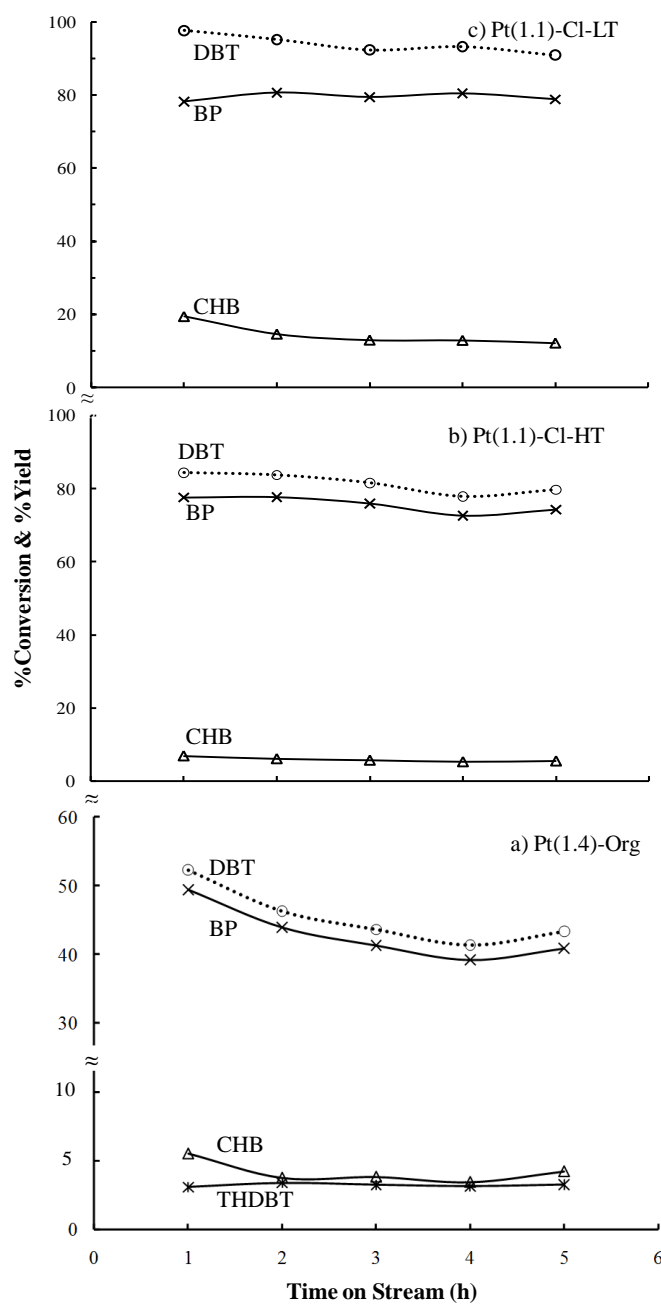
Fig. 5. Evolution with time on stream of the conversion of dibenzothiophene over the prepared Pt/γ-Al$_2$O$_3$ catalysts: a)Pt(1.4)-Org; b)Pt(1.1)-Cl-HT; c)Pt(1.1)-Cl-LT. Reaction conditions: T = 583 K, P = 5 MPa, liquid feed flow 30 mL/h, H$_2$/liquid feed ratio = 500 NL/L.
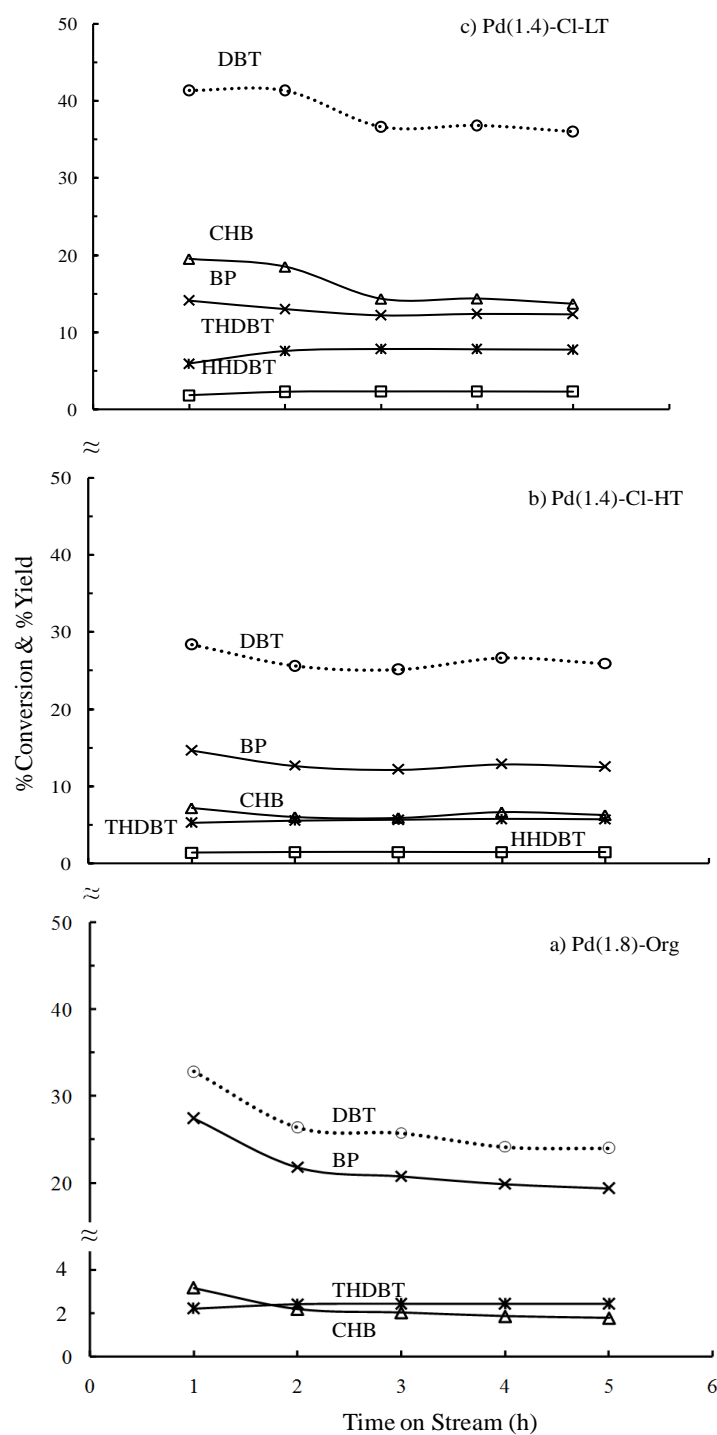
Fig. 6. Evolution with time on stream of the conversion of dibenzothiophene over the prepared Pd/γ-Al$_2$O$_3$ catalysts: a)Pd(1.8)-Org; b)Pd(1.4)-Cl-HT; c)Pt(1.4)-Cl-LT.

Examining the behavior of those catalysts prepared from the acetylacetonate precursors (Figs. 5a and 6a), it is noticed that, regardless of the noble metal, these catalysts are very selective to DDS, thus yielding biphenyl as the main reaction product, and very low amounts of cyclohexylbenzene and TH-dibenzothiophene. Part of the DDS active sites of these two catalysts is irreversibly poisoned at the beginning of the reaction. Furthermore, it can be said that a higher number of DDS active sites of the catalysts prepared from acetylacetonates are deactivated at the beginning of the reaction as compared to those prepared from chlorides. For the catalysts prepared from chlorides, the low temperature treatment enhanced the conversion of dibenzothiophene for both Pt and Pd as compared with the high temperature treatment. On the other hand, the selectivity HYD to DDS depends essentially on the nature of the noble metal for chlorided Pt and Pd/γ-Al$_2$O$_3$. Both samples of chlorided Pt/γ-Al$_2$O$_3$ are markedly selective to DDS (Figs. 5b and 5c), whereas over chlorided Pd/γ-Al$_2$O$_3$ HYD becomes more competitive to DDS (Fig. 6b) and overcomes DDS when the low temperature treatment is used (Fig. 6c). In fact, it is observed that for Pd(1.4)-Cl-LT the yield to cyclohexylbenzene is higher than the yield to biphenyl.

At this point, it was decided to correlate the reactivity of dibenzothiophene over the different Pt and Pd/γ-Al$_2$O$_3$ catalysts and the chemical properties of these materials, in order to gain better insight into the factors that control the development of HYD over both noble metals.

3.2.1. Relationship between the dispersion of Pt and Pd and the HDS of dibenzothiophene

Figs. 7a and 7b feature the steady state $\%C_{DBT}$ and S_{HYD} as function of the Pt/Al XPS atomic ratio and Pd/Al XPS atomic ratio, respectively; such ratios are considered to be semi-quantitative descriptors of dispersion in supported catalysts [52-54]. It can be seen that there is no apparent correlation between these variables, regardless the noble metal. The same qualitative result can be obtained by plotting $\%C_{DBT}$ and S_{HYD} as a function of the H_2 uptake (not shown) for both noble metals. In agreement with the present results, Niquille-Röthlisberger and Prins [3] discarded particle size effects in the HDS of dibenzothiophene and 4,6-dimethyl-DBT over Pd and Pt/γ-Al$_2$O$_3$. Consequently, the drastic changes in the catalytic performance of the prepared noble metal catalyst is rather related to nature of the precursors, and for those materials prepared from chlorides with the change in the pretreatment conditions.

3.2.2. Role of the use of chloride precursors in the hydrodesulfurization performance of Pt and Pd/γ-Al$_2$O$_3$.

As appointed before, the Pt and Pd catalysts prepared from chlorides are more active in the hydrodesulfurization reaction than those prepared from acetylacetonates. The presence of residual chlorine on the surface of the catalysts was verified by XPS for the calcined materials. In Chapter III (Part II: Section 3.2.) it has been demonstrated that residual chlorine is not eliminated after reduction in the activation stage. Literature reports agree with this [21, 23, 25, 32, 40]. NH$_3$ chemisorption measurements (Table 1) demonstrated an increase in the number of acidic sites of the chlorided catalysts. It is often considered that an increase in support's acidity enhances hydrodesulfurization and hydrogenation reaction

rates, as well as the sulfur tolerance of noble metals [4, 6, 7, 14-18]. This has been ascribed to the generation of electron deficient noble metal particles [14, 17, 18] and to the formation of additional hydrogenation sites on the metal-support interface which result from hydrogen spillover from the metal to the support [15-17, 34]. The electron deficiency of Pt and Pd reduces its affinity to sulfur and therefore weakens the metal-S bonds formed during the hydrodesulfurization reactions [1, 14, 17]. On the other hand, a bifunctional hydrodesulfurization mechanism has been often proposed [16, 55, 56]. Simon et al. [16] TPD studies on the decomposition of thiophene over Pt-supported zeolites reached the conclusion that the Brønsted acidic sites of the carriers in the proximity of Pt can act simultaneously as adsorption and hydrodesulfurization sites, the HDS activity of such metal-support interface sites being significantly enhanced by spilt-over hydrogen from Pt. From NH_3 chemisorption it is not possible to distinguish between Brønsted and Lewis acidic sites, but, as discussed before, the use of the chloride precursors besides an increase in the concentration of acidic sites of the catalysts causes a change in the distribution of the weak, medium and strong acidic sites which also depends on the type of noble metal. For Pt, such redistribution mostly increases the catalytic activity but not the HYD selectivity (Fig. 5). This is not the case of Pd, for which the increase in HDS is due mainly to an enhancement of the conversion of dibenzothiophene via HYD (Fig. 6). The increase in the selectivity to HYD is particularly higher after the low temperature treatment (approximately twofold). Chou and Vannice [34] tested a series of Pd catalysts supported in several carriers of different acidic properties, C, SiO_2, Al_2O_3 SiO_2-Al_2O_3 and TiO_2, and modifying the reduction temperature of those catalysts prepared from $PdCl_2$, in the hydrogenation of benzene. The highest turnover frequencies in the reaction where

registered for those Pd catalysts prepared with PdCl$_2$ and reduced at low temperature (448 K). They attributed this trend to the creation of additional Brønsted acidic sites on the carrier by the action of the HCl generated during the low temperature treatment; such acidic sites being transformed into strong Lewis acidic sites with the increase in reaction temperature [34, 51]. In conclusion, not only the presence of surface chlorine on the noble metals enhances the rate of hydrodesulfurization but the conditions of the pretreatment are very significant, in particular the reduction temperature during activation which can, aside from increasing dibenzothiophene conversion, help developing the HYD route of hydrodesulfurization especially over Pd catalysts.

3.2.3. *Factors controlling the development of HYD*

The development of HYD is highly desirable for deep hydrodesulfurization. The characterization and catalytic results presented so far evidence that HYD selectivity is always low for Pt catalysts, whereas it can be modulated over Pd catalysts basically by changing the acidic balance of the Al$_2$O$_3$ carrier. It is worth the while then to review and re-consider the mechanism of hydrodesulfurization of dibenzothiophene type molecules and compare it with copious experimental evidence in the field of aromatics hydrogenation over noble metal supported catalysts, with the aim of reconciling the catalytic behavior of the present materials. To do this, it must first be reminded that the formation of a π-complex between the aromatic backbone of dibenzothiophene and the catalytic active phase is a pre-requisite to HYD as in the case of aromatics hydrogenation [57-59] and that it has been assumed that the final sulfur withdrawal step in HYD is common to the one in DDS [3, 57]. A key factor controlling all hydrogenation reactions is the intrinsic capacity of the metal to

transfer hydrogen to the reacting molecule. This property is indirectly reflected by the measurements of H_2 chemisorption. It has been shown in Table 1, that the Pt catalysts have a higher H_2 uptake capacity than Pd (See also Chapter III, Part II: Section 3.2.). Such difference has been used in this Thesis to explain the higher intrinsic rate of hydrogenation of Pt compared to that of Pd and also linked to the development of HYD by a correlation with stereoselectivity differences in the hydrogenation of certain molecules such as o-xylene [60] and tetralin [61]. An additional factor has been encountered to play a significant role in the development of HYD over Pd in this Chapter; the acidic balance of the alumina carrier. It is known that alumina carriers possess mostly Lewis acidic sites [47, 48] and that sulfur from H_2S [62] and thiophene [56] can be adsorbed and even dissociated under certain reaction conditions [56]. Table 1 and Fig 4 demonstrate that the γ-Al_2O_3 support and those catalysts prepared from acetylacetonates have similar acidic properties. Contrary to the chlorided catalysts, in this case both the Pt(1.4)-Org and Pd(1.8)-Org catalysts show a high DDS selectivity. Sarbak [56] proposed that a decrease in the number of the stronger Lewis acidic sites of γ-Al_2O_3 enhances the DDS rate of hydrodesulfurization of thiophene by promoting the σ-adsorption of the molecule through the sulfur heteroatom on the weaker Lewis CUS vacancies of γ-Al_2O_3. Considering the mechanism of adsorption of the Pt(acac)$_2$ and Pd(acac)$_2$ precursors on the stronger Al^{3+} CUS sites of alumina [27] it is possible to speculate that DDS is thus favored particularly for Pd, because the strong selectivity to DDS of Pt remained rather unmodified at the conditions of the present study.
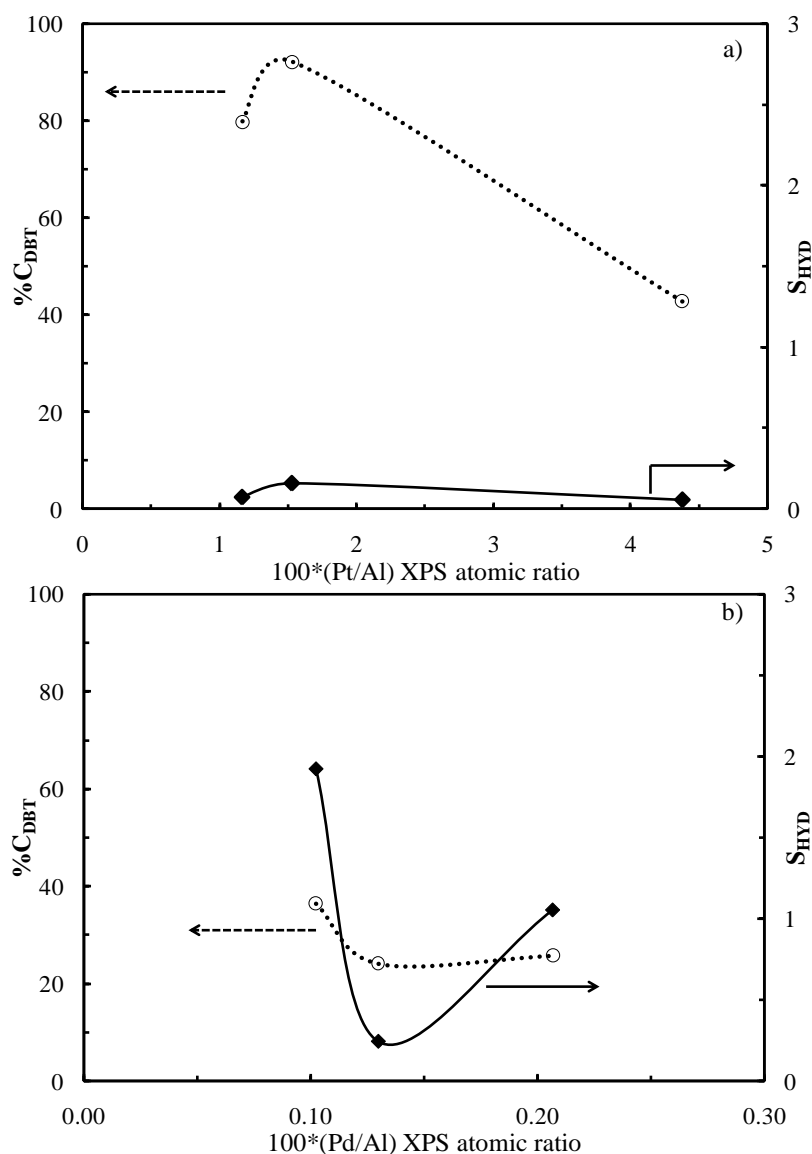
Fig. 7. Steady state conversion of dibenzothiophene (%C_{DBT}) and selectivity to HYD (S_{HYD}) plotted against the Pt,Pd/Al XPS atomic ratio. a)Pt/Al and b)Pd/Al.

On the other hand, if the presence of residual chlorine particularly enhances the number of stronger Lewis acidic sites of γ-Al_2O_3 and to a certain extent the apparition of Brønsted acidic sites [47-49, 56], and the noble metals are attached to the –OH groups of the carrier instead than to the Al^{3+} CUS sites of alumina this type of interaction between the

dibenzothiophene molecule and the support would be certainly disfavored, thus promoting HYD. Furthermore, stronger Lewis acidic sites have been also proposed to play a very important role in inducing an electronic interaction between the metal and the support which causes electron enrichment of the metal particles and thus enhances the rate of hydrogenation of aromatics [63]. When the low temperature pretreatment is applied the highest activity is registered for both Pt and Pd, but, whereas the HYD selectivity remains basically at the same level for Pt, it is significantly enhanced for Pd; in this case, cyclohexylbenzene becomes the main reaction product, while the yields of TH-dibenzothiophene and HH-dibenzothiophene are basically constant. As previously stated, it has been determined that when low temperature reduction of chlorided Pd catalysts is performed additional Brønsted acidic sites are created in the Al_2O_3 support as compared to reduction at higher temperatures [34, 49]. Several authors [15, 16, 34, 41] have proposed that in a bifunctional mechanism of hydrogenation these additional sites provide new hydrogenation active centers when in close proximity to the metallic phase. Such new hydrogenation sites would be responsible for the very high selectivity displayed by the chlorided Pd catalyst treated at low temperature. A final aspect to be considered in establishing a relationship between the mechanism of aromatics hydrogenation and the development of HYD is that an increase in acidity conducts to a decrease in the *cis*-decalin selectivity during tetralin hydrogenation over noble metals [63, 64]. Discarding the isomerization of subsequent isomerization of *cis*-decalin to *trans*-decalin it is recognized that the intrinsic increase in the selectivity to *trans*-decalin produced requires the *rollover* of the reaction intermediates over the catalytic surface [60, 61, 65], i.e. a consecutive adsorption-desorption of the octalin intermediate. In the previous Chapters (II and III) it has

been proposed that within the mechanistic dynamics of the HYD route of hydrodesulfurization of dibenzothiophene also a *rollover* mechanism is involved during the change in the adsorption mode of the dibenzothiophene partially hydrogenated intermediates on the active sites as to perform the final scission step of the S heteroatom. In this sense, very recent literature reports have indeed identified the presence of *cis*- and *trans*-TH-dibenzothiophene intermediates during the hydrodesulfurization of dibenzothiophene [10, 66], which give support to the hypothesis of the involvement of such mechanism in the hydrodesulfurization of such type of compounds.

4. Conclusions

In this Chapter it was demonstrated that the use of chloride precursors to prepare γ-Al$_2$O$_3$ supported Pt and Pd catalysts enhances the conversion of dibenzothiophene at typical hydrotreatment reaction conditions. The reactivity of dibenzothiophene is linked to the type of noble metal. Thus, it was confirmed that highly active Pt is always selective to the direct route of hydrodesulfurization, while less active Pd tends to develop the hydrogenation route of hydrodesulfurization when prepared from a chlorided precursor. Low temperature pretreatment of the chlorided catalysts, implicating reduction at 473 K, was found to enhance catalytic activity in both cases, and for Pd/γ-Al$_2$O$_3$ it doubled dibenzothiophene conversion via HYD, with cyclohexylbenzene as the main reaction product. It was established that these catalytic trends are related to changes induced by residual chlorine in the chemical state of the noble metals and in particular to a modification of the distribution of weak, medium and strong acidic sites of the catalysts. Such modification is thus very important to improve the selectivity to HYD of the catalytic materials prepared in this

Thesis. Therefore, in the final Chapter of the Thesis, it will be demonstrated that, indeed, a "soft" change in the acidic balance of the support of Pd-Pt alloyed catalysts makes this system even more selective to HYD than any other conventional and previous catalyst presented in open literature.

References

[1] Y. Yoshimura, M. Toba, T. Matsui, M. Harada, Y. Ichihashi, K.K. Bando, H. Yasuda, H. Ishihara, Y. Morita, T. Kameoka, Appl. Catal. A: Gen. 322 (2007) 152.

[2] H. Guo, Y. Sun, R. Prins, Catal. Today 130 (2008) 249.

[3] A. Niquille-Röthlisberger, R. Prins, J. Catal. 242 (2006) 207.

[4] V.L. Barrio, P.L. Arias, J.F. Cambra, M.B. Güemez, B. Pawelec, J.L.G. Fierro, Fuel 82 (2003) 501.

[5] V.G. Baldovino-Medrano, S.A. Giraldo, A. Centeno, Fuel 87 (2008) 1917.

[6] H.R. Reinhoudt, R. Troost, A.D. van Langeveld, S.T. Sie, J.A.R. van Veen, J.A. Moulijn, Fuel Proc. Tech. 61 (1999) 133.

[7] D.D. Whitehurst, T. Isoda, I. Mochida, Adv. Catal. 42 (1998) 345.

[8] S.K. Bej, S.K. Maity, U.T. Turaga, Energy Fuels 18 (2004) 1227.

[9] H. Yang, C. Fairbridge, Z. Ring, Energy Fuels 17 (2003) 387.

[10] C.-M. Wang, T.-C. Tsai, I. Wang, J. Catal. 262 (2009) 206.

[11] G. Pérot, Catal. Today 86 (2003) 111.

[12] M. Breysse, G. Djega-Mariadassou, S. Pessayre, C. Geantet, M. Vrinat, G. Pérot, M. Lemaire, Catal. Today 84 (2003) 129.

[13] F. Richard, T. Boita, G. Pérot, Appl. Catal. A: Gen. 320 (2007) 69.

[14] A. Stanislaus, B.H. Cooper, Catal. Rev.-Sci. Eng. 36 (1994) 75.

[15] L.J. Simon, J.G. van Ommen, A. Jentys, J.A. Lercher, Catal. Today 73 (2002) 105.

[16] L.J. Simon, M. Rep, J.G. van Ommen, J.A. Lercher, Appl. Catal. A Gen. 218 (2001) 161.

[17] A. Yu. Stakheev, L.M. Kustov, Appl. Catal. A: Gen. 188 (1999) 3.

[18] W.M.H. Sachtler, Catal. Today 15 (1992) 419.

[19] E.H. Van Broekhoven, V. Ponec, Prog. Surf. Sci. 19 (1985) 351.

[20] D. Łomot, W. Juszczyk, Z. Karpiński, Applied Catal. A: Gen. 155 (1997) 99.

[21] H. Karhu, A. Kalantar, I. J. Väyrynen, T. Salmi, D. Yu. Murzin, Appl. Catal. A: Gen. 247 (2003) 283.

[22] L.M. Tosta Simplício, S. Teixeira Brandão, E. Andrade Sales, L. Lietti, F. Bozon-Verduraz, Appl. Catal. B: Environ. 63 (2006) 9.

[23] C.-P. Hwang, C.-T. Yeh, J. Mol. Catal. A: Chem. 112 (1996) 295.

[24] P. Reyes, M. Oportus, G. Pecchi, R. Fréty, B. Moraweck, Catal. Lett. 37 (1996) 193.

[25] A.R. Sethuraman, B.H. Davis, Catal. Lett. 18 (1993) 401.

[26] H. Lieske, G. Lietz, H. Spindler, J. Völter, J. Catal. 81 (1983) 8.

[27] J.A. Rob van Veen, G. Jonkers, W.H. Hesselink, J. Chem. Soc. Faraday Trans. I 85 (1989) 389.

[28] W.A. Spieker, J.R. Regalbuto, Chem. Eng. Sci. 56 (2001) 3491.

[29] R.S. Monteiro, L.C. Dieguez, M. Schmal, Catal. Today 65 (2001) 77.

[30] J.Z. Shyu, K. Otto, Appl. Surf. Sci. 32 (1988) 246.

[31] N. Mahata, V. Vishwanathan, J. Catal. 196 (2000) 262.

[32] V.G. Baldovino-Medrano, S.A. Giraldo, A. Centeno, J. Mol. Cat. A Chem. 301 (2009) 127.

[33] D.C. Koningsberger, M. Vaarkamp, Phys. B: Cond. Matt. 208-209 (1995) 633.

[34] P. Chou, M.A. Vannice, J. Catal. 107 (1987) 129.

[35] J. Hancsóka, S. Magyar, K. Juhásza, D. Kallo, Top. Catal. 45 (2007) 207.

[36] W. Palczewska, Adv. Catal. 24 (1975) 245.

[37] F. Bertinchamps, A. Attianese, M.M. Mestdagh, E.M. Gaigneaux, Catal. Today 112 (2006) 165.

[38] Y. Wang, R.T. Yang, J. Catal. 260 (2008) 198.

[39] V.G. Baldovino-Medrano, S.A. Giraldo, A. Centeno, J. Catal. (2009) DOI: 10.1016/j.jcat.2009.08.004.

[40] S.D. Jackson, J. Willis, G.D. Mclellan, G. Webb, M.B.T. Keegan, R.B. Moyes, S. Simpson, P.B. Wells, R. Whyman, J. Catal. 139 (1993) 191.

[41] A. Sarkany, G. Stefler, J.W. Hightower, Appl. Catal. A: Gen. 127 (1995) 77.

[42] E. Lesage-Rosenberg, G. Vlaic, H. Dexpert, P. Lagarde, E. Freund, Appl. Catal. 22 (1986) 211.

[43] Cr. Conţescu, M.I. Vass, Appl. Catal. 33 (1987) 259.

[44] Z.C. Zhang, B.C. Beard, Appl. Catal. A: Gen. 188 (1999) 229.

[45] D. Roth, P. Gélin, M. Primet, E. Tena, Appl. Catal. A: Gen. 203 (2000) 37.

[46] G. Tonetto, M.L. Ferreira, D.E. Damiani, J. Mol. Catal. A: Chem. 171 (2001) 123.

[47] R.R Bailey, J.P Wightman, J. Colloid Inter. Sci. 70 (1979) 112.

[48] J.B. Peri, J. Phys. Chem. 70 (1966) 1482.

[49] M. Marczewski, M. Derewinski, St. Malinowski, Canad. J. Chem. Eng. 61 (1983) 93.

[50] E.W. Qian, K. Otani, L. Li, A. Ishihara, T. Kabe, J. Catal. 221 (2004) 294.

[51] E. Dhainaut, H. Charcosset, C. Cachet, L. de Mourgues, Appl. Catal. 2 (1982) 75.

[52] Y. Okamoto, T. Imanaka, S. Teranishi, J. Phys. Chem. 85 (1981) 3798.

[53] B.M. Reddy, B. Chowdhury, P.G. Smirniotis, Appl. Catal. A: Gen. 211 (2001) 19.

[54] N.K. Nag, Catal. Lett. 24 (1994) 37.

[55] M. Zdražil, Appl. Catal. 4 (1982) 107.

[56] Z. Sarbak, Appl. Catal. A: Gen. 159 (1997) 147.

[57] H. Yang, C. Fairbridge, Z. Ring, Energy Fuels 17 (2003) 387.

[58] N.K. Nag, Appl. Catal. 10 (1984) 53.

[59] J.J. Rooney, G. Webb, J. Catal. 3 (1964) 488.

[60] A.K. Neyestanaki, P. Mäki-Arvela, H. Backman, H. Karhu, T. Salmi, J. Väyrynen, D.Yu. Murzin, J. Mol. Catal. A 193 (2003) 237.

[61] S. Dokjampa, T. Rirksomboon, S. Osuwan, S. Jongpatiwut, D.E. Resasco, Catal. Today 123 (2007) 218.

[62] C.R. Apesteguia, J.F. Plaza De Los Reyes, T.F. Garetto, J.M. Parera, Appl. Catal. 4 (1982) 5.

[63] M.F. Williams, B. Fonfé, C. Woltz, A. Jentys, J.A.R. van Veen, J.A. Lercher, J. Catal. 251 (2007) 497.

[64] B.-C. Kang, T.-C. Huang, Chem. Eng. J. Biochem. Eng. J. 63 (1996) 27.

[65] Y. Inoue, J.M. Herrmann, H. Schmidt, R.L. Burwell Jr., J.B. Butt, J.B. Cohen, J. Catal. 53 (1978) 401.

[66] H. Wang, R. Prins, J. Catal. 258 (2008) 153.

Chapter V: Highly HYD selective Pd-Pt/support hydrotreating catalysts for the high pressure desulfurization of DBT type molecules

Abstract

A silica-alumina supported Pd-Pt bimetallic catalyst was found to be highly active in dibenzothiophene hydrodesulfurization with preferential selectivity to the hydrogenation (HYD) route of hydrodesulfurization at the expense of the direct removal of sulfur. In addition, it was demonstrated that for Pd-Pt catalysts selectivity to HYD can be drastically changed by a "soft" change in the nature of the carrier.

Keywords: Pd-Pt, SiO_2-Al_2O_3 support, hydrodesulfurization of dibenzothiophene, HYD reaction route.

1. Introduction

The development of the hydrogenation (HYD) route of desulfurization of dibenzothiophene (DBT) type molecules is urged in order to accomplish deep hydrodesulfurization (HDS) of heavy stock oils [1-3]. The main advantage of HYD is that it makes more flexible the aromatic structure of dibenzothiophene [3], which in turn reduces the steric hindrance of highly refractory di-β-dibenzothiophenes, such as 4,6-dimethyl-DBT [1-3]. In spite of the large amount of reports claiming new more active CoMo and NiMo sulfided catalysts, none of them have proven preferential conversion of dibenzothiophene via HYD so far [1-6]. This is due to the fact that the role of Co and Ni as promoters is mainly to enhance the direct C-S-C bond scission function of the MoS_2 active phase [4, Chapter I]. Also, to increase the selectivity to HYD over the direct desulfurization route (DDS), the active phase of the catalyst should be able to selectively adsorb the dibenzothiophene molecule in a flat π-mode through one of its aromatic rings and perform its HYD rather than binding

and breaking the S heteroatom in a "single" step [7]. Furthermore, DDS is the favored thermodynamic pathway under standard reaction conditions [8]. In Chapter III it has been demonstrated that the supported Pd-Pt system possess high activity in the hydrodesulfurization of dibenzothiophene, and exhibits better selectivity to HYD than conventional sulfided CoMo and NiMo catalysts. Other studies have shown that the hydrogenating capacity and thiotolerance of Pd-Pt catalysts allow them to perform the hydrodesulfurization of 4,6-dimethyl-DBT via HYD [9-12]. In spite of this, even over Pd-Pt neither preferential dibenzothiophene hydrodesulfurization via HYD has been achieved nor has HYD been effectively controlled only by "soft" changes in the nature of the carrier. This has been achieved in this work, where highly HYD selective Pd-Pt catalysts were developed for the high-pressure hydrodesulfurization of dibenzothiophene as a function of slight changes in the nature of the support.

2. Experimental

2.1. Catalysts preparation

Four bimetallic Pd-Pt catalysts, supported in different carriers, with a Pd/(Pd + Pt) = 0.8 molar ratio were prepared by incipient wetness co-impregnation. Supports used comprised: home-made SiO_2, Al_2O_3 and SiO_2-Al_2O_3, Si/Al molar ratio = 0.1, and Procatalyse γ-Al_2O_3 . Home-made carriers were prepared adapting the method presented by Cai et al. [13] for MCM. In a typical synthesis of 10g of support, c.a. 430 mL of deionized water and 27 mL of NH_4OH (Merck, reagent grade) were heated at 353 K under vigorous stirring. Then, approximately 8 g of the cationic surfactant, hexadecyltrimethylammonium bromide (CTAB) (Merck, 98%), was added to the mixture until complete dilution. Afterward, appropriate amounts of silica (tetraethyl orthosilicate, Merck) and/or aluminum

trisecbutoxide (Merck) were added slowly to this solution. A 0.125(CTAB):1(silica and/or aluminum precursors) molar ratio was used in all preparations. All throughout the preparation process, the pH was allowed to remain at its natural value (pH = 13 - 14). The resulting white slurry was filtered and dried at ambient conditions. To eliminate the surfactant a Soxhlet extraction was carried out for 24 h using an ethanol (250 mL) - HNO_3 (5 mL) solution. Solids were then pressed into pellets, calcined at 773 K for 2 h in air flow (100 mL/min), and grounded to a particle diameter = 0.18 - 0.6 mm. All supports were calcined for 4 h in air flow at 773 K before impregnation of the metals. Palladium and Platinum precursors used were $PdCl_2$, Pd(II) acetylacetonate ($Pd(acac)_2$), Pt(II) acetylacetonate ($Pt(acac)_2$) and $H_2PtCl_6.4H_2O$ (all provided by Sigma-Aldrich), respectively. A mixed solution of chloride ($PdCl_2$ or chloroplatinate) or organometallic precursors was prepared and impregnated onto the support. Amounts of Pt and Pd precursors were adjusted to obtain the desired metallic contents. In the case of chloride precursors, preparation was performed following the recipe presented in Chapter III (Part I, Section 2.1.). The organometallic precursors were simultaneously diluted in hot toluene. The calcination of the impregnated solids was performed with the same protocol as presented in Chapter III (Part I, Section 2.1.). Two conventional CoMo and NiMo catalysts were also prepared for comparison purposes. Catalysts labels are presented in Table 1.

2.2. Catalysts characterization

2.2.1. Textural properties and metallic contents

The metallic contents of the catalysts were established by atomic absorption technique and by Inductively Coupled Plasma-Atomic Emission Spectrometry (ICP-AES) measurements. The latter being performed in an Iris Advantage apparatus from Jarrell Ash Corporation.

BET surface area, pore volume, distribution and pore size; using the BJH method, were determined by nitrogen adsorption-desorption isotherms in a Nova 1300 (Quantachrome) apparatus.

2.2.2. CO chemisorption

CO chemisorption measurements were conducted using the procedure presented in Chapter III.

2.2.3. Temperature programmed desorption (TPD) of ammonia

Ammonia TPD was carried out in the same apparatus described for TPR analysis (Chapter III, Part II: Section 2.2.3.) experiments. Samples of the catalysts (c.a. 0.15 g) were reduced under H_2 flow at 673 K; according to the activation procedure described in Chapter III, before the analysis. During this process it was checked that the MS signal (m/z = 17 and 18) was flat. After this step, the system was cooled down until the temperature selected to chemisorb NH_3 (308 K). To do this, a flow of NH_3 (5 vol. %)/He was passed through the reactor. Physisorbed NH_3 was eliminated from the catalyst by flowing pure He until obtaining flat NH_3 signals in the MS detector (m/z = 15, 16 and 17). TPD analysis was then performed by desorbing the chemisorbed ammonia by heating, at 10 K/min, until 873 K. The MS signal m/z = 16 was selected for analysis. The classification of the acidic sites according to their strength was defined in agreement to the methodology used in ammonia chemisorption measurements (see Chapter IV, Section 2.2.2.), and obtained from an integration of the area under the TPD curve in the specified temperature range. Hence, weak acid sites are those corresponding to the temperature range $308 \text{ K} \leq \text{T} < 423 \text{ K}$; medium acid sites: $423 \text{ K} \leq \text{T} < 623 \text{ K}$ and strong acid sites $\text{T} \geq 623 \text{ K}$.

2.2.4. FTIR analysis of adsorbed pyridine

Fourier transformed infrared spectra of pre-adsorbed pyridine (FTIR-Py) were recorded with an IFS55 Equinox spectrometer (Brücker) equipped with an MCT detector using 100 scans and a resolution of 4 cm^{-1}. Catalysts and supports powders were pressed into self-supported wafers (15 mg, 13 mm diameter) and placed in a homemade IR cell. Samples were first degasified under vacuum (10^{-6} mbar) at 773 K for 2 h. A first spectrum of the samples, taken as a reference, was then recorded after cooling to room temperature. Degasified samples were exposed to 10 mbar of pyridine for 30 min. Afterwards, the FTIR-Py spectra were recorded after evacuation (10^{-6} mbar) for 1 h at room temperature, 373, 473 and 573 K.

2.3. Catalytic tests

The hydrodesulfurization of dibenzothiophene was performed at the same conditions described in Chapter III, Part II: Section 2.3. The Pd-Pt catalysts were activated by reduction in H$_2$ flow, while conventional CoMo and NiMo were sulfided with a 15vol.% H$_2$S in H$_2$ mixture (for further details see Chapters I and III).

Activity, products distribution and selectivity to HYD were defined according to expressions presented in Chapters I and II.

3. Results and discussion

Table 1 presents the textural properties and the results of CO chemisorption of the prepared materials. It can be observed that the catalysts supported on the home-made carriers possess better textural properties as compared to commercial γ-Al$_2$O$_3$. The catalyst supported on SiO$_2$ displays the highest BET surface area but its average pore diameter is lower than that

of the γ-Al_2O_3 supported catalysts. The lowest average pore diameter was registered for the Pd(1.0)-Pt(0.5)/Al-Si catalyst. In spite of these differences, the N_2 adsorption-desorption isotherms (not shown) of all of these materials showed that they are mesoporous. The metallic contents of the catalysts do not exceed a total metallic content (Pd + Pt) of 1.5 wt.%, with a constant Pd/(Pd+Pt) molar ratio of 0.8. On the other hand, the measurements of CO chemisorption indicate the following tendency in dispersion: Pd(1.0)-Pt(0.5)/Al-Si $\geq$ Pd(1.0)-Pt(0.5)-Cl/Al^{Proc} > Pd(1.0)-Pt(0.5)/Al^{Proc} $\approx$ Pd(1.0)-Pt(0.5)/Al^{HM} $\approx$ Pd(0.7)-Pt(0.4)/Si. Therefore, the Pd-Pt alloys are better dispersed either by employing chlorided precursors in the preparation process of by its deposition on the mixed oxide Al_2O_3-SiO_2 support.

Fig. 1 shows the average steady state HYD selectivity (S_{HYD}) in the hydrodesulfurization of dibenzothiophene for the prepared Pd-Pt catalysts and the two NiMo and CoMo conventional catalysts; the latter being tested at iso-conversion reaction conditions, as to allow a direct comparison with Pd(1.0)-Pt(0.5)-Cl/Al^{Proc} and Pd(1.0)-Pt(0.5)/Al-Si. Both MoS_2-based catalysts display a very low S_{HYD} in agreement with previous literature reports [1-6]. For the Pd-Pt system, S_{HYD} drastically varies as a function of the carrier used. Thus, S_{HYD} follows the order: Pd(1.0)-Pt(0.5)/Al-Si > Pd(1.0)-Pt(0.5)-Cl/Al^{Proc} > Pd(0.7)-Pt(0.4)/Si > Pd(1.0)-Pt(0.5)/Al^{Proc} > Pd(1.0)-Pt(0.5)/Al^{HM}. The fact that a very sharp enhancement of S_{HYD} is obtained over Pd-Pt with only "soft" changes in the nature of the carrier employed is rather un-precedent in HDS literature ([1-6, 14-17] and references therein).

Table 1. Textural properties and CO chemisorption measurements on the prepared Pd-Pt catalysts.

Catalyst[†]	S_{BET} (m^2/g)	D_p (Å)	V_p (cm^3/g)	CO Chemisorption	
				n_{ads}^{STP} (µmol CO/µmol metal)	%Dispersion
Pd(0.7)-Pt(0.4)/Si	1008.6	87	2.2	0.30	22
Pd(1.0)-Pt(0.5)/Al^{HM}	332.5	102	0.9	0.29	22
Pd(1.0)-Pt(0.5)/Al^{Proc}	205.9	114	0.6	0.30	23
Pd(1.0)-Pt(0.5)-Cl/Al^{Proc}	199.2	112	0.6	0.37	30
Pd(1.0)-Pt(0.5)/Al-Si	286.4	55	0.4	0.43	32

[†]Metallic contents (wt.%) of the catalysts are indicated in parentheses. Codes for the carriers are: Si = home made SiO_2; Al^{HM} = home made Al_2O_3; Al^{Proc} = commercial *Procatalyse* Al_2O_3; Al-Si = home made Al_2O_3 - SiO_2 mixed oxide support (Si/Al ratio = 0.2). The index −Cl indicates use of chlorided precursors.

Table 2 shows the average steady state performance of the catalytic materials in the hydrodesulfurization reaction. The results show that for Pd(1.0)-Pt(0.5)/Al-Si the HYD route of hydrodesulfurization is completely developed as it is evidenced by the fact that cyclohexylbenzene is the main reaction product. It must be remarked that the metallic content of all of the prepared Pd-Pt catalysts in this work is much lower than those contents reported by Kabe et al. [10]. These authors [10] observed almost complete conversion of dibenzothiophene to cyclohexylbenzene over a 2 wt.% Pt - 10 wt.% Pd catalyst. Their results indicated that it is possible to develop the HYD route of hydrodesulfurization of the dibenzothiophene molecule over Pd-Pt alloys, but it was necessary to design a Pd-Pt catalytic system with a similar good performance but employing lower noble metal contents. Such high Pt and Pd loads seem prohibitive to the commercial HDS processes. On the other hand, Niquille-Röthlisberger and Prins [11] have prepared high HDS performance low content noble metal catalysts and developed the HYD route of hydrodesulfurization for 4,6-dimethyl-DBT. However, for this model molecule DDS is practically unfeasible [7]. From this standpoint the HDS performance of Pd(1.0)-Pt(0.5)/Al-Si is quite extraordinary

and relevant to the future design of highly HYD selective catalytic materials aimed to be employed in deep HDS processes. Important differences in S_{HYD} and products distribution as a function of the support must be commented. In first place, partially hydrogenated intermediates in high amounts are registered for the Pd-Pt catalysts and not for CoMo and NiMo. It may be noted that significant amounts of such intermediates (Table 2) were detected for the silica supported Pd-Pt catalyst (Pd(0.7)-Pt(0.4)/Si). This indicates that this material is able to develop HYD but it seems to experience certain level of limitation regarding the ability to perform the final C-S-C bond scission step in HYD as compared to the other Pd-Pt catalysts which yielded lower amounts of such intermediates.
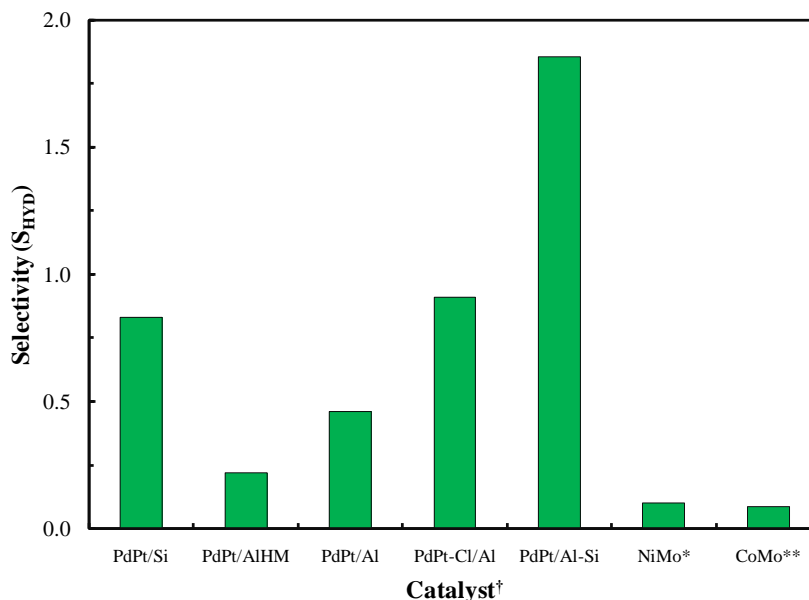
Fig. 1. Steady state average total HYD (S_{HYD}) selectivity for the prepared catalysts. Catalysts' codes modified to fit graphic's screen as follows: PdPt/Si = Pd(0.7)-Pt(0.4)/Si; PdPt/Al HM = Pd(1.0)-Pt(0.5)/Al^{HM}; PdPt/Al = Pd(1.0)-Pt(0.5)/Al^{Proc}; PdPt-Cl/Al = Pd(1.0)-Pt(0.5)-Cl/Al^{Proc}; and PdPt/Al-Si = Pd(1.0)-Pt(0.5)/Al-Si. [*]NiMo catalyst tested at 563 K. [**]CoMo catalyst tested at 573 K.

On the other hand, if one compares the performance of the catalysts supported on alumina (Pd(1.0)-Pt(0.5)/Al^{HM} and Pd(1.0)-Pt(0.5)/Al^{Proc}) but prepared from the same precursor, it is

important to remark how HYD over Pd-Pt is highly susceptible to a probable change in the nature of the alumina support. It is known that the surface chemistry of every alumina is rather complex [18] and it can influence the catalytic activity in HDS [19], but not usually HYD selectivity in dibenzothiophene hydrodesulfurization. The results for these two alumina supported materials catalysts are similar to those presented by Niquille-Röthlisberger and Prins [11], who reported that Pd-Pt/γ-Al$_2$O$_3$ catalysts, prepared from nitrate precursors, have a better selectivity to DDS over HYD, and also displayed low amounts of non-desulfurized dibenzothiophene intermediates. This can be very advantageous when performing the HDS of non-sterically hindered dibenzothiophenes which in turn require less hydrogen consumption in the removing of sulfur [2].

Table 2. Average steady state conversion and products distribution in the hydrodesulfurization of dibenzothiophene for the different supported Pd-Pt catalysts and conventional NiMo and CoMo.

Catalyst	$\%C_{DBT}$	$\%y_{CHB}$	$\%y_{BP}$	$\%y_{HHDBT}$	$\%y_{THDBT}$
Pd(0.7)-Pt(0.4)/Si	40	11.7	21.9	1.2	5.3
Pd(1.0)-Pt(0.5)/Al^{HM}	40	5.3	32.6	0.2	1.6
Pd(1.0)-Pt(0.5)/Al^{Proc}	44	9.8	30.2	0.7	3.5
Pd(1.0)-Pt(0.5)-Cl/Al^{Proc}	70	31.4	36.8	0.3	1.9
Pd(1.0)-Pt(0.5)/Al-Si	76	46.4	26.6	0.5	2.5
NiMo	78	7.1	70.9	0.0	0.0
CoMo	75	6.0	69.4	0.0	0.0

In general, the alumina supported Pd-Pt catalysts prepared from organometallic precursors possess a higher DDS selectivity ($\%y_{BP}$) compared to Pd(0.7)-Pt(0.4)/Si. Moreover, as mentioned before, the C-S-C bond breaking capacity of alumina supported Pd-Pt catalysts is higher than that of Pd(0.7)-Pt(0.4)/Si. Therefore, the differences in the nature of the carriers are clearly modulating the selectivity in hydrodesulfurization over Pd-Pt. Although

extensive information exists concerning the effect of support on hydrodesulfurization reactions over MoS_2 based catalysts [1-3, 5, 6, 15-17, 20], regarding Pd-Pt catalysts, to author's knowledge, there are no works in open literature analyzing the effect of the support on the selectivity of this catalytic system in the hydrodesulfurization of dibenzothiophene. On the other hand, comparing the behavior of the alumina supported catalysts prepared from chloride precursors (Pd(1.0)-Pt(0.5)-Cl/Al^{Proc}) with those prepared from the organometallic precursors it is clear that the nature of the precursors of the active elements can also induce changes in the materials which manipulate both the activity and selectivity over Pd-Pt. Comparatively, the yield of cyclohexylbenzene is significantly enhanced for Pd(1.0)-Pt(0.5)-Cl/Al^{Proc} in regard to that of Pd(1.0)-Pt(0.5)/Al^{Proc}. In addition, the $\%C_{DBT}$ of the latter catalyst (Pd(1.0)-Pt(0.5)/Al^{Proc}) is c.a. 44%, while in the former (Pd(1.0)-Pt(0.5)-Cl/Al^{Proc}) it reaches 70%. A comparison of the products distribution shows that the use of chloride precursors mostly favors conversion of dibenzothiophene via HYD. Therefore, even the possible presence of Cl ions remaining attached to the alumina surface [21] can have a deep impact in the development of HYD over Pd-Pt catalysts. The effect of residual chlorine was clearly evidenced in the precedent Chapter (Chapter IV) for monometallic Pt and Pd/γ-Al$_2$O$_3$. Besides enhancing the catalytic activity, the changes in the acidic balance of the alumina carrier induced by this halogen were found to promote the development of HYD over Pd. This last evidence confirm that in the bimetallic Pd-Pt alloys, Pd is the active metal providing the active centers responsible for the high selectivity of Pd-Pt to the HYD route of hydrodesulfurization. The acidic

balance of the carriers used in this study was analyzed by ammonia TPD; results are presented in Table 3.

Table 3. Results of ammonia TPD characterization for the prepared catalytic materials.

Catalyst	10^8x(Total acidity/g cat.)[†]	10^3x(Total acidity/m^2)	Weak acid sites (%)	Medium acid sites (%)	Strong acid sites (%)
SiO$_2$	8.4	8.3	100	0	0
Pd(0.7)-Pt(0.4)/Si	12.7	12.6	99	1	0
Al$_2$O$_3$	6.9	21.1	47	50	3
Pd(1.0)-Pt(0.5)/Al^{HM}	6.1	18.3	59	38	4
Al$_2$O$_3$-Procatalyse	5.3	24.3	52	43	4
Pd(1.0)-Pt(0.5)/Al^{Proc}	5.6	27.0	62	34	4
Pd(1.0)-Pt(0.5)-Cl/Al^{Proc}	7.3	36.9	45	48	7
SiO$_2$-Al$_2$O$_3$-(Si/Al = 0.2)	7.4	22.7	58	39	2
Pd(1.0)-Pt(0.5)/Al-Si	6.7	23.5	50	45	5

[†]Total acidity corresponds to the integrated area under the TPD curve.

Little differences in total acidity are observed between the carriers and the supported catalysts. The distribution of acid sites for SiO$_2$ and the corresponding Pd-Pt catalyst shows that these materials possess a small amount of acid sites which are weak. The total acidity (total acidity/m^2) of the other materials followed the order: Pd(1.0)-Pt(0.5)-Cl/Al^{Proc} > Pd(1.0)-Pt(0.5)/Al^{Proc} > Pd(1.0)-Pt(0.5)/Al-Si > Pd(1.0)-Pt(0.5)/Al^{HM}. The distribution of acid sites of these catalysts shows that these acid sites are mostly weak and medium in strength with the presence of few strong acid sites. On the other hand, FTIR-Py (Fig. 2) showed that the catalysts Pd(1.0)-Pt(0.5)-Cl/Al^{Proc} and Pd(1.0)-Pt(0.5)/Al-Si possess a certain number of Brønsted acid sites. Furthermore, the latter displayed H-Bonded pyridine sites that can be transformed into additional weak Brønsted acid sites. The catalyst Pd(0.7)-Pt(0.4)/Si only showed H-Bonded pyridine sites, whereas Pd(1.0)-Pt(0.5)-Cl/Al^{Proc} and Pd(1.0)-Pt(0.5)/Al^{HM} only presented the bands attributed to Lewis acid sites (Fig. 2). The

differences between the distributions of acid sites among the catalysts are quite slight, thus the materials can be said to be distinguished by "soft" modifications of their acid balance. To try to provide a reasonable explanation to the catalytic trends registered we should take a little while in revising some literature findings concerning the relationship between acidity and hydrodesulfurization. Acidity can enhance hydrodesulfurization rates as well as thiotolerance of noble metal based catalysts [14, 22, 23]. Galindo and de los Reyes [23] found a correlation between thiophene hydrodesulfurization, thiotolerance and acidity for alumina-titania Pd-Pt supported catalysts. Barrio et al. [14] ascribed the high activity of Pd-Pt/ASA catalysts in the hydrodesulfurization of dibenzothiophene and hydrogenation of naphthalene partly to strong Brønsted acidic sites. However, they did not present results on HYD selectivity, but reported that compared to monometallic Pd/ASA a Pd-Pt/ASA catalyst displayed a much higher C-S-C hydrogenolysis capacity. For conventional MoS_2 based catalysts it has been claimed that an increase in support's acidity promotes HYD pathway [5, 6, 16, 24, 25], but only minor increases are reported. Concerning, the results presented in this Chapter, it is useful to recall that the Pd-Pt catalyst supported on SiO_2 exhibited a S_{HYD} similar to that of Pd(1.0)-Pt(0.5)-Cl/Al^{Proc}, nonetheless, as noticed before, Pd(0.7)-Pt(0.4)/Si produces a significant amount of partially hydrogenated intermediates. It is known that the acidity of SiO_2 is due to the presence of silanol groups of diverse nature: single, geminal, vicinal [26].

Fig. 2. FTIR-Py spectra (T=373K) of the different Pd-Pt catalysts.
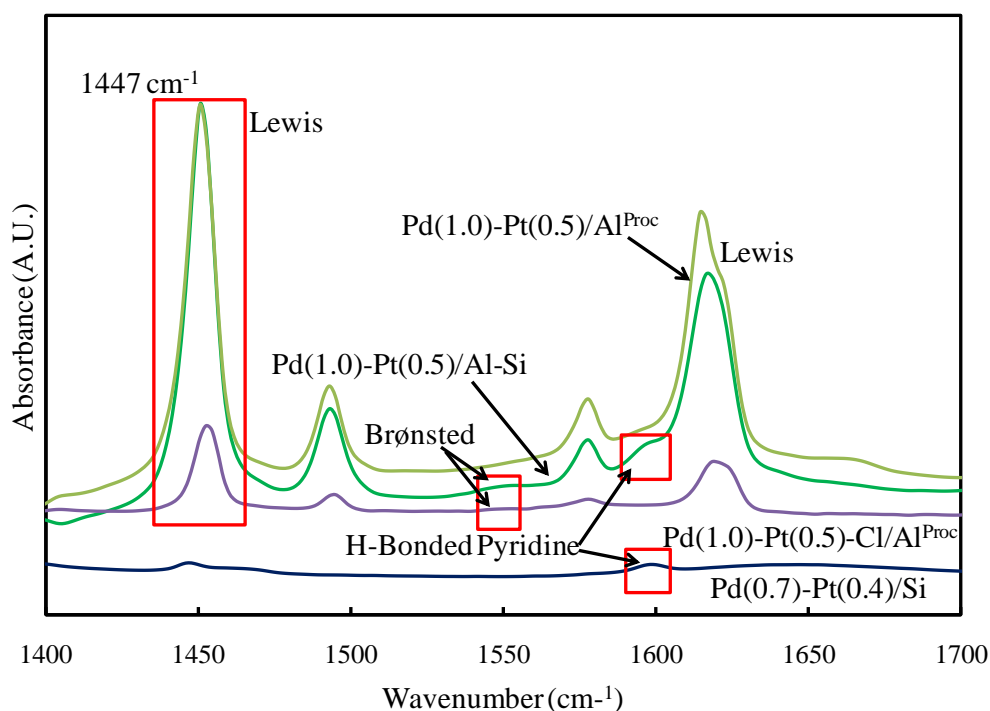
Pyridine is bonded to these silanol groups by hydrogen bonds (Fig. 2). In the course of a reduction process, as that performed during the activation of the catalysts, such groups can be converted to Brønsted acid sites [27, 28]. From such consideration the high selectivity to HYD of this material can be partly explained, given that hydrogenation reaction rates are enhanced by Brønsted acid sites. In the previous Chapter it was demonstrated that when reduction of a γ-Al$_2$O$_3$ supported Pd catalyst, prepared from a chloride precursors, is performed at low temperature HYD selectivity is boosted. This was attributed to the generation of additional weak Brønsted acid sites located in the proximity of the noble metal active sites which can act as additional hydrogenation centers. On the other hand, the Lewis acid sites present on γ-Al$_2$O$_3$ can be also playing a role in the hydrodesulfurization reaction and more precisely in the selectivity.

The effect of residual chlorine is not present for the catalysts Pd(1.0)-Pt(0.5)/Al^{HM} and Pd(1.0)-Pt(0.5)/Al^{Proc}, which have the same activity than Pd(0.7)-Pt(0.4)/Si, but are comparatively more selective to DDS. In Chapter IV the possible participation of Al^{3+} CUS sites Lewis acid sites of the carrier in the hydrodesulfurization reaction was postulated in agreement to the mechanism proposed by Sarbak [29]. As in the case of monometallic Pd/γ-Al$_2$O$_3$ prepared from a chlorided Pd precursor and pretreated at reduced 773 K (Chapter IV, Section 3.2.), over the bimetallic Pd(1.0)-Pt(0.5)-Cl/Al^{Proc} catalyst HYD is very competitive to DDS, but dibenzothiophene is not preferentially converted via HYD. Therefore, the author proposes that in the bimetallic Pd(1.0)-Pt(0.5)-Cl/Al^{Proc} catalyst the presence of residual chlorine promotes the simultaneous formation of additional Brønsted and Lewis acid sites which can be contributing to improve the dynamic transformation of dibenzothiophene over the catalytic surface by a bifunctional mechanism. Within this line of thought, the outstanding performance of Pd(1.0)-Pt(0.5)/Al-Si can be ascribed to a more proper distribution of the Brønsted and Lewis acid sites of this material as compared to the others. Diverse authors agree that the combination of Al$_2$O$_3$ and SiO$_2$ in a mixed oxide carrier possesses a higher concentration of Brønsted acid sites compared to both single oxides. At the low Si/Al ratio used in this Thesis, though neither the total acidity of Pd(1.0)-Pt(0.5)/Al-Si nor the distribution of the acid sites, according to their strength, is very different from that of the other catalysts, it is possible that this "soft" change in the distribution of the Brønsted and Lewis acid sites is deeply implicated in the observed catalytic behavior. This aspect is very important because highly acidic supports tend to favor undesirable side reactions during hydrodesulfurization [30] and are additionally more

susceptible to poisoning from hydrodenitrogenation [31]. Finally, the superiority of the Pd-Pt system for deep HDS is fully demonstrated from the present results, because only over this type of materials the HYD/DDS selectivity in hydrodesulfurization can be so acutely manipulated and specifically adjusted to a definite requirement of the process; in this sense, it is important to notice that in order to observe non-trivial changes in the HYD/DDS selectivity of dibenzothiophene over conventional Co(Ni)Mo sulfided catalysts drastic changes in the nature of the support or the active phase must be made. Large amounts of literature on the subject indicate so.

4. Conclusions

It has been found that the hydrodesulfurization of dibenzothiophene can be selectively oriented to the HYD reaction pathway over a silica-alumina supported Pd-Pt catalyst of very low Si/Al ratio. The correlation of the catalytic results with the acid characteristics of the supported Pd-Pt materials shows that the reaction pathway in the hydrodesulfurization of dibenzothiophene over Pd-Pt can be directed to HYD only by inducing "soft" changes in the acid balance of the carrier. Therefore, these catalysts are certainly very promising for deep hydrodesulfurization in which sterically hindered di-β-dibenzothiophenes are to be treated, but also the flexibility of their functionalities would allow its use in other hydrodesulfurization processes requiring other type of selectivity; such as those where DDS is preferred. The results of this Chapter are so encouraging that surely will inspire new research investigating the properties and application of such kind of materials in other fields of catalysis science.

References

[1] C. Song and X. Ma, Intern. J. Green Energy, 1 (2004) 167.

[2] D.D. Whitehurst, T. Isoda and I. Mochida, Adv. Catal. 42 (1998) 345.

[3] S.K. Bej, S.K. Maity and U.T. Turaga, Energy Fuels 18 (2004) 1227.

[4] J. Mijoin, G. Pérot, F. Bataille, J.L. Lemberton, M. Breysse and S. Kasztelan, Catal. Lett. 71 (2001) 139.

[5] B. Pawelec, T. Halachev, A. Olivas and T.A. Zepeda, Appl. Catal. A: Gen. 348 (2008) 30.

[6] T.A. Zepeda, B. Pawelec, J.L.G. Fierro, A. Olivas, S. Fuentes and T. Halachev, Microp. Mesop. Mat. 111 (2008) 157.

[7] H. Yang, C. Fairbridge and Z. Ring, Energy Fuels 17 (2003) 387.

[8] M.L. Vrinat, Appl. Catal. 6 (1983) 137).

[9] H.R. Reinhoudt, R. Troost, A.D. van Langeveld, S.T. Sie, J.A.R. van Veen and J.A. Moulijn, Fuel Proc. Tech. 61 (1999) 133.

[10] T. Kabe,W. Qian, Y. Hirai, L. Li and A. Ishihara, J. Catal. 190 (2000) 191.

[11] A. Niquille-Röthlisberger and R. Prins, J. Catal. 242 (2006) 207.

[12] A. Niquille-Röthlisberger and R. Prins, Catal. Today 123 (2007) 198.

[13] Q. Cai, Z.-S. Luo, W.-Q. Pang, Y.-W. Fan, X.-H. Chen and F.-Z. Cui, Chem. Mater. 13 (2001) 258.

[14] V.L. Barrio, P.L. Arias, J.F. Cambra, M.B. Güemez, B. Pawelec and J.L.G. Fierro, Fuel 82 (2003) 501.

[15] "Effects of Support in Hydrotreating Catalysis for Ultra-clean Fuels" Catal. Today 86 (2003) 1-288.

[16] G. Pérot, Catal. Today 86 (2003) 111.

[17] J. Ancheyta and G.F. Froment (Eds) "International Symposium on Advances in Hydroprocessing of Oils Fractions (ISAHOF 2007)" Catal. Today 130 (2008) 1-264.

[18] J.A. Kelber, Surf. Sci. Rep. 62 (2007) 271.

[19] M. Adachi and C. Contescu, J.A. Schwarz, J. Catal. 162 (1996) 66.

[20] S.A. Giraldo and A. Centeno, Catal. Today 133–135 (2008) 255.

[21] S.D. Jackson, J. Willis, G.D. Mclellan, G. Webb, M.B.T. Keegan, R.B. Moyes, S. Simpson, P.B. Wells and R. Whyman, J. Catal. 139 (1993) 191.

[22] A. Stanislaus and B.H. Cooper, Catal. Rev.-Sci. Eng. 36 (1994) 75.

[23] I.R. Galindo and J.A. de los Reyes, Fuel Proc. Tech. 88 (2007) 859.

[24] C. Pophal, F. Kameda, K. Hoshino, S. Yoshinaka and K. Segawa, Catal. Today 39 (1997) 21.

[25] H. Kim, J.J. Lee and S.H. Moon, Appl. Catal. B: Env. 44 (2003) 287.

[26] S.K. Parida, S. Dash, S. Patel, B.K. Mishra, Adv. Colloid Interf. Sci. 121 (2006)77.

[27] T.S. Mahadevan, S.H. Garofalini, J. Phys. Chem. C 112 (2008) 1507.

[28] L. Peng, W. Qisui, L. Xi, Z. Chaocan, Colloid. Surf. A: Physicochem. Eng. Aspects 334 (2009) 112–115.

[29] Z. Sarbak, Appl. Catal. A: Gen. 159 (1997) 147.

[30] H. Guo, Y. Sun and R. Prins, Catal. Today 130 (2008) 249.

[31] E. Furimsky and F.E. Massoth, Catal. Rev. 47 (2005) 297.

General Conclusions

In this Ph.D. Thesis the design of a series of catalytic materials for the selective hydrodesulfurization of dibenzothiophenes via HYD was made. To achieve this purpose the author has performed an in-depth review of HDT literature and by its analysis a series of experiments were critically designed from a scientific perspective. These experiments were sequentially carried out and thoroughly discussed confronting them with relevant scientific literature in every step of the way. In this manner, as the reader goes through each Chapter of the Thesis, he will find that each one of them provides suitable experimental evidence combined with literature in catalysis science which sets a solid scientific-engineering basis to arrive to the consecution of the primary objective of this Thesis: to obtain a catalytic system highly efficient for the selective HDS of dibenzothiophene via HYD by a rational tuning of the characteristics of the active phase of the catalyst with the acid-base characteristics of the support. Furthermore, by using the proposed methodology new insights into the nature of the active sites implicated in the HYD route of hydrodesulfurization, and the specific mechanism of the HYD route of hydrodesulfurization of dibenzothiophene were obtained.

In particular, a combination of a Pd-Pt active phase of a determined Pd/(Pd+Pt) atomic ratio (0.8) with a SiO_2-Al_2O_3 carrier of low Si/Al ratio (0.2) was found to convert non-sterically hindered dibenzothiophene prevalently via HYD. By doing this, such material is an excellent candidate to perform the ultra-deep hydrodesulfurization of heavy oil refinery streams, because it can efficiently perform the hydrodesulfurization of di-β-dibenzothiophenes which have been determined to react mainly via HYD. Furthermore, the "soft" acid properties of the SiO_2-Al_2O_3 carrier are very advantageous in order to prevent poisoning by extensive coking and strong adsorption of basic nitrogen containing molecules due to parallel HDA and HDN reactions.

During the course of this research it was demonstrated that at the selected Pd/(Pd+Pt) atomic ratio the Pd-Pt active phase is able to endure H_2S inhibition and is capable of efficiently perform the hydrodesulfurization of dibenzothiophene with good selectivity to HYD in the presence of aromatics; more precisely naphthalene. Moreover, this Pd-Pt catalyst is very active in both reactions when they are performed simultaneously; as it corresponds to a real scenario in a refinery reactor unit. As it is demonstrated, the hydrogenating function of the Pd-Pt alloys is very strong but depends on the Pd/(Pd-Pt) atomic ratio. For a Pd/(Pd+Pt) atomic ratio of 0.8, the selectivity to hydrogenation reactions; HYD reaction route and/or aromatics hydrogenation, always prevails over hydrodesulfurization and/or the DDS route of desulfurization of dibenzothiophene. One aspect that must be remarked is the flexibility of the active phase of the Pd-Pt alloy in the hydrodesulfurization reaction which can be adapted to different requirements of selectivity by adjusting the Pd/(Pd+Pt) molar ratio used in the preparation. For example, if a highly DDS selective material is desired, thus consuming less hydrogen in the HDS reaction, very low Pd/(Pd+Pt) atomic ratios should be used; i.e. higher concentrations of Pt than of Pd, whereas if a highly HYD or aromatics hydrogenation selective material is required, deep HDT of heavy oil cuts, the Pd/(Pd+Pt) molar ratio should be adjusted to values around 0.8; i.e. a Pd rich alloy with low amounts of Pt. This is partly possible due to the fact that both noble metals possess remarkable differences in activity and selectivity in the hydrodesulfurization reaction. While Pt is highly active and selective to DDS, Pd is less active but displays intensive competition between the HYD and DDS pathways. When alloyed, the bimetallic Pd-Pt system does not present synergy in the hydrodesulfurization of dibenzothiophene, but, instead, it displays a synergy effect in the development of the HYD route of hydrodesulfurization. This synergy effect is in correspondence with the one observed in reactions of aromatics hydrogenation under H_2S atmospheres. The properties of the Pd-Pt active phase responsible for such trends were

investigated by correlating the dynamics of the HYD reaction mechanism with the mechanism of naphthalene hydrogenation. In this sense, naphthalene hydrogenation was proved to be a very useful probe molecule for the *in situ* determination of certain surface characteristics of the working catalyst. As a result, it was possible to describe the HYD mechanism as a dynamic equilibrium between surface hydrogenation-dehydrogenation-C-S-C bond breaking reactions which in the case of the Pd-Pt system can be controlled from the Pd/(Pd+Pt) molar ratio of the alloy.

By the use of a series of surface characterization techniques which complemented the results obtained in the model naphthalene hydrogenation reaction, it was possible to determine some key characteristics of the Pd-Pt alloys which allow this system to efficiently develop HYD. Therefore, the Pd-like character of the Pd-Pt active phase in HDT was verified and the existence of an interaction between electron deficient $Pd^{\delta+}$ particles and platinum was detected. In addition, a direct correlation between the hydrogen chemisorption capacity of the Pd-Pt catalysts and the synergy in HYD was found.

Another factor playing an important role in the development of HYD over Pd-Pt catalysts is the metal-support interaction, and, in this case, those chemical properties related to the acidic balance of the support. It was proved that important enhancement in the catalytic functionalities of the Pd-Pt system can be obtained from slight modifications either in the nature of the carrier or in the modification of γ-Al_2O_3 by the presence of residual chlorine. From the point of view of the acidic properties of the carriers, it was demonstrated that "soft" changes in the acid balance of the catalysts induce drastic changes in the HYD/DDS selectivity. Consequently, to prepare supported Pd-Pt materials with a very strong hydrogenation function, apt for deep hydrodesulfurization reactions, it is not necessary to use highly acidic carriers with strong Brønsted acid sites; this kind of sites being promoters of undesirable side reactions often leading to poisoning. This last finding is very significant in

the field of catalytic hydrotreatment because it is normally assumed that there is a straight relationship between the increase in the number and strength of acid sites and the performance in hydrotreating reactions.

List of Publications

Published

V.G. Baldovino-Medrano, S.A. Giraldo, A. Centeno. "Reactivity of dibenzothiophene type molecules over Pd catalysts". Journal of Molecular Catalysis A: Chemical 301 (2009) 127–133.

V.G. Baldovino-Medrano, S.A. Giraldo, A. Centeno. "The functionalities of Pt/γ-Al$_2$O$_3$ catalysts in simultaneous HDS and HDA reactions". Fuel 87 (2008) 1917-1926.

In Press

V.G. Baldovino-Medrano, S.A. Giraldo, A. Centeno. "Highly HYD selective Pd-Pt/support hydrotreating catalysts for the high pressure desulfurization of DBT type molecules". Catal. Lett. (2009) DOI:10.1007/s10562-009-9919-9.

V.G. Baldovino-Medrano, S.A. Giraldo, A. Centeno. "Comportamiento de catalizadores PtMo/γ-Al$_2$O$_3$-B$_2$O$_3$ en reacciones de hidrodesaromatización de naftaleno y hidrodesulfuración de dibenzotiofeno" Información Tecnológica ISSN 0718-0764, Vol. 20 (6) (2009).

Accepted

V.G. Baldovino-Medrano, P. Eloy, E.M. Gaigneaux, S.A. Giraldo, A. Centeno. "Pd-Pt catalysts for the hydrodesulfurization of DBT type molecules: Development of the HYD route of hydrodesulfurization." Journal of Catalysis (2009) In Revision.

Under Review

V.G. Baldovino-Medrano, S.A. Giraldo, A. Centeno. "High pressure hydrodesulfurization and hydrogenation over bimetallic Pt-Mo catalysts." Fuel (2009).

V.G. Baldovino-Medrano, P. Eloy, E.M. Gaigneaux, S.A. Giraldo, A. Centeno. "Factors controlling the development of the HYD route of desulfurization of DBT over γ-alumina supported Pt and Pd catalysts" Catalysis Today (2009).

Symposia and Congresses

V.G. Baldovino-Medrano, P. Eloy, E.M. Gaigneaux, S.A. Giraldo, A. Centeno. "Factors controlling the development of the HYD route of desulfurization of DBT over γ-alumina supported Pt and Pd catalysts" En: J. Ancheyta, G.F. Froment (Eds) "Proceedings of the International Symposium on Advances in Hydroprocessing of Oil Fractions (ISAHOF 2009)" To be held at Ixtapa-Zihuatanejo, México, June 14-18 - 2009.

V.G. Baldovino-Medrano, S.A. Giraldo, A. Centeno. "Comparative performance of γ-alumina supported Pt and Pd catalysts for the hydrodesulfurization of dibenzothiophene" En: Process Engineering Publisher (Eds) "Summaries 1, Reaction Engineering, 18th International Congress of Chemical and Process Engineering CHISA 2008" ISBN 978-80-02-02048-6, Prague, Czech Republic (2008) p. 19.

V.G. Baldovino-Medrano, S.A. Giraldo, A. Centeno. "Comportamiento de catalizadores PtMo/γ-Al$_2$O$_3$-B$_2$O$_3$ en reacciones de HDA de naftaleno y HDS de dibenzotiofeno". En: Sociedad Española de Catálisis y Universidad de Málaga (Eds) "Memorias del XXI Simposio Iberoamericano de Catálisis, SICAT 2008" ISBN 978-84-691-4234-9, Junio (2008) Benalmádena-Costa, España, p. IV-500.

V.G. Baldovino-Medrano, S.A. Giraldo, A. Centeno. "Evaluación de las funcionalidades de catalizadores NiMo/γ-Al$_2$O$_3$-B$_2$O$_3$ en reacciones de HDA de naftaleno y HDS de dibenzotiofeno." En: Sociedad Española de Catálisis y Universidad de Málaga (Eds) "Memorias del XXI Simposio Iberoamericano de Catálisis, SICAT 2008" ISBN 978-84-691-4234-9, Benalmádena-Costa, España (2008) p. IV-1086.

V.G. Baldovino-Medrano, S.A. Giraldo, A. Centeno. "Análisis del estado del azufre y el paladio y su relación con el desempeño catalítico en HDT". En: "Memorias del V Simposio Colombiano de Catálisis (V SICCAT)", Bucaramanga, Colombia (2007).

K. Rojas-Restrepo, L.E. González-Ardila, V.G. Baldovino-Medrano, S.A. Giraldo, A. Centeno. "Influencia de la incorporación de boro al catalizador NiMo/γ-Al$_2$O$_3$ sobre su función hidrogenante en reacciones de HDT". En: "Memorias del V Simposio Colombiano de Catálisis (V SICCAT)", Bucaramanga, Colombia (2007).